Hygrothermal Analysis of Vacuum Insulation Panels in New and Retrofit Walls for Canada

by

Brock Conley

A thesis submitted to the Faculty of Graduate and Postdoctoral Affairs in partial fulfillment of the requirements for the degree of

Doctor of Philosophy

in

Mechanical Engineering

Carleton University
Ottawa, Ontario

Abstract

In Canada, residential buildings account for 16.7% of the total secondary energy end use and 12.7% of the total greenhouse gas emissions. Of these percentages, space heating and cooling account for about two-thirds of the total. As buildings are being built to higher standards, an air-tight, resilient, and thermally efficient building enclosure could be used to meet the targeted energy efficiency in new and retrofit construction. The research program was aimed at the use of vacuum insulation panels (VIPs) encapsulated within expanded polystyrene (EPS) board to form an exterior insulation system for use in new and retrofit construction nationwide. The program utilized experimental and numerical methods to evaluate the insulation system under steady-state thermal and transient hygrothermal conditions.

The experimental study was split into two categories: steady-state thermal conductivity testing and in-situ hygrothermal monitoring. The steady-state testing, performed with a guarded hot-box at Carleton University, found that a 200 mm by 300 mm (8" x 12") VIP in the exterior insulation with a 1:1 VIP to EPS insulated area ratio on a code-built wood-frame wall would have an effective thermal resistance of R-5.1 to R-6.3 m^2K/W. It was observed after the in-situ monitoring, performed at CanmetENERGY-Ottawa, that the backer material for the VIP-insulated system did not affect the long-term potential for mould growth or moisture-related damage in the assembly.

The numerical study was performed using Wärme Und Feuchte Instationär (WUFI) Pro 6.1 and WUFI 2D. The hygrothermal model was validated using the in-situ monitored data from 2016 to 2020 for Ottawa, CA. A methodology to model VIP insulated wall assemblies for building envelope retrofits was presented and performed in multiple cities across Canada. It was observed that masonry clad buildings (e.g., brick veneer) and wet climates (e.g., Vancouver and St. John's)

had a higher potential to experience mould growth in new and retrofit buildings, for a similar envelope construction in a dryer climate. Finally, a screening study of eleven simulation inputs was performed using WUFI Pro 6.1 by following the Morris Method, a One-At-a-Time (OAT) screening procedure that compares the standard deviation and mean of the peak mould index. Non-linear effects were observed for all the screened simulation inputs, and the inputs that had the greatest effect on the mould index were the vapour permeability of the insulation, inclusion of a rainscreen, the designated vapour control strategy and initial moisture content of the materials for a given exterior climate to which wall assemblies were subjected.

Acknowledgements

I would like to first thank the past and present students from the Solar Energy Systems Laboratory, the Carleton University Centre for Advanced Building Envelope Research, and the Building Performance Research Centre as well as the faculty and staff in the Mechanical and Aerospace Engineering, and Civil Engineering departments at Carleton University. Your guidance and support were invaluable to my research program and my development as a researcher in the field of building science and building performance.

I would like to thank Dr. Cynthia A. Cruickshank and Dr. Christopher Baldwin for continuing to support, guide, and advise me during my studies. I am so grateful for the opportunities you have given me during the last 7 years including the side projects, research proposals, design of experiments, workshop participation, allowing me to attend building physics conferences, and writing a book chapter. I look forward to continuing to work together in the future.

To the team at Natural Resources Canada including Meli, Mark, Anil, Alex, Silvio and Sébastien, who included me in their research team part-time during my studies. I feel very lucky and fortunate to be given the opportunity to work in your group.

To all my family (Paul, Alison, John, Greg, Curtis), my in-laws (Guy and Martha), grandparents (John, Ingrid, Mary) and friends who are as close as family, thank you for encouraging me during this journey. And those who are no longer with us, you are missed, and I will always remember your support in helping me be who I am today.

Finally, my wife, Alexandra MacLeod; your quiet support throughout my whole degree helped me get to the finish line. You are the most exceptional woman and I look forward to starting our life adventure together.

Nomenclature

A	m^2	area
ρ	kg/m^3	density
DI	-	drying index
E_j^i	-	elementary effect
H	J/m^3	enthalpy of moist building material
h	J/kg	evaporation enthalpy
λ	W/m·K	heat conductivity of moist material
$q"$	W/m^2	heat flux
D	m^2/s	liquid transport coefficient
k_2	-	moderation of growth as mould index approaches its peak
Q	L/hr	moisture source
w	Kg/m^3	moisture content
MI	-	moisture index
k_1	-	mould growth intensity
M	-	mould index
σ	-	non-linear effect of the input
R	L/hr	rainwater
φ, RH	-	relative humidity
c	J/kg·K	specific heat
SQ	-	surface quality (0 for sawn surface/non-wood, 1 for kiln-dried)
ϑ, T	K *or* °C	temperature

MC	%	temperature and species corrected moisture content
E	W·h	the energy input to the metering chamber
μ^*	-	the measure of influence on the input
W	-	timber species (0 for pine, 1 for spruce)
t	h *or* s	time
μ	-	vapour diffusion resistance factor of dry material
δ	kg/m·s·Pa	vapour permeability
u	m^3/m^3	water content
p	Pa	water vapour partial pressure
WI	-	wetting index

subscript

v	vapour
sat	saturated or saturation
w	wall
o	initial
p	pressure
crit	critical

Table of Contents

List of Tables

List of Figures

List of Appendices

Chapter 1: Introduction

The residential building sector in Canada is comprised of 15 million total units [1] and consumes about 16.7% of the national energy consumption and is responsible for 12.7% of the total greenhouse gas (GHG) emissions in 2018 [2]. The energy consumption trends in Canada are like other regions across the globe, as buildings in the United States and Europe account for 40% and 38% of their energy use, respectively [3, 4]. Space conditioning accounts for the greatest percentage of energy use in the residential sector and varies between 49% and 64% across the listed regions [3, 4]. Within Canadian residential buildings, space heating and cooling accounts for 67% of the total energy consumption in this sector followed by energy consumption by domestic water heating (17%) and appliances (13%). Based on the significant difference between residential energy consumed from space heating and cooling and the other consumers, it is apparent that reducing space conditioning loads should be the target of energy efficiency measures.

The building envelope acts as a barrier between the indoor and outdoor conditions that suppress the energy transfer between the environments. The indoor space uses heating and cooling systems to offset the energy transfer through the enclosure to maintain comfortable interior air conditions. The space conditioning loads can be decreased by improving the building enclosure, such as the effective thermal resistance and airtightness. The effective thermal resistance in the envelope combines the thermal bridging caused by structural components and penetrations, such as windows and doors. By increasing the effective thermal resistance and air-tightness of the building envelope, the space conditioning loads will decrease, and the energy performance will improve. By increasing the amount of insulation, improving the air leakage, or replacing older windows in the building envelope, the largest usage of energy consumption in residential buildings

can be decreased. Therefore, improving the building envelopes of residential buildings could significantly impact the total energy consumption in Canada's building sector.

Additionally, Canada has committed to achieving net-zero emissions by 2050, which will have an impact on the design and construction of the residential building sector and the energy consumed by those buildings. In 2050, it is expected that about 70% of the occupied residential buildings are already built today. As such, Canada has aimed to make new to make new buildings more energy efficient, retrofit the existing residential buildings, including fuel switching if necessary, and to support these actions with new buildings codes that adopt a net-zero energy ready model building code by 2030 [5].

The current building stock data compiled by Statistics Canada [6] has separated residential dwellings into their decade of construction. According to the data acquired from the 2011 census, 72% of occupied residential buildings in Canada were built before 1990 and 38% were built before 1970. Similarly in Ontario, 72% of occupied residential buildings were built before 1990, while occupied dwellings built before 1970 accounted for 40%. When Canada aims to reach their net-zero emissions target, these buildings will be between 60 and 80 years old, and in need of significant repair.

Due to the distribution of occupied building vintages in Canada, a large majority of people live in buildings constructed at a time with different iterations of building codes and different construction requirements. An example is the revisions in building codes from 1960 to 2017. The National Building Code of Canada [7] in 1970 prescribed a minimum insulation level based on the number of total annual degree-days and the type of fuel supplied to space conditioning systems. The highest minimum level of insulation the code prescribed for above-grade walls in 1970 was RSI 1.76 m^2K/W (R10.0 $ft^2°F·h/(BTU)$. For comparison, the current Ontario Building Code

prescribes the above-grade wall to be at least RSI 3.87 m^2K/W (R22.0 $ft^{2\circ}F{\cdot}h/(BTU)$ [8] and quantifies the change in building enclosures over the past 50 years. Currently, the National Energy Code of Canada for Buildings (NECB) prescribes a maximum overall thermal transmittance of 0.290 $\frac{W}{m^2K}$ to 0.165 $\frac{W}{m^2K}$, which excludes doors and assemblies that transmit light [9]. Along with the changing of building codes and minimum insulation levels, there has also been an increase in more ambitious voluntary codes and standards focused on energy efficient housing.

Voluntary codes and performance standards for residential buildings have been increasing in number with a drive towards energy efficiency and Net-Zero homes. A common theme through the voluntary codes for building energy efficiency is to increase the thermal insulation level far above code-built homes, sometimes exceeding RSI 7.0 m^2K/W (R40 $ft^{2\circ}F{\cdot}h$ /(BTU). However, these standards would have a minimal impact if they were only implemented in new construction based on current housing forecasts. Based on forecasted housing stock presented in Figure 1-1, dwellings built pre-1970s will still account for roughly 35% of the occupied dwellings in 2030. The insulation in those homes, whether in the attic, below or above-grade walls, is possibly below the current building code and well below the voluntary codes if they have not been renovated recently. The disparity in space conditioning energy consumption between older buildings in Canada as of 2014 is illustrated in Figure 1-2. Residential dwellings constructed before 1960 accounted for 30% of the total space heating energy while dwellings built before 1984 accounted for 60% of the total space heating energy, which was a disproportionate compared to the percentage of units from those vintages. Therefore, renovating the building envelope of older dwellings should be a focal point for making significant progress in reducing the energy consumption of residential buildings in Canada.

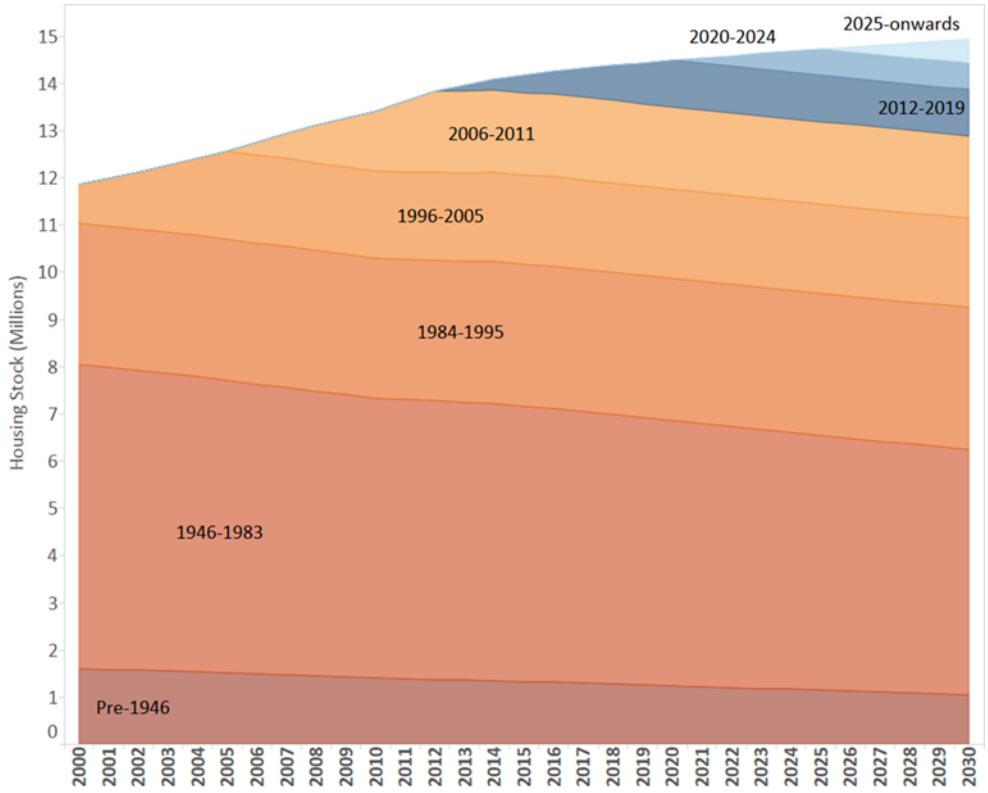

Figure 1-1: The number of homes by vintage, based on changes in the National Energy Code for Buildings [10]

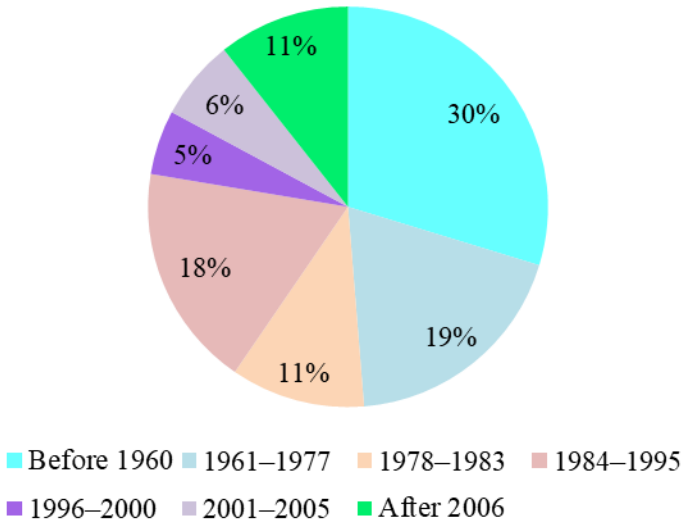

Figure 1-2: Heating energy consumed by residential buildings in Canada sorted by vintage [10, 11]

1.1 Building Envelopes

The building envelope encompasses all the components used to separate the interior and exterior environments. The envelope includes the roof, foundation, exterior walls, windows, and doors. The purpose of the envelope is to control rain, air, vapour, and heat transfer between the interior and exterior. The municipal, provincial, and national building codes dictate the components within the assembly; however, a simplified wall assembly consists of 3 main components: cladding, control layers and structural [12].

A basic wall concept, shown in Figure 1-3, uses those 3 components to create a comfortable and durable wall assembly. The structural component is the physical makeup of the building and the ability to withstand the loads. The control components include rain, air, vapour, and thermal control within the envelope. These control components are meant to keep the structure dry and long lasting. Examples of these components would be membranes, insulation and rainscreens. To best protect the structure, it is suggested that these components are placed on the exterior. This would minimize the effect of moisture, moist air, or extreme temperatures on the structure. The primary function of the cladding is to provide ultraviolet and rain control for the envelope, as well as aesthetics. This should also be applied to the exterior of the control layers to improve the lifespan of those materials. The basic principle is to keep the components protected from environmental conditions and last for their entire service life. This perfect wall concept can be applied to foundation, slab, and roof components as well. [12]

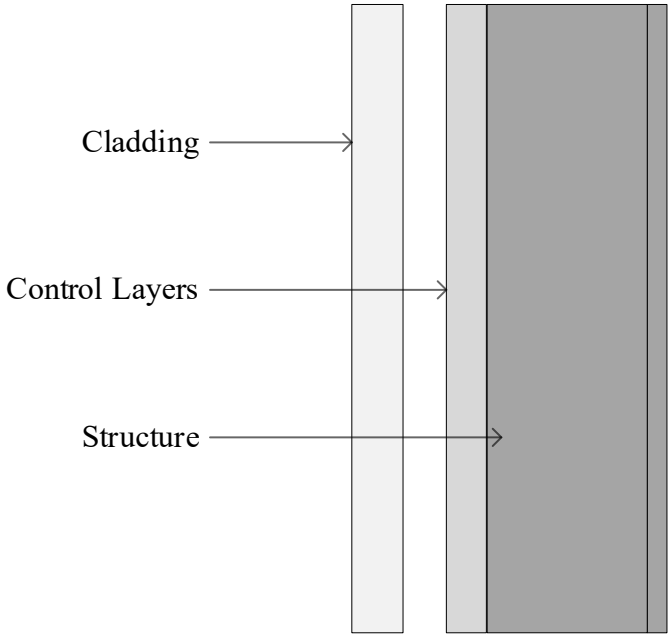

Figure 1-3 Concept of the perfect wall [12]

Thermal control in the envelope will have the greatest impact on energy consumption in residential buildings. The thermal control, or insulation, added to the envelope will directly reduce the amount of energy required to condition the interior space. However, the insulation levels of many existing dwellings do not meet the current or likely future (e.g., 2050) requirements from the national building energy codes. Air control layers can also improve the building energy efficiency as infiltration and exfiltration rates decrease. As such, retrofitting the building envelope with greater thermal and air control presents an opportunity to improve the energy efficiency, comfort, and maintain the indoor quality of the existing building if done properly.

In the building context, examples of retrofits would include adding mechanicals (e.g., air conditioning, central heating etc.), thermal storage, modifying the building envelope (e.g., insulation, new windows, doors), and adding renewables, such as photovoltaics to an already existing home. Motivation for the occupant or homeowner for retrofitting a building may come from a social, maintenance, environmental or energy efficiency perspective, among others. The

building retrofit may be undertaken to address a single component in the building, one or multiple systems of the building, or the deep retrofit where much of the building is changed. Specifically, retrofitting or improving the building envelope is an approach to reduce the overall energy consumption. After a building envelope retrofit, the total amount of energy will be reduced and the amount of energy required by renewable sources on- or off-site to reach NZEr will be reduced, offsetting the high level of consumption. By retrofitting the building envelope of older homes, which commonly have lower insulation levels and decreased air tightness, the capacity of mechanical systems and photovoltaics to match the energy consumed to energy produced is reduced. The building envelope retrofit directly impacts the other systems in the building, and the retrofit can be approached from either the interior or exterior.

At the interior of the sheathing, a retrofit or renovation would consist of adding or replacing the insulation between the structural members or adding insulation on the interior of the structural members. Meanwhile, retrofitting the exterior of the envelope could be performed by removing and replacing exterior materials up to the sheathing or by adding insulation directly on top of the cladding. For both types of retrofits, many considerations need to be made during the design: heat, air and moisture (HAM) transfer through the assembly, architectural considerations, including construction, installation, aesthetics, and total cost of the retrofit. These considerations should be weighted during the design process to determine the appropriate means of improving the envelope by retrofit.

It is important to note that for both the interior and exterior approaches, the building envelope thickness increases. The space inside or around the dwelling is an asset to the homeowner and retrofitting the envelope will encroach on those spaces. The value of livable floor area in a home is rising and could be upwards of $200 per square foot [13]. A similar issue could exist

around the exterior perimeter of the building as it approaches the minimum necessary setback from the property lines. A solution would be to address minimizing the increase of wall thickness and augmenting the RSI-value of the envelope.

Retrofitting the interior can provide many thermal benefits, however, concerns regarding the moisture control and installation make this approach less appealing. If the cavity between the structural members does not contain insulation or has low quality insulation, it represents an opportunity to improve the envelope by adding blown in or high performing batt insulation. Another option would be to remove the gypsum board and vapour barrier and install a double stud wall with 2x4 lumber with the cavities filled with insulation. While the effective thermal resistance of these envelopes would be improved, the moisture movement through the assembly would need to be carefully considered. The impact of improving the interior insulation would result in a lower surface temperature at the sheathing, which could lead to dew point temperature and condensation formation concerns. Additionally, this type of retrofit will be intrusive and disruptive to occupants and in the case of a double stud wall, would reduce the livable floor area within the dwelling. These issues could detract from the attractiveness of the retrofit application and cause occupants to opt for an exterior retrofit instead.

An exterior building envelope retrofit can provide similar thermal benefits as the interior retrofit as well as minimize the disruption to the interior space of the occupants during construction. Different exterior approaches exist that would provide a thermal performance comparable to or exceeding what an interior retrofit would provide. Additional layers of rigid foam board can be added to the exterior to obtain the necessary RSI value however, the building is limited by the minimum setbacks for the property. When retrofitting the exterior, the building envelope can be upgraded but the total thickness, property lines and moisture levels within the

assembly remain a concern as well as accounting for other envelope elements such as penetrations and connections to the roof or foundation.

1.1.1 Condensation Plane

A condensation plane is a point within the assembly where the temperature is cold enough to produce condensation for a given exterior and interior relative humidity. In walls with thermal insulation, the chance of condensation increases when the relative humidity of the ambient air approaches 80%. A condensation plane will exist in the assembly independent of climate, however, it can create a problem during the winter months in cold climate regions when the relative humidity level is higher at the inboard surfaces because the surface temperature is low. Assemblies situated in a cold climate during the winter months, the condensation plane moves further inboard to the assembly. By maintaining a higher level of insulation on the exterior as opposed to the interior, the sheathing temperature remains warmer during the winter and is less at risk of forming condensation at the surface.

Condensation formation can occur during the heating season from exfiltration or during the cooling season with infiltration. Condensation may occur due to insufficient insulation during the winter, a thermal bridge that causes a localized cold surface temperatures in the assembly, or air leakage through the assembly.

1.1.2 Air Leakage

Air moving from one boundary of the building envelope to the other is commonly referred to as air leakage. Air that is permitted to travel from the interior of the assembly is called exfiltration, while air travelling in the opposite direction is infiltration however, both can impact the durability of the building assembly. The air leakage characteristics of a building envelope are closely related to the air tightness of the building, measured in air changes per hour, where an

assembly that contains air leakage paths or a high-volume flow rate of air leakage would be reflected in the air tightness of the building. To follow the NECB, the air barrier system used in a building needs a normalized air leakage rate not greater than 1.25 $\frac{L}{sm^2}$ under a pressure differential of 75 Pa.

From a durability standpoint, air leakage can bring excess moisture into assembly in the form of (1) bulk moisture that can be trapped, or (2) water vapour, which can condense on a surface or increase the relative humidity. The direction of the air leakage is dependent on the pressure difference between the interior and exterior, which can be impacted by ventilation within the space and wind-driven pressures on the exterior of the building. Minimizing air leakage and leakage paths have been addressed in residential construction through the addition of weather resistance barriers and building wraps that improve the overall air tightness of the building. However, unintended cracks and leaks from either boundary can exist at the seams or joints in the building envelope.

1.1.3 Thermal Bridging

Thermal bridging is a localized area or plane in which the heat transfer is greater compared to the adjacent or surrounding area [14]. In a building envelope, thermal bridging exists as a heat flow pathway that has a high heat transfer rate that surrounds materials in the assembly. Thermal bridges in the building envelope can exist as higher thermal conductivity materials surrounding low conductivity materials, penetrations through the envelope, especially the thermal control layer, and discontinuities in the thermal control layer, such as gaps or intersections [15]. Some examples of thermal bridges in the building envelope include steel or wood-framed studs, fasteners or components used to clad the envelope, and mechanicals or electrical penetrations through the envelope such as plumbing and electrical conduits.

The thermal bridges not only affect the building efficiency but could also cause condensation issues within the assembly, if not designed properly. In cold climates, a significant thermal bridge in the enclosure will cause a localized cold temperature which could be below the interior dewpoint. If this is the case, it is possible that with sufficient humidity, the surface may experience condensation. A well designed enclosure and thermal control layer will consider thermal bridging and minimize its effects on the heat and moisture transport through the assembly.

1.2 Thin, High-Performance Envelope Solutions

In this research, a thin, high RSI-value envelope assembly will be defined as an above-grade wall assembly that has an effective thermal resistance of RSI 7.0 m^2K/W (R40 $h{\cdot}°F{\cdot}ft^2/BTU$) with a total thickness less than or equal to current building code minimums. A benefit of a thin high-performance assembly is that home energy efficiency can improve without sacrificing the valuable space inside or outside the building. These restrictions require high performing insulation for the building and as such, common building insulations alone may not be enough. The potential use of vacuum insulation panels (VIPs) has been investigated as a solution to the building insulation retrofit issue however, they also present further challenges to integration.

A VIP is a porous material enclosed in a metallic foil with an internal pressure maintained near 10 mbar, such that conduction and convection through the panel are effectively eliminated [16]. The VIP can provide a thermal resistance of RSI 7.0 (R40 $h{\cdot}°F{\cdot}ft^2/BTU$) for a 25.4 mm (1”) thickness [17], showing promise for meeting the thermal performance targets necessary for the building envelope. However, some challenges hinder the use of VIPs in building envelopes. First, the panels are very fragile, such that if the VIP’s foil enclosure is punctured or broken and the internal vacuum is lost, the thermal performance benefits above conventional insulation are nearly lost. The risk of a puncture during installation from a stray nail or mishandling should be

considered during design and construction. Secondly, the panels contain a significant change in RSI-value at the edges and do not act as continuous insulation when applied to the exterior of the envelope [18]. These issues need to be considered before the integration of VIPs into a building envelope. Despite their challenges, VIP has the lowest thermal conductivity compared to other available ultra-low thermal conductivity insulations [18].

A proposed solution for fragile insulation materials would be encasing them within existing insulation and creating a composite insulation system for the envelope that could be applied to the above-grade, below grade or in the roof systems. This composite system could be built on-site however, the preferred option would be to prefabricate the system off-site in a controlled setting. The off-site fabrication or prefabrication would allow for improved quality control. A panelized wall system utilizes off-site construction in a controlled environment. The prefabricated components are delivered to the construction site after quality assurance and control, then installed on the building with minimal time exposed to environmental conditions. The benefits of panelized construction compared to the traditional on-site construction commonly seen across Canada is the potential to reduce construction time, higher quality control and cost savings from labour and material waste.

VIPs could be integrated into a panelized insulation system to create a thin, high-performance insulation panel with high-quality control. By integrating the VIPs into a panelized approach, it would be possible to improve quality control, reduce the risk of pre-mature failure and build a low-conductivity wall assembly. The VIPs would be placed into an insulation panel and surrounded by a type of rigid foam insulation, as shown in Figure 1-4. Before completing the insulation panel with a backer material, it would be possible to perform quality control and assurance that each VIP has not failed during installation.

Figure 1-4: Example of unfinished composite insulation system with VIPs with extruded polystyrene (XPS)

The function of the panelized system could change based on the backer board material. The system could function purely as an insulation system if the panel is finished with an insulation backer material. However, the system can include a structural component by finishing the panel with an OSB or plywood backer material. These two distinctions will be separated into two different types of VIP panelized insulation systems: a composite insulation panel (CIP) and a structural insulation panel (SIP).

The two types of panelized wall systems are presented for evaluation. The panelized insulation and structural system were designed with Type 2 expanded polystyrene (EPS), VIP and OSB. The panel types were created with 1200 mm by 2400 mm (4’ by 8’) by 38 mm (1-1/2”) thick EPS sheet with 200 mm by 300 mm (8”x12”) voids for VIPs insulation. In this design, the blanks were prefabricated into the EPS sheet such that it could accommodate 24 VIPs, sized 200 mm by 300 mm (8”x12”), as shown in Figure 1-5. By using this size of VIPs and that patterned layout, the panelized modules could be applied to wood-framed walls that use 300 mm (12”) on-center spacing by installing the panel vertically or 400 mm (16”) on-centre spacing by installing the panel horizontally. This pattern would provide 100 mm (4”) fastening space for the panels to be clad onto the framing as well as lower the amount of potential thermal resistance loss if the VIP is punctured during the installation process.

Finally, the panelized insulation system is finished with a printed structural or insulated backer board, shown in Figure 1-6, to fully enclose the panel. The blue printed location identifies the VIP locations to the builder and limits the number of avoidable punctures in the VIP. With the design, it is expected that either panel could meet the demand for low profile, high-performance continuous insulation system, with an expected overall thermal resistance of R-4.2 m^2K/W (R-25 $h \cdot °F \cdot ft^2/BTU$), greater than 140 mm (5-1/2") of fibreglass insulation in a thinner profile.

The research program was built upon previous work by the author, in which the thermal performance of VIPs and VIPs encapsulated in rigid foam boards were evaluated using numerical and experimental methods. The research, performed between 2015 and 2017, investigated the thermal conductivity of VIPs, including the thermal bridging around the edges, as well as potential methods to minimize thermal bridging when installed in a building envelope. The research concluded that the VIP insulated wall systems had greater than an RSI 7.0 $\frac{m^2K}{W}$ thermal resistance but needed sufficient hygrothermal analysis before it could be used in Canadian building enclosures safely.

The research scope included the hygrothermal evaluation of a wood-framed wall assembly insulated with fibreglass batt insulation and the composite insulation panel (CIP) and the structural insulation panel (SIP). The evaluation was performed using 1D and 2D numerical modelling, and steady-state thermal resistance evaluation in a guarded hot box at Carleton University and in-situ field monitoring at CanmetENERGY-Ottawa. The opaque portion of the building envelope was evaluated, as such windows, doors or penetrations were outside the research scope. Additionally, the building properties outside of the opaque wall were assumed to comply with NECB and were not altered, unless specified, as they were outside the scope of the research scope.

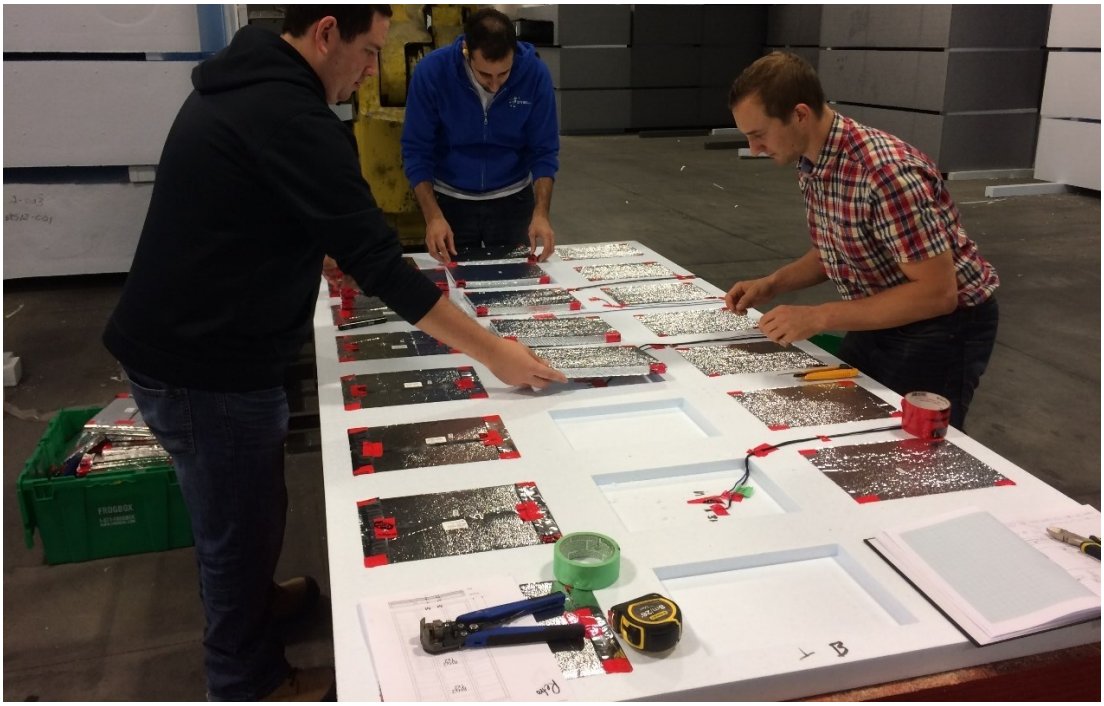

Figure 1-5: Visual of VIP pocket with EPS composite insulation panel

Figure 1-6: Finished CIP (left) and SIP (right) wall systems with printed markers on backer board

1.3 Research Questions

The research questions that will be answered through this work are listed below. The answers to these questions will highlight that creating thin, high performing building envelopes apply to Canada and can address the thermal and hygrothermal needs of the present and future.

1. How can thin, high-performance building envelopes be designed to achieve necessary thermal and hygrothermal criteria in Canada?
2. Can the thermal and moisture risks involved with installing vacuum insulation panels within building envelopes be mitigated to provide reliable performance?
3. Can the thin, high-performance building envelope applied to a newly constructed residential building be the solution for a building undergoing an envelope retrofit?
4. Is the thin, high-performance solution sufficiently robust to avoid the failure criteria when exposed to different environmental conditions and climates in Canada?
5. How does the hygrothermal performance of novel new or retrofit construction solutions perform compared to current building envelope retrofit practices?
6. How can a side-by-side comparison between potential building envelope retrofit designs be assessed with lab data as opposed to multiple years of measured data?

1.4 Research Contributions

From the studies presented in the thesis, the following were identified as contributions to research in building envelopes:

- Determine the thermal resistance of a high-performance building envelope panel with VIPs by using steady-state testing in a guarded hot-box and steady-state 1D and 2D simulations.
- Conduct experiments to measure the heat losses by thermal bridging, specifically on the edges of VIPs.

- Conduct and commission an 8’ by 8’ in-situ evaluation of a high-performance building envelope with VIPs to determine the moisture permeation and durability of the assembly.
- Produce an experimentally-validated model of the high-performance building envelopes with VIPs. Through simulation, determine the sensitivity of input parameters and initial conditions to the hygrothermal model to assess the best practices during construction.
- Produce a method to model exterior building envelope retrofit options applicable for Canadian housing. The modelling method will be a tool to inform and create guidelines on the risk of a building envelope retrofit for a given different climate, initial construction and envelope retrofit.

1.5 Thesis Outline

The remainder of the thesis is broken down as follows:

- Chapter 2 presents a detailed literature review related to the study, including previous laboratory, in-situ, and numerical studies about moisture control in building envelopes, building envelope retrofits and vacuum insulated building envelopes.
- Chapter 3 presents the experimental set-ups used in this work, including the equipment required for measuring the hygrothermal performance of two different thin, high-performance panelized solutions using vacuum insulation panels under steady-state and transient in-situ conditions.
- Chapter 4 presents the numerical modelling used to evaluate the two panelized insulation systems, including a description of the programs used for the study, an outline of best modelling practices, the assumptions used for modelling inputs (e.g., material properties, moisture sources, and boundary conditions etc.) and description of the parametric study of modelling inputs.

- Chapter 5 presents the measured results and calculated errors from the experimental steady-state and in-situ studies for two different panelized designs using vacuum insulation panels on wood-framed construction as well as an analysis of the results and their impact on Canadian construction.
- Chapter 6 presents the results from the numerical modelling of the above-grade wall assemblies for a variety of test cases including baseline hygrothermal performance for existing Canadian housing, the hygrothermal performance of a high-performance enclosure with vacuum insulation panels across Canada for new and retrofit construction cases and a comparison between numerical and measured in-situ data.
- Chapter 7 presents the conclusions of this work and a discussion on the future work that could build on this study.

Chapter 2: Literature Review

A literature review about the state-of-the-art building envelope construction and the effects of heat, air and moisture transport through the assembly was examined and is presented in the following section. This chapter presents different materials used in high-performance wall assemblies, the necessary moisture control layers and links to durability issues that may arise. These topics are supported by experimental data from in-situ field studies and computational modelling with 2D and 3D hygrothermal software. Finally, the gaps in the literature are identified at the end of the chapter.

2.1 Building Envelope Durability

Durability in the building envelope is defined as the ability to perform its functions to the required levels over a period in its service environment under the influence of its environment or self-ageing process [19]. This applied to the building envelope as a system and to the components and materials within the assembly individually. For residential building envelopes, the cladding and structural system sets are most commonly wood or lightweight steel frame structure with any of the cladding types listed in Table 2-1. This would apply to any type of construction (new or retrofit), with any set of cladding and structural systems and in-service conditions.

Exposure to environmental (or in-service) conditions can negatively impact the life span of building envelopes that are expected to exceed the duration of the building. The exterior surface of the assembly is exposed to thermal cycling, wind-driven rain, and direct and diffuse solar radiation, all of which will contribute to the durability of the assembly. At the interior boundary, the temperature and humidity are controlled however, there may be periods where the temperature or humidity may vary outside of typical conditions. In those situations, the interior surface may be exposed to low temperatures or high levels of humidity that can create hygrothermal issues within

the assembly. In addition to the boundary conditions imposed on the interior and exterior surfaces, there may be water intrusion into the assembly. The ability for the envelope to dry after wetting events, either by vapour diffusion, air leakage or bulk wetting, and its ability to maintain air conditions that do not promote decay within the assembly is an indicator of a resilience and durable envelope system. Evaluating the durability of an envelope system is essential in determining whether the enclosure will satisfy its entire service life.

The durability can be designed using experimental and numerical methods and is described by ISO 13823 – General principles on the design of structures for durability [20]. Within the standard, principles and procedures are recommended for the verification of the durability of structures based on the predicted environmental conditions that may cause degradation leading to failure. For a given building envelope design where the durability will be assessed, a set of environmental actions (e.g., climate loads, interior conditions, wall configuration, hygrothermal properties of components) that would cause degradation and failure of the designed operation to fully assess the design life. When the design life does not exceed the design service life, that is the period where the assembly or component is expected to perform without maintenance, repair or failure, then the wall assembly would be considered not durable [19, 21, 22, 23].

For the Canadian context in building envelopes, the Canadian Standards Association (CSA) S478-2019 Guidelines on Durability in Buildings [23] is referenced in the National Building Code of Canada [7] and is used to assist designers in creating durable buildings. The standard provides a range of expected service life of building components and assemblies; citing that costly and intrusive maintenance should only occur between every 50-99 years.

For exterior walls, the standard notes that the design service life would be expected to be equal to the building life (50-99) years and that above-grade exterior walls with insulation have

durability implications in the cladding and structure. The failure in the building envelope would be costly to repair and commonly reveals itself as moisture damage, condensation, uneven temperature distribution, poor indoor air quality or discoloration. Therefore, testing must be carried out beforehand to ensure that the envelope system is durable. This can be done through demonstrated effectiveness, modelling the service life and deterioration and a wide array of testing, including laboratory testing under controlled and simulated conditions, durability tests of assemblies and components, and finally, full-scale assemblies field testing to determine the transport mechanisms. The assembly and material testing are quintessential in evaluating the durability and the design service life of new envelope assemblies and materials, the definition of the failure needs to be explored.

Table 2-1: Environmental actions and effects that may lead to hygrothermal degradation for selected wall assemblies within National Building Code Part 9 housing [19]

Envelope Assembly Type			Degradation of Structure or connectors arising from		Degradation of cladding arising from	
Cladding Type	**Metal Connectors**	**Wall Structure**	**Environmental Actions**	**Action Effects**	**Environmental Actions**	**Action Effects**
Masonry Veneer	Ties, anchors, fasteners	Light-weight Wood-Frame	Fungal growth and fungal decay	Mould growth & wood decay	Freeze-thaw	Spalling, disintegration
Wood-Based	Fasteners	Light-weight Wood-Frame	Above & metal corrosion	Wood decay; fastener failure	Fungal growth and decay	Mould growth & wood rot
Cement-Based	Fasteners	Light-weight Wood-Frame	Above & metal corrosion	Wood decay; fastener failure	Freeze-thaw	Disintegration
Plastic	Fasteners	Light-weight Wood-Frame	Above & metal corrosion	Wood decay; fastener failure	Oxidation	Crazing, cracking
EIFS	Fasteners	Light-weight Wood-Frame	Above & metal corrosion	Wood decay; fastener failure	Oxidation	Crazing, cracking
MV, W, CB, P, M, EIFS	Fasteners	Light-weight steel frame	Above & metal corrosion	LGSS failure fastener failure	Above	Above

2.1.1 Moisture Control

Moisture is present in all climates and is a factor in deterioration processes with the envelopes, and therefore moisture control is necessary to ensure that no durability issues arise during the service life of the assembly [24]. Moisture control refers to the ability to protect or inhibit moisture from accumulating within the assembly [25]. The controls may be material or details added to the envelope (e.g., vapour retarder, weather-resistant barrier) or by control at the boundaries (e.g., humidity control, drainage planes) [26]. The moisture in the envelope is expected to be cyclic over time through convection, diffusion, capillary suction, and bulk wetting caused by the environmental effects. The building envelope durability is based on the ability of moisture to egress from the envelopes and avoid accumulation. High moisture conditions for prolonged periods will lead to decay and a shorter service life [19]. The objective of these following studies was to find the relationship between moisture and durability issues within building envelopes, techniques and designs effective for managing moisture in cold climates, and steps for addressing moisture-related concerns in building envelopes.

The United State Environmental Protection Agency (EPA) [27] developed Moisture Control Guidance for Building Design, Construction and Maintenance which outlines best practices for avoiding moisture-related issues regarding building envelopes, occupant comfort and space conditioning. It specifies that moisture control is important to protect occupant health and the building from mechanical, physical, or chemical damage [27]. It adds that moisture control does not require everything to be dry but needs to have the ability to dry out. Excess moisture can cause bacterial growth or chemical reactions within the HVAC systems may be transmitted to the occupant by the lack of fresh ventilation. Finally, the building materials that are exposed to these conditions for prolonged periods may cause swelling, rot, deterioration, freeze-thaw damage, or

reduction in insulation values. It clearly outlines that moisture within the building can lead to long-term issues that impact many different disciplines of the building.

Moisture control strategies can be summarized into 3 groups [25]:

1. Control moisture entry
2. Control of moisture accumulation
3. Removal of moisture

The control strategies can be used together for the best possible control. When the strategies are used in combination, it offers the most resiliency against any given moisture-related conditions. For example, control of moisture entering the wall may not be the best control if the moisture already exists within the assembly from construction. A balanced moisture control strategy for moisture entry, accumulation, and removal is important for building envelopes and ensuring durability and long service lives [25]. It is practically impossible to remove all moisture driving forces and moisture sources for the wall assembly so passive mitigations strategies such as dying need to be available to the wall assembly [28].

Moisture can be introduced to the envelope through multiple mechanisms, also known as wetting. The biggest concern is bulk wetting or liquid capillary suction by rainwater entry or leaks. Other forms of wetting include air transport (also referred to as air leakage) and vapour diffusion, however, these are generally on a much smaller scale. The source of the wetting can occur from either the exterior or interior environments and an effective moisture control strategy should account for both sources and will be based on both climates [25, 29].

Exterior climates in North America can be separated into 5 hygrothermal regions. In a severe-cold and cold climate, which covers most of Canada, the envelope will need to be protected from wetting by the interior and exterior while maintaining the ability to dry towards the exteriors.

Air and vapour barriers are installed towards the warm interior surfaces to limit wetting by moist air and vapour diffusion [25]. Additionally, using mechanical ventilation to keep moisture levels in the interior space helps to avoid wetting and moisture accumulation. The use of vapour permeable barriers on the exterior allows excess moisture in the building envelope to dry and leave the assembly without accumulating. Materials such as exterior sheathing, building papers and drainage planes are permeable and promote drying to the exterior [25]. It is best to ensure that if moisture does enter, it will still be able to escape over time, which makes selecting the right interior barrier for a given wall assembly especially important.

Table 2-2: Hygrothermal regions in North America [25]

Region	Description
Severe-Cold	A region with approximately 8,000 heating degree days or greater
Cold	A region with between 4,500 and 8,000 heating degree days
Mixed-Humid	A region that receives more than 500 mm (20”) of annual precipitation, greater than 4,500 heating degree days, and monthly average outdoor temperature below 7°C (45°F) during the winter months
Hot-Humid	A region that receives more than 500 mm (20”) of annual precipitation, and monthly average outdoor temperature above 7°C (45°F) throughout the year
Hot-Dry	A region that receives less than 500 mm (20”) of annual precipitation, and monthly average outdoor temperature above 7°C (45°F) throughout the year.
Mixed-Dry	A region that receives less than 500 mm (20”) of annual precipitation, has ~4,500 heating degree days or less, and a monthly average outdoor temperature below 7°C (45°F) during the winter months

Interior vapour barriers are meant to slow or eliminate the migration of moisture in the envelope and are separated into classes based on the rate at which they slow the permeation of moisture [26]. Vapour barriers are effectively used to prevent wetting of the building enclosure; however, they also prevent moisture from escaping the assembly, essentially lowering the drying potential. These barriers are grouped based on their permeability in perms and into classes (Class I, Class II and Class III). The recommended use of vapour barriers is to not install more barriers when a more permeable solution would suffice [26].

Another type of barrier used in building enclosures is smart barriers, which are a moisture adaptive air barrier system. The smart membranes have a moisture dependent vapour permeability, such that the vapour permeance of the film changes to the surrounding conditions. For example, the during the summer, the membrane allows for inward drying of the construction, and during the winter the membrane the membrane has a higher permeance to prevent condensation. In a wood-framed wall assembly in Canada, this smart barrier would be best applied as the interior vapour control since it promotes inward drying during the summer and does not allow wetting by vapour diffusion from the interior during the winter. While long-term durability benefits exist, it has not become a current best practice in Canada and was not evaluated in this research program.

2.1.2 Failure Criteria

The durability and design service life of an envelope assembly and materials are dependent on the environment and in-service conditions that are expected. Moisture in the building envelope was found as the primary means of durability failure in the previous section. Therefore, the envelope needs to maintain a balance of moisture wetting and drying to avoid moisture accumulation in the assembly. Mould growth is an indicator of elevated moisture levels at the material surface, and while it does not cause degradation of the building materials, is the main

indicator of hygrothermal performance. During modelling and experimental evaluations, a standard was published by the American Society of Heating, Refrigeration, Air Conditioning and Ventilation (ASHRAE) titled ASHRAE 160 [30] has outlined several parameters that are indicative of the durability. Recently, ASHRAE has adapted their failure criteria for moisture control in building assemblies from moisture content percentage in organic materials to the mould growth index at the surface of materials. ASHRAE has set the following as conditions required to minimize problems associated with mould growth on the surface, and apply to every layer within the building envelope except for the exterior surface:

- Mould growth index less than 3.0
- 30-day running average surface relative humidity is less than 80% when the 30-day running average surface temperature is between 5°C and 40°C,
- 7-day running average surface relative humidity is less than 98% when the 7-day running average surface temperature is between 5°C and 40°C, and
- 24-hour running average surface relative humidity is less than 100% when the 24-hour running average surface temperature is between 5°C and 40°C.

The standard suggests that some materials may be more resistant to mould growth for longer periods if the surface has been chemically treated or the material is more naturally resistant. However, criteria outlined in the standard are commonplace in evaluating the durability of building envelopes.

An empirical relationship of the potential for mould growth on a surface based on the surface temperature, surface relative humidity and time has been developed and validated by Hukka and Viitanen [31]. The mould index, M, is a mathematical representation based on regression analysis of the effects from surface temperature and relative humidity through a series

of laboratory studies. Hukka and Viitanen observed that mould growth was favourable within a temperature range of 0°C and 50°C however, the relative humidity necessary to facilitate mould growth varies through the temperature range [32]. The critical relative humidity, RH_{crit}, for mould growth for the temperature range, observed during their experimental investigation, is:

$$RH_{\text{crit}} = \begin{cases} -0.00267T^3 + 0.160T^2 - 3.13T + 100.0, & \text{when } T \leq 20°C \\ RH_{\text{min}} \text{ when } T > 20°C \end{cases} \quad \text{2-1}$$

For wood and wood-based materials, RH_{min} is 80% relative humidity and will vary for other materials due to their difference in resistance to mould growth. The values were determined through experimental studies by holding materials at a constant relative humidity for a predetermined time and evaluating the effects of micro- and macroscopic mould growth on the materials. Their experimental findings and related visual observations of the surface from the research lead to the conclusion that mould growth would start with these relationships, but new relationships should be developed to describe mould growth after it has begun.

Mould Index is used to describe the level of organic activity that could be present at the surface [31]. The index is measured on a scale of 0 to 6 and each integer of the mould index represents a level of fungi growth on the surface, where 0 would be no growth initiated up to 6 where heavy and tight fungal growth has occurred on the entire surface. A full description of mould growth rates and the relationship to the index is provided in Table 2-3.

Table 2-3: Description of mould growth rate for a given mould index [33]

Index	Description of Growth Rate
0	No Growth
1	Small amounts of mould on the surface (microscopic), initial stages of growth
2	Several local mould growth colonies on the surface (microscopic)
3	Visual findings of mould on the surface, <10% coverage or <%50 coverage of mould (microscopic)
4	Visual findings of mould on surface, 10%-50% coverage or >%50 coverage of mould (microscopic)
5	Plenty of growth on the surface, >50% visual coverage
6	Heavy and tight growth, coverage around 100%

A mathematical model was developed required context and led to a discretization of visual inspections related to the parameter. From their experience, they concluded that the maximum mould index value that could occur on the surface assumed a parabolic form as a function of the relative humidity at the surface and the critical relative humidity at a given temperature, shown in the form of Equation 2-2 [31].

$$M_{\max} = 1 + 7\left(\frac{RH_{\text{crit}} - RH}{RH_{\text{crit}} - 100}\right) - 2\left(\frac{RH_{\text{crit}} - RH}{RH_{\text{crit}} - 100}\right)^2 \qquad 2\text{-}2$$

During the laboratory testing of different building materials at 97% relative humidity and 22°C, different rates of fungal growth, or increasing mould index, were observed. This led to the development of four material sensitivity classes: Very sensitive, sensitive, medium resistant and resistant. These materials were classified based on the length of time it took to reach an elevated mould index. For instance, at 97% RH and 22°C, very sensitive materials will take under 7 weeks for the mould index to exceed 5, while a resistance material under the same conditions will reach a mould index of about 1 after 120 weeks. The mathematical relationship was extended to a function of time, as well as surface quality, wood species, current air conditions at the surface and

two sensitivity class factors, shown in Equation 2-3. The factor k_1 represents the mould growth intensity and k_2 represents the moderation of growth as the mould index begins to approach its peak value, both are a function of material sensitivity class, and the values can be found in Table 2-4. Also, W is the timber species (0 for pine, 1 for spruce), SQ is the surface quality (0 for sawn surface and non-wood materials, 1 for kiln-dried quality).

$$\frac{dM}{dt} = \frac{1}{7\exp(-0.68lnT - 13.9lnRH + 0.14W - 0.33SQ + 66.02)} k_1 k_2 \qquad 2\text{-}3$$

Table 2-4: Coefficients for sensitivity classes of materials

Sensitivity Class	$\boldsymbol{k_1}$		$\boldsymbol{k_2(M_{max})}$			$\boldsymbol{RH_{min}}$
	$M < 1$	$M > 1$	A	B	C	%
Very Sensitive	1	2	1	7	2	80
Sensitive	0.578	0.386	0.3	6	1	80
Medium Resistant	0.072	0.097	0	5	1.5	85
Resistant	0.033	0.014	0	3	1	85

The mould index has been adopted as the failure criteria by ASHRAE and can be applied to any of the surfaces [30]. The mould index summarizes the mould growth potential with a single number for a given set of surface air conditions which makes helps to compare different building assemblies. These conditions may be generated from controlled or in-situ monitoring, or through hygrothermal modelling.

While the ASHRAE 160 criterion has been criticized for being too conservative and predicting failure within assemblies when post-mortem analysis showed no deterioration [34], it remains the moisture control standard of choice for building enclosure designers.

2.2 High-Performance Envelopes

The building envelope creates a boundary between the interior conditioned space and the exterior environment. The boundary's primary function is to manage the heat, air, and moisture transport between the two sets of environmental (indoor and outdoor) conditions. This led to the development of high-performance envelopes designated by high R-values and a high level of air tightness. The HAM transport through these assemblies and the progress made towards the impact on high-performing assemblies.

High-performance envelopes are not limited to limiting the heat flow through the building components (e.g., walls, roof, windows, and foundation). They are also airtight, have minimal thermal bridging, limit the heat flows, ensure human comfort, and provide moisture control that leads to long service lives [35, 36]. A universal definition does not exist, as climates are diverse and provide different loads however, it is accepted that the level of thermal control provided in a high-performance enclosure exceeds what is locally mandated. For this research project, an enclosure thermal resistance of R-7.0 m^2K/W (R-40 $ft^2°F·h/BTU$) with moisture control and airtightness will be considered a high-performance envelope, as the research is focused on building envelopes in cold climates.

The International Energy Agency (IEA), founded in 1974, has created research programs, referred to as Annexes, about energy consumption for buildings and communities (EBC), with a specific theme about the heat and mass transport in building envelopes. The IEA has developed programs that study the effects of HAM transport, building details, long-term performance and retrofitting applications since the theme's inception. For this research program, the following Annexes were reviewed in detail:

1. Annex 24: Heat, Air and Moisture Transport – Completed 1995 [37]

2. Annex 32: Integral Building Envelope Performance Assessment – Completed 1999 [38]
3. Annex 39: High-performance Thermal Insulation Systems (HiPTI) – Completed 2005 [39]
4. Annex 41: Whole Building Heat, Air and Moisture Response (MOIST-ENG) – Completed 2007 [40]
5. Annex 65: Long Term Performance of Super-Insulating Materials in Building Components and Systems – Ongoing 2018 (initial end date). [41]

These Annexes reviewed the fundamentals of HAM transfer through building envelopes and began investigating the design of high-performance building insulation and envelopes. IEA has supported other studies on the effects of building envelopes on thermal comfort (Annex 69), roof and fenestration systems (Annex 12, 14 and 19) and the retrofitting of buildings with a historic designation (Annex 76). These Annexes were outside the scope of this research proposal.

Annex 24 studied the physics of HAM-transfer specific to well-insulated building envelopes and the relationships between thermal performance and durability of the wall system. The studies covered a range of computer modelling, studying the environmental conditions, material property testing of building materials and experimental verification of HAM response within envelopes. Each contingent utilized its HAM transfer software and highlighted a set of environmental effects that impact the HAM performance of the assembly; (1) initial construction moisture, (2) solar gain, (3) wind-driven rain, (4) air leakage, (5) exfiltration, and (6) capillary suction. They found that the most important parameters for hygrothermal performance of a well-insulated building were exfiltration, initial moisture, latent heat, and wind-driven rain, in that order of importance. Additionally, they noted that while full- and simplified models can provide a qualitative assessment of the hygrothermal performance, the simplified models are restricted capability as a design tool due to their inability to determine whether the assembly is acceptable.

The project was studied across multiple countries and with different interior and exterior conditions, therefore Annex 24 elaborated on two concepts to compare the various climates and results: Indoor Climate Classes (ICC) and Moisture Durability Reference Year (MDRY). The ICC is used to define the indoor climate based on the maximum allowable internal vapour pressure before condensation will occur for benchmark or code-built assemblies. This is meant to represent a worst-case scenario for buildings in different climates. Likewise, the MDRY is a composite year with the most severe moisture load in 10 years. The MDRY uses monthly averages of air temperature, relative humidity, vapour pressure and the monthly total solar gain on a horizontal surface to assess the building envelope. An issue with this weather file is that it neglects the effects of wind-driven rain, which was deemed important through their earlier modelling, however, that can be assessed by using different reference weather files currently available (e.g., ASHRAE Weather Reference Year (WRY), Typical Mean Years (TMY), etc.). The ability to compare different climates and interior conditions is essential to assessing the robustness and durability of a building envelope.

EBC-Annex 24 completed their project with experimental analyses of in-situ testing and were able to conclude about the durability risk and certain building details after assessing various building envelope components of the roofs and walls. They were able to comment that while vapour retarders may be necessary for certain ICC, construction moisture and air-tightness are the most important parameters that can limit the durability of the assembly.

EBC-Annex 32 was interested in research and developing two areas: assessment methodologies and evaluation methodologies with design tools. The objective of assessment methodologies was to create a systematic approach based on a set of performance criteria, that included the envelope, climate, building and internal systems, to best optimize the construction of

the building envelope from an energy perspective. The systematic approach used heat and mass transport, acoustics, light, fire, service life, costs, and sustainability of the building envelope. Each of the performance criteria was graded on a scale of 1 to 5 to compare the designs of new construction and retrofitting buildings. But it acknowledged that costs, thermal insulation, and sustainability are easy to include in the optimization, while the remaining parameters are related to general regulations. The Annex concluded by stating that their methodology can create an efficient construction process and better use of resources when designing building envelopes.

Following Annex 24 and 32, the IEA started EBC-Annex 39 to develop high-performance insulations that can be implemented into building envelopes. The main objectives outlined in the Annex were the basic material development, application development, and demonstration of the new thermal insulation. There was a heavy focus during their studies on vacuum insulation panels (VIPs) as a method to accomplish highly insulated building envelopes, however, the limited data on the material and in-use performance was the motivator for the research program. During the material testing stage, the effective thermal resistance and thermal bridging for varying cores, foils and sizes of panels were evaluated. Also, the service life assessment of the panels was made during laboratory testing, while they were exposed to high temperature and humidity to assess their impact on the internal gas pressure and internal moisture content. The increase in internal gas pressure and moisture content are compared to the change in the VIP conductivity. After the material testing, there were many VIPs installed in new and existing buildings in Germany and Switzerland. This allowed them to make judgements about the installation practices and monitor the performance in-situ for increased data about the service life. Additionally, the Annex concluded that the life cycle energy assessment is dominated by the high energy consumption of production.

In their future outlooks, VIP cost, confidence in the technology and quality assurance as barriers before VIPs can be implemented into the market.

Finally, EBC-Annex 41aimed to combine the previous research and investigate the HAM transfer within the whole building. The project objectives included basic research, development of hygrothermal models, as well as field and material testing of envelope parts. The Annex focused on creating a set of hygrothermal simulation and verification exercises to evaluate the building envelope. The six common exercises involved varying the indoor boundary conditions for the moisture sources, isothermal and non-isothermal at the room level, verification with inter-model comparison, adding real-world infiltration flows and finally, experimental work to validate the models. The Annex was able to validate several existing and new whole-building HAM software tools and was able to generate sets of data that could be used to validate future upgrades to the software with indoor climate data collection.

The IEA-Annex EBC research programs targeted building envelopes during the past 25 years, with focus on HAM transfer with building envelopes and whole buildings, and later research on low thermal conductivity materials and their usage in high-performance building envelopes. The research work and evaluation exercise or methodologies are commonly used in the following research project found throughout the literature review.

2.3 Moisture Control and Durability Assessment

Durability and moisture control within buildings is a necessary component in building envelope design. For new and retrofit construction, the surrounding environment, control layers and exterior cladding all have a significant impact on the performance over the service life. As a result, all the conditions that may impact the building envelope and the HAM transfer should be studied and evaluated before being implemented into practice. The following section includes a

survey of experimental and numerical simulation studies used to evaluate building envelope designs for cold and mixed climates across North America and Europe.

The ASHRAE Standard 160 [30] has become the reference document for moisture control and design, along with the assessment. However, there are different methods that other researchers have applied the evaluation criteria. Lacasse and Morelli [42] estimated the long-term durability of wood-frame structures using by applying a limit-states design approach to the performance of the assembly. They did a numerical evaluation of a wood-frame stucco clad wall assembly in different climates in Canada. The OSB sheathing was the focus of the evaluation since damage and/or mould formation would lead to an underperforming design. They separated the OSB into 4 main regions of focus: (1) OSB Sliver, (2) Back of OSB, (3) Whole OSB and (4) OSB-Fiber interface. The OSB "sliver" was a 1 mm slice of the exterior face of the OSB in contact with the membrane. The Back OSB was the 10 mm inboard of the OSB Sliver. The whole OSB was the whole 11 mm thickness of the OSB. OSB-Fiber interface was focused on the interior surface of the OSB.

The authors stated that the National Research Council Institute for Research in Construction (NRC-IRC) currently assesses the hygrothermal performance of wall assemblies by comparing the RHT-Index and Mould Index to a wall assembly with known or accepted performance observed through in-service performance in the field. They note that subjecting the wall assemblies to climate loads for a specified period may have merit for evaluating hygrothermal performance, but that it has not been fully explored.

2.3.1 Moisture Response of Wall Assemblies

Hall et al. [43] performed lab studies that compared the effects of moisture on organic materials in envelopes (e.g., gypsum, OSB and dimensional lumber). Their objective was to assess

the moisture levels with the level's thresholds associated with performance issues. Their study included laboratory material testing, hygrothermal modelling and field testing to fully verify their results. Their experimental testing involved measuring the moisture of wood- and gypsum-based materials that were held at 75% RH and 21°C (70°F) until the material reaches equilibrium. Hygrothermal modelling was a performance to determine the influence of varying moisture levels in the field studies and to approximate the periods of elevated relative humidity. Their 4 case studies were 3 buildings in New Jersey and 1 building in Central Texas. The researchers took handheld moisture readings of the existing buildings for multiple years, aligned with the hygrothermal simulations. While the handheld results showed elevated moisture levels exceeding the failure criteria threshold, destructive testing at the end of the study showed that no visual moisture-related damage or biological growth was noticed. The study does not define whether they were simply taking a macroscopic look at the assembly, since microscopic coverage of mould growth may exist.

Smegal and Straube [44] investigated the performance of 17 different wall assemblies in the Pacific Northwest climate, specifically Portland, Oregon. They modelled the hygrothermal performance of wall assemblies that included variations in the vapour control layers, framing, exterior or interior insulation, and structural members. They had additional criteria to assess the overall performance based on the (1) thermal control between RSI2.5-RSI7.2 (R14-R41), (2) Durability, (3) Constructability, (4) Cost, and (5) Material Use. The thermal control of the wall assemblies was evaluated using THERM by modelling the wall assemblies in plain view and using an effective conductivity for the measured assembly in elevation view. This captures the effects of the thermal bridges in the assembly. They used constant film coefficients at the interior and exterior

boundary conditions (8.3 W/m^{2}K and 34.0 W/m^{2}K, respectively) and framing factors (amount of lumber in the assembly of 23% for 400 mm (16") O.C walls and 19% for 600 mm (24") O.C walls.

They assessed the long-term durability of the wall assemblies by modelling the assemblies in Wärme Und Feuchte Instationär (WUFI) Pro for the indicated region. The durability criteria grouped rain control, drying of water leakage events, condensation, built-in moisture, and susceptibility of different building materials to moisture-related issues. They set the interior relative humidity for these simulations to a sinusoidal condition varying from a minimum of 40% in the winter to a maximum of 60% in the summer based on the correlation to occupancy behaviour and ventilation strategies. They used the condensation potential based on air leakage from the interior and the moisture content of the sheathing to assess the durability of 17 different wall assemblies.

They concluded that the exterior insulation is effective at limiting the condensation potential during the winter, even if air tightness details are compromised. Excluding cost and material use from their evaluation, the results clearly show from a thermal control, durability, and constructability standpoint that assemblies with advanced framing with exterior insulation were the best to use in that region and would likely translate to colder climates. The thermal control and durability are similarly related to the project goals of this project, since the evaluation practice will be similar, and provides a comparison for the high-performance wall assembly studies for this project.

The previous study by Smegal and Straube is supported by the report prepared by Lepage, Schumacher and Lukachko [45]. They modelled the moisture response 9 highly insulated walls built using advanced wood-framing or concrete masonry units with WUFI Pro 5.1. They noticed that many factors impacted the moisture-related risks in high R-value walls, including but not

limited to climate, insulation type, location, and cladding type which are known parameters. However, there have been new, high-performing insulation materials, changing indoor environment conditions and expectations, and new performance standards that have been introduced. They were interested in the role of insulation levels, air leakage, and vapour diffusion on moisture-related issues for different indoor and outdoor climates. They evaluated 9 different wall assemblies and defined High R-value walls as effective R-values of at least double the code required thermal resistance.

Following their hygrothermal evaluations of the wall assemblies and varied hygrothermal parameters, they came to the following conclusions:

1. The location of the insulation (exterior versus interior) is as important as the amount, as exterior insulation provides more moisture resilience since cavity insulation hinders drying and increases the condensation potential (lower sheathing temperature).
2. Exterior insulated walls are less affected by air leakage, especially if the interior relative humidity is maintained to an adequate level for the climate.
3. The main barriers to High R-value assemblies using typical insulation materials are the initial capital investment.

Additionally, they noted that more approaches to High R-value walls, including super insulation materials, include studying small- and full-scale assembly mock-ups to empirically verify the models.

In Sweden, Abdul Hamid and Wallentén [46] studied the performance of interior insulated masonry buildings by in-situ measurements and numerical simulations using WUFI Pro. The main objective was to measure and evaluate the moisture-related risks for two case study buildings in

Sweden (Lund and Örebro) with interior or exterior insulation which can be used to validate a realistic use case model. They validated the model by comparing the temperature and relative humidity from the numerical and experimental methods and found that the only diverging results were related to the accuracy of the solar data available. Otherwise, they conclude that current simulation practices are enough when hygrothermal inputs are varied for different in-use applications.

The performance of similar assemblies for new constructions in different climates has also been studied by Trainor, Straube and Smegal [47, 29, 35], for which they came to the same conclusions about High R-value building envelopes and the associated moisture concerns. They evaluated timber and masonry walls with a varying set of external conditions, insulation levels, and moisture control layers or strategies to minimize long-term moisture-related degradation.

2.3.2 Highly Insulated Enclosures

Building a highly insulated enclosure can improve the energy consumption and greenhouse gas emissions of an occupied building. However, there are existing research questions about the hygrothermal transfers within the wall assembly for that type of construction. The heat transfer through the enclosure is reduced, but in some cases so is the air and vapour movement in the enclosure. Researchers have used experimental and numerical methods to measure and approximate the risk of various types of wall assemblies in Canada.

The National Research Council (NRC) Institute for Research in Construction (IRC) evaluated the hygrothermal response by field testing highly insulated wood-frame wall assemblies at the NRC Field Exposure of Walls Facility (FEWF) and numerical simulation using the hygIRC model. The researchers at NRC, in collaboration with clients, Canadian Mortgage and Housing

Corporation (CMHC), and Natural Resources Canada (NRCan) analyzed the hygrothermal response of six different wall assemblies through field exposure and modelling.

The 6 wall assemblies were varied by their outboard exterior insulation, inboard insulation, and wood framing [48]. The constant between all the wood-frame wall assemblies was a 12 mm interior gypsum board painted with a 6 mm polyethylene vapour and air barrier and an 11 mm oriented strand board sheathing panel. The rest of the wood-frame wall assembly details are described in Table 2-5. The proposed wall assemblies were finished with a sheathing membrane, 19 mm strapping and air space with vinyl siding. Finally, a 3 mm x 368 mm deficiency was included in the air barriers to promote measured exfiltration through the wall assemblies.

The FEWF facility in Ottawa, CA could accommodate three 1219 mm by 1029 mm (4’ by 6’) wood-frame wall assemblies at a time, so the project involved monitoring walls W1, W2, and W3 in Year 1, and changed the samples to W4, W5, W6 in Year 2. The wall assemblies were instrumented with thermocouples, relative humidity, and heat flux (HF) plates to measure the hygrothermal response to the boundary conditions.

The boundary conditions of the field study were separated into 4 Phases to test the durability of the enclosure. The relative humidity varied between 35% and 50% RH at 21°C and had a period where the interior deficiency was open or closed; the exterior deficiency was always open. The walls were exposed to the environmental elements in Ottawa, CA. Their main deficiency period occurred during 3 weeks in May for all the wall assemblies as the expected worst case.

The authors found that there was a low risk of condensation and moisture-related decay in their study and verified this observation by calculating a low mould index for the monitored period. They determined that a low surface temperature of the OSB sheathing panel meant there was a low

risk to mould and fungal growth, as well as the ability of moisture to dissipate from within the wall assembly.

Table 2-5: NRC Wall Assemblies from the Highly Insulated Wood-Frame Walls project [48]

Wall Assembly	Wood Framing	Inboard Insulation	Outboard Insulation	Nominal R-value $\frac{m^2K}{W}\left(\frac{ft^2\cdot°F}{BTU}\right)$
REF	38 mm x 140 mm (2x6-nominal)	140 mm glass fibre	None	(R19)
W1	38 mm x 140 mm (2x6-nominal)	140 mm glass fibre	25 mm EPS	(R27)
W2	38 mm x 140 mm (2x6-nominal)	140 mm glass fibre	51 mm XPS	(R35)
W3	38 mm x 140 mm (2x6-nominal)	140 mm glass fibre	76 mm Mineral Fibre Insulation	(R35)
W4	38 mm x 140 mm (2x6-nominal)	51 mm XPS + 140 mm glass fibre	None	(R35)
W5	38 x 230 mm (2x10-nominal)	61 mm SPF +168 mm glass fibre insulation	None	(R45)
W6	38 mm x 280 (2x12-nominal)	280 mm cellulose fibre insulation	None	(R40)

For the numerical simulations, hygIRC was used to perform 2D hygrothermal simulations of the wood-frame wall assemblies [49, 50]. A numerical simulation was performed for each of the proposed wood-frame wall assemblies for a 1 year simulation period. The numerical study also varied the location and air leakage rates in addition to the wall construction. The average and maximum mould index at the regions of interest (top plate, bottom plate, interface of the sheathing

and insulation) were calculated and used to compare the relative performance to the code-built reference wall.

The results using the hygIRC model showed that the walls with outboard exterior insulation had a lower mould index compared to the code-compliant wood-frame wall [49, 50]. It also showed that the location had a large impact on the calculated mould index and that St. John's (NL) had the greatest overall average mould index in comparison to the other cities evaluated.

This research led to the development of 3 more wood-frame wall assemblies between RSI 5.1 (R29) and RSI 7.6 (R43) [51]. A total of 9 wood-frame wall assemblies were simulated using HOT2000 model to determine whether the wall assemblies would meet the 2030 net-zero energy target for new and retrofitted existing wood-frame construction. Based on their simplified calculations of energy consumption compared to energy generation in low-rise residential construction, it was confirmed that above-grade wall assemblies with thermal insulation values between R35 and R50 would be capable of achieving a net-zero energy status for certain locations in Canada [52]. While the results were promising, the authors noted that the assessment was higher level and that the quality of workmanship of high-quality materials, specifically the continuity of air and vapour barriers was important to ensure there is no premature failure of the building materials.

Building panels used thermal and air control, as well as structural loads, have been explored by in simulation and field measurements. A multi-functional wood composite panel (MFP) using laminated OSB skins with two types of insulation cores (wood-fibre and XPS) was evaluated using hygrothermal models in different climatic regions in Canada [53, 54] using WUFI Pro and field measurements. They found that the measured and simulated results were within 5%, and they did not observe a significant performance difference between the two panel types. The results are

consistent with previous results in Japan with plywood-faced with low-density wood-fibre insulation [55].

2.3.3 Enclosures with Low Conductivity Materials

There have been multiple studies investigating the use of low-conductivity materials as interior and exterior insulation in residential buildings. The materials used were varying sizes and thicknesses of VIPs and aerogel blankets applied inboard and outboard of the sheathing. A common issue noted in the studies was the poor economic feasibility of using low-conductivity or super insulation materials (SIMs) as building insulation when typical payback periods using energy savings and material costs are considered.

The Canadian Construction Materials Centre (CCMC) and NRC developed a technical guide outlining test protocols and criteria for assessing the compliance of VIPS with the NBC in 2018 [56]. The technical guide was used to evaluate the components of VIPs as well as the properties of a finished VIP, shown in Table 2-6 and Table 2-7. The technical guide provides a list of material properties to be measured or defined. From a hygrothermal performance standpoint, the thermal resistance at (a) beginning, (b) failure, and (c) changing over varied cycles of temperature and relative humidity for the finished panel are important and are frequent questions when designing VIPs into the building enclosure. Since VIPs have different core materials, foil barriers, and sealing details, these values, in addition to the others listed, will vary from manufacturer to manufacturer and VIP to VIP. The technical guide is useful in being able to compare different VIPs and making an informed decision during the design stage.

Table 2-6: Properties of VIP components

Component	Property
Barrier	Tensile strength
Barrier with Seam	Tensile Strength
Core	Density Thermal Conductivity Moisture sorption at 22°C and varying RH%

Table 2-7: Properties of a finished VIP

VIP Thickness	Property
	Dimensional tolerances Flatness Squareness
Maximum thickness produced	Compressive strength
All thicknesses	Flexural strength
25 mm thick specimen and all other thicknesses	Initial thermal resistance Thermal resistance at failure Change in thermal resistance following exposure to specific constant RH and T Change in thermal resistance following exposure to cycles of temperature and RH
n/a	Estimated long-term thermal resistance at 15 years

The authors also looked at the performance of two different VIP walls: a spandrel panel in a curtain wall and a non-load-bearing steel stud wall. They found the VIP provided greater thermal resistance than traditional materials, even if punctured. VIPs complied with the NBC under the described conditions. Future investigations will look at improving the service life assessment and enhancing the service life to 25 years. They noted the need for extra planning during construction and design since the VIPs cannot be cut on-site as another barrier that needs to be eliminated.

VIPs were identified as an insulation technology to build high-performance enclosures. The insulation has been used to build thick wall assemblies over R-10.4 m^2K/W [57, 58] with in-situ and numerical validation. However, they can also be applied to the envelope to create thin, high-performance assemblies as the exterior insulation on their own [59, 17], as interior insulation [60] or as a part of a composite panel [61, 62, 63, 64, 65, 66]. The conclusions from the projects

found that VIPs were effective at providing thermal control for high-performance enclosures and have anecdotally noted the best building practices include off- and on-site quality control.

Thermal bridging at the seams and edges of VIPs has been identified as a concern for the insulation material [67]. The thermal bridging along the highly conductive barrier may significantly reduce the thermal effectiveness of the VIP that should be considered during the design stage. Numerical and experimental studies have been undertaken to reduce the thermal bridging by using larger panels, filling gaps at edges with airflow resistance material and overlapping VIPs with multiple layers of insulation [68, 69, 70, 71]. The studies found that the mechanisms were effective at limiting the thermal bridging effects from VIPs.

The long-term thermal performance of VIPs was identified as a limitation for integration into the building envelopes. The aging of VIPs is governed by (1) the gas and vapour transmission properties of the barrier material, (2) thermal sensitivity of the core material to pressure increases, (3) integrity of the seams and (4) effectiveness of the desiccant. The thermal resistance for VIPs will decrease from air- and moisture entry into the panel and cause an increase in heat transfer by convection (air pressure) and conductivity (moisture content of core material) within the panel [67, 16, 72, 73]. From experimental and numerical studies on the subject, it was found that for VIPs in cold climates it would require at least 20 years to double in thermal conductivity with proper moisture control [74, 75, 76, 77, 73]. The service life of the panels is dependent on the surrounding conditions, moisture control and the composition of the VIP barrier and core material. However, more information is needed on this topic to have a firm conclusion in practice. A useful contribution to the science would be the evaluation of VIPs after in-situ use and evaluating their current thermal conductivity. The measured data, in addition to the in-use conditions, would increase the confidence in VIP service life.

Durability characterization and in-service conditions on VIPs in a highly insulated wood-framed enclosure for a tiny home was performed between 2018 and 2021 [78]. The tiny house was insulated with VIPs on the exterior of the building and spray foam insulation in the cavities to create an insulated and air-tight enclosure. The building envelope data was monitored with simulated interior moisture loads for occupancy. The study found that VIPs performed 28-40% greater than a wall without VIPs and were built to 50% of the thickness for a traditional high performance envelope, contributing to significant space savings in the tiny home. Based on the measured data, the VIPs were not exposed to harsh hygrothermal conditions and could achieve a service life greater than 40 years.

VIPs have also been analyzed in moderate climates as well. The energy modelling of new builds and retrofits with VIPs in middle latitude locations, such as Italy, analyzes the energy savings. It was found that when compared to a traditional wall, buildings in middle latitudes could experience an energy saving of 40% during the winter, 9% during the summer, and approximately 22% in total annual energy demand. Other design factors such as building orientation and window-to-wall ratio influenced the energy demand more than the exterior wall composition and would be better for high-efficiency homes in cold climates.

When evaluating wall assemblies with VIPs, overestimating the total thermal resistance is possible if the thermal bridges along the VIP perimeter is not considered. Moore investigated the impact of using different standard calculation methods and numerical simulation techniques, including the parallel path and isothermal planes methods, and used a guarded hot-box to validate the results [79]. He concluded that the thermal resistance of steel stud wall with VIPs may be overestimated by 38% if the joints and edges are unaccounted for in 2D simulations. He found that the 3D simulations were generally more accurate than 2D simulations, however, 2D simulations

using VIP effective thermal conductivity derived from the surrounding thermal bridges and center of panel thermal conductivity were equally as accurate.

Aerogels are another innovative material that provides a low-thermal conductivity super insulation material for buildings. Incorporating the material into the building envelope has several challenges, including production energy demand, production cost, moisture sensitivity, flammability, and thermal stability [80]. The hygrothermal performance of aerogel blankets used within traditional masonry walls in a cold, humid climate, like Ottawa, CA has been evaluated [81]. A numerical study was performed using WUFI Pro and the results were validated with measured in-situ data. Furthermore, a numerical study was performed to compare different wall configurations using the same aerogel blanket and varying hygrothermal parameters such as wind-driven rain exposure, wall orientation, initial construction conditions, and indoor and outdoor climates. Their results were like the previous studies that interior insulated, and un-insulated assemblies carry additional moisture-related risks based on the data analysis and comparison to ASHRAE 160, mould growth models, condensation potential, and drying rates.

2.3.4 Hygrothermal Parametric Study

A report prepared by the Institute of Research Construction (IRC) from the National Research Council (NRC) in Ottawa, CA reported on the hygrothermal response of exterior wall systems when parameters such as climate, moisture control, cladding types, and materials are changed [82]. The report focuses on stucco, exterior insulated fenestration systems (EIFS), masonry and vinyl-cladding wood-framed buildings in North America. They studied the predicted hygrothermal response using the hygIRC model under a specified wetting condition. The research team used laboratory testing on reference walls to evaluate the amount of rainwater penetration past the water control layer and into the stud cavity for a 50 mm penetration or defect in the

sheathing membrane. They developed a relationship for the moisture source, Q, in litre per hour based on the rainwater on the surface, R_{w}, and a water entry function based on the pressure difference across the wall, P_{w}. The water entry function was specific to a reference wall for a 50 mm gap in caulking around a penetration and would be specific to the type of defect and wall assembly. The moisture source took the following form:

$$Q = R_{\mathrm{w}} \cdot f(P_{\mathrm{w}}) \qquad 2\text{-}4$$

Another output from this report was the concept and calculation of the Moisture Index (MI). The index was used to qualitatively compare different climatic conditions, such as a hot-dry climate to a cold-dry or cold-wet climate. The index is a function of two terms: the Wetting Index (WI) and the Drying Index (DI). WI in this study was based on the annual rainfall, while the DI was based on the potential for evaporation. The MI was found using the following expression:

$$MI = \sqrt{WI_{\mathrm{normalized}}^2 + (1 - DI_{\mathrm{normalized}})^2} \qquad 2\text{-}5$$

The research team calculated a MI between 0 and 1.4 for 383 North American locations and produced five climate zones based on moisture load severity, shown in Figure 2-1.

Table 2-8: Moisture Index calculated using weather records for Canadian locations [82]

Location	MI	Location	MI
Vancouver, BC	1.09	Ottawa, ON	0.93
Victoria, BC	1.00	Toronto, ON	0.92
Fredericton, NB	0.99	Edmonton, AB	0.89
Iqaluit, NU	0.97	Winnipeg, MB	0.86
Montreal, QC	0.94	Calgary, AB	0.81
Windsor, ON	0.94		

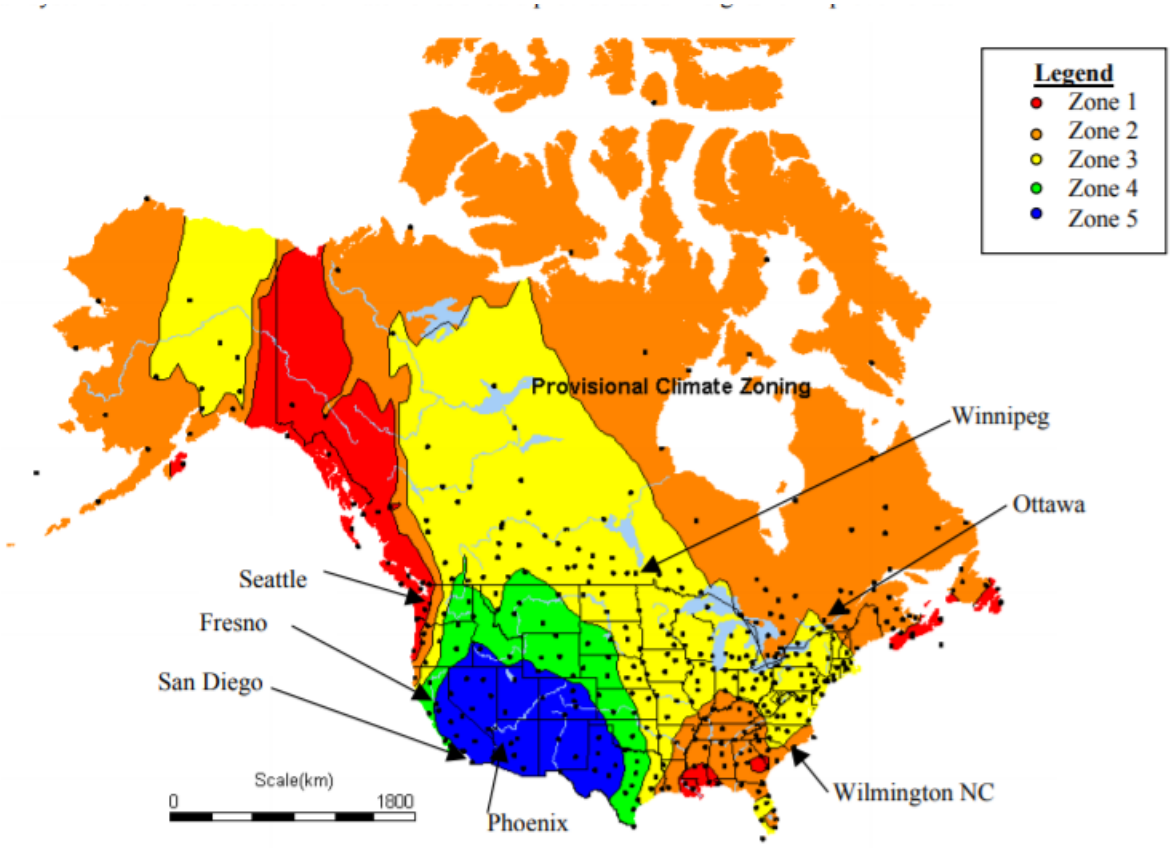

Figure 2-1: Climate zones based on moisture severity according to [82]

They used a relative humidity and temperature (RHT) index to compare the changes in hygrothermal response. The RHT index used the 10-day average temperature and relative humidity at the sensitive layers of the assembly, where RH_c, T_c are the critical relative humidity and temperature for the project. The index is calculated for each timestep of the simulation, and a higher RHT-index value indicated that there was an increased severity of hygrothermal response and damage.

$$RHT\ (x) = \sum (RH - RH_c)(T - T_c) \qquad 2\text{-}6$$

The critical values can be set by the user however, the authors noted that the nominal conditions for the initiation of damage would begin at 95% and 5°C, while initiation of mould growth would conservatively begin at 80% and 5°C.

In summary, the researchers concluded that the RHT(95) response was sensitive to the flow rate of water entry in the stud cavity and the severity of the climate, and that evaporative drying through multiple layers can be very slow. From their observations, they concluded that it was more important to limit the moisture penetration, as it has greater potential to lead to failure. Additionally, the RHT index for colder climates tended to be lower in the analyzed wall assemblies because the sheathing temperature would dip below 5°C; outside of the critical temperature for the RHT index. Finally, they note that it is important to understand the design climate for the enclosure and use the Four Ds strategy: Deflect, Drain, Dry, and use Durable materials. However, their results did not specifically address the effect of the input simulation parameters that were selected.

A study has been completed on the sensitivity of input parameters to the wall and material scale. The material properties in hygrothermal modelling [83, 84, 85] and found that the modelling was most sensitive to thermal conductivity, specific heat, water storage capacity and water vapour permeability. At the building level, sensitivity studies have been performed to investigate the effect of moisture properties on the energy consumption of the buildings [86] by computing the variance of the output and input interaction effects on the output. The importance of moisture effects impacts the building envelope durability as well as the energy performance. However, for building envelope modelling for durability, there are significantly more parameters than the material properties, nor were these analyses performed using WUFI.

A parametric assessment for the hygrothermal performance of a brick wall was evaluated using a small sample of numerical inputs [87]. The brick material properties, indoor and outdoor climate, wall thickness, and interior insulation were varied in the numerical simulation with experimental validation. Unfortunately, the results from both studies did not converge and added that the cost of evaluating specific material properties of specific materials may not be worthwhile.

2.4 Building Envelope Retrofit Studies

Many of the studies and results previously presented were directly related to new construction and instrumenting existing buildings to validate numerical simulations. However, as was presented in the introduction, the existing dwellings in the residential sector, that will require refurbishment or be rebuilt, represent a larger portion of the energy savings potential compared to new constructions. Retrofitting the building envelope can offer a significant improvement on the overall energy consumption of a home and would reduce the necessity of high capacity mechanicals in a potentially leaky, old home. Like the experimental and numerical studies presented in the previous section, these retrofit projects predominantly featured insulation systems using conventional construction materials, however, some advanced techniques and low conductivity materials are also presented.

2.4.1 Building Envelope Retrofits with Conventional Insulation

Kolaitis et al. [88] compared internal and external retrofitted insulation systems with numerical simulations. They compared the use of interior and exterior insulation in retrofits for a mid-level, multistory building, which is representative of the Greek building stock. The thermal (TRYNSYS) and hygric (1D thermal with dew point method) parameters were evaluated and compared to different constructions. Their analysis showed that a building retrofitted with internal insulation was outperformed on an energy basis by a building retrofitted with exterior insulation

by about 8%, while also lowering the condensation potential on an annual basis. However, they added that the cost of adding interior insulation was 34.23 €/m^2 compared to 80.00 €/m^2 for exterior insulation, which significantly increases the payback period. The study was based in a warmer climate, therefore, the envelope retrofit, and associated payback period would be shorter in a cold climate, like those in Canada, without comparing the cost required to purchase the energy.

A study by Stovall et al. [89] also found, by retrofitting wall assemblies and evaluating the thermal performance under steady-state conditions in a guarded hot-box that the exterior insulation provides better energy savings. They studied 5 different retrofit practices for different wall assemblies with insulated cavities and showed that the exterior retrofit consistently performed better.

Aregi and Little [90] performed an experimental and simulation-based study of a retrofitted envelope in Ireland. The mainstream retrofit case included adding low-cost insulation to the interior of the assembly with vapour-closed foil facing and plasterboard finish. Their proposed retrofit assembly was adding more insulation to the interior wall without any vapour control layers or membranes. Transient numerical simulations using a hygrothermal modelling program named WUFI 2D. They found that preserving drying capacity is more important than preventing vapour ingress from the room and the addition of impervious layers may result in moisture accumulation. They also compared the mainstream retrofit to their proposed retrofit solution as well as the current condition and original condition of the building for their analysis.

Ueno [91] performed an analysis on 3 case studies where a wood-frame building was retrofitted with exterior insulation. This retrofit substantially increased the R-value of existing walls and can be detailed to substantially improve overall building airtightness. The addition of 4 in. of polyisocyanurate foam is a nominal change from roughly RSI 2.3 to RSI 6.9 (R-13 to R-39);

factor of 3 increase) with roughly 2/3 of the thermal resistance outboard of the condensing surface (interior face of the existing sheathing boards) after the retrofit. The case study included three homes from different vintages: a 1915 single family home, a 1930 duplex, and an 1850 single family home. Ueno performed hygrothermal studies of all the buildings, which included a sensitivity study for water intrusion at different layers of the retrofitted envelope. They observed that the vapour permeance of the exterior insulation had a significant effect on the drying potential of the retrofitted assemblies, such that XPS tended to accumulate moisture over time. From this study, EPS would be better than XPS for retrofitting due to its open-cell formation and its increased vapour permeance.

Retrofit projects involving prefabricated components have been investigated using OSB skins and EPS insulation for low-rise residential in Ottawa, CA [92, 93]. The Prefabricated Exterior Energy Retrofit (PEER) program from NRCan used prefabricated exterior wall panels to overclad the exterior of the buildings [94]. The project aims to develop, test and validated a prefabricated building envelope system for retrofitting Canadian homes from the exterior. The pilot project showed that a prefabricated exterior envelope retrofit is possible and includes numerical modelling, analysis of thermal bridging components and in-situ monitoring of the hygrothermal data [95]. The project showed that a high-performance enclosure is possible using conventional materials.

An energy efficient retrofit was performed on a 1950s multi-dwelling house in Sweden that included a building envelope retrofit [96, 97]. The building was retrofitted with an exterior insulation and finishing system (EIFS) composed of mineral wool and a thick layer of mineral scratch rendering. The coupled in-situ measurements and hygrothermal simulations showed that

the existing moisture in the assembly was able to dry quickly and provide sufficient moisture control post-retrofit for the climate.

Exterior retrofits for arctic climates have been explored to reduce building energy loads. A test wood-framed building with a cavity filled with insulation with a polyethylene vapour retarder had the exterior retrofitted with EPS or spray-applied polyurethane foam insulation [98]. The test unit varied the percentage of interior insulation compared to the total around the building between 32-100% to understand the impact of insulation ratio on condensation and drying rates. The building showed potential for mould growth and rot as an inadequate ability to prevent moisture accumulation during the winter and a limited ability to release moisture in the summer relative to their control wall assembly [98].

2.4.2 Envelope Retrofits with Low-Conductivity Materials

Further to conventional insulation, the prospect of adding low conductivity or super insulation materials into building envelope retrofits has been studied. In Sweden, Johansson et al. [99] added VIPs to a historical brick building to slow the rate of building degradation. They instrumented the existing building with temperature, relative humidity and moisture content sensors in the brick, mortar and VIPs and built a climatic chamber around the instrumented area to maintain constant interior conditions. Hygrothermal simulations were performed using one- and two-dimensional modelling in software and showed that over time the wall could be damaged from freeze thaw cycles based on the moisture accumulation.

Further to this study, the moisture content and relative humidity of the wood framing were measured for the pilot project. It was found that for a wood-framed building with brick veneer with an interior retrofit, the wood moisture content did not differ between conventional insulation and

VIPs. However, in the VIP retrofit, the surface temperature of the wood was found to be colder and therefore had higher relative humidity at the surface. Additionally, it was noted that the drying potential was lower when VIPs were used [99].

In Canada's Yukon, VIPs were added to a commercial building to monitor the VIP performance and degradation as an exterior building insulation retrofit in extremely cold temperatures [17, 100, 101, 102]. The 560 mm x 460 mm x 12 mm VIPs were sandwiched between two 25 mm layers of extruded polystyrene (XPS) as exterior insulation over the top of a masonry block wall in 2011 by researchers and technologists from NRC, Yukon Housing Corporation and Yukon College. Their goal was to increase the effective thermal resistance above 8.8 m^2K/W, aligned with the expectation for a net-zero ready building.

They have published works from the initial design stages, the on-site construction, and the hygrothermal monitoring since 2011. The researchers installed thermistors at the material interfaces and monitored the thermal performance of the VIPs by the percentage of delta temperature. They also used thermal imaging to support their claims that the VIPs were not damaged during installation. After 5 and 8 years of monitoring, the researchers concluded that VIPs were maintaining their thermal performance based on the in-situ measured data. Overall, less than 0.9% change in thermal resistance year over year was observed. They are intending to continue collecting data for the foreseeable future to continue monitoring the degradation under in-service conditions. The authors also noted that they expect costs of VIPs to drop over time to make the product more viable as the financial cases for vacuum insulation for buildings are challenging.

Interior retrofits for high-performance buildings typically involved a significant amount of interior floor space, For the financial case of VIP insulated retrofits to balance, the interior floor

area savings need to be included when adding interior wall insulation is the only viable avenue. This may be the case in heritage buildings, buildings where access to the exterior for retrofit is limited or not feasible. A thermo-economic study showed that VIPs may be more economically sustainable compared to conventional insulation materials when the space savings and ability for increased rental income are factored into the discounted payback period of the retrofit when rental value is high [103]. Other factors such as climate zone, insulation thickness and heating system efficiency influence the final economic result as well, while VIP ageing effects did not.

In exterior or interior retrofits with VIPs, the thermal bridges along the VIP edges could introduce significant changes in building efficiency [104]. Modelling a building energy consumption in EnergyPlus, the change in energy between a wall accounting for the VIP thermal bridging and ignoring it varied between 3-10%. While limitations of the study included Thermal bridging in high-performance enclosures can create heat flow paths that short-circuit the low-conductivity insulation.

2.5 Knowledge Gaps

The summary of major studies performed with project objectives ranging from high-performance materials and enclosures showed many variables will affect the thermal and hygrothermal evaluations.

- New and retrofitted constructions can be through evaluated using similar hygrothermal modelling practices however, their initial parameters must be varied, such as initial conditions for initial construction moisture or initial degradation;
- The durability of these assemblies is impacted by many variables from the environment, all of which contribute to the durability and the long-term performance;

- The sensitivity of the variables is dependent on the wall assembly components, such as the vapour and thermal control layers, and they should all be considered to accurately determine the durability of the envelope;
- In-depth hygrothermal or retrofit studies using low conductivity materials were extremely limited, and act as another barrier before the materials can be seriously considered as a replacement;
- The thermal and hygrothermal benefits need to not only surpass the economic aspects, but also the ease of constructability required for a construction site.

It becomes clear from the number of studies that support the conclusion that retrofitting the exterior provides better HAM performance than the interior retrofit. The main barriers to exterior envelope retrofits are the initial capital investment and significant disruption to the occupants caused by lengthy demolition and construction. The air tightness and effective thermal resistance of the building will be increased, however, adding 150 mm (6”) of insulation to the exterior may not be feasible due to space limitations.

Chapter 3: Experimental Approach

An experimental approach was taken to answer the research questions and address the knowledge gaps found in the literature utilized two different test facilities and procedures. The high-performance composite insulation panel (CIP) and structural insulation panel (SIP) assemblies were evaluated in a guarded hot-box at Carleton University to measure thermal performance under steady-state conditions, and at the CanmetENERGY Building Envelope Test Hut (CE-BETH) to measure the hygrothermal performance under in-situ conditions. During steady-state testing, the effective R-value of the baseline and high-performance assemblies were measured. The wall assembly underwent quality assurance after installation and testing by use of infrared thermal imaging. The durability of the baseline and high-performance wall assemblies was assessed after 4-year in-situ monitoring at CE-BETH. The experimental methods used during both studies are described in the following section, including a description of the test facilities, instrumentation, experimental error, sample preparation, and monitoring plans.

3.1 Guarded Hot-box Steady-State Testing

A guarded hot-box located at Carleton University was used to study the base and high-performance wall assemblies under steady-state operation. These tests were performed from August 2016 to June 2018. A schematic of the guarded hot-box utilized is shown in Figure 3-1. The guarded hot-box consists of a three-chamber test apparatus capable of maintaining steady-state conditions to accurately monitor and measure the heat flow through a wall sample placed between the chambers in the surround panel.

The guarded hot-box is used to measure the thermal resistance of a wall assembly sample by controlling the temperature difference across a wall sample and indirectly measuring the heat flow from the metering chamber to the guard chamber [58, 69, 62].

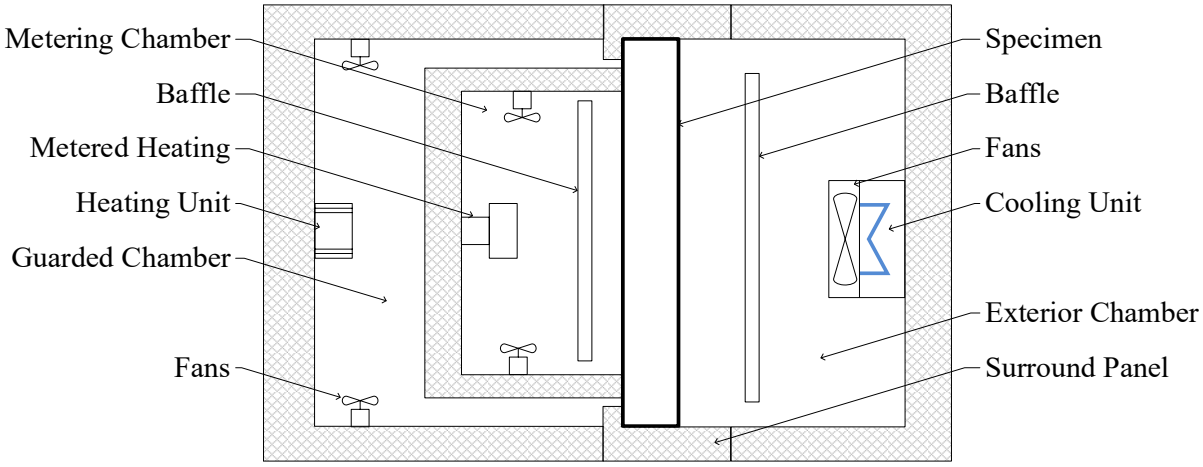

Figure 3-1: Guarded hot-box schematic with labels

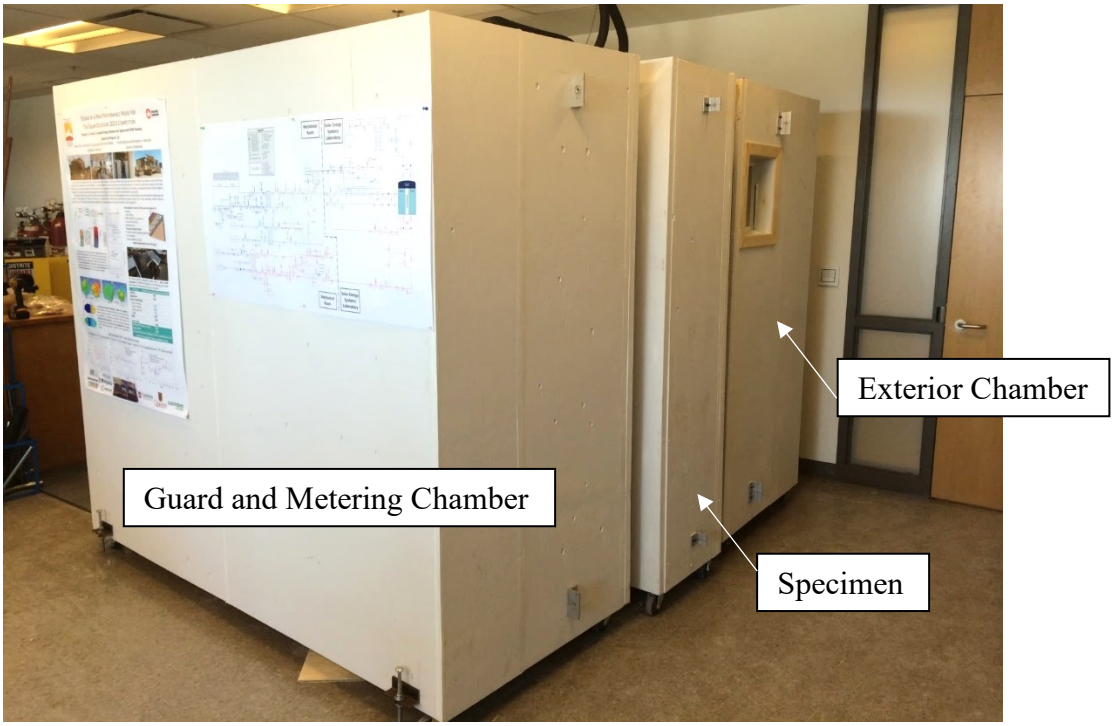

Figure 3-2: Guarded hot-box pictured at Carleton University

The three chambers are (1) the exterior chamber, (2) the metering chamber, and (3) the guarded chamber. The exterior chamber is used to simulate outdoor temperature conditions through a fan and chiller system that is directly tied to the laboratory and building infrastructure. The exterior chamber is operated at temperatures between -30°C to 10°C, depending on the

climatic conditions required by the test procedure. The guarded and metering chambers are used to simulate interior conditions. The chambers are operated at the same temperature set-points to effectively create one-dimensional heat flow from the metering chamber to the climate change through the wall sample. This is an important characteristic since the metering chamber contains most instrumentation used to evaluate the wall assembly thermal performance.

The wall assembly sample is installed in the surround panel and then placed between the exterior and the guarded chambers. The chambers and panels are pressed together using clamps to create an airtight seal with the aid of compressible gaskets adhered to the contact surfaces. The airtight seal and gaskets limit a source of error from the experiment and therefore very important in maintaining a one-dimensional heat flow between metering and the exterior chamber.

After the guarded hot-box chambers were pressed together with the sample in the center, the apparatus was turned on and chambers started to reach their temperature setpoints.

3.1.1 Instrumentation and Monitoring

The guard hot-box was outfitted with a National Instruments (NI) CompactDAQ data acquisition system and a Delta control system to accommodate the thermocouples, heat flux plates, thermistors, relative humidity, and power monitoring. The data acquisition system is connected to a local desktop with the LabVIEW user interface. The NI system is used to manage the 128 analog inputs and 4 pulse counter inputs that are logged and saved to a comma-separated variable (.CSV) file for analysis. The guarded hot-box instrument specifications are included in Table 3-1.

Table 3-1: Instrumentation included in the guarded hot-box.

Instrument	Manufacturer	Product	Unit	Error	Quantity
Thermocouple	Omega	Type-T	°C	±0.46	80
Heat Flux Plate	Huskeflux		W/m^2	± 5%	9
Power Monitoring	WattNode Pulse Transducer		Wh	+0.375 Wh	1
Relative Humidity	Vaisala		%	0%-90%, ±3% 90%-100%, ±5%	3
Thermistor		10 kΩ	°C	±1°C	8

Instruments were placed in all 3 chambers to measure air and surface conditions. There are a total of 23 thermocouples, 3 heat flux plates, 1 relative humidity sensor, 1 pressure transducer, and 1 power monitoring system installed in the metering chamber. A thermocouple was placed on each surface inside the metering box and was used to calculate the heat flow between the guard and metering chamber. There were 6 thermocouples were placed in a grid in the air curtain between the baffle and the specimen. There were 12 thermocouples and 3 heat flux plates in the metering chamber with slack and adhered to the interior surface of the specimen in a 4 x 3 grid, following ASTM C-1363 [105], or where the measured heat flow was desired (e.g., thermal bridges, the center of VIP, etc.). The relative humidity and pressure transducers were stationary near the center of the metering chamber. The power monitoring system was connected to the electrical resistance heaters inside the metering chamber and used to measure the energy input to the metering chamber.

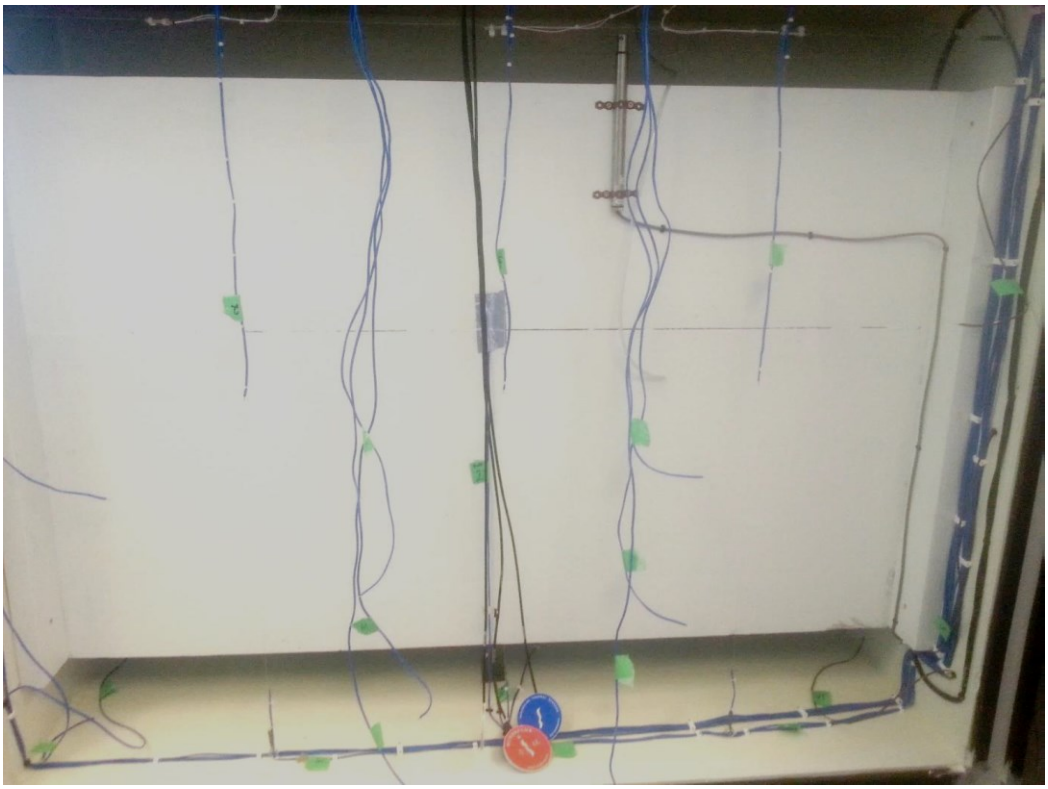

Figure 3-3: Picture of the metering chamber with instrumentation disconnected from the sample

The guard chamber surrounding the metering chamber only contained thermocouples. Five thermocouples were placed on the exterior surface of the metering chamber, to calculate the heat flow through the walls. An additional 8 thermocouples were used to measure the specimen surface temperature and were distributed evenly along the perimeter. A matching set of 8 thermocouples was added to the exterior chamber. The instrumentation in the guard chamber was used to ensure that there was limited heat flow between the metering and guard chambers and provide a buffer between the metering chamber and the environment.

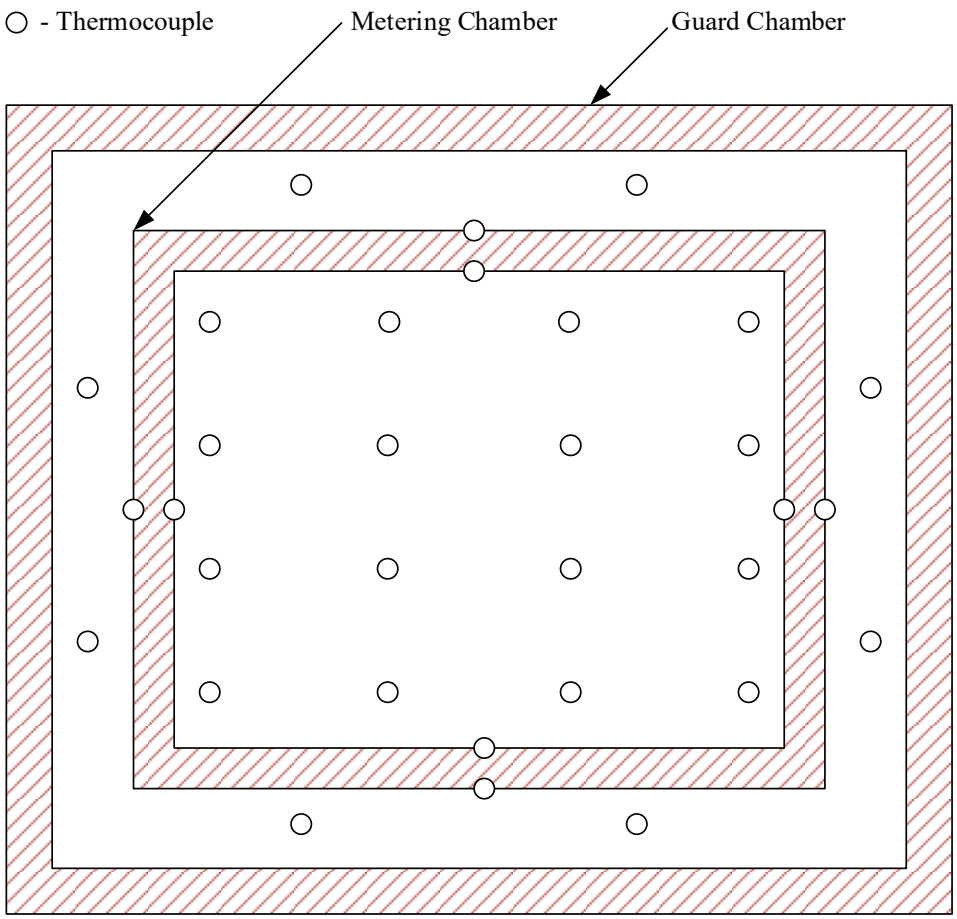

Figure 3-4: Matching thermocouples on both sides of the specimen and metering box during steady-state testing

The exterior chamber was outfitted with 23 thermocouples, 3 heat flux plates, and a relative humidity sensor permanently installed, as well as 50 pairs of quick connect junctions for additional thermocouples, heat flux sensors, or other voltage-based instruments that were required. The instrumentation was arranged similarly to the metering chamber and guarded chamber. There were 12 thermocouples were placed on the specimen surface in a 4 x 3 grid, as well as 8 thermocouples on the surface placed evenly around the perimeter. The heat flux plates were placed on the specimen surface with tape and conductive paste to ensure good contact with the surface. The quick-connect junctions, depicted in Figure 3-5, were used to connect thermocouple and heat flux plates that were embedded within the wall assembly. Those sensors were used to measure the

temperature profile of wall assembly, temperature gradients along an insulation plane, and the heat flux at thermal bridges. The leads of the embedded sensors were terminated with an Omega miniature thermocouple connector or screw terminal block and were wired back to the data acquisition system through the enclosure.

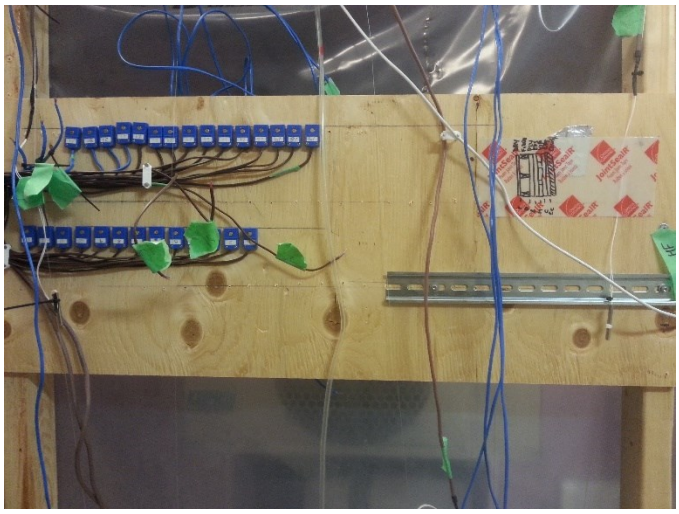

Figure 3-5: Exterior chamber quick connect junctions

The instrumentation was used to measure the effective thermal resistance of the panelized insulation systems and the thermal bridging at the edges of the VIPs when the guarded hot-box was operating under steady-state conditions.

3.1.2 Thermal Resistance and Thermal Conductivity

The instrumentation and monitoring used in the guarded hot-box are described in the following section, as well as the calibration of sensors and apparatus, and how the guarded hot-box was used to evaluate the proposed wall assemblies for this project scope.

Before measuring the data points of interest, the guarded hot-box must be held at steady-state conditions. Using the instrumentation in the chambers, steady-state conditions are met when the following criteria must be met for 5 consecutive test periods, according to ASTM C1363 [105]:

- the average specimen surface temperature in the metering chamber did not vary by more than ± 0.25°C;
- the average specimen surface temperature in the exterior chamber did not vary by more than ± 0.25°C;
- the average temperature within the air curtain did not vary by more than ± 0.25°C;
- the average energy input to the metering chamber did not vary by more than ± 1%.

When steady-state conditions inside the guarded hot-box are met, the energy input (E), the interior and exterior surface temperature (T) and heat fluxes (q''), can be measured. The effective thermal resistance of the wall assembly (R_{eff}) and thermal resistance from the heat flux measurements (R_{HF}) can be calculated based on those measurements. R_{eff} was calculated through Equation 3-1 using the averaged measurements from 5 consecutive steady-state periods.

$$R_{\text{eff}} = \frac{\Delta T \cdot A \cdot t}{E} \qquad 3\text{-}1$$

where ΔT is the temperature difference between the interior and exterior surfaces of the wall assembly in °C, A is the metering chamber area in contact with the sample measured in m^2, t is the elapsed time of the test period in hours, and E is the energy input to the metering chamber, measured with power monitoring system, in W·h.

Another parameter that can be determined from the data is the thermal resistance at a point, R_{HF}, by Equation 3-2 with the use of the heat flux plates.

$$R_{\text{HF}} = \frac{\Delta T}{q''} \qquad 3\text{-}2$$

where ΔT is the measured temperature difference across the material in °C, and q'' is the measured heat flux in W/m^2 under steady-state conditions. This calculation was performed when the R-value of materials (e.g., VIP, VIP edges, EPS etc.,), R-value at thermal bridges (e.g., studs) or any other point in the assembly was different.

In summary, the guarded hot-box system is equipped with a National Instruments data acquisition, and Delta control system. National instruments interfaces with LabVIEW, which is a graphical programming interface used to operate experimental test systems, to take and store the measurements onto the local computer. The test parameters, such as averaging periods, measurement intervals, required test periods and analog inputs from the data acquisition are programmed into and executed by LabVIEW. Meanwhile, the Delta control system interfaces with Oracle and controls the heating and cooling of the chambers. The control system monitors the temperatures in the chambers and triggers the chiller, fan, or heaters if necessary. Greater detail of the instrumentation, data acquisition or controls of the Carleton University guarded hot-box can be found in Conley [68].

3.1.3 Calibration and Error

The thermocouples and guarded hot-box used in the system was calibrated before any studies took place. The thermocouples were calibrated before calibrating the guarded hot-box facility. The calibration procedure followed the procedure from Baldwin [106] and ASTM E220-19 [107]. The procedure used a resistance temperature detector (RTD) probe and the water-based Fluke 7008 micro bath. The guarded hot-box used 5 different spools of Type T thermocouple wire and all 5 wires were calibrated. Three samples were taken from each spool in three different lengths, and the junction was submerged into the calibration bath along with the RTD. The RTD was connected to a digital multimeter (DMM) and was controlled by the LabVIEW user interface to read the resistance measurements through a serial connection. The thermocouple samples were connected to the NI 9213 voltage differential card and the voltage difference and cold junction temperature (CJC) were read by LabVIEW.

The calibration bath was maintained to a constant temperature while the RTD, thermocouple, and CJC readings were logged simultaneously. The calibration bath range was initially performed from a 5°C to 95°C with the micro bath filled with water, however, it was later performed from -5°C to 95°C with a glycol solution to verify the relationship did not significantly vary below 0°C. Upon start-up, the temperature bath was allowed 60 minutes to settle to the lowest temperature of the range. After the calibration bath has reached a steady temperature, the measurement period was 5 minutes with a 20-second measurement resolution for a total of 15 readings from each of the RTD, CJC, and thermocouples. The calibration bath temperature increased by 2°C and another set of measurements was taken after the setpoint was reached. This continued until a set of measurements were completed for the entire calibration range, and a 6th order polynomial correlation was created with cold junction compensation, in the form of:

$$T = aV^6 + bV^5 + cV^4 + dV^3 + eV^2 + fV + g + CJC \qquad 3\text{-}3$$

where the measured voltage is in mV and the CJC is the measured cold junction temperature. The coefficients from the calibration procedure are provided in Table 3-2 and they were integrated into the LabVIEW monitoring program.

Table 3-2: Calibrated coefficients for each spool of thermocouple wire

Coefficient	a	b	c	d	e	f	g
Roll 1	0.0034	-0.0146	-0.0149	0.1455	-0.6962	24.67	0.1171
Roll 2	0.0059	-0.0246	-0.0313	0.2509	-0.8073	24.69	0.1012
Roll 3	0.0012	-0.1032	-0.0018	0.1559	0.8044	24.65	-0.0348
Roll 4	-0.0003	0.0067	-0.0012	0.1413	-0.7922	24.65	-0.0708
Roll 5	0.0178	-0.0578	-0.1193	0.5068	-0.7246	23.95	-0.0121

The next step was to calibrate the guarded hot-box by measuring a homogenous sample of known thermal conductivity. A 500 mm (2") thick sheet of extruded polystyrene (XPS) was installed in the surround panel and was used to calibrate the guarded hot-box. The guarded hot-box was closed and operational for 34 hours with setpoints of -20°C and 20°C in the climate and metering chamber, respectively. Under steady-state conditions, the measured thermal resistance was 1.96±0.1 m^2K/W compared to an expected thermal resistance of 1.91 m^2K/W. The expected thermal resistance was the sum of the thermal conductivity through the XPS (1.76 m^2K/W) as well as the film resistances at the interior (0.03 m^2K/W) and exterior surfaces (0.12 m^2K/W). Therefore, the difference between the known sample and the measurement from the guard hot-box was within the range of experimental error and the testing of high-performance materials could begin.

Further information on the calibration and uncertainty in the effective thermal resistance and thermal resistance calculated using measured heat flux in the guarded hot-box can be found in Conley [68].

3.1.4 Quality Assurance

After the steady-state testing was completed, it was possible to utilize infrared thermography (IRT) to qualitatively assess thermal bridges, possibly air leakage, or weak points within the assembly. This guarded hot-box orientation was especially beneficial in performing non-destructive assessments of VIPs that were installed in the wall assembly. Generally, a quality VIP will be rigid, and the foil will be taught to the porous core because of the vacuum present inside the panel. In some cases, the VIPs may seem acceptable based on that criterion during installation, but it may provide a below require in-service thermal resistance. It was observed that

some VIPs would appear to be high-quality but after IRT inspection after installation, it was found that they were broken and provided a much lower thermal resistance than expected.

To perform the IRT studies, the guarded and metering chambers are unclamped from the system and removed, such that the wall assembly sample remained clamped to the exterior chamber while the interior face is exposed to the interior environment, as shown schematically in Figure 3-6. The thermal camera is used to capture images of the interior facing surface, which would measure the radiation from each pixel of the image and correlates the measurement to a temperature. The lights in the environment were turned off and the blinds were shut to minimize the impact on the radiation emitted by the interior surface of the sample. IRT was an important aspect of the quality assurance and assessing the thermal bridging impact of the VIPs.

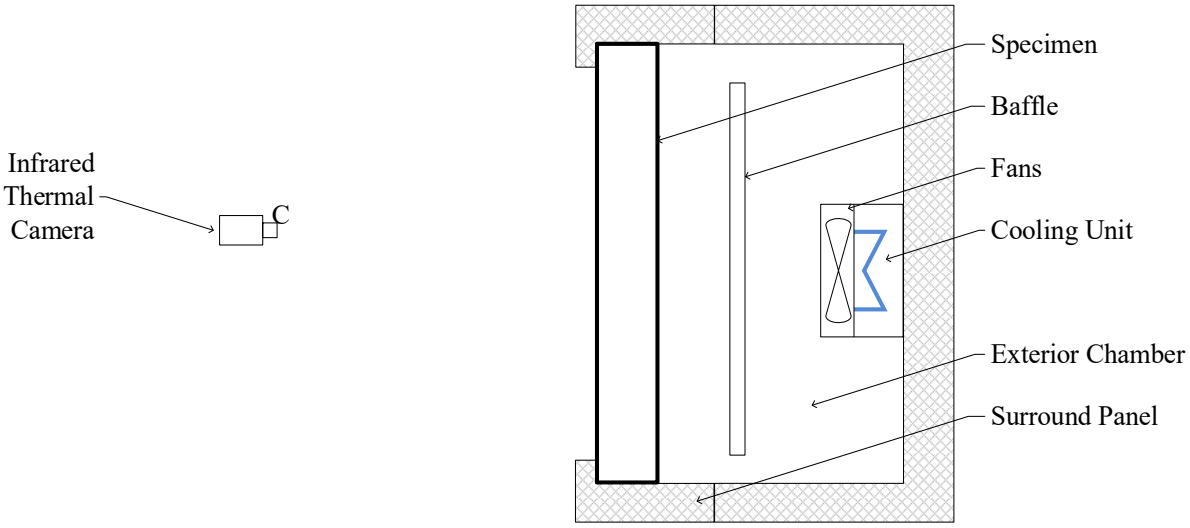

Figure 3-6: Infrared thermography set-up with a guarded hot-box system

3.1.5 Wall Assembly Monitoring Plan

The CIP and SIP panelized approaches were evaluated in the guarded hot-box as (1) only the panelized system, and (2) a part of a finished above-grade wall assembly. The benefits of evaluating the panelized insulation on its own is the ability to verify that there are no compromised

VIPs in the system through infrared thermography and measure the effective thermal conductivity of the insulation system. A photo from the laboratory of the interior surface of the panelized systems is presented in Figures 3-7 and 3-8. For reference, a plywood surface was added to the CIP assembly to provide some rigidity and ease of fastening. Additionally, the insulation of the SIP panel was inboard of the OSB and fastened to the surround panel. Not shown is a gasket inside the surround panel or the applied air barrier on the exterior face of each panelized system before testing and instrumentation.

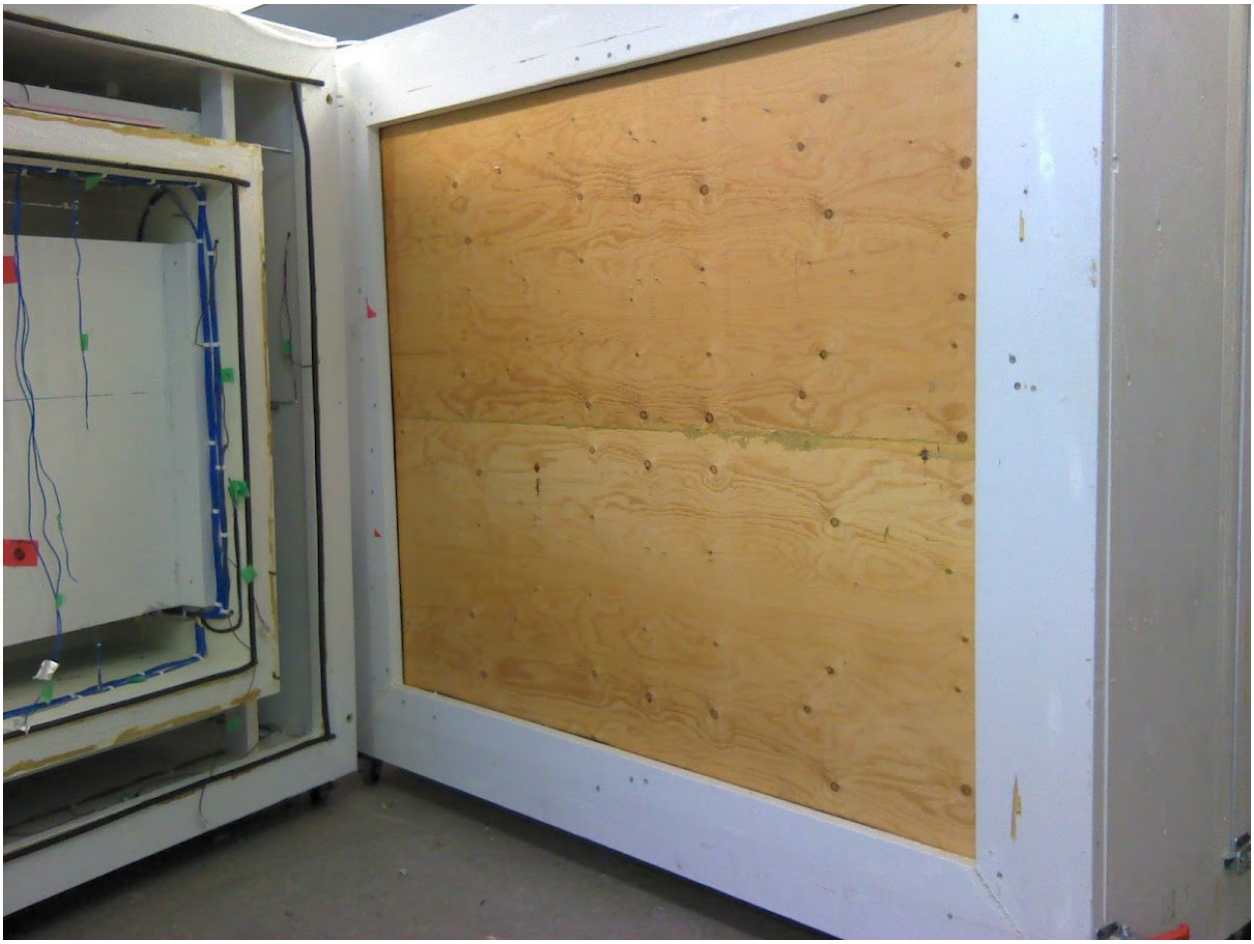

Figure 3-7: Photos of CIP system installed before testing in the guarded hot-box. Plywood is used as a structural base for the CIP panel for (1) rigidity, (2) fastening purposes, and (3) air sealing details.

Figure 3-8: Photos of SIP system installed before testing in the guarded hot-box.

A follow-up test of the panelized systems on a completed wall assembly would allow some verification of the results and an effective thermal resistance value for a completed wall assembly. A base wall used a wood-framed wall built 400 mm (16”) on-center (O.C.) with fibreglass filled cavities, vapour barrier and 10 mm (3/8”) gypsum board. The exterior was finished with a Tyvek weather barrier, 1x3 strapping and vinyl siding to minimize and/or eliminate the air leakage between the climate and metering chambers, shown in section view in Figure 3-9.

Additional thermocouples were installed within the panels and the base wall to measure the temperature profile through the assembly. The thermocouples were placed at each material interface and were connected to the data acquisition system through the miniature TC ports in the

exterior chamber. The location of each thermocouple is presented in Figure 3-10 for the complete wall assembly. The instrumentation embedded in the panel was also used for evaluating the panelized system only.

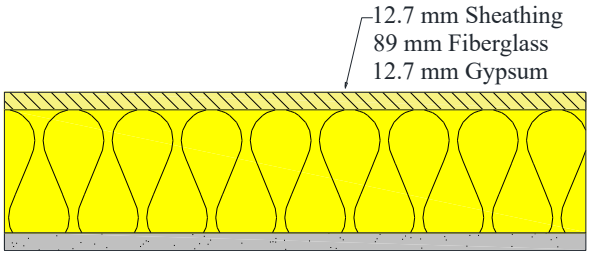

Figure 3-9: Section view of the base wall.

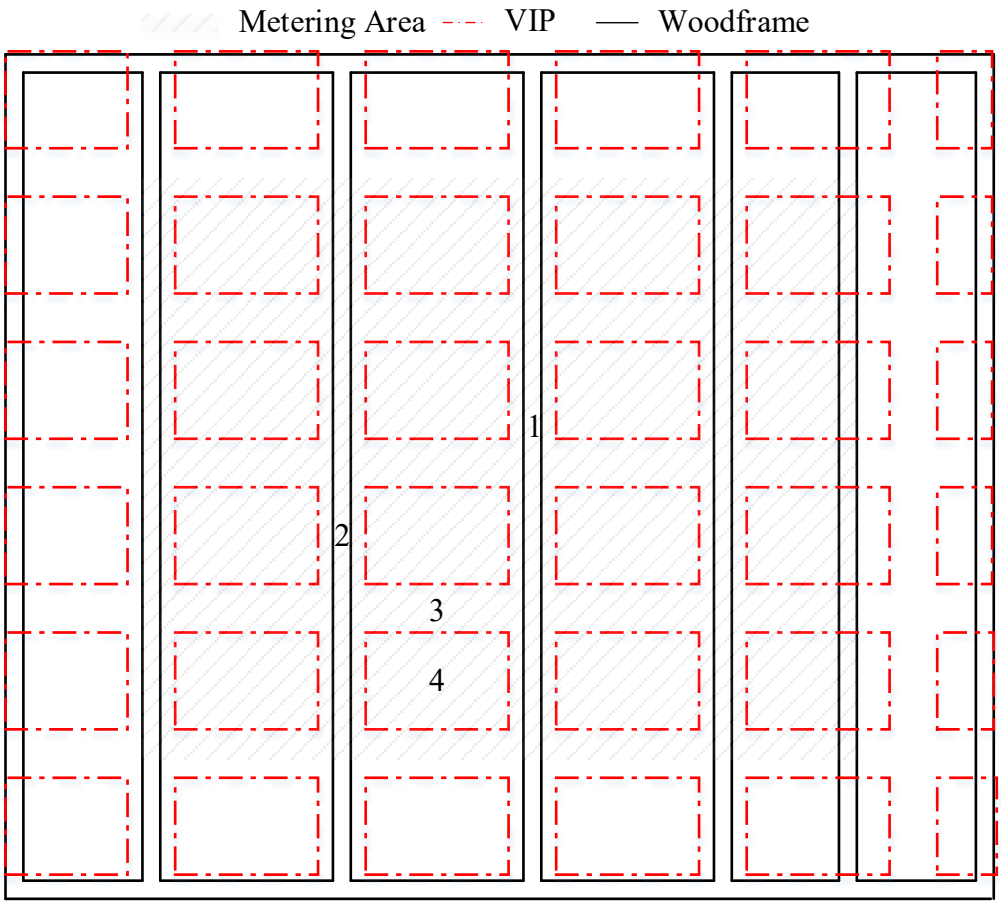

Figure 3-10: Instrumentation plan for the guarded hot-box assemblies including the metering box.

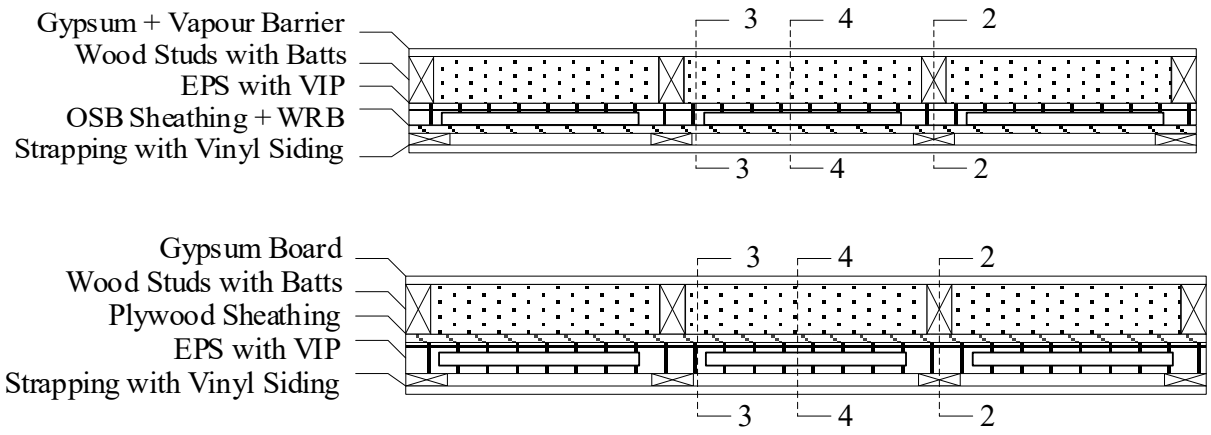

Figure 3-11: Section view wall assemblies evaluated from sections 2, 3, and 4 denotes. Thermocouples were placed at each interface.

3.1.6 VIP Edge Effect

In addition to evaluating the effective thermal resistance of the panelized system and the complete wall assembly, the variable VIP performance was known to exist but not yet quantified. The thermal conductivity was known to change near the edge of a VIP as thermal bridging would exist. A layout of 30 AWG Type-T thermocouples was installed in the pocket of the EPS before installing the VIP and laminating the panels. A total of 38 thermocouples were placed on the warm side of the VIP, denoted by the red indicators in Figure 3-12. Within the first 76 mm of each VIP edge, a total of 28 thermocouples were placed at 12.7 mm spacing. An additional 5 thermocouples were placed along the centerline at 25.4 mm spacing, including one placed at the center of the VIP. A final 5 thermocouples were placed at other points in the field of the panel to compare to the centerline temperature measurements.

The same 30 AWG Type-T thermocouples were placed on the VIP centerline spaced by 50.8 mm from 50.8 mm off the edge (on EPS) to 50.8 mm off the VIP edge (on EPS). The outermost thermocouple was aligned with a stud to measure the temperature at the lowest thermal resistance in the wall assembly. The thermal resistance along the VIP cannot be calculated since a

heat flux sensor could not be included in the instrumentation plan due to space restrictions. Under steady-state conditions, the temperature gradient was used to provide a qualitative assessment of the thermal bridging present in the assembly.

After inserting the VIP into the EPS pocket, a set of thermocouples were added to the cold side, denoted by the blue markers. The sensor distribution did not require as much density because the exterior surface was close to the exterior boundary conditions that were held to a constant temperature. Therefore, it was expected that the temperature at the interface would be far more uniform compared to the pocket surface. Secondary, the guarded hot-box setup could only handle accommodate an extra 50 sensors embedded in the assembly.

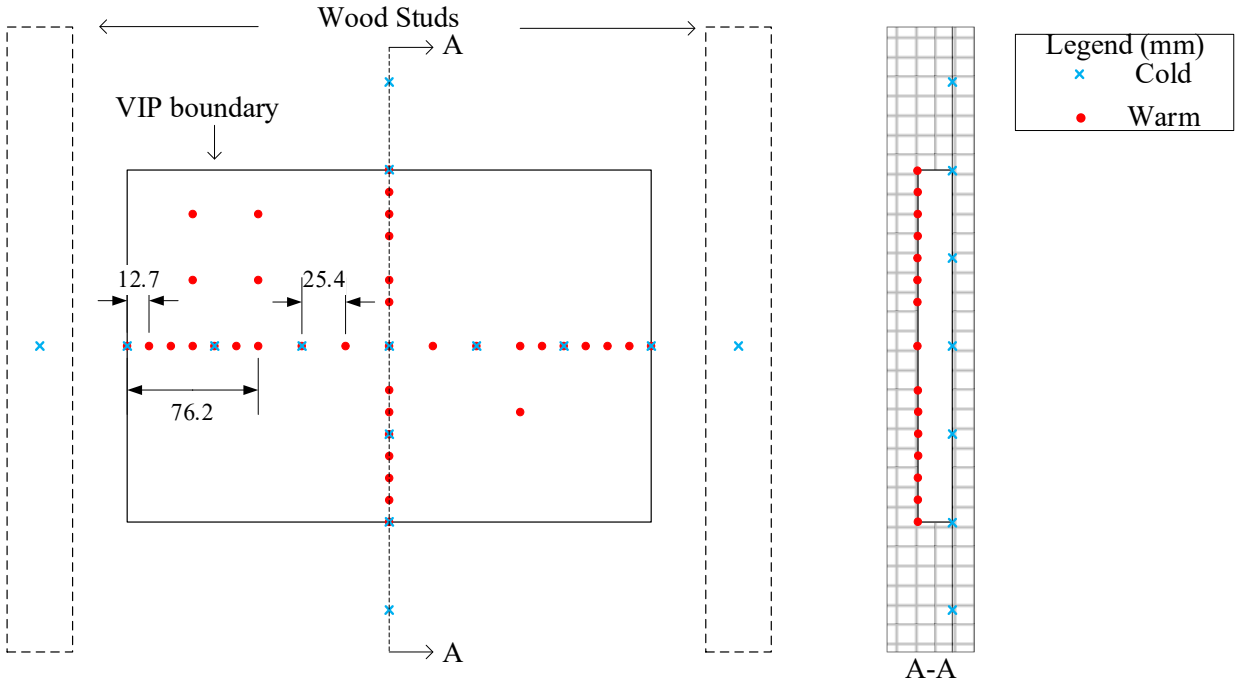

Figure 3-12: Instrumentation plan for evaluating the edge effects of the VIPs in plan (left) and section (right)

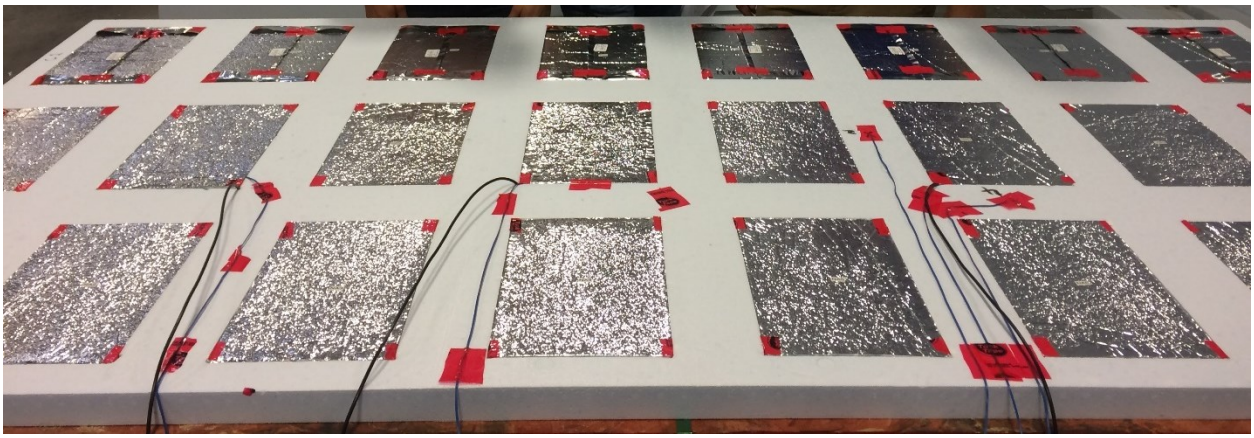

Figure 3-13: Photo of instrumented VIP before laminating EPS backer

3.1.7 Guarded Hot-box Summary

The guarded hot-box was used to evaluate scaled wall assemblies under steady-state conditions. In total, two types of panelized insulation systems were evaluated with two different manufacturers of VIPs. Additionally, heat flux plates were placed at the center of the VIPs outboard of the exterior panelized system to measure the thermal resistance at specific points, thermocouples at each interface to measure the temperature profile through the assembly, and the thermocouples around the VIP to measure the temperature variation in that plane.

3.2 In-Situ Monitoring

The CanmetENERGY Building Envelope Test Hut (CE-BETH) was used to determine the experimental in-situ hygrothermal performance of the prototype, high-performance wall assemblies. CE-BETH, shown in Figure 3-14, is an in-situ building envelope evaluation facility that monitors wall assemblies exposed to environmental conditions, such as wind-driven rain, solar exposure, temperature, and relative humidity with controlled interior temperature and relative humidity setpoints. The in-situ testing is important in evaluating building envelopes since the monitoring is performed under in-service conditions and incorporates construction penetrations

and defects that are assumed during the modelling. In this study, Bays A and C were used, and the center Bay was used for a separate experimental study.

The facility contains three large openings able to accommodate one 2.4 m x 2.4 m (8’ x 8’) specimen per opening or two 1.2 m x 2.4 m (4’x 8’) specimens that could be used for side-by-side evaluations of different wall assemblies (e.g., baseline and high-performance). The openings face the East direction and have limited shading on the exterior surface. The facility floor has less insulation than the walls and roof and generally lacks air tightness. However, it is raised off the ground such that the bottom of the openings remained above the level of snow cover during the winter periods.

Figure 3-14: CanmetENERGY Building Envelope Test Hut (CE-BETH) situated at Bells Corners Campus

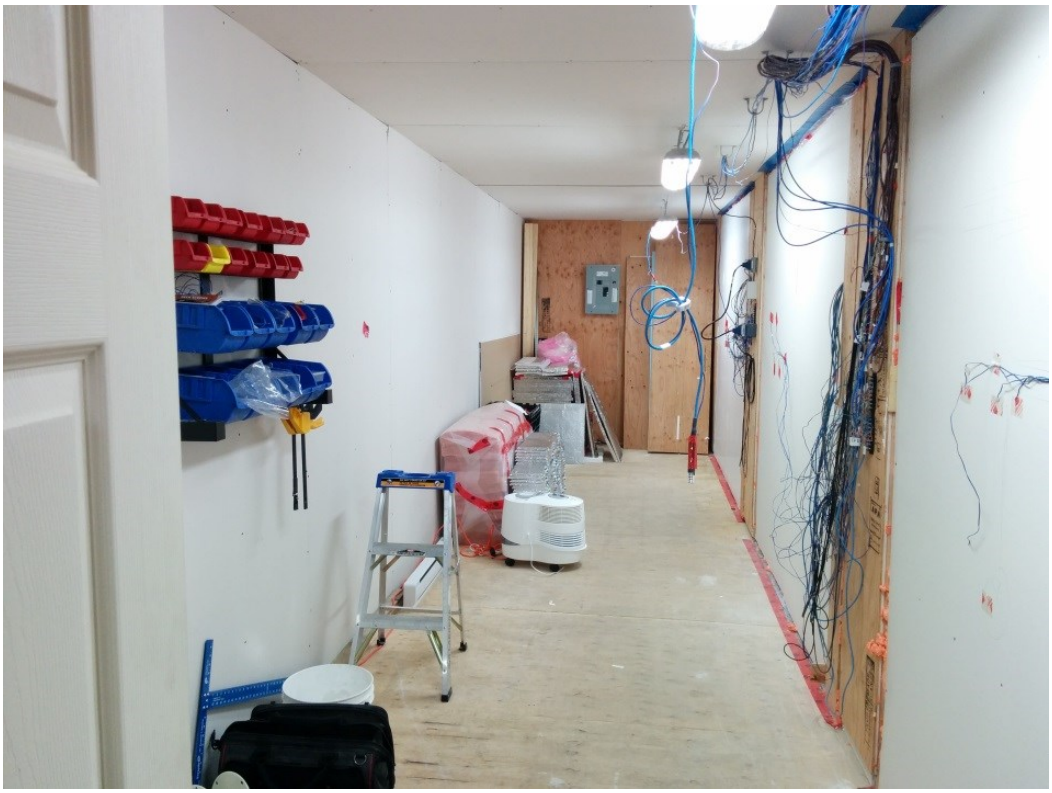

Figure 3-15: Interior of CE-BETH showing the instrumentation and interior surfaces of samples

The interior of the facility is framed with 2x4 dimensional lumber, sprayed with closed-cell foam to insulate, and air seal the container. The container was purchased and used and contained significant dents and holes that required patching making it challenging to the frame. The interior was finished with drywall and paint, as seen in Figure 3-15. The baseboard heaters, humidifiers, and instrumentation can also be seen in the figure. Not shown is the portable air conditioner that provided cooling and dehumidification, NI-RIO DAQ, and the local desktop used to collect data and control the interior conditions.

3.2.1 Instrumentation and Monitoring

The facility was equipped with data logger equipment and various measurement devices capable of handling over 230 measurements per 10-minute period. The instrumentation was used to measure the heat, air, and moisture (HAM) transfer through the assembly. In addition to the

permanent instrumentation and data acquisition equipment, there are infrared thermal imaging devices on-site and the ability to depressurize the facility to detect air sealing or leakage through qualitative evaluations with smoke pencils or thermography. For each of the wall assemblies, the moisture content, temperature, and relative humidity were measured through sensors that utilized a combination of NI and Structural Monitoring Technology (SMT) data loggers. The voltage and resistance-based measurements were taken at 10-minute intervals and averaged hourly to evaluate the measured data to the failure criteria. The NI system was used to measure the voltage-based thermocouples, heat flux plates and relative humidity sensors, while the SMT system was used to measure the resistance-based point moisture measurement (PMM) and moisture content sensors (MCs). The NI system featured a NI-RIO connected to LabVIEW [108] on a local desktop computer inside the test facility. The SMT system featured eight SMT A3 (8R) dataloggers located next to the wall assembly and a 48-channel multiplexer located near the local desktop. The A3s were powered by batteries and transmitted the data through a wireless receiver to the desktop. The multiplexer was powered by the exiting electrical and connected directly to the local computer through CAT5/RJ45 connection.

The facility experienced blackouts during the monitoring period over the past 3 years, and the data loggers connected to the facility infrastructure would not collect measurements during this period, unlike the battery-powered SMT A3 data logger. During these blackout periods, there were limited measurements and a loss of control over the interior conditions of the test facility.

3.2.2 In-Situ Preparation

The test bays were split into 2 bays that could accommodate two wall specimens 1.22 m by 2.44 m (4’ by 8’). This setup would allow for a direct side-by-side comparison between the high-performance assemblies and a reference wall that used the equivalent thickness of standard

exterior insulation. The two samples would be exposed to the same interior and exterior boundary conditions and the difference in hygrothermal performance could be measured and compared.

The rough opening in the facility was cut larger than dimensional lumber was used to make the openings square and to the proper size. The rough openings framed sections with the gaps spray foamed for air and water tightness and to create a barrier between the wall specimens and existing walls. This buffer was important to eliminate any lateral heat, air or moisture transfer between the monitored walls and the facility structure.

The monitored walls were both wood-framed assemblies and the wood framing was the first portion that was installed. Since the openings were square, the wood framing was added to the opening. In Bay A, a wood-frame was built using 2x6 dimensional lumber built on 405 mm (16”) on centre spacing and was built to represent new construction in Ottawa. Stud cavities were insulated with R-19 fibreglass batt insulation and finished with a 6-mil polyethylene vapour barrier and 10 mm painted gypsum board on the interior. In Bay C, a wood-framed wall using 2x4 dimensional lumber was built using 405 mm (16”) on-center spacing and was built to represent a home built before 1984 in Ottawa. A 10 mm (3/8”) plywood was used as the sheathing and the cavities were insulated with R-13 fibreglass batt insulation. The wall was finished with a painted gypsum board on the interior and did not use any interior vapour control to represent pre-1960 construction.

On the exterior of the wood-frame, the bulk water, air, vapour, and thermal control layers were included. The walls in Bay A and C contained many similar elements. The exterior insulation in each bay was split in half. One half would be insulated using a high-performance panel and the other half of the wall assembly was insulated using an equal thickness of EPS insulation and would represent the baseline wall assembly. Additionally, a Tyvek weather-resistant barrier (WRB) was

stapled to the sheathing, behind the insulation, to control the air and bulk water between the sheathing and exterior insulation. Finally, the whole exterior was finished with vinyl siding and with a 0.75” unventilated air space providing additional bulk water control. The differences between the two bays were in Bay A featured a 4x8 SIP panel using 200 mm by 300 mm (8” by 12”) VIPs as the exterior insulation with the sheathing facing outboard while Bay C featured 1220 mm by 2440 mm (4’by 8’) CIP panel using 200 mm by 300 mm (8” by 12”) VIPs as the exterior insulation. After the walls were finished, the seams around the opening were taped and another bead of spray foam was applied around the exterior to minimize air leakage paths.

Some limitations were caused by the in-situ preparation and construction of the wall assemblies. First, installing the wall assemblies into the rough openings utilized spray foam to eliminate the gaps and provide proper sealing. This would be successful the first time however, at the end of the monitoring period, it will be difficult to install a new sample and obtain the same level of air tightness detailing. A better process for creating an airtight, possibly with the use of membranes, tapes, and gaskets, would be suggested. Secondly, the facility was insulated with spray foam and many holes needed to be fixed in the enclosure. It is suspected that some leaks existed in the roof as during the spring the floor would show new water damage. The water found a path along with the spray foam and therefore it was not possible to determine the source. This unexpected water source was unlikely to affect the monitored assemblies, but the importance of having an enclosure that is air and water-tight was noted.

3.2.3 Monitoring Plan for Assemblies

The monitoring objective was to establish the CIP and SIP panels would pass the failure criteria when exposed to in-situ environmental conditions over a minimum of 3 years of monitoring. The failure criteria are based on the peak mould index, which used the temperature,

relative humidity, and moisture content at the surface of organic materials to calculate the mould index at each timestep. The monitoring plan was built to ensure that the expected and worst cases were measured during the test period, and redundancies were added to ensure sufficient data would be acquired.

The measurement locations were selected based on the highest expected moisture content of organic material and what could be used to validate a hygrothermal model with temperature and relative humidity measurements. The hygrothermal monitoring followed suggestions from literature with amendments to measure the effect caused by VIPs. The materials most susceptible to conditions that would promote mould growth were the inner surface of the sheathing and the structural framing, specifically the bottom plate.

The OSB sheathing was an organic material that would fall in the sensitive material class for the mould index. Additionally, the sheathing would be exposed to environmental conditions including air movement and vapour diffusion and very little if any bulk wetting due to the heat and moisture control layers outboard. The interior surface of the sheathing was instrumented with point moisture measurement (PMM), temperature and relative humidity sensors. The PMMs measure moisture content by reading the resistance between two stainless steel screws in the wood, like a handheld moisture unit. The sensors are operable under the expected temperature conditions. The measured resistance was correlated to a wood moisture content by Equation 3-4.

$$MC = \left[\frac{R_s + (0.567 - 0.0260T + 0.000051T^2)}{0.881(1.0056^T)} - b\right] \div a \qquad 3\text{-}4$$

where R_s is the measured resistance, T is the measured temperature of the wood in °C, a and b are species correction regression coefficients, that can be found in the Wood Handbook [109]. Stainless steel screws were used, and the screws were exposed through the thickness of the

sheathing. Since the screws were not insulated, the measured resistance would be the path of least resistance. It was possible to obtain insulated nails that would only read the resistance at the exposed tips. The PMMs have an integrated thermistor that was used to approximate the sheathing surface temperature and compensate for the moisture content.

PMM sensors were placed on the sheathing at 4 different locations on the sheathing of the high-performance wall assemblies: (1) point insulated with VIP, (2) point along the edge of the VIP, (3) point behind the EPS and, (4) point nearest to a stud. These locations were selected since they are the four unique cross sections in the wall assembly. Those sections would have different thermal and moisture properties and would therefore present different long-term results.

Relative humidity sensors were placed in similar locations as the moisture content sensors. The relative humidity was measured in the same four locations and was also placed on the surface. The sensor was placed on the surface instead of midspan in the cavity because the surface conditions were more important than assuming the entire cavity would be exposed to the same air conditions to get the air conditions at the surface of wood-based materials. Two sensor manufacturers were used and taped to the sheathing while keeping the measurement area exposed to the air near the surface. A Vaisala HMP60 [110] humidity and temperature probes were placed in position 1, a point on the sheathing insulated by a VIP. The probe was designed to be rugged and long-lasting and 1 instrument was installed in each wall assembly.

Honeywell HIH-503 [111] humidity sensors were placed in monitoring locations 1 through 4. These sensors were selected due to their low voltage requirements, low profile size, suitable accuracy, and cost-effectiveness. The sensors were powered with a 5VDC supply, and the voltage output was read by the NI data acquisition system. The uncorrected relative humidity was converted using Equation 3-6. Since there was no onboard temperature, a thermocouple was

attached to the sheathing surface next to the humidity sensor or was tied to the humidity sensor. The measured temperature from the thermocouple was used to compensate for humidity and used to measure the temperature profile through the assembly, shown by Equation 3-7.

$$V_{\text{out}} = V_{\text{supply}}(0.00636 \cdot RH_{\text{sensor}} + 0.1515) \quad 3\text{-}5$$

$$RH_{\text{sensor}} = \left(\frac{V_{\text{out}}}{V_{\text{supply}}} - 0.1515\right) * 0.00636 \quad 3\text{-}6$$

$$RH_{\text{corrected}} = \frac{RH_{\text{sensor}}}{1.0546 - 0.00216 \cdot T} \quad 3\text{-}7$$

Humidity sensor placement on the inner OSB surface is shown in the plan view drawing in Figure 3-16, along with the temperature and moisture content sensors.

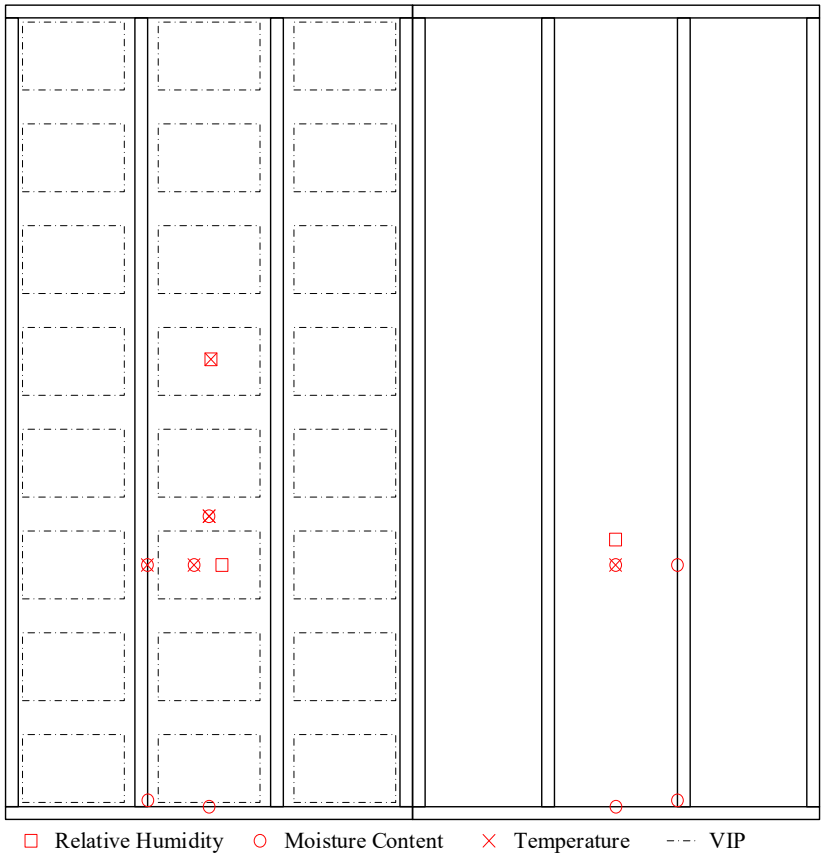

Figure 3-16: Plan view drawing of sensors installed in retrofit and new construction wall assembly

Temperature sensors, specifically thermocouples, were placed throughout the wall assembly. Type-T thermocouples from Omega Environmental were used and were calibrated in the same procedure as the guarded hot-box. The thermocouples were placed at each material interface for each of the 4 cross sections and are depicted schematically in Figure 3-17. Those measurements would be used to capture the temperature profile through the assembly as well as compensate for any moisture content or relative humidity sensors.

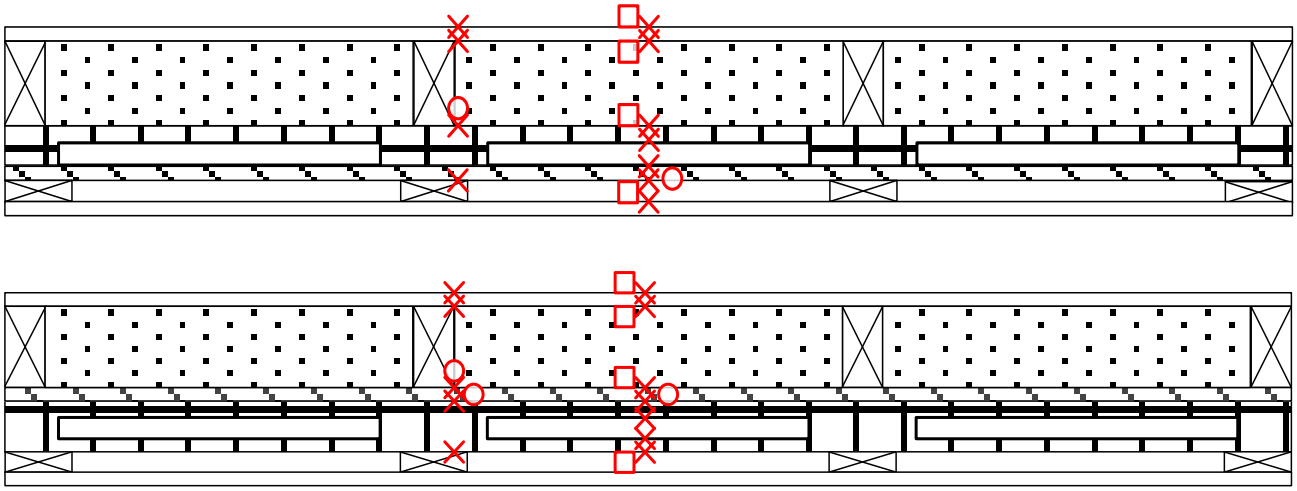

Figure 3-17: Section view for the instrumentation for new construction (top) and retrofit (bottom) walls. Same legend as instrumentation in Plan View.

The bulk of the instrumentation was concentrated on the inner OSB surface within the wall cavities, shown in Figure 3-18. The moisture content sensors were screwed into the OSB with stainless steel screws and have a thermistor onboard. The relative humidity sensors were taped to the wall with tape while keeping the sensor exposed to the air. One set of heat flux plates was applied to the 6-mil vapour barrier with heat flux paste and taped with nearby thermocouples (blue wires). The wall assemblies were finished with 12 mm drywall and painted with latex paint, shown in Figure 3-19, with thermocouples measuring the interior surface temperature. From the exterior, the new construction and retrofit wall assemblies can be seen in Figure 3-20 and Figure 3-21 before

the vinyl siding is installed. The printed marks on the CIP panel can be seen on the retrofit wall assembly however, the markings are covered by the Tyvek barrier in the new construction assembly.

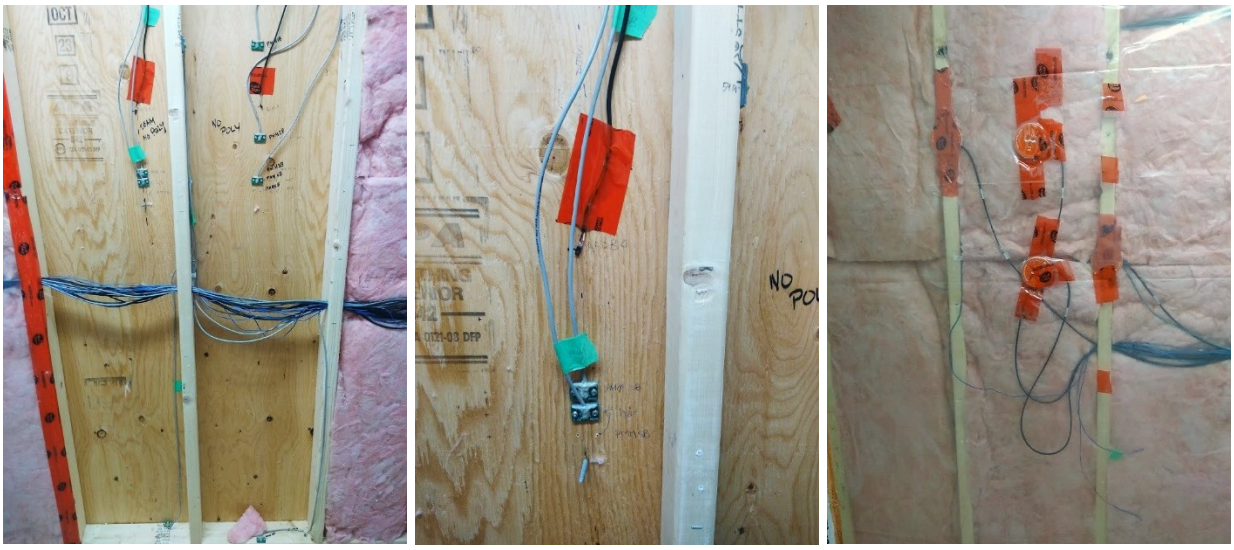

Figure 3-18: Pictures of instrumentation installed inside the wall cavities at CE-BETH

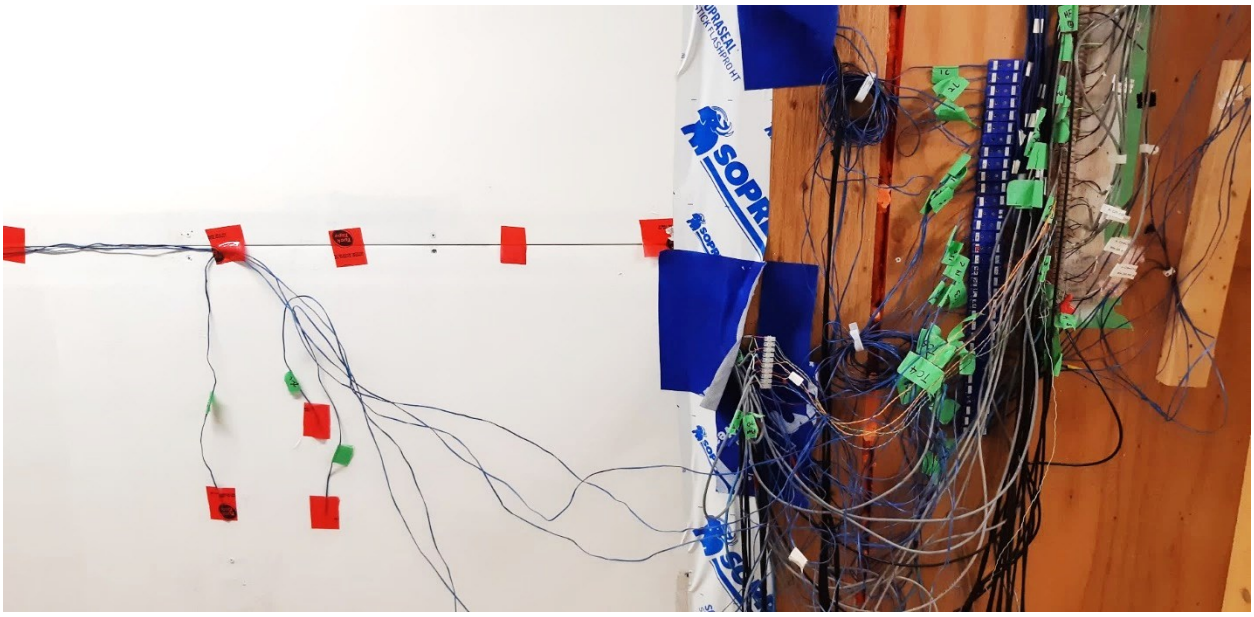

Figure 3-19: Pictures of instrumentation on interior surface and data acquisition junctions at CE-BETH.

Figure 3-20: Exterior photo of the in-situ monitored retrofit wall assembly at CE-BETH.

Figure 3-21: Exterior photo of the in-situ monitored new construction wall assembly at CE-BETH.

3.2.4 Sensor Error and Limitations

The instrumentation used for the CIP and SIP wall assemblies at CE-BETH is listed in Table 3-3, including the manufacturer, calibrated, or listed error, and the total quantity of instruments for the project. The uncertainty on the measurements that include the sensor error is presented in Appendix E.

Table 3-3: Instrumentation included in CE-BETH and in-situ monitoring

Instrument	Manufacturer	Product	Unit	Error	Quantity
Thermocouple	Omega		°C	±0.46	60
Heat Flux Plate	Huskeflux		W/m^2	±5%	16
Relative Humidity	Vaisala		%RH	0%-90%, ±3% 90%-100%, ±5%	6
Relative Humidity	Honeywell		%RH	0%-10%, ± 7% 11%-89%, ±3% 90%-100%, ±7%	16
Thermistor	SMT		°C	±1°C	12
Point Moisture Measurement (PMM)	SMT	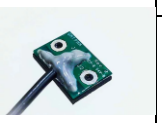	%MC	~3%MC	40

3.2.5 Boundary Conditions

The interior conditions of CE-BETH are controlled by monitoring the air temperature and relative humidity at two midpoints in the facility. The monitoring points are inputs to the control schema created in LabVIEW, where a digital output is sent to heating, cooling, or humidification systems as necessary. The control response is nearly instantaneous, however, losses of power or empty humidifiers can lead to interior conditions diverging from the prescribed set-points. The

interior set-points are listed below and were varied seasonally to investigate the effect the interior conditions have on the hygrothermal performance of the wall assembly.

1. 22°C temperature, 37.5% ±2.5% relative humidity during the 2017 winter.
2. 23°C temperature, uncontrolled humidity (allowed to float) during summer 2017;
3. 22°C temperature, 42.5% ±2.5% controlled humidity during the 2018 winter;
4. 23°C temperature, uncontrolled humidity (allowed to float) during summer 2018;

The hourly running average of measured interior conditions throughout the test is plotted in Figure 3-22. The conditions were selected to represent a set of circumstances that were loosely related to ASHRAE criteria for prescribed interior conditions. During winter 2016, a "worst-case" scenario of high interior humidity over the winter, greater than the 40% prescribed by ASHRAE when the exterior temperature is less than -10°C. During the 2017 and 2016 winters, the relative humidity was set at 40% and 42.5%. However, due to a lack of airtightness through the floor, frequent loss of power, and insufficient humidification the relative humidity set-point was commonly below the 40% set-point during the winter in 2017 and averaged about 35% RH. During the summer months, the interior temperature was controlled to 22°C, the same as ASHRAE, however, the relative humidity could float since the same unit was used to control both parameters. The exterior of the assemblies was exposed to the elements; consequently, the assemblies were subject to all the real-world moisture transfer phenomena, including vapour diffusion, air infiltration/exfiltration, wind-driven rain, and solar vapour drive.

The exterior conditions in Ottawa, Canada vary seasonally, from cold, humid winter periods (December, January, February) to hot, humid summer periods (June, July, August). The amount of precipitation is nearly constant throughout the year and is shown graphically in Figure 3-23, since the beginning of 2017.

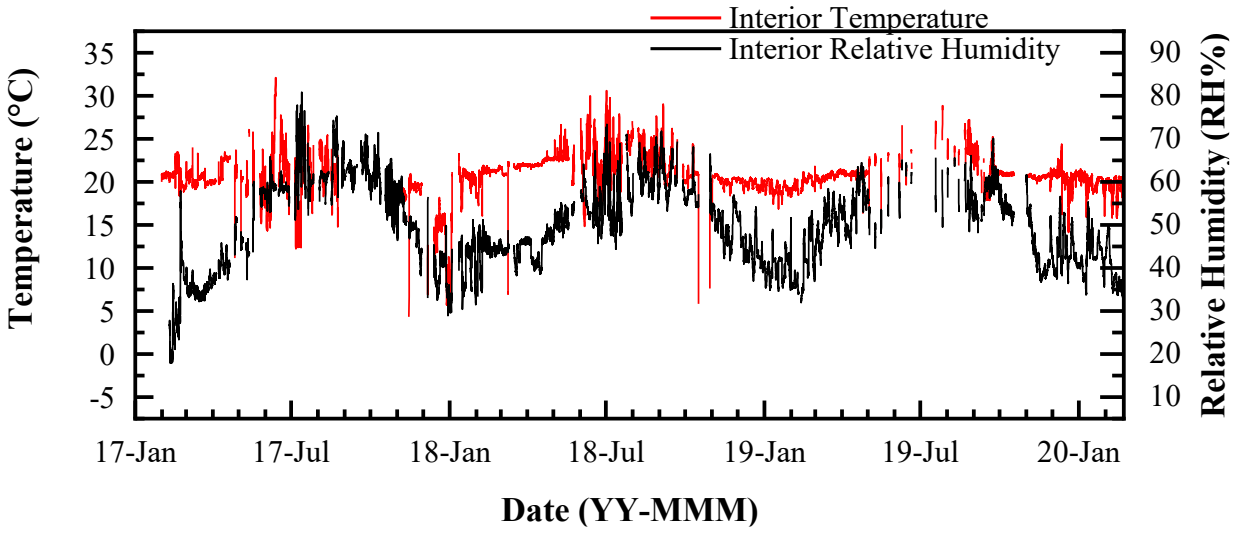

Figure 3-22: Interior boundary condition at CE-BETH from January 2017 to February 2020

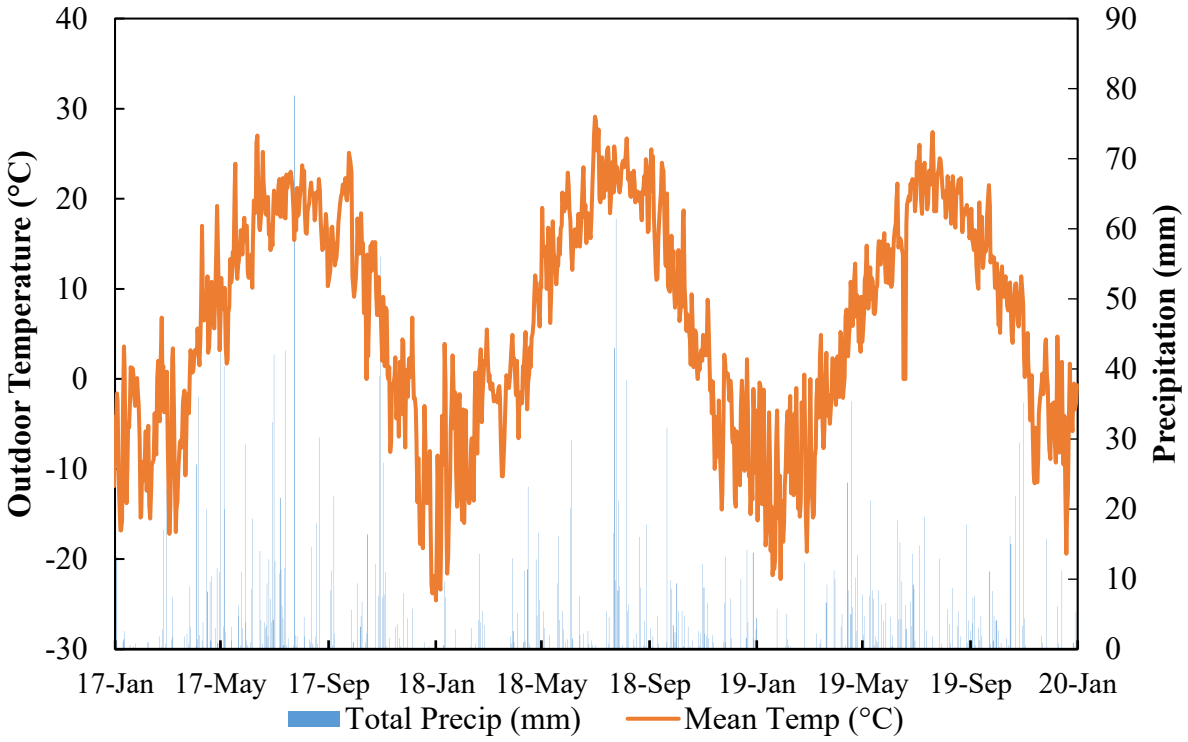

Figure 3-23: Exterior precipitation and average outdoor temperature in Ottawa, CA from 2017 to 2020. Data was obtained from Environment Canada [112]

3.3 Summary

The experimental methodologies followed will aid in answering the research questions and determine whether VIPs encased in insulation would be suitable for a Canadian climate. The guarded hot-box steady-state testing was used to find the effective thermal resistance of prototype panels, which were compared to literature, and theoretical and numerical calculations based on the material properties provided by the manufacturers. The thermal results from the experimental study will be integrated into numerical analysis and used to improve the prototype to an optimal solution. The in-situ hygrothermal monitoring was an invaluable exercise that provided real, in-use data that can be compared to numerical analysis. The hygrothermal monitoring was used to ascertain that introducing VIPs did not cause a moisture risk to the organic materials in the assembly and can be used to verify the numerical modelling can be reproduced to analyze VIPs in the wall assembly.

Chapter 4: Numerical Approach

The numerical objective was to evaluate the durability and risk of reduced in-service life caused by moisture-related risks of VIPs into Canadian building stock with the supporting experimental data.

4.1 Thermal Model

Two steady-state thermal models were selected to perform the numerical analysis to achieve research objectives 1 and 4. The effective thermal resistance of wall assemblies was evaluated using numerical analyses and compared to the experimental data. THERM [113], a two-dimensional steady-state modelling software developed by Lawrence Berkley National Labs (LBLN), was used to evaluate the effective thermal resistance and thermal bridges in new and retrofit wall assemblies.

THERM 7.7 is a computer program used to analyze two-dimensional steady-state heat transfer of building enclosure components. The computer program can be used to compute the steady-state heat transfer through building envelope components such as windows, walls, foundations, roofs, doors, and floor-to-wall connections among other thermal bridges that may exist in the building. It uses the finite element method to compute the heat transfer by conduction and radiation through building components. The program includes features such as the capability to import 2D computer-aided drawing files, a built-in material library and a boundary condition library [114]. The results analysis tools built-in to the program can visualize the temperature and predict condensation planes for a given set of temperature and humidity conditions and heat fluxes using isotherms, constant flux vectors and coloured infrared and flux magnitude.

While THERM provides a user-friendly interface to model building envelopes, it does have some limitations. The program cannot incorporate variation in material properties, such as thermal

conductivity dependent on temperature. Research has shown that thermal conductivity decreases as material temperature decreases, however for this study, these factors are not sufficiently significant in a highly insulated enclosure since the variance in thermal conductivity varies much less than the overall thermal resistance of the wall assemblies being evaluated. Additionally, the drawing and batch processing of the program is significantly limited. For complex geometries and studies where VIP material properties were varied, the program does not offer a feature to import drawings from other THERM files or the ability to perform batch processing.

The thermal modelling was limited to 2D simulations using THERM as the point thermal bridges caused by the VIP were not considered since the VIPs were encased within a foam board and surrounded by excess insulation. To address this issue, an effective thermal resistance that encompasses the edge effects and thermal bridging surrounding the panel was used and using 3D thermal modelling would not significantly improve the accuracy of the thermal resistance [79].

4.2 Hygrothermal Model

Two hygrothermal modelling programs were selected to perform annual simulations of the proposed wall assemblies under a variety of expected boundary and initial conditions to meet the research objectives 3 and 4, as well as support objective 2. The hygrothermal modelling program WUFI was developed by Künzel [115] selected to perform the simultaneous transient heat and moisture transfer in multi-layered wall assemblies. These modelling programs were selected since it has been validated against EN 15026 and a variety of test cases [116, 117, 118]. Additionally, the program is used by building scientists, architects, and researchers worldwide. WUFI Pro and WUFI 2D were the two hygrothermal models developed by Fraunhofer Institute in Germany. The models use a coupled equation and numerical solution to resolve the moisture conditions and evaluate the transient moisture and thermal conditions at each timestep in the wall assembly. WUFI

Pro was used to evaluate the one-dimensional transient hygrothermal conditions throughout the proposed wall assemblies. WUFI 2D was used to evaluate the two-dimensional transient hygrothermal conditions through the wall assembly and assess whether there is a need for evaluating wall assemblies in two or three dimensions.

WUFI utilizes a coupled equation and numerical solution to resolve the moisture conditions at each timestep. Equation 4-1 represents the heat storage and transport in the building material with the moisture-dependent thermal conductivity and vapour enthalpy flow, related to heat absorbed by water evaporation from one surface and condensing on another surface where H is the enthalpy of the moisture building material in J/m^3, ϑ is the temperature in K, λ is the thermal conductivity of the building material in W/m·K, h_{v} is the evaporation enthalpy of water to vapour in J/kg, δ is the vapour permeability in kg/m·s·Pa, μ is the vapour diffusion resistance factor of dry material, φ is the relative humidity in %, t is the timestep in seconds, and p is the water vapour partial pressure at saturation in Pa.

$$\frac{\partial H}{\partial \vartheta}\frac{\partial \vartheta}{\partial t} = \nabla(\lambda \nabla \vartheta) + h_{\mathrm{v}} \nabla \left(\frac{\delta}{\mu} \nabla(\varphi p_{\mathrm{sat}}) \right) \qquad 4\text{-}1$$

Equation 4-2 represents the moisture storage of a given material on the left-hand side and the liquid transport by surface diffusion and capillary suction, and vapour transport on the right-hand side, where w is the moisture content of the material in kg of water per m^3 of material, and D is the liquid transport coefficient in m^2/s.

$$\frac{\partial w}{\partial \varphi}\frac{\partial \varphi}{\partial t} = \nabla \left(\left(D_{\varphi} \nabla \varphi \right) + \delta_p \nabla(\varphi p_{\mathrm{sat}}) \right) \qquad 4\text{-}2$$

The heat and moisture transport equations are similar as the material storage is described on the left-hand side and the heat and moisture transport is described on the right-hand side. In two

dimensional system, the heat and moisture transport take the form of Equations 4-3 and 4-4 when the anisotropic properties (directional dependent properties for building assemblies) are considered.

$$\frac{\partial H}{\partial \vartheta}\frac{\partial \vartheta}{\partial t} = \frac{\partial}{\partial x}\left(\lambda_x \frac{\partial \vartheta}{\partial x}\right) + \frac{\partial}{\partial_y}\left(\lambda_y \frac{\partial \vartheta}{\partial y}\right) + h_v \frac{\partial}{\partial x}\left(\delta_{px} \frac{\partial \varphi p_{sat}}{\partial x}\right) + h_v \frac{\partial}{\partial y}\left(\delta_{py} \frac{\partial \varphi p_{sat}}{\partial y}\right) \quad 4\text{-}3$$

$$\frac{\partial w}{\partial \varphi}\frac{\partial \varphi}{\partial t} = \frac{\partial}{\partial x}\left(D_{\varphi x} \frac{\partial \varphi}{\partial y} + \delta_{px} \frac{\partial \varphi p_{sat}}{\partial x}\right) + \frac{\partial}{\partial y}\left(D_{\varphi y} \frac{\partial \varphi}{\partial y} + \delta_{py} \frac{\partial \varphi p_{sat}}{\partial y}\right) \quad 4\text{-}4$$

Furthermore, the one-dimensional coordinates can be further derived from the previous equations for heat and moisture transport in building materials, where ρ is the density in kg/m^3 and u is the water content in m^3/m^3.

$$\frac{\partial H}{\partial \vartheta}\frac{\partial \vartheta}{\partial t} = \frac{\partial}{\partial x}\left(\lambda \frac{\partial \vartheta}{\partial x}\right) + h_v \frac{\partial}{\partial x}\left(\frac{\delta}{\mu}\frac{\partial p}{\partial x}\right) \quad 4\text{-}5$$

$$\rho_w \frac{\partial u}{\partial \varphi}\frac{\partial \varphi}{\partial t} = \frac{\partial}{\partial x}\left(\rho_w D_w \frac{\partial u}{\partial \phi}\frac{\partial \varphi}{\partial x}\right) + \frac{\partial}{\partial x}\left(\frac{\delta}{\mu}\frac{\partial p}{\partial x}\right) \quad 4\text{-}6$$

The differential equations are discretized using an implicit differential volume method and iteratively solved using the flow chart in Figure 4-1. The model was validated for one and two-dimensional applications with experimental results from a cellular concrete flat roof assembly (one-dimensional) [115] and a masonry stone wall (two-dimensional) [115]. The one-dimensional model showed good agreement between the experimental data and the model results. Künzel noted that the two-dimensional model has no fundamental differences from the one-dimensional model but set up a two-dimensional experiment to validate those assumptions [115]. The moisture distribution of a lime silica brick was measured after wetting in liquid for 72 and 120 days was measured and compared to the calculations from the model. The results show some differences that could be attributed to the behaviour of the masonry stone which seemed to be more sensitive

to non-linear material parameters than the one-dimensional model. Overall, the comparison between the experimental results and the WUFI model (WUFI-2D) showed that the model was suitable to calculate the moisture transport in a system.

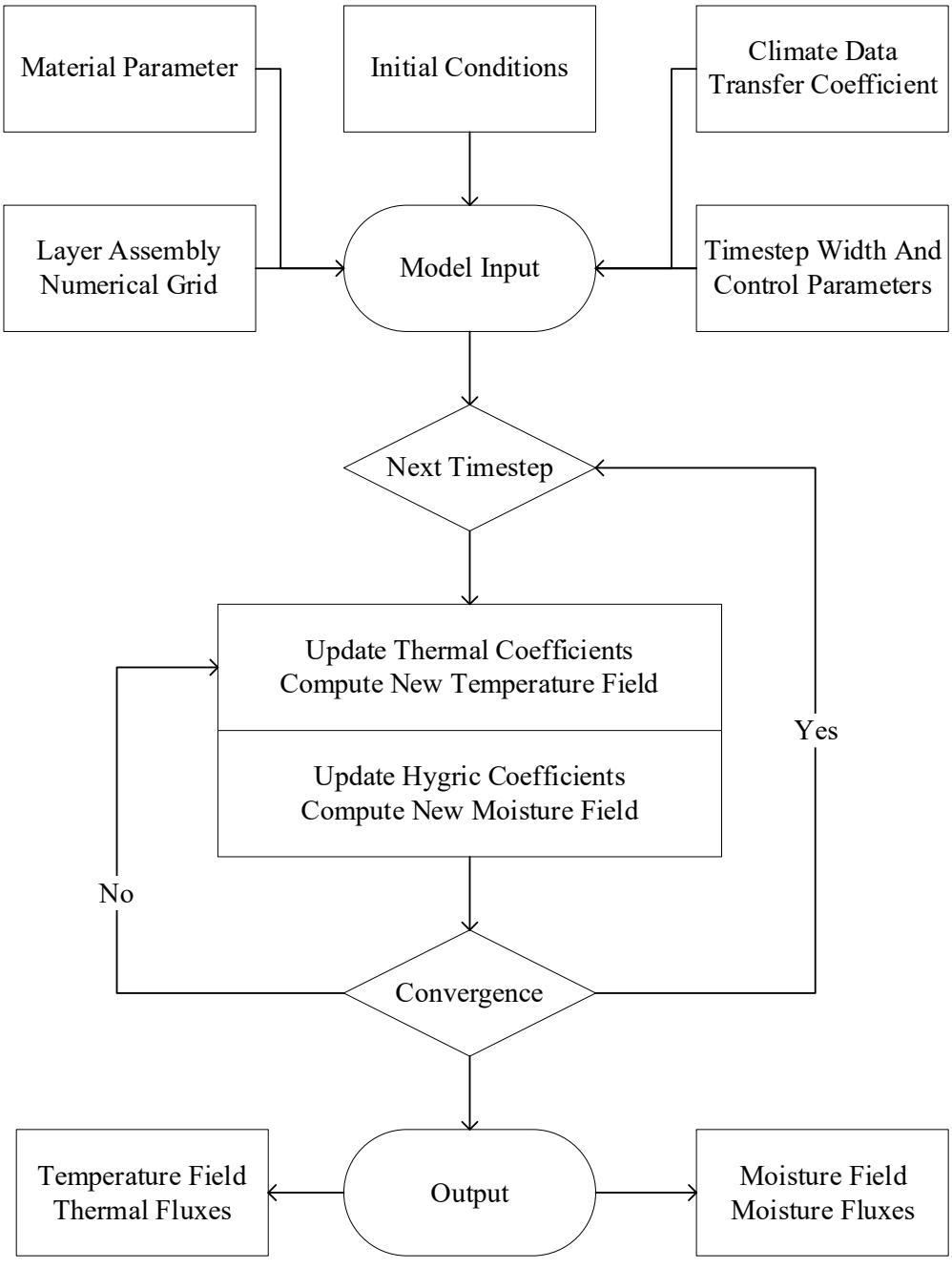

Figure 4-1: Flow chart used for the WUFI model [115]

Some limitations of the calculation model were tied to the time dependence of the material properties. Practically, during wetting and drying of capillary active materials may cause long-term irreversible changes in the hygric transport properties. Changes such as carbonation, material hardening or changes in pore structure for brick and concrete. The WUFI model does not account for these changes over the short- or long-term during calculation. These changes can be accounted for by creating multiple simulations with proper linking, coefficients, material properties and modified coefficients for annual changes, however, it may not be efficient as WUFI is not well suited to handling a chain of models that incorporate end conditions as initial conditions. The model does not include short-term time dependence of material properties caused by swelling or shrinking however, it is not expected that changes in material properties over time would produce a significant source of error for this study. Additionally, the long-term degradation of VIPs or other materials in 20+ year range were not included in the research scope, and as such material changes were not included in the modelling.

The software has a built-in material library and boundary conditions with hygric transport properties, indoor environment, and weather files. The library includes measured material and weather data from building science laboratories worldwide as well as engineered climate files for moisture design control and energy calculations. Specifically, the North American database includes collaborators from the National Institute of Standards, ASHRAE, RDH Building Science and the National Research Council, amongst others. The database includes most, if not all, materials required to build an enclosure such as insulation, building materials, masonry, air, and water membranes and building boards and siding. In the instance when a material is unavailable or properties need to be edited, new materials can be imported or created.

The WUFI library also contains interior and exterior boundary conditions. The indoor boundary condition, or indoor climate, has four different built-in boundary conditions available to the user. The indoor climates are based on international standards [30, 119, 120] and control the indoor temperature and relative humidity based on factors such as occupancy, outdoor temperature, design moisture load and air tightness. The outdoor climate includes weather files from ASHRAE 160 weather files for moisture-control design analysis in buildings as well as the ability to import or create weather files from other data sets.

4.3 Simulation Design

The hygrothermal performance of new and retrofit wall assemblies was going to be calculated using the WUFI model in both one- and two-dimensions. The basis of the wall assemblies as described in Chapter 1, as a wood-framed wall insulated with a combination of VIP and rigid foam insulation outboard. The numerical simulations were performed to represent new and retrofit construction and were used to verify the experimental results and further assess whether a VIP insulated wall assembly would be suitable under a variety of different circumstances, such as environmental conditions, control layers, exterior cladding, and initial moisture conditions. The boundary conditions, material properties, initial conditions and weather files selected for new and retrofit wall assemblies are described below.

4.3.1 VIP Wall Construction

The simulations were designed to represent the wall assemblies built, instrumented, and monitored at CE-BETH. A one-dimensional cross section was set up for the VIP insulated sheathing and another for the EPS insulated sheathing. The basic wall construction, shown in Figure 4-2 and described in Table 4-1 was used to evaluate the hygrothermal performance of the wall assembly. The materials were selected from the WUFI material database. The database

contained thermal and hygric properties for many building materials. The database has compiled measured material properties necessary for an accurate hygrothermal simulation from laboratories worldwide.

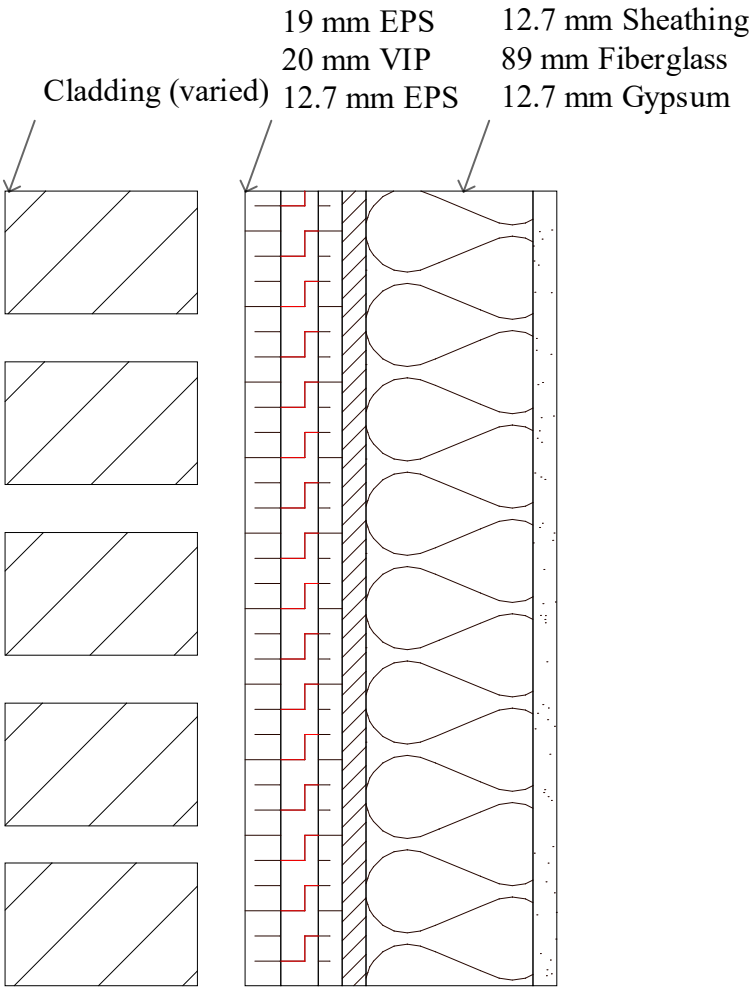

Figure 4-2: Generic layer assembly used in WUFI for hygrothermal analysis.

Table 4-1: List of materials used during WUFI simulation.

	Material	Thickness (mm)	WUFI Material Name
Layer 1	Vinyl Siding	10.5	Composite Wood Siding
Layer 2	Drain and Ventilated Rainscreen	20	20 mm Air Layer (no additional moisture)
Layer 3	Expanded Polystyrene	6.25	Expanded Polystyrene Insulation
Layer 4	Vacuum Insulation	20	VIP Generic (0.007 W/m^2K)
Layer 5	Expanded Polystyrene	6.25	Expanded Polystyrene Insulation
Layer 6	Weather-resistant barrier	0.1	60 min Building Paper
Layer 7	Oriented Strand Board	12.5	Oriented Strand Board
Layer 8	Fiberglass Batt Insulation	89	Low-Density Glass Fibre Insulation
Layer 9	Gypsum Board	12.7	Gypsum Board (USA)

*Material properties are provided in Appendix A.

The materials were selected from the North American sub-section and most of the materials were evaluated by ORNL or NRC. It was assumed that the materials used in the in-situ study had similar thermal and hygric properties as those used in the numerical study. The thermal data provided by the manufacturer was used in the modelling however, no hygric properties were provided so the defaults in the material library were used. The materials in the database are common materials, except for VIPs, and the hygric properties from the database were reviewed and found to be acceptable as they were measured from academic or research institutions, and manufacturer provided data. The VIP Generic (0.007 W/m^2K) was used in the simulation study,

and it was found to provide a suitable relationship for the material. The hygric conditions were similar as the material has a high water vapour diffusion resistance and low thermal conductivity. The exact composition of the VIP was not a relevant factor as the vapour barrier and thermal resistance provided by the material would cause the largest impact on the moisture resiliency of the assembly. One notable variable with the material as the thermal conductivity was independent of moisture and temperature. The issue is significant since during the first 5 years, it is expected that the moisture accumulation would not significantly change the VIP thermal conductivity due to the desiccant within the panel during the initial period. Also, the simulated thermal conductivity was higher than expected since the thermal conductivity for VIPs is lower at colder temperatures. As such, the material was deemed acceptable for use in the simulation.

4.3.2 Air and Moisture Sources

Since building envelopes experience wetting predominantly by bulk water, air transport and vapour diffusion, it was essential to properly model those sources through hygrothermal simulation. The air- and moisture-transport mechanisms are simplified in the model to ignore the solid-phase aspect of moisture (e.g., ice, frost) for porous materials in a multi-layered assembly.

Bulk wetting is liquid water introduced into the envelope because of wind-driven rain (WDR) penetration and rain run-off but could also be caused by leaks and system failures, that are not commonly modelled. The wind-driven rain was identified as the main bulk wetting moisture source in the enclosure. The cladding and water control layers are used to protect the enclosure from bulk water exposure; however, it is expected that a certain amount will penetrate those layers. There are driving rain models [121, 122, 123] to provide a simplified estimate of rainwater that impinges along with the cladding based on the total rain, wind speed and direction. Based on the modelling strategies proposed by Lstiburek et al. [124], it is assumed that 30% of the wind-driven

rain bounces off the wall, while 70% adheres to the cladding surface by capillary flow and vapour diffusion. Further, it was assumed that 1% of the 70% adhered to the wall assembly penetrated the backside of the cladding, and 1% of the 1% penetrates the water-control layer and enters the sheathing, as shown in Figure 4-3. The failure or imperfection of another system would lead to an unpredictable and challenging to quantify the amount that would vary on a case-by-case basis.

The 1% of WDR hygrothermal modelling assumption was evaluated against measured water entry using a scaled laboratory setup. Their findings showed that the 1% WDR assumption was very conservation for imperfections such as joints and penetrations [125]. However, since the assumption is recognized by ASHRAE 160 for moisture design, the 1% and 0.01% WDR moisture sources were used in the WUFI Pro and WUFI 2D. The sources were applied across the back 10 mm or 25% of the material, whichever was smaller.

The airflow through the building enclosure is a three-dimensional phenomenon that will be represented in a one-dimensional model. Twelve airflow pathways for exfiltration and infiltration in a built multilayer wall assembly can be identified in a building envelope [124]. The airflow pathways can be approximated for modelling into four airflow pathways: ventilated rainscreen, inner lining leakage, outer lining leakage and the insulated sheathing leakage. The sizes and air change rates of airspaces for different cladding options are provided in Table 4-2 and were incorporated into the WUFI model.

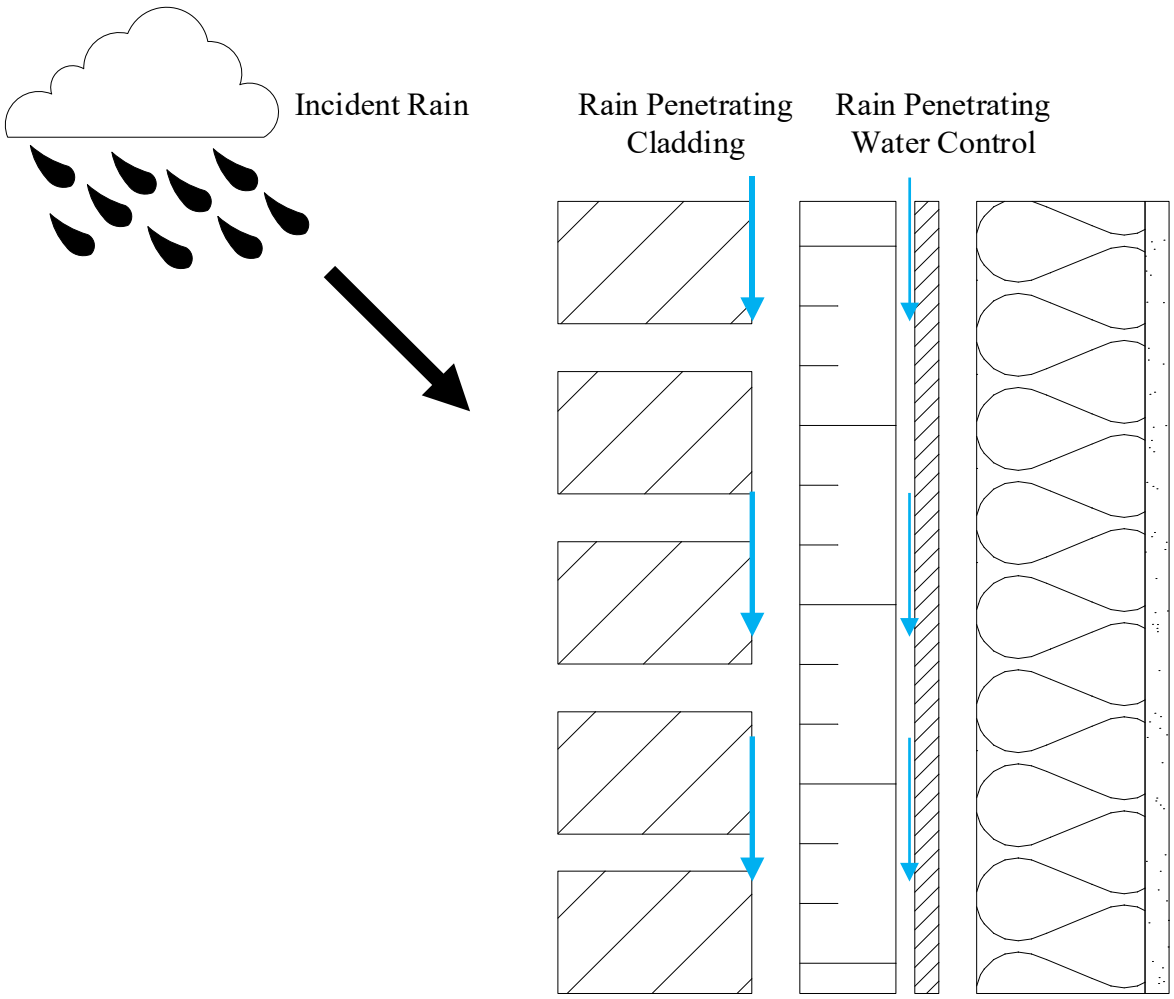

Figure 4-3: Wind-driven rain wetting mechanisms in a wall according to J. Lstiburek et al. [124]

The four pathways are shown on a simplified drawing of a wood-framed wall section with the outdoor air on the left and the indoor air on the right in Figure 4-4. The ventilated rainscreen is modelled using the built-in air gap connected to the exterior air with a high air change rate. The other leakages were approximated by adding a 5 mm airspace at the appropriate locations. Two airspaces were placed at the interface of the cavity insulation and the sheathing to represent the inner and outer lining leakages. The inner lining leakage is connected to the interior air and simulates the movement of air transported from the conditioned interior into the insulated cavity.

The outer lining leakage is coupled to the outdoor air and simulates the infiltration of the exterior air into the insulated cavity. In the case of an assembly with an insulated sheathing, a 5 mm airspace was included at the interface of the exterior insulation and the sheathing. The airspace was coupled with the exterior air and simulates the outdoor air flanking behind the insulation. These air flows are used to simulate imperfect assemblies and are used for a conservative estimate of durability.

Table 4-2: Ventilation size and rates for airspaces in multilayered assemblies [124]

	Flow Rate (m^3/h per m^2)	Gap (mm)	ACH (1/h)
Wood Siding	0.17	5	20
Vinyl Siding	0.85	5	200
Brick Veneer	0.25	25	10
Stucco (vented	0.17	10	10
Stucco (directly applied)	n/a	n/a	0
Sheathing Leakage*	0.085	5	10

* Refers to outer-lining leakage, inner-lining leakage, and insulating sheathing leakage.

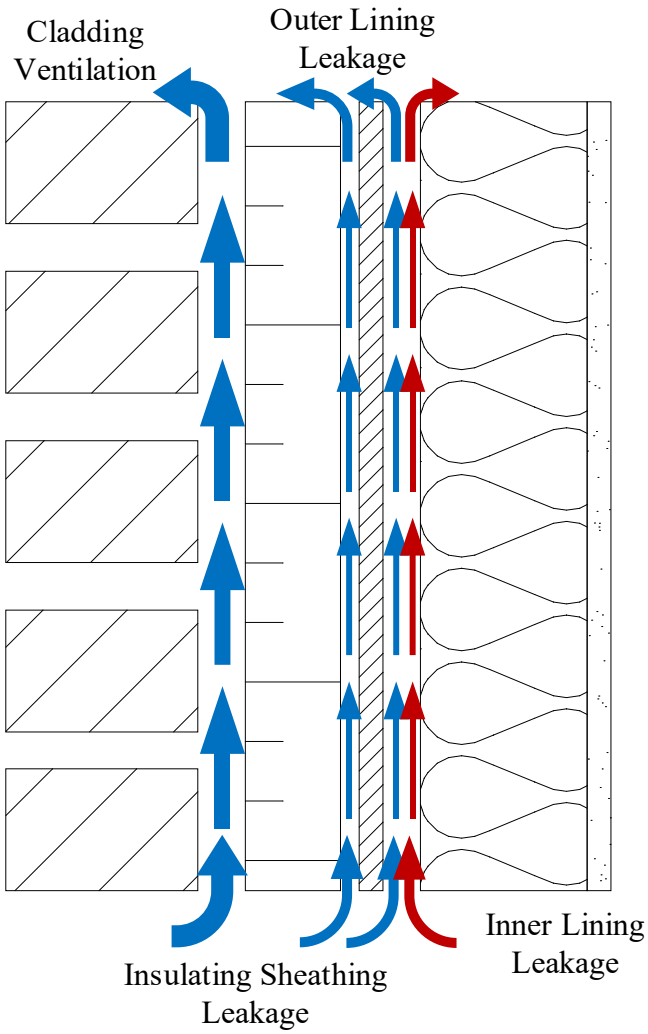

Figure 4-4: Airflow mechanisms in a wall according to J. Lstiburek et al. [124]

In the context of the wall assemblies with VIPs, these air and moisture sources are important to integrate into the simulation because the VIPs cause a lower drying potential in the assembly. The air and moisture sources are integrated into the material assembly provided in the previous section and are represented in WUFI as shown by Figure 4-5.

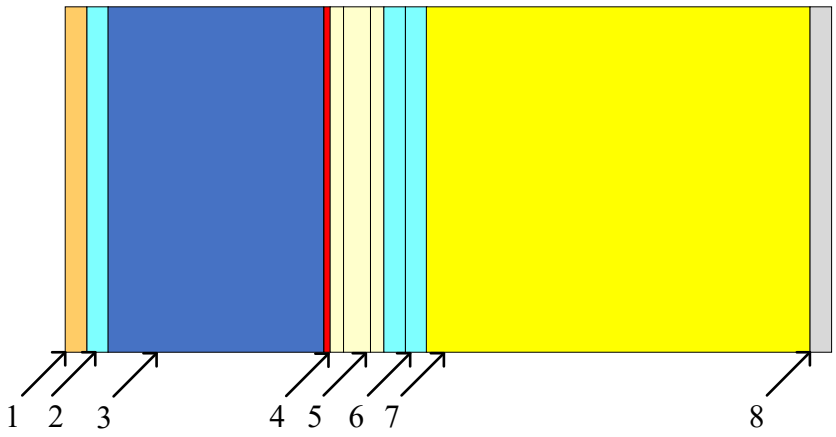

Figure 4-5: WUFI geometry includes materials, air spaces and moisture sources.

1. Exterior Cladding with 1% WDR moisture source at the interior surface
2. Ventilated air space with 25-100 ACH air source tied to the exterior air
3. Exterior insulation with 10 ACH air source tied to the exterior air
4. Air control layer
5. Wood sheathing divided into 3 components with a 0.01% WDR moisture source at the exterior surface
6. Air layers with outer and inner lining leakage with two 10 ACH rates
7. Inboard insulation
8. Gypsum board with vapour control layer

4.3.3 Initial Conditions

The material initial conditions differed depending on whether new or retrofit construction was being simulated. The temperature and relative humidity or moisture content of each material and airspace in the geometry need to be assigned by the user. The initial conditions can be assigned as a constant temperature and relative humidity across the assembly or assigned by each material or node, if that resolution is required.

For new construction, the initial conditions of the materials were assigned as a constant 20°C and 80% RH for the whole assembly. These values were assumed based on the expectation that the materials would be able to dry if there were exposed to a rain event during construction.

These values are likely to vary during the construction process for a building fabricated on-site. The values could have a significant amount of variance for uncontrollable factors such as rain events, leaks before completion and the season when the construction was completed.

These initial temperatures and relative humidity would be different for a prefabricated unit built in a covered facility. The initial moisture content would be lower with a prefabrication method since the duration of on-site construction before the materials are wrapped would be shorter. A prefabricated building could still be exposed to wetting during the installation on-site. However, the period for that to occur is much smaller and therefore the risk of enclosing wet materials is significantly lower.

For retrofitted assemblies, the conditions of moisture and relative humidity would vary building by building. The assembly, indoor and outdoor conditions, and orientation would greatly influence the initial conditions for a building undergoing an exterior envelope retrofit. WUFI can be used to determine what the approximate initial conditions could be for the existing building enclosure, while the materials used to complete the retrofit with initial conditions are consistent with new construction.

For the simulations presented, the following structure was followed to assess the performance of new construction and retrofit construction with VIPs. Using the logic presented in Figure 4-6, the final MC/T profile is used as the initial conditions were selected for the hygrothermal simulations of retrofit construction.

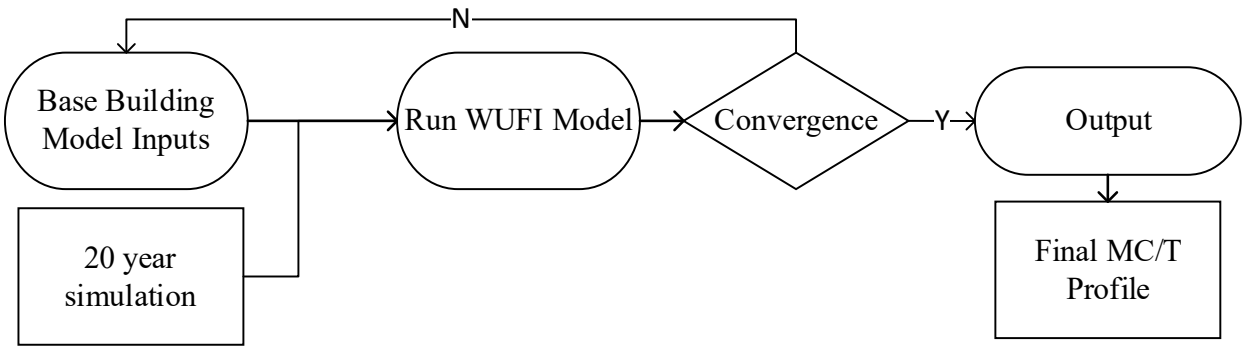

Figure 4-6: Process for determining the initial conditions for the materials using WUFI Pro

4.3.4 Boundary Conditions

The indoor and outdoor boundary conditions were selected based on the expected in-use conditions and common practices from building science experts. The indoor conditions provided in the simulation are the time series of temperature and relative humidity. For moisture control design, there are guidelines provided by ASHRAE 160 [30], EN 15026 [119] and ISO 13788 [126]. ASHRAE 160, the American standard, indoor climate used the outdoor temperature, building volume, air exchange rate, air conditioning type and a defined moisture generation rate to determine the indoor temperature and relative humidity. While at first glance this may seem more accurate, the increased number of inputs may lead to increased uncertainty due to the number of assumptions needed to create the indoor climate. The European standard, EN 15026, generated the indoor climate based on a simpler set of conditions. The indoor climate was based on the outdoor temperature and a moisture design load that can be varied between low, medium, and high. Finally, the ISO 13788 indoor climate used a constant temperature during the simulation but varies the indoor moisture load with the outdoor climate temperature. The indoor boundary conditions can be adjusted to fit your region and modelling requirements. If a simplified indoor climate was desired, the temperature and relative humidity can be represented by a sine curve with a user-defined mean value, amplitude, and date of peak values.

The software has a library of climate files for over 140 cities worldwide. There are specific parameters that must be included in the outdoor climate files to compute the calculation: outdoor temperature and relative humidity, normal rain and wind vectors or wind-driven rain, solar radiation data unless the component under investigation was completely shaded and barometric pressure. These parameters have the biggest effect on moisture damage and drying potential in building envelopes and are required to have an accurate simulation. Other parameters that could be included were cloud cover and long-wave irradiation however, these have a much smaller impact on the thermal and hygric calculations and performance.

The WUFI built-in climate library has weather files for moisture design created by ASHRAE and ORNL focused on North American cities. For example, Ottawa, CA has 5 weather files built into the software: Cold Year, Warm Year, ASHRAE Year 1, ASHRAE Year 2, and ASHRAE Year 3. The Cold and Warm Year weather files were created by ORNL based on the raw weather data from ASHRAE to provide a reference cold and warm year for energy system and moisture control design. The ASHRAE Year was a dataset used to represent the most severe moisture conditions related to building envelopes according to ASHRAE RP-1325 [127]. These datasets were considered the three most severe weather conditions for moisture damage out of the measured 10-year period. Otherwise, user-defined weather files, such as measured data or prepared datasets for moisture design, can be imported into the software and used as the outdoor climate. When the data in the weather file is inaccurate or missing, it is possible to interpolate between the data points in most cases. Hygrothermal effects are slow, therefore any short-term events in the weather file have a minor effect on the long-term result.

4.4 Comparison to Measured CE-BETH Data

The in-situ measured data was compared to the validated hygrothermal model, WUFI Pro 6.1. The measured boundary conditions from CE-BETH and laboratory measured material properties at the Carleton University laboratory were used in the WUFI model. Otherwise, best practices were used to assume the air and moisture sources. There were uncontrolled and unmeasured variables in the model that could not be directly measured or accounted for during the monitoring.

The initial design iteration of the VIP integrated building envelope included thermal and hygrothermal experimental evaluation. The composite panels were exposed to the environmental conditions beginning in October 2016 with data collection beginning at the end of January 2017. The conclusions from the data are valuable pieces of information that may be used to determine the durability; however, their utility is enhanced by experimentally validating hygrothermal models. The hygrothermal modelling is 1-D or 2-D finite element computation of the heat and mass transfer through the building materials. The boundary conditions are interior conditions, exterior weather conditions, amount and location of rainwater penetration, and sun exposure.

The initial data of the in-situ monitoring was used to compared to a hygrothermal model of the two designed wall assemblies by using measured indoor and outdoor conditions, and material properties (e.g., VIP thermal conductivity) from laboratory studies performed at Carleton University. The interior conditions from CE-BETH were set to 21°C and 40% RH during the heating season and 22°C and a free-floating relative humidity during the cooling season, frequently above 60% RH indoors. The simulated exterior boundary conditions used weather data from a local weather station nearby the test facility and supplemented by the Ottawa airport weather station if there are significant gaps in the monitoring. The readings include temperature, relative

humidity, dew point temperature, precipitation, wind velocity, horizontal radiation, and diffuse radiation.

Thermal and moisture readings from the experiment and simulations were compared to using the root mean squared (RSME) method. The measured temperature and relative humidity was compared to the modelled values over the duration of the test period. The most accurate sensors in the assembly were selected for comparison and when the RSME is within the sensor error, it is assumed there is good agreement between the model and measured values.

The VIPs used in the assembly do not have homogenous thermal conductivity and will vary near the edge of the panel. To capture these effects, the VIP center of panel thermal conductivity provided by the manufacturer and experimentally measured thermal conductivity (center and edges) will be modelled.

The moisture content and relative humidity were measured at various locations in the wall assembly from October 2016 until September 2020 and will be compared with the hygrothermal model. The moisture content calculations from the hygrothermal simulations will be compared to the measured values from CE-BETH.

There will be challenges associated with this process since the control of the in-situ test facility and detection of air leakage paths has encountered difficulties and equipment failure (e.g., water penetration and power outages during the test period). However, the process will be performed nonetheless since the ability to properly validate the models with experimental data increases the confidence when different assemblies for new and retrofit construction in Ottawa and across Canada are evaluated.

The quality of workmanship, improper detailing, and material degradation over time may lead to unpredicted hygrothermal performance. The hygrothermal model does not allow for defects

and material decay to be incorporated into the simulation however, moisture sources and material properties can be adjusted to account for the imperfections. When the experimental results are compared to the model, using these adjustments would be useful in correlating wetting and drying mechanisms within the assembly. In isolation, this would be too conservative of a durability assessment since the wall assembly the exposure to worst-case conditions that could be a symptom of worse problems in the envelope. There would be a significant benefit in assessing the incremental impact of each potential imperfection or input parameter to the model.

Additionally, the collected data were compared to the results from a WUFI 2D model. Since the moisture transfer in the system is three-dimensional, it is expected that a 2D model will better represent the measured data when symmetry in the panel is assumed. The measured boundary conditions and material properties used in the WUFI Pro simulations were also used in the 2D simulation, along with best modelling practices for above-grade wall hygrothermal modelling.

4.5 Parametric Study

After validating the hygrothermal modelling of a wall assembly in Ottawa, Canada with the experimental data, performing simulations with varied input parameters is needed. This run of simulations is needed to determine the effects of (1) different construction practices, (2) the current state of the building envelope during retrofit or (3) imperfections in building materials or barriers have on the durability and robustness of the designed assembly.

The sensitivity analysis (SA) was defined as the capacity of the model to respond to changes in the simulation. The SA objective was to assess the WUFI's response to changing inputs and its relation to the impact on the durability of highly insulated building envelope design, specifically vacuum insulated envelopes. The SA covered many process variables therefore a

screening process was used to limit the complexity and number of simulations required. The WUFI sensitivity study was performed by simulating an Ontario code-built wall assembly using the Ottawa weather files as the outdoor boundary condition. For comparison purposes, the moisture content, relative humidity, and temperature of the sheathing throughout the simulated period from each simulation were exported. The mould index calculated from humidity and moisture content was used to evaluate the model response to the input changes. In addition to the comparison between each simulation, the cases were evaluated against the failure criteria.

4.5.1 Process Variables

The set of process variables for the SA was determined through literature, controls and boundary conditions, assumptions in modelling wall assemblies and specific construction details. From each simulation, the relative humidity and moisture content for each time step will be output and compared to the failure criteria proposed previously as well as the baseline performance. The selected process variables are included in Table 4-3 with the prescribed set-points.

For cold climate buildings, it is important to control the interior moisture load since vapour diffusion or convention can drive moisture into the wall assembly from the interior. Elevated moisture conditions can be caused by a lack of dehumidification during high moisture load events, such as cooking, bathing, and high occupant density. During these periods, the air can be exhausted or controlled however, there may be some vapour may escape through the envelope.

The warm, moist air can leak through the assembly with the risk of condensing on a cold surface. The response from the wall assembly and its ability to allow excess moisture in the assembly to dry after these periods of elevated moisture is an indication of its drying potential and long-term durability. For the parametric study, it was decided to represent the interior conditions using a SINE curve and vary the peak and average annual relative humidity. The varying relative

humidity profile could illustrate (1) a lack of humidity control resulting in higher peaks in the summer and (2) a high occupancy building with higher annual mean humidity. It is important to evaluate these parameters since the interior conditions are closely tied to the moisture levels observed inside the walls.

Table 4-3: Variations for initial conditions and inputs to the hygrothermal software

Model inputs	Inputs Levels		
Indoor Conditions	Sine Curve (low)	Sine Curve (med)	Sine Curve (high)
Wetting Plane	Inboard of cladding	Inboard of rainscreen	Outboard of WRB
Amount of wind-driven rain	1.0%	2.0%	5.0%
Initial moisture	80% RH	85% RH	90% RH
Construction completion	Spring (May 1st)	Summer (July 1st)	Fall (Oct. 1st)
Outboard construction	XPS with rainscreen	EPS with rainscreen	XPS without rainscreen
Vapour Control	Interior vapour barrier	Interior vapour permeable barrier	No interior vapour barrier
Orientation	East	North	South
Timestep	1 hr	0.5 hour	0.33 hour

The wetting plane is where the wind-driven rain passes through the cladding and is deposited within the assembly. Rainwater penetration is a source of bulk moisture load in the assembly; however, buildings are constructed to limit the amount of bulk moisture penetration. Overhangs and drainage planes are effective features of an envelope for limiting bulk moisture penetration. Overhangs are located at the top of the wall and limit the amount of rain that encounters the wall, while the drainage plane is located behind the cladding where any penetrating water can drain or dry out. Commonly, the wetting plane is inboard of the cladding (drainage

plane), however in different constructions or assemblies with imperfections, the rainwater can penetrate up to or beyond the weather resistance barrier as a worst-case scenario.

The amount of moisture penetration is another issue caused by wind-driven rain onto the assembly. Even a small amount of bulk moisture in an assembly can cause issues and the assembly will need the ability to dry out. The amount of penetrated bulk water can vary by construction and imperfections however, ASHRAE suggests that 1.0% of the wind-driven rain penetrating the assembly should be used to represent a leak at the wetting plane during simulations. This value was adjusted up to 5% to represent the worst-case scenario that is likely to be seen in construction, according to ASHRAE [30]. Varying the input fraction of bulk moisture levels penetrating the envelope to wind-driven rain onto the vertical surface in the simulation tool, the drying potential when exposed to high levels will be assessed.

During construction, the building materials are exposed to environmental conditions without protection which causes elevated moisture contents in the building materials after completing construction. This initial moisture content of the materials is described as construction moisture and could be detrimental if the assembly is not able to dry from the initial conditions. The construction moisture content of the sheathing or vertical framing members can reach values of 30% to 35% at the beginning of the test period and those values were used in simulation tools to evaluate the drying rates. Another factor of construction moisture is seasonally when the construction is completed, depending on whether the moisture is being driven inward or outward through the assembly. The sensitivity study on construction moisture and completion with construction moisture values of 25%, 30%, and 35% while also varying the season of completion to spring, summer, and fall.

The final components that will be varied through the sensitivity study are the orientation of the envelope and the materials in the assembly. Sun exposure on the vertical wall assembly impacts the vapour drive in the assembly and temperature gradient which are directly related to the moisture levels within the assembly. The sensitivity of vertical wall to facing direction will be assessed by varying the facing direction from North, South, and East/West. East and West facing envelopes do not experience significant differences in sun exposure when compared to the difference between North and South facing vertical walls. In addition to the facing direction of the vertical wall, the amount of exterior insulation and vapour control layers will be varied. The initial designs had a similar thickness of exterior insulation with differences in VIP performance and vapour control layers. For the sensitivity study, the coverage area of VIP and interior vapour control layers will be varied. The VIP coverage affects the vapour permeability of the exterior insulation and the effective thermal resistance. Eliminating or limiting the interior vapour control increases the interior moisture to move through the assembly through diffusion or convection. The two parameters are related since the VIPs have been shown that they act as a vapour barrier exterior of the sheathing and could entrap moisture within the assembly causing long-term durability issues. Therefore, the two parameters will be varied and determine what combination of VIP coverage and interior vapour control creates durability issues within the assembly.

After this study, the results were used to help with input selection for the following broader study of high-performance building envelopes (new construction and retrofit) in different locales operated under different interior conditions.

4.5.2 Morris Method

There are many variables included in the study that would cause an intensive computationally intensive global SA. Therefore, a screening process was used to determine the

relative effect of the inputs by lowering the number of required simulations by discretizing the inputs into levels. The non-influential inputs can be found with a small number of simulations, and a simplified SA can be performed. A screening method called "One At a Time" (OAT) design was selected and followed the Morris method [128]. The inputs were classified into 3 groups when implementing the Morris Method: negligible effects, linear effects, and non-linear effects. In this sense, the Morris method of sampling is qualitative but is capable to rank the inputs from greatest to least effective.

Through the Morris method to screen the input variables, the total number of simulations needed was much lower. The number of required simulations is $N = r(k + 1)$, where k is the number of inputs and r is the sample size. Since there were ten input variables assigned three levels each the Morris method requires 36 simulations are required to screen the inputs. The screening method is like a global sensitivity analysis; however, it requires much less computational time. A limitation of the process is that the results do not quantify the effects of the inputs on outputs and do not allow self-verification.

The simulation matrix was created using a random number generator in Excel to select the level for each input parameter. The randomly selected input parameters for 36 simulations were run using WUFI Pro 6.5. From the hygrothermal model, the inner and outer OSB sheathing surface relative humidity and temperatures were exported and used to calculate the mould index for each simulation. The peak mould index from each simulation was used as the output for the function, and the elementary impact, E_j^i, was calculated using Equation 4-7.

$$E_j^i = \frac{f(X^i + \Delta e_j) - f(X^i)}{\Delta} \qquad 4\text{-}7$$

where X^{i} is the i-th input and Δe_{j} is the incremental change of the j-th input. The elementary impact is calculated for every simulation and is used to find the influence and non-linear effects of the input on the model through Equations 4-8 and 4-9

$$\mu_{\mathrm{j}}^{*} = \frac{1}{r}\sum_{\mathrm{i}=1}^{r}\left|E_{\mathrm{j}}^{\mathrm{i}}\right| \tag{4-8}$$

where μ_j^* is a measure of the influence of the j-th input on the output. The larger the value, the more the j-th input contributes to the dispersion of the output.

$$\sigma_{\mathrm{j}} = \sqrt{\frac{1}{r}\sum_{\mathrm{i}=1}^{r}\left(E_{\mathrm{j}}^{\mathrm{i}} - \frac{1}{r}\sum_{\mathrm{i}=1}^{r}E_{\mathrm{j}}^{\mathrm{i}}\right)^{2}} \tag{4-9}$$

where σ_j is a measure of non-linear and/or interaction effects of the j-th input. If the value is small, elementary effects have low variations on the support of the input.

Thus, the effect of a change is the same all along the support suggesting a linear relationship between the studied input and the output. If larger, less likely the linearity hypothesis is. Thus, a large value will be considered to have non-linear effects or be implied in interaction with at least 1 other variable.

The Morris Method, a local sensitivity analysis, was selected instead of a global sensitivity analysis, such as the Sobel and Monte Carlo methods, due to the complexity involved with designing the input files for WUFI given the large number of input variables and levels that were desired. The Monte Carlo method is used to predict the possibility of a variety of outcomes by assigning a random number with a range of a variable in the model and repeating to attain an estimate of the uncertainty [129, 130]. The method required many more numerical results that were not efficiently possible using the WUFI Pro software. However, the Morris Method, while required

$n(k+1)$ simulations, the number was far less than the Monte Carlo methods for estimating error. Due to the limitation in software, the Morris Method was selected to screen the input variables for the impact and uncertainty.

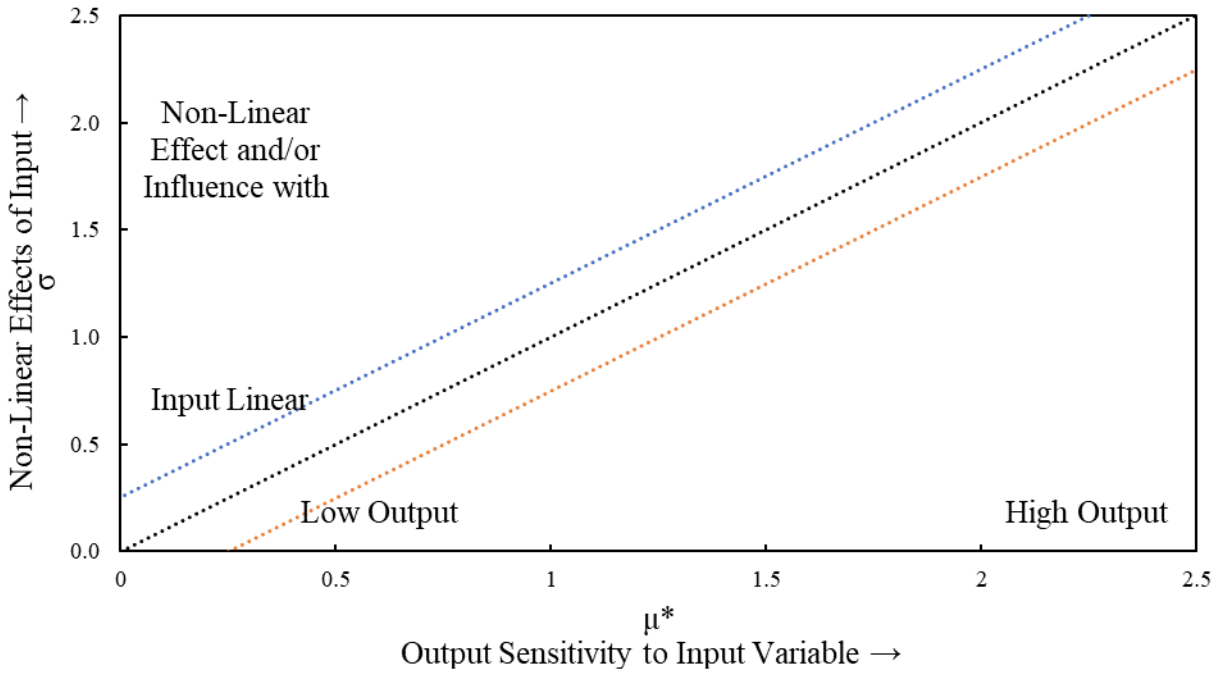

Figure 4-7: Examples plot and regions of interest for the Morris Method parameter screening

4.6 Assessment for Canada

After the sensitivity of the variables was determined, the hygrothermal performance of the proposed wall assemblies across Canada could be simulated with greater confidence.

4.6.1 City Selection

The objective for varying the climates used in this study was to evaluate the building envelope solutions across Canada. The variety of climates includes (1) cold and wet (2) cold and dry (3) very cold and dry (3) moderate and wet (4) moderate and dry. The selected locations would give an indicator of whether the building envelope designs would be durable in Canada, or it would highlight their limitations in certain regions. The mean temperature and annual driving rain were

the main influencers of long-term hygrothermal performance, however, the amount of solar and orientation may also impact the results, but not to the same extent as the former variables.

Table 4-4: Weather information about selected climates

City	HDD (°Day)	CDD (°Day)	Mean Temperature (°C)	Max Temperature (°C)	Min Temperature (°C)	Annual Driving Rain (mm/a)
Ottawa, ON*	4311	344	6.5	33.9	-35	779.9
Quebec, QC*	5131	127	5.1	32.2	-29.4	964.2
Vancouver, BC*	2776	71	9.1	27.2	-11.1	1169.1
Winnipeg, MN*	5708	202	2.3	32.2	-40.0	585.3
Calgary, AB*	5110	46	2.7	30.6	-30.6	450.6
Edmonton, AB**	5439	62	1.9	28.0	-36.0	566.3
St. John's, NFLD*	4703	30	4.1	26.1	-17.2	1116
Whitehorse, YK***	7171	4	-1.6	18.4	-21.1	310

**According to ASHRAE Year 1 weather files*
***According to ORNL standard weather files*
****According to CWEC files*

By varying the location and climate across Canada, the feasibility of the retrofit solutions can be assessed. This information would provide insight into how each high-performance construction can be implemented nationwide and the risks associated with that location. It is

anticipated that some solutions that are feasible in Ottawa may fail in Vancouver since their exterior conditions are different. The list of selected cities is provided in Table 4-4.

4.6.2 Above-Grade Wall Construction

The suggested vintages were based on the updates to the building codes as well as descriptions found through the National Energy Use Database [131], EnerGuide for Houses database [132] and Survey of Household energy use [133]. For each vintage, a cladding of brick, wood siding and vinyl siding should be considered based on their usage in the building stock. The lumber used before 1984 was commonly 2x4 filled with batt insulation on 406 mm (16") O.C spacing however, the R-value increased over time as the industry developed insulation with lower thermal conductivity. However, it is possible to see 600 mm (24") O.C spacing for new constructions in 2019, which would provide sufficient structural strength and a higher effective R-value for the envelope. For vapour barriers and membranes, interior vapour control layers (e.g., 6 mil polyethylene and kraft paper) were used after 1961, and kraft paper has been sparingly used in Canada since 1978. The exterior vapour control layers have changed as materials improve, however some form of building paper on the exterior sheathing has always been used. Finally, the sheathing could have been applied to the exterior without insulation outboard, which could have residual moisture effects on the sheathing. This could lead to high moisture levels in the sheathing depending on the season that the retrofit takes place, which is an important consideration for these simulations.

Retrofitting the building envelope is a solution that offers many practical challenges. These challenges include initial moisture levels caused by the envelopes being in service, adapting the assembly to reduce the risk of moisture-related issues long-term, and changing the air leakage paths through the assembly. These moisture-related challenges must also be balanced with

attaining the high thermal performance goal and construction challenges of applying added insulation to an existing building. Those issues are limiting the progress or applicability of these types of projects but could be a positive way to facilitate the use of high-performance insulation in the building sector.

One method to ease the construction difficulties of retrofits would be to include an element of prefabrication in the process. From this prefabricated process, a wall panel (e.g., structural insulation panel, wood-framed, etc.) would be manufactured and sized for the building undergoing a retrofit. Since these panels were completed in a controlled setting it would be an opportunity to insulate the assembly with VIPs. The VIPs could be embedded within the wall panel and would be installed off the construction site. This would have a greater chance of maximizing their lifespan.

The outcome of this research was a substantial assessment of the durability of retrofitting many different vintages and constructions of homes in Ottawa. Additionally, the long-term moisture performance of high-performance retrofit panels was evaluated. Following the assessment of vintages and retrofits in Ottawa, Canada, the simulations will be modified to understand whether the same retrofit solutions applied in Ottawa, can be applied nationwide however, Canada possess a wide array of outdoor conditions.

4.7 Summary

In total, 3 numerical models were used to evaluate the thermal and hygrothermal performance of the VIP insulation system. THERM was used to simulate the steady-state heat flow conditions through the assembly and calculate the expected thermal resistance including the thermal bridging. WUFI Pro was used to simulate the hygrothermal performance of a VIP insulation system in Ottawa as well as 9 other Canadian cities that have different outdoor climate

conditions. The simulation inputs were screened using the Morris Method. A validation study was performed using WUFI Pro with the measured boundary conditions from the in-situ monitoring. Finally, a WUFI 2D model was used to evaluate the clear field wall of the insulation system. The calculated moisture and temperature from WUFI 2D would be compared to the WUFI Pro and in-situ results for the same position in the wall assembly.

From these studies, the long-term durability, and the feasibility of vacuum insulation panels for a high-performance enclosure were assessed.

Chapter 5: Experimental Results

The following Chapter presents the experimental results from vacuum-insulated panelized wall systems evaluated using the guarded hot-box and the CanmetENERGY Building Envelope Test Hut (CE-BETH). The vacuum insulated wall assemblies were evaluated according to the experimental method described in Chapter 3. The boundary conditions and monitored data for the in-situ VIP insulated assemblies are presented.

5.1 Steady-State Thermal Performance

The insulation panels were evaluated under steady-state conditions within the guarded hot-box to measure the effective thermal resistance and thermal resistance of the VIPs. In summary, the insulation panel uses a 50% VIP coverage area intending to improve the constructability and moisture performance of the system, with an anticipated slight reduction in thermal performance. The unknown reduction in effective thermal resistance was expected by reducing the coverage area of VIPs and replacing it with high thermal conductivity insulation, such as EPS. The guarded hot-box was used to measure the insulation panel performance, and ensure it met the minimum requirement of R-4.2 m^2K/W (R-25 $h \cdot °F \cdot ft^2/BTU$).

A structural insulation panel (SIP) and a composite insulation panel (CIP) with VIP and EPS insulation were designed. The SIP panel is an insulated sheathing product that featured an oriented strand board (OSB) backer for structural support. The panel type was designed to be applied to new homes; however, it would also be suitable for retrofit applications. The CIP design used EPS as the backer material. This panel would be used for retrofitting envelopes, where an additional sheathing or nailing base may not be necessary or could be applied as an exterior insulation panel for new homes. The two panel types included a combination of EPS and VIP as the insulation with printing on the exterior face to outline the VIPs to avoid puncture.

VIPs from different manufacturers were used to assess the impact on the overall thermal performance. Previous research has shown that VIP manufacturing and material processes impact the edge effects and effective thermal resistance of VIPs. In total there were 4 unique samples tested, one of each type of panel with a different set of VIPs. Each sample was evaluated at steady-state conditions as a complete wall assembly, as well as an individual component.

A 2x4 wood-framed wall at 16" O.C. with fibreglass batt-filled cavities, gypsum board and plywood sheathing were built and instrumented at Carleton University. The VIP-EPS samples were fastened onto the frames and installed in the guarded hot-box. Before beginning operation, 1x3 strapping and vinyl siding to replicate the whole assembly that would be built on-site.

Since this iteration of the project included evaluating VIPs with the same dimensions, the instrumentation strategies were similar for each test. Thermocouples were installed at each material interface to measure the temperature profiles through the assembly and assess whether steady-state conditions were met. Heat flux plates were added directly in line with the VIP, edge of the VIP and in line with the EPS gap to measure the change in heat flux of the unique cross sections. The instrumentation was installed in the VIP pocket during the initial sample fabrication at the manufacturing plant. Instrumentation was added before the VIPs were added to the EPS sheets, and before the final lamination of the backer material. After lamination, the instrumentation and VIPs are inaccessible without destructive testing since the back material is adhered to the VIPs and would destroy the panel if the backer was removed. Therefore, the instrumentation needed to be planned and placed carefully to limit any damage to the wiring. Unfortunately, there were a couple of thermocouples there were damaged during lamination and some adjacent sensors were used for the analysis.

The thermal performance of the assemblies was evaluated under steady-state conditions with the guarded hot-box and the results are summarized in Table 5-1. The high-performance assemblies are compared to a baseline assembly of the equivalent thickness of Type 2 EPS insulation as the exterior insulation as opposed to the VIP-EPS composite panel. It is apparent that the thermal improvements made by the VIP-EPS composite vary between 20% and 31%, however, remained below the minimum prescribed thermal performance in the project objectives. Figure 5-1 illustrates the measured steady-state conditions by the plotted temperature profile in the assembly. Over 24 hours, the temperatures were within 0.25°C except for the climate and metering surfaces that varied due to the mechanical equipment power cycling.

Table 5-1: Summary of steady-state effective RSI-value from guarded hot-box testing

Assembly	New Construction (m^2K/W)	Retrofit (m^2K/W)
Baseline	4.8 (nominal)	4.2 (nominal)
High-Performance – VIP1	6.3 (effective)	5.1 (effective)
High-Performance – VIP2	6.2 (effective)	-

Following the full-wall assembly evaluation in the guarded hot-box, the SIP and CIP insulation systems were installed in the guarded hot-box to measure the thermal resistance with the base wall excluded. The CIP and SIP systems were fastened to the guarded hot-box's surround panel, and in the case of the CIP, a plywood sheathing was included as well to provide structure for the panel. The panels were faced with a weather barrier on the exterior and spray foamed at the seams to reduce air leakage into the guarded hot-box. In addition to measuring the thermal resistance, two other items were of interest: (1) temperature profiles along the VIP surfaces for thermal bridging, and (2) non-destructive quality assurance that the VIPs remained intact during construction and instrumentation. To do this, extra thermocouples were added on either side of the

VIPs, and the guarded hot-box was set up in its infrared imaging orientation with the metering and guard chambers removed.

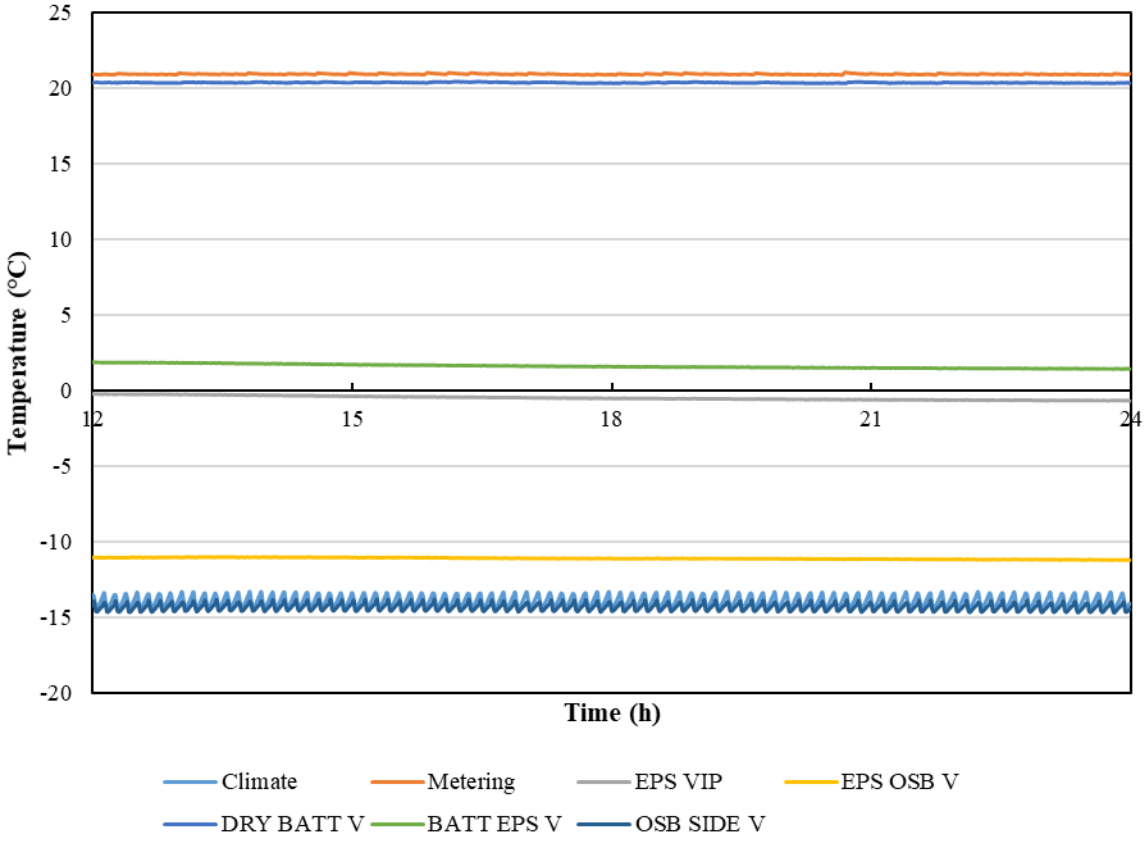

Figure 5-1: Measured surface temperature profile of SIP panel during steady-state testing in guarded hot-box

The guarded hot-box chambers were connected to monitor the steady-state conditions and measure the effective thermal resistance of the panels for a set of 5 consecutive measurement periods under steady-state conditions. Following the test period, the metering and guarded chambers were removed from the apparatus, and an infrared camera was used to capture the temperature at the sheathing surface. The captured infrared image in Figure 5-2 shows that the VIPs were intact based on the surface temperature being significantly warm that the surrounding area. The higher interior surface temperature showed a higher level of insulation from the EPS compared to the VIPs.

There are colder surfaces shown in the infrared image. Along the periphery, voids in the insulation system exist from the 1220 mm by 2440 mm (4’ by 8’) panels being cut to fit in the guarded hot-box. Additionally, the seam along the center is where the insulation panels were butted together. While it was filled with spray foam it still contributed as a significant thermal bridge. Unfortunately, under this test setup, the significance of the thermal bridges in the panel caused the effective thermal resistance to never reach the prescribed steady-state conditions. Therefore, the thermal resistance results were not successful.

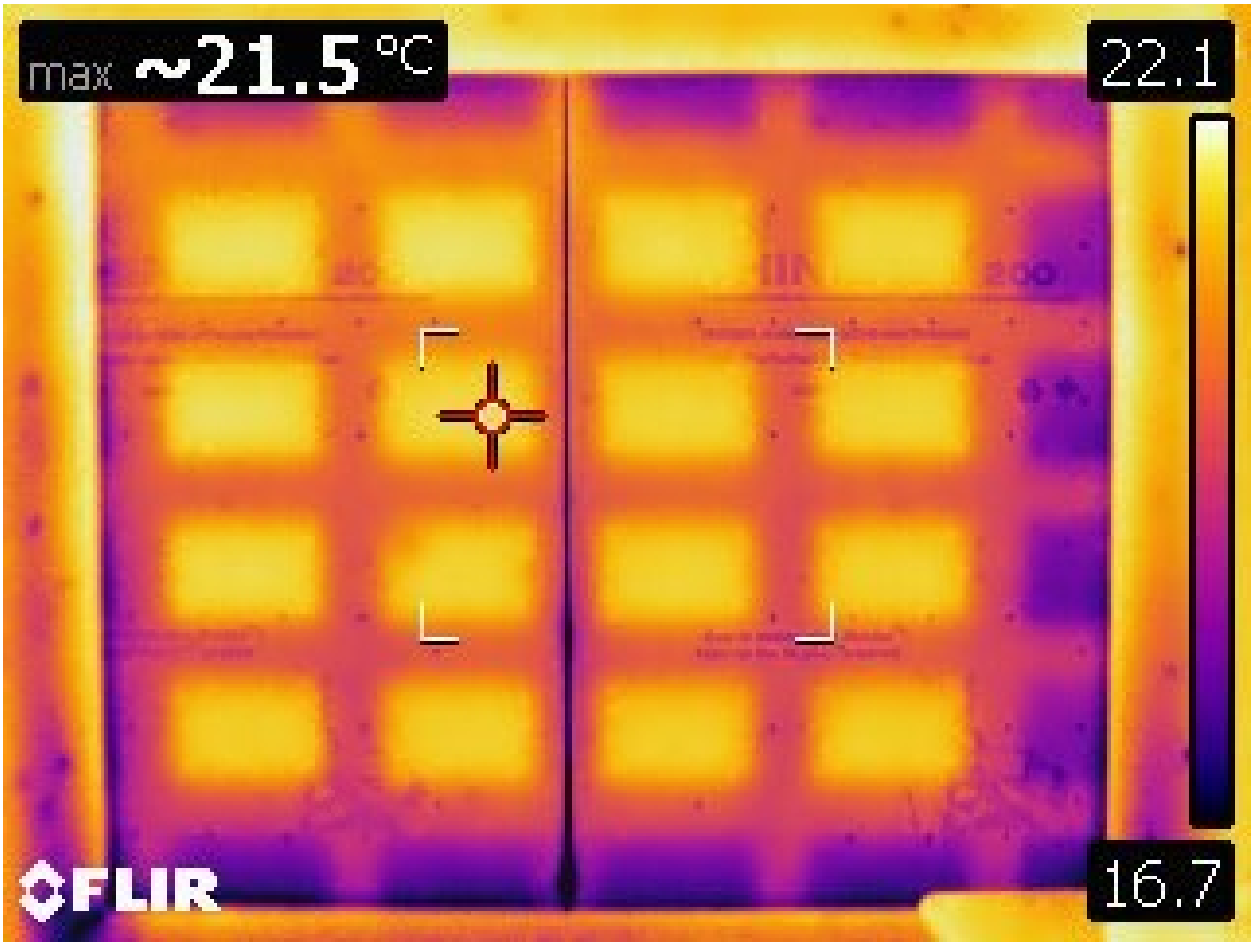

Figure 5-2: Infrared image from the retrofit EPS-VIP assembly, outlining VIPs

The first iteration of thermal resistance testing with VIPs from the first manufacturer was lower than expected. The overall drop in performance was attributed to higher than expected

thermal bridging or lower effective thermal conductivity of the VIP. Therefore, thermocouples were added inside the EPS pocket (warm-side of the VIP) to measure the temperature profile along the VIP surface and temperature difference across the VIP.

Thermocouples were placed at measured increments behind the VIP (within the EPS pocket) and on the VIP surface before the panel was laminated such that the sensors were embedded in the panel with the leads accessible on the outside. Under steady-state conditions, temperatures were measured and used to qualitatively assess the thermal bridges.

Instrumenting the pocket and the warm side of the VIP was better because that plane is insulated from the climate setpoint and its cyclic temperature. The temperature variation in the EPS pocket was heavily influenced by the change in apparent thermal conductivity and thermal bridge and was therefore a better interface to the instrument.

On the warm side of the VIP, a total of 6 thermocouples were added in the first 76 mm (3”) of each VIP edge and were placed in a straight line towards the center at 12 mm (0.5”) intervals, followed by 25 mm (1”) intervals along the long edge, shown in Figure 5-3. Thermocouples were not added at 12 mm intervals for the entire panel due to previous research, the temperature difference and edge effects of the VIP were limited to 50 mm (2”) from the edge. An extra inch of high-resolution instrumentation was added if the edge effects were more significant than other VIPs evaluated. Additional thermocouples were added in the top left and bottom right quadrants to verify the temperature profile behind the VIP.

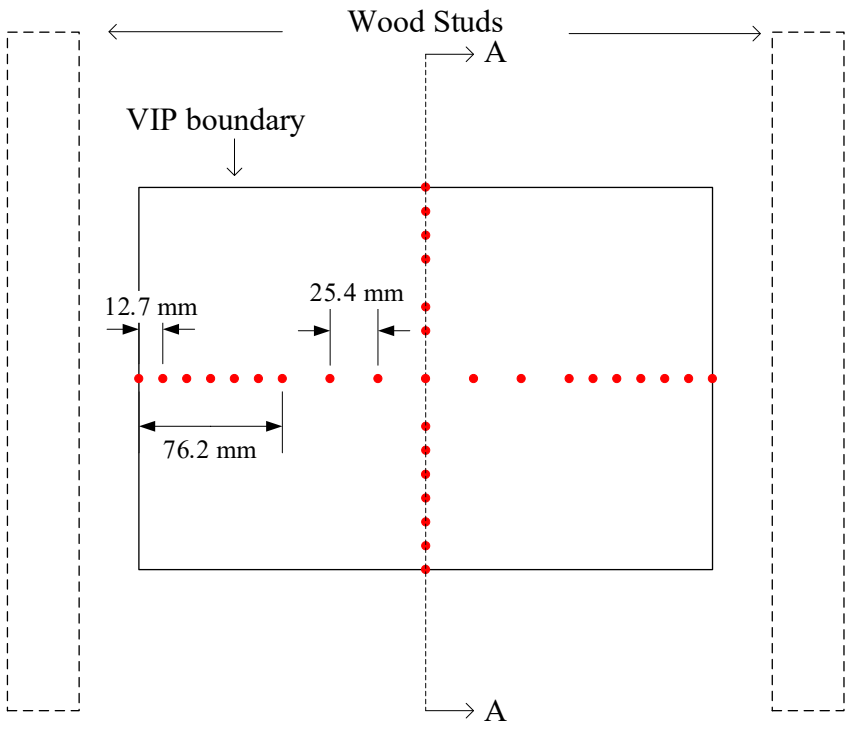

Figure 5-3: Thermocouples placed in the EPS pocket to measure the VIP inboard surface temperature

The CIP system with the heavily instrumented VIP pocket was installed on a base wall in the guarded hot-box with the 3 chambers connected. After steady-state conditions were met, the measured temperatures were recorded for 15 hours at 1-minute timesteps. The averaged value for each position was plotted in Figure 5-4, and the average temperature difference was plotted in Figure 5-5.

The measured surface temperatures inboard of the VIP and the area insulated by EPS showed that thermal bridging was located at the edges. Under steady-state conditions, a thermal bridge along the panel existed and the VIP thermal conductivity was not constant based on the inboard temperature plotted in Figure 5-4. At the edge of the VIP panel, a 3.5°C to 5°C smaller temperature difference compared to the center of the VIP, which indicates a lower thermal conductivity.

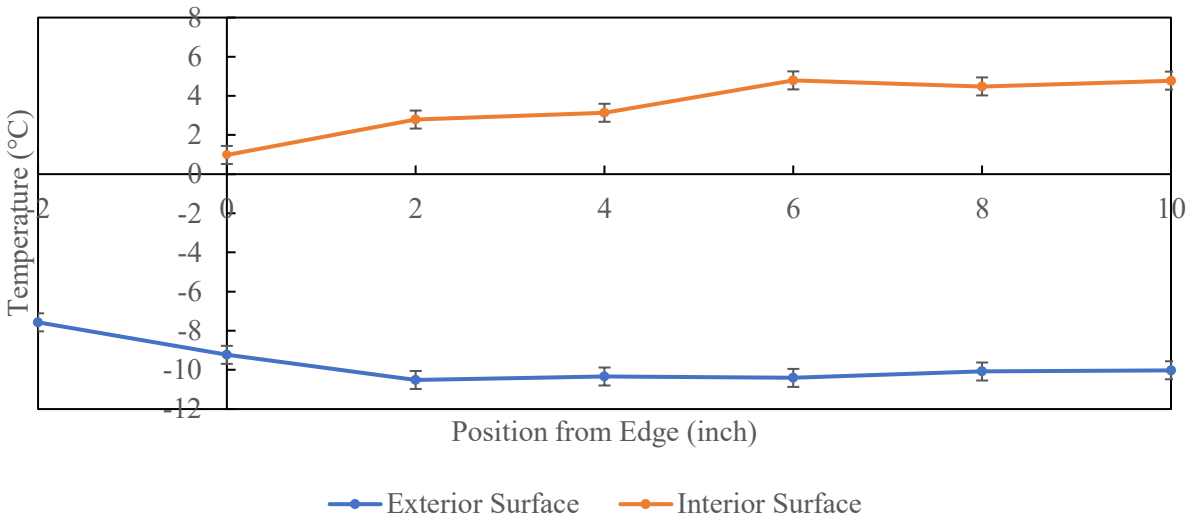

Figure 5-4: Measured temperature along the VIP surface under steady-state conditions

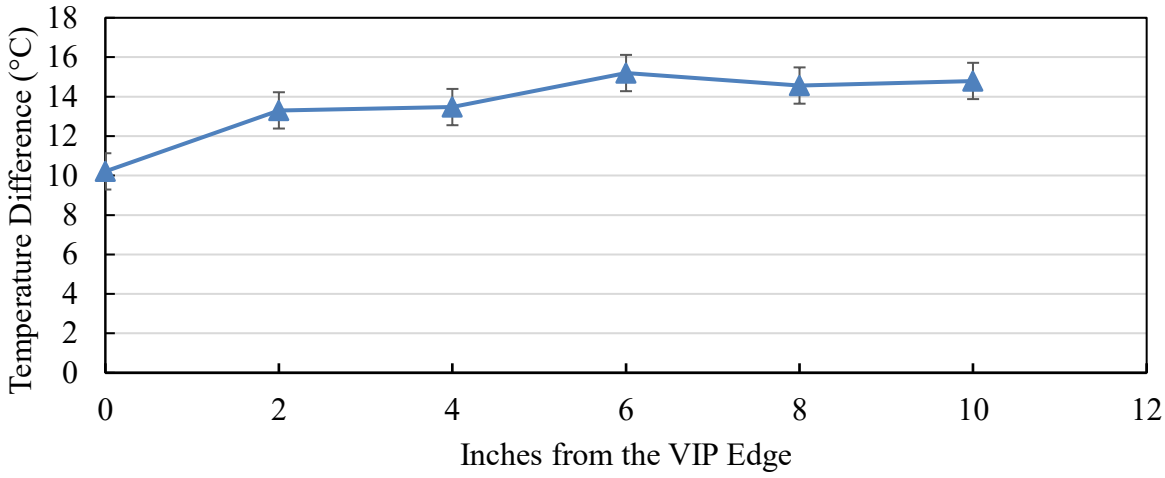

Figure 5-5: Measured temperature difference across VIP with error bars under steady-state conditions

This information can be directly applied to selecting the proper size of VIP. A conservative estimate from this work shows that 50 mm (2”) from the edge would have lower thermal conductivity and should not be assumed to have the same thermal conductivity as the center. Therefore, to improve the overall thermal resistance, the optimized panel design would be a minimized perimeter to cross sectional area ratio. For example, a square VIP panel with the

maximum area would be the solution to maximize the effective thermal resistance of a wall assembly.

In a practical sense, the optimized design for a VIP factoring the constructability was more challenging to quantify because of its subjective nature. The minimum required nail area was assumed as the stud width plus 6.35 mm (1/4”) based on the anecdotal usage of installing the CIP and SIP insulation systems. Another constraint was the VIPs must fit within the wood studs to minimize risk of a puncture during installation. Therefore, for a wood-frame wall built on 400 mm centers, the most thermally efficient design within the safety parameters was a 350 mm x 350 mm VIP panel, drawn in Figure 5-6. Alternatively, a wood-frame wall built on 300 mm centers using the same design assumptions would be a panelized system with 250 mm x 250 mm VIPs.

In summary, the steady-state studies showed that the SIP and CIP insulation systems were found to perform below the outlined threshold due to VIP thermal bridging and insufficient VIP insulated area. The VIPs were found to not have been damaged during installation into the EPS sheets, lamination, transportation, and cladding onto a wood-framed assembly according to the thermal imaging. Finally, the thermocouple measurements with the panelized system showed that there was a temperature gradient along and a change in temperature difference across the VIP when the distance from the edge was varied. From the observations, a new VIP size was suggested to the industry partner that would balance the constructability and thermal performance of a panelized insulation system.

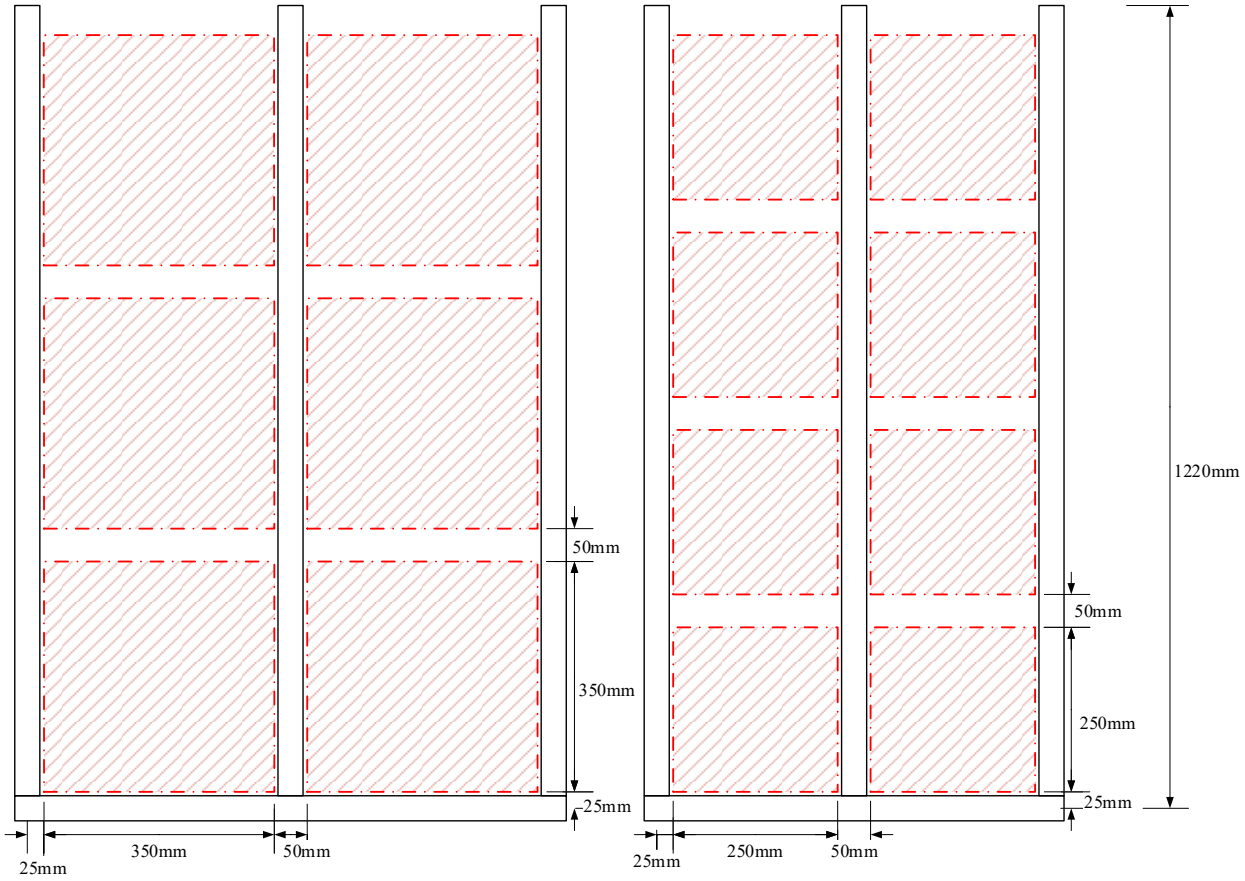

Figure 5-6: Suggested VIP size to balance the effective thermal performance and minimize the risk of puncture for 400 mm spacing (left), 300 mm spacing (right)

5.2 Hygrothermal Monitoring

The hygrothermal monitoring was undertaken from October 2016 through December 2020, although the data monitoring was affected by remote computing issues and intermittent power outages. The monitoring took place at the CanmetENERGY-Ottawa campus in Ottawa, CA at the building envelope test hut. Temperature, relative humidity, and wood moisture content were measured in 4 wall assemblies; two baseline walls and two high-performance walls insulated with vacuum insulation panels. The results from the data acquisition and monitoring are described in the following sections.

5.2.1 Moisture Content and Calculated Relative Humidity

In materials sensitive to mould growth in the in-situ assemblies, the moisture content was measured with point moisture measurement (PMM) sensors. The moisture content sensors were placed in the sheathing of the high-performance and baseline assemblies of the new construction and retrofit specimens. The PMMs were fastened into the sheathing and used to monitor the moisture levels in the sheathing.

In the high-performance retrofit assembly, the measured moisture content is presented in Figure 5-7 for January 2017 to March 2019. The moisture content was measured at points on the sheathing insulated by VIP (1), EPS (2), 50 mm from the edge of the VIP (3) and along the seam of the VIP (4). The general trends for the moisture content were observed first. The amount of moisture in the assembly is low for the first winter until July 2017. During the summer, the sheathing experienced wetting due to two likely factors:

1. High temperature and relative humidity conditions outdoors during the summer cause moisture air and vapour diffusion to be driven towards the cool, air-conditioned interior.
2. The bulk wetting from rainfall increased the runoff from the flat roof possibly increasing the amount of bulk water that penetrated the cladding and ventilated cavity.

The first factor is an expected seasonal event that occurs when the vapour pressure of the conditioned indoors is lower than the vapour pressure outdoors. The second factor is a situation specific wetting caused by a prolonged 3-day rainfall July 11th-13th 2017, and a composition of the test facility causing an increase in the volume of water that needed to be shed by the cladding and ventilated cavity. Additionally, the WRB was applied on the sheathing and was sealed with tape to the test facility so the assembly would not be susceptible to bulk water leakage.

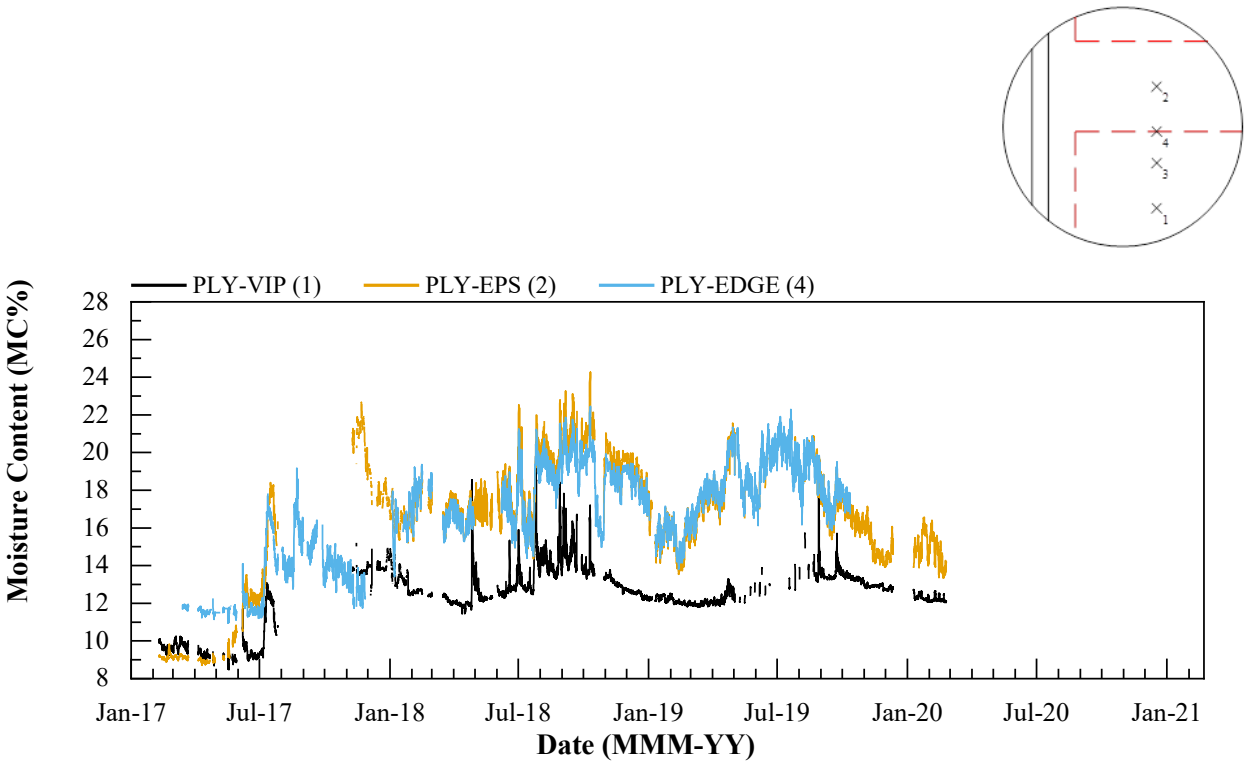

Figure 5-7: Measured moisture content of the plywood sheathing for a retrofit with VIPs

The measured moisture content showed similar trends for the following two years in 2018 and 2019 for the individual points. The moisture contents at each point began to increase quickly between March and April and peaked around the same time, between July 2018 and October 2019. From October to March, the moisture content of the sheathing decreased, likely through vapour diffusion towards the exterior as the vapour pressure gradient was towards the exterior during the winter months.

In the new construction assembly, the OSB sheathing was located outboard of the insulation and was therefore exposed to different conditions compared to the retrofit assembly. The measured OSB moisture content for the monitoring period was plotted in Figure 5-8, in addition to the measured moisture content of the wood studs. An increase in the OSB sheathing moisture content was observed during the winter, as the material temperature and, subsequently,

the moisture storage capacity decreased. During the spring, the measured moisture content in the OSB decreased to below 12% within 2-3 months. This would be caused by the material temperature and moisture capacity increasing as the outdoor temperature increases. Another factor was the low water vapour resistance towards the exterior since the OSB was placed outboard of the insulation and was only covered with the Tyvek building paper, which was open to water vapour transmission.

A seasonal change in the measured wood stud moisture content at the EPS interface was observed. The wood stud had a short time where the moisture content was measured as greater than 20% MC. The wood stud was protected from all forms of wetting by the exterior insulation and the interior vapour barrier, and as such, did not high moisture conditions were not found to occur at this location.

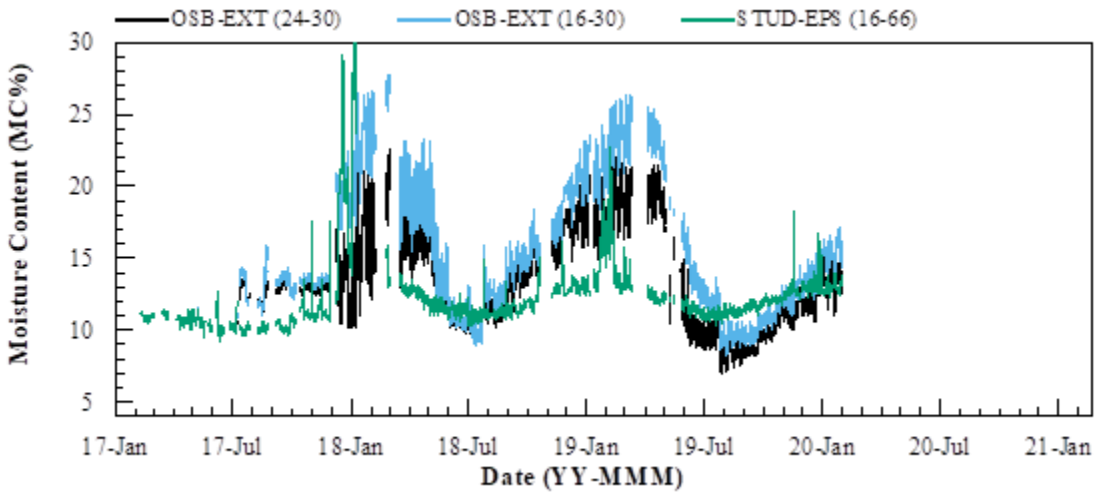

Figure 5-8: Measured moisture content of the VIP insulated OSB sheathing of the new construction wall

5.2.2 In-Situ Temperature Measurements

The temperature and relative humidity were measured on surfaces of the building enclosure within the high-performance and baseline assemblies for new and retrofit construction. The measurements were taken with the thermistors and thermocouples, the relative humidity sensors

were measured using Honeywell sensors and the surface relative humidity was calculated based on the moisture content measurements and the equilibrium moisture content relationship in Equation 5-1 from the Wood Handbook [109] where MC is the temperature and species corrected moisture content.

$$RH_{\mathrm{MC}} = \left(1 - e^{\left(-26.655 * \mathrm{MC}^{1.55}\right)}\right) * 100 \qquad 5\text{-}1$$

The temperature through the assembly is plotted in Figure 5-9 and Figure 5-10 for the retrofit assembly. From both plots, the interior temperature was maintained between 20°C and 25°C. There were brief periods where the temperature would drop below the setpoint during the winter due to power outages and control-related issues. The EPS-EXT temperature was representative of the outdoor surface temperature, as the temperature dips near -30°C in the winter months annually and reached 40°C during the summer. On this surface, the measured temperature of the solar effects on the wall assembly were observed since the outdoor temperature in Ottawa, CA can be colder than the measured -25°C and is not warmer than 30°C as frequently as it was measured.

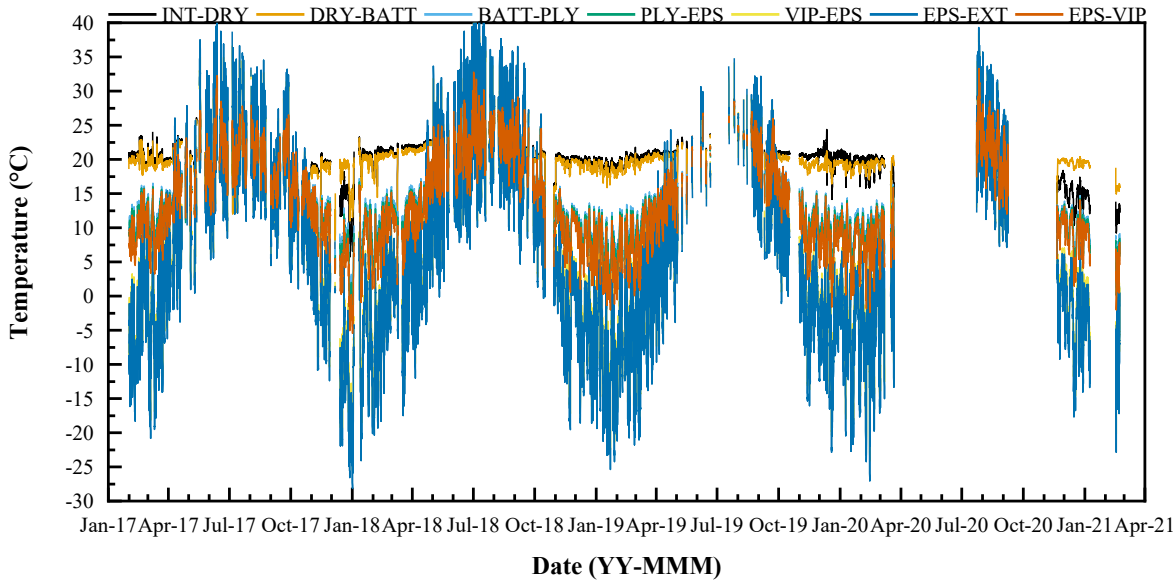

Figure 5-9: Surface temperature profile through the retrofit assembly through VIP insulated area

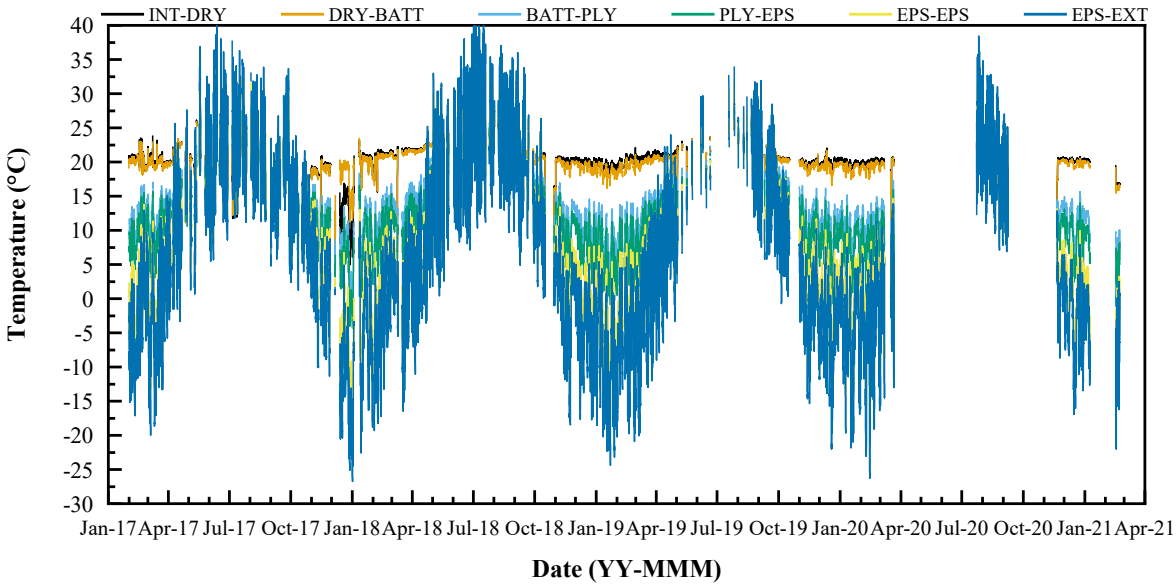

Figure 5-10: Surface temperature profile through the retrofit assembly through EPS insulated area for the monitoring period

In both plots, the surface temperature was measured at each material interface. The BATT-PLY and PLY-EPS are the interior and exterior surface temperatures of the plywood, respectively. The plywood material is considered sensitive to mould growth. Figure 5-11 shows the sheathing temperature over the monitoring period without the boundary conditions measured by the Type T

thermocouples. The sheathing area insulated VIP and the VIP edge are depicted on the plots. It shows that the surface is warmer for both those points compared to the sheathing surface insulated by EPS in the baseline and high-performance wall assemblies. The measurements are shown during a cold month with the highest average temperature gradient during the monitored period. The measured temperature on the interior surface of the VIP is shown on the same plot through the EPS-VIP line. The VIP provided an increase in the sheathing surface temperature.

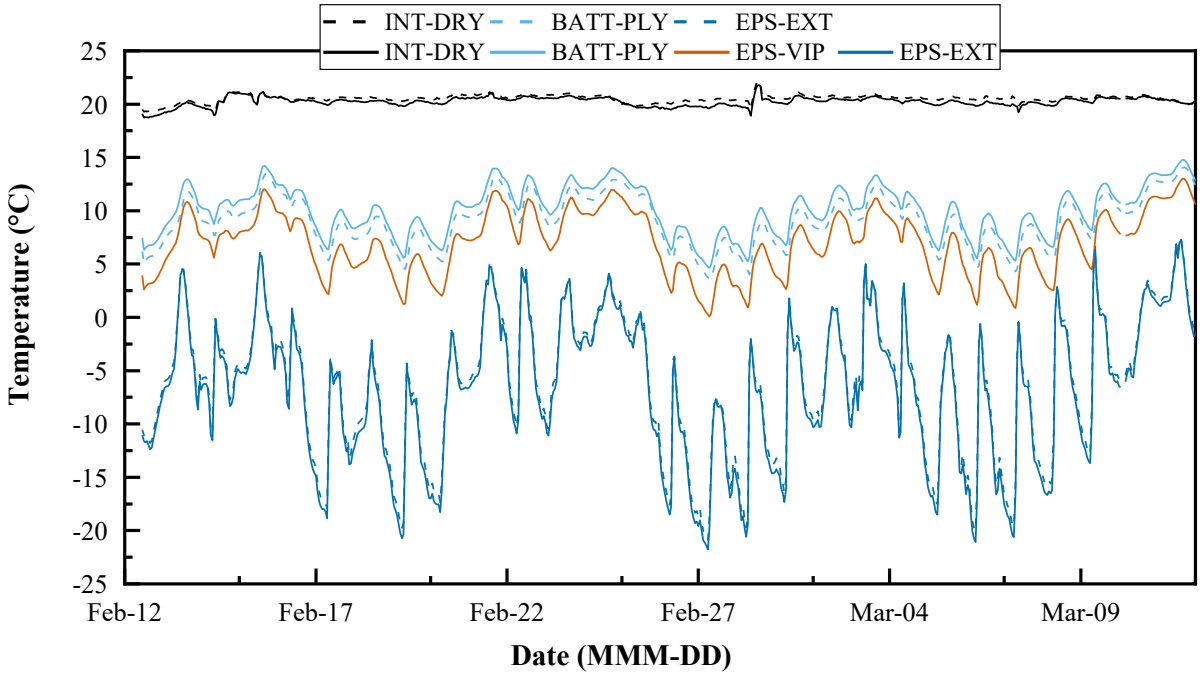

Figure 5-11: Sheathing temperature of the retrofit assembly insulated by EPS (dashed line) and VIP from February 12th, 2019, to March 12th, 2019 (cold month).

The sheathing inner surface temperature was measured by the second set of sensors and data acquisition system, the same results were measured. The plotted second set of data for the entire monitoring period was plotted in Figure 5-12, and the effect of the VIPs was evident. The sheathing temperature insulated VIPs and the edge of VIP are consistently higher than the sheathing in the baseline wall assembly and the EPS insulated area in the high-performance wall assembly.

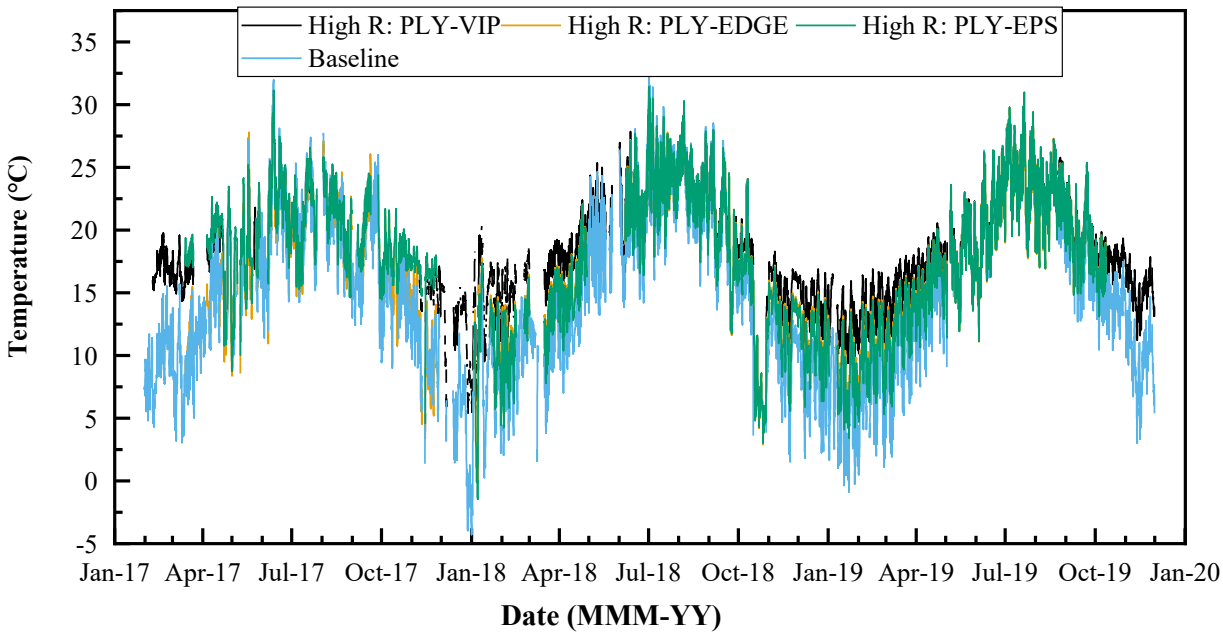

Figure 5-12: Sheathing inner surface temperature of the retrofit assembly insulated by EPS and VIP from January 2017 to January 2020

The sheathing temperature during a cold month is plotted in Figure 5-13, along with the calculated dewpoint of the interior air temperature. The real risk of condensation occurs when warm, moist indoor air flows through the assembly and reaches a surface temperature lower than the dewpoint. During the cold month in 2019 plotted in Figure 5-13, the measured interior sheathing surface temperature dropped below the interior dewpoint when insulated by the EPS and the VIP edge. This would imply that condensation at these locations on the surface would be possible if proper air sealing was not applied to the interior. The interior air would need to leak and flow to the surface for condensation to occur. The sheathing surface insulated with VIPs was kept above the dewpoint during the cold month and did not show a risk of periodic condensation.

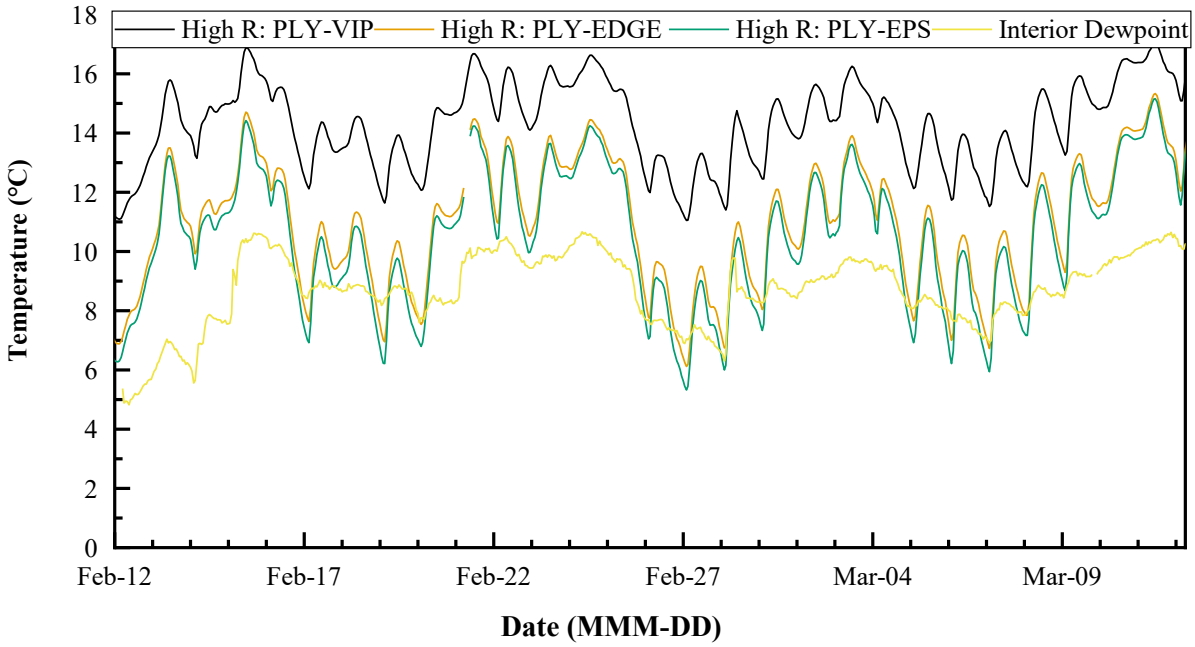

Figure 5-13: Inner sheathing surface temperature of the high-performance assembly insulated by EPS and VIP from February 12th, 2019, to March 12th, 2019, measured by thermistors

In the new construction assembly with the SIP system, the sheathing temperature was colder since it was outboard of the insulation. In Figure 5-14, the surface temperature on either side of the sheathing is plotted during a cold period from February 2019 to March 2019 with the baseline wall assembly. There was little difference between the measured surface temperature in the rainscreen and the inner surface of the outboard sheathing, meaning the sheathing temperature is very close to the outdoor temperature during the winter, except when there is significant solar irradiation on the surface. While this would seem like a potential condensation issue, the sheathing would have a higher vapour permeability and drying potential since little insulation and material is limiting its ability to dry.

The sheathing temperature in the baseline assembly was plotted in Figure 5-14 for comparison and it was expectedly warmer. The baseline assembly was insulated with 38 mm (1.5”)

of EPS outboard. The measured temperature varied less, due to the lower heat flow at the layer, and the lowest temperatures were higher than the high-performance assembly.

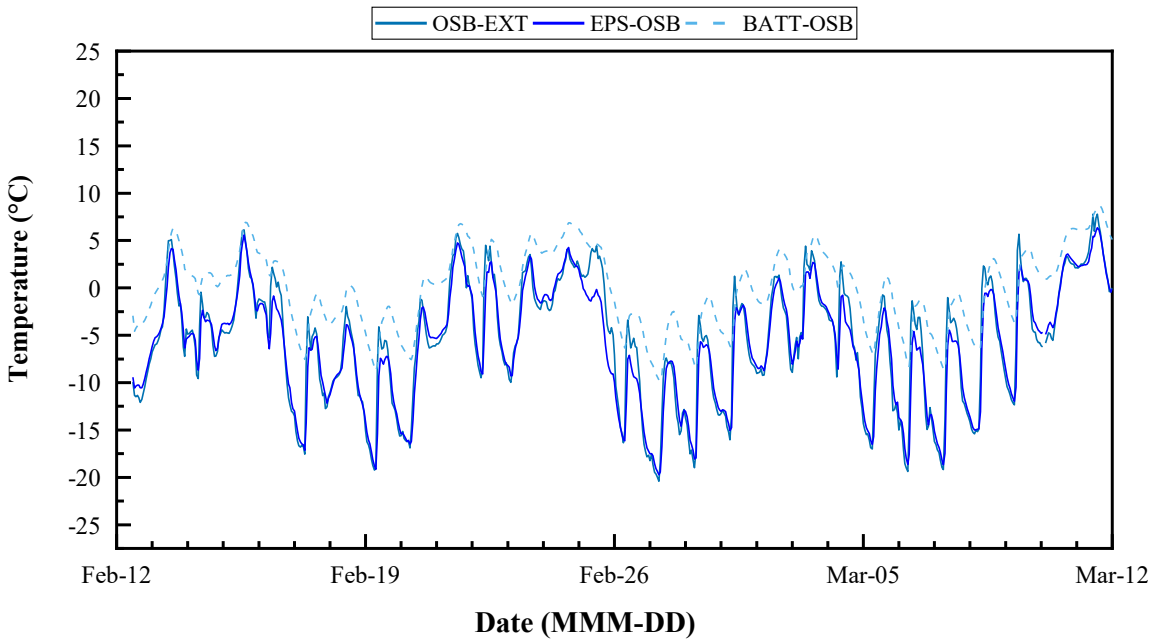

Figure 5-14: Sheathing temperature of the new construction assembly insulated by EPS and VIP during from February 12th, 2019, to March 12th, 2019, measured by thermistors. Baseline sheathing surface temperature is shown as the dashed line.

The temperature was monitored at each material surface in the new and retrofit assemblies and the difference between VIP and EPS insulated areas was observed and compared to the baseline and interior dewpoint assemblies. As expected, the in-situ measurements displayed that the sheathing temperature was warmer when it was insulated with VIPs, and the risk of condensation at the sheathing insulated by VIPs was minimal based on the measurements.

5.2.3 Relative Humidity at the Sheathing

In the high-performance retrofit assembly, the same points were monitored at the same locations as the moisture content readings. The relative humidity measured in the stud cavity at the sheathing surface was measured using the Honeywell sensors and is plotted in Figure 5-15 for the duration of the monitored period.

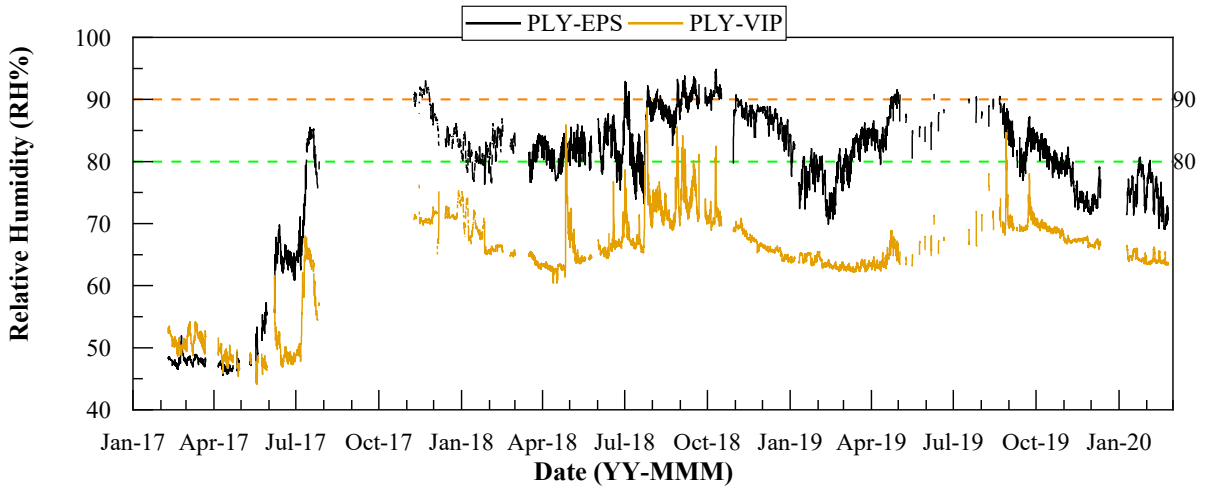

Figure 5-15: Measured relative humidity at the sheathing's inner surface for a retrofit insulated with VIPs

In the new construction wall assembly with the SIP system, the Honeywell sensors did not provide the long-term performance that was desired, as observed by the large variances and frequently measuring above 100% RH during the monitoring. The sensors were placed behind the WRB and the sheathing to measure the humidity at the exterior surface and were essentially measuring the humidity in the rainscreen, which was consistent with the outdoor humidity. Unfortunately, the sensors did not provide reliable data about the hygrothermal performance of the relative humidity at the sheathing surface, and the data will not be presented.

The calculated relative humidity at these points plotted in Figure 5-16 is less conclusive regarding the long-term durability of the assembly. For a significant amount of time from October 2017 through to August 2018, the relative humidity is above the threshold for durability, according to the failure criteria. It appears that the Sheathing-EPS section in the assembly, which is the most vapour permeable, experiences a drying period during the fall of 2017 and winter of 2018, and was very sensitive to the high humidity during the summer of 2018. While the Sheathing-VIP also experienced these spikes in relative humidity, due to precipitation, and high outdoor humidity

during the summer. However, it was not as volatile at other measured points along the sheathing surface.

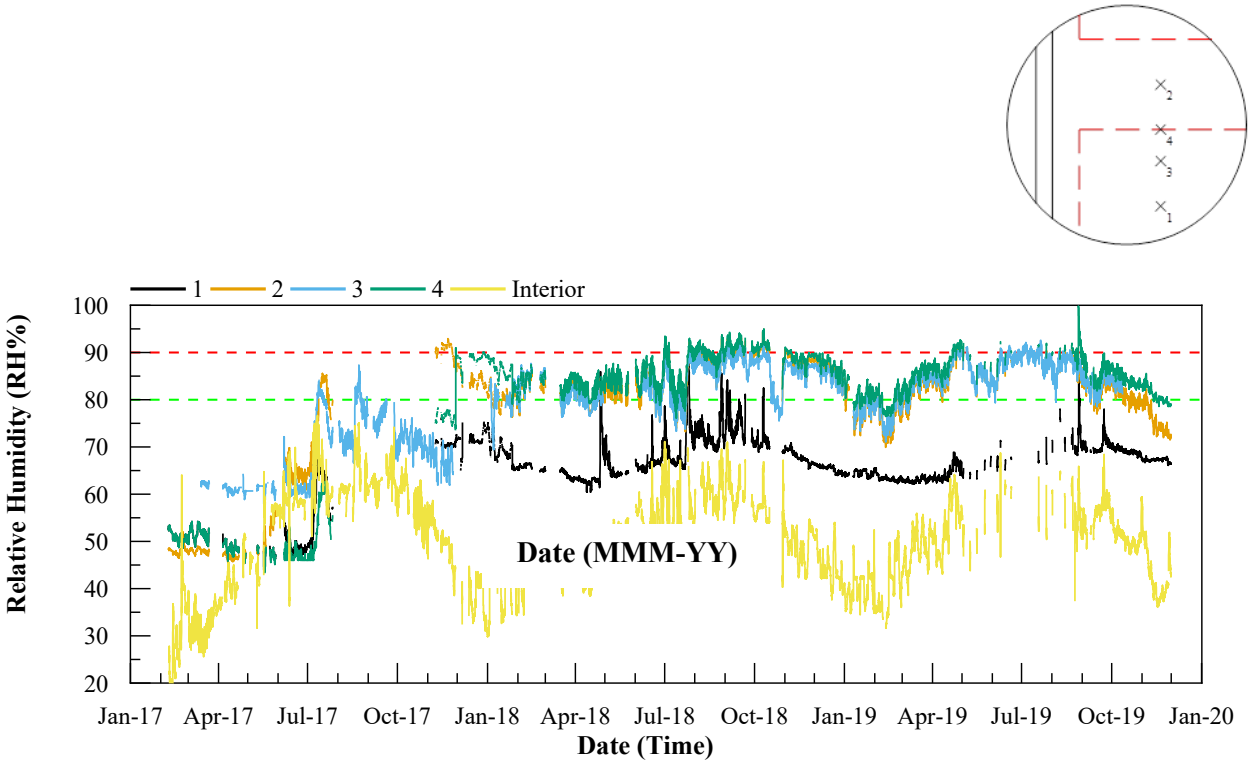

Figure 5-16: Calculated relative humidity at the sheathing surface for a retrofit insulated with VIPs

In the new construction wall assembly, the sheathing did not have insulation outboard and the calculated relative humidity, shown in Figure 5-17, had a similar trend to the moisture content results. During the winter, when the temperature decreased, the moisture capacity of the air decreased so the relative humidity increases. The mould index will be calculated at this surface to determine whether there may be issues with this design for the given in-situ conditions.

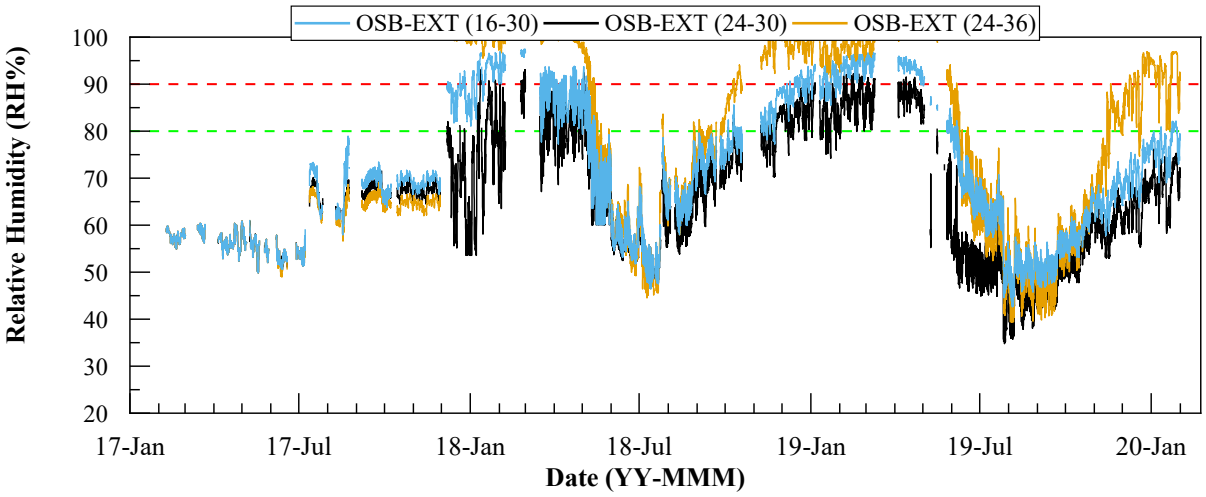

Figure 5-17: Calculated relative humidity at the sheathing surface for a new build insulated with VIPs

5.2.4 Evaluation Criteria and Mould Index

The measured temperature, relative humidity and moisture content were used to evaluate the building envelope assemblies against the outlined criteria to determine whether there is a risk for failure. In previous iterations of ASHRAE 160, the humidity at surfaces was used to evaluate whether the building enclosure was a durable design. However, after it was found to be too strict and acceptable wall assemblies would fail the evaluation. Therefore, a mould index and critical relative humidity criteria were developed to better assess the building envelopes. For these assemblies, both evaluation criteria were used to assess the high-performance and baseline assemblies.

The first evaluation criteria followed a modified version of the old ASHRAE 160 standard. The standard outlined the following conditions necessary to minimize mould growth on all surfaces of components of the building envelopes assembly [30]:

(a) 30-day running average surface RH < 80% when the 30-day running average surface temperature is between 5°C and 40°C.

(b) 7-day running average surface RH < 98% when the 7-day running average surface temperature is between 5°C and 40°C.

(c) 24-hour running average surface RH < 100% when the 24-hour running average surface temperature is between 5°C and 40°C.

If a wall assembly did not pass one of these conditions, it was considered a failure and did not pass the moisture control design threshold. These criteria were found to be too strict and would indicate that a wall known to be safe had conditions favourable for mould growth [34]. Therefore, for this study, the criteria were modified to compare the performance of the wall assemblies. This is apparent in Table 5-2 and Figure 5-18, as the baseline assembly was above 80%RH for nearly 4000 hours, or 166 days, during the monitoring period. The 30-day moving average relative humidity at the inner sheathing surface was shown to have significant variation between the baseline and high-performance assemblies.

Table 5-2: Number of unaveraged hours spent on evaluation criterion RH Conditions

Construction		RH > 80%	RH > 98%	RH = 100%
New	Baseline	3999	0	0
	EPS Insulated	9273	4734	0
	VIP Insulated	4309	0	0
Retrofit	Baseline	4968	0	0
	EPS Insulated	10413	0	0
	VIP Insulated	187	0	0

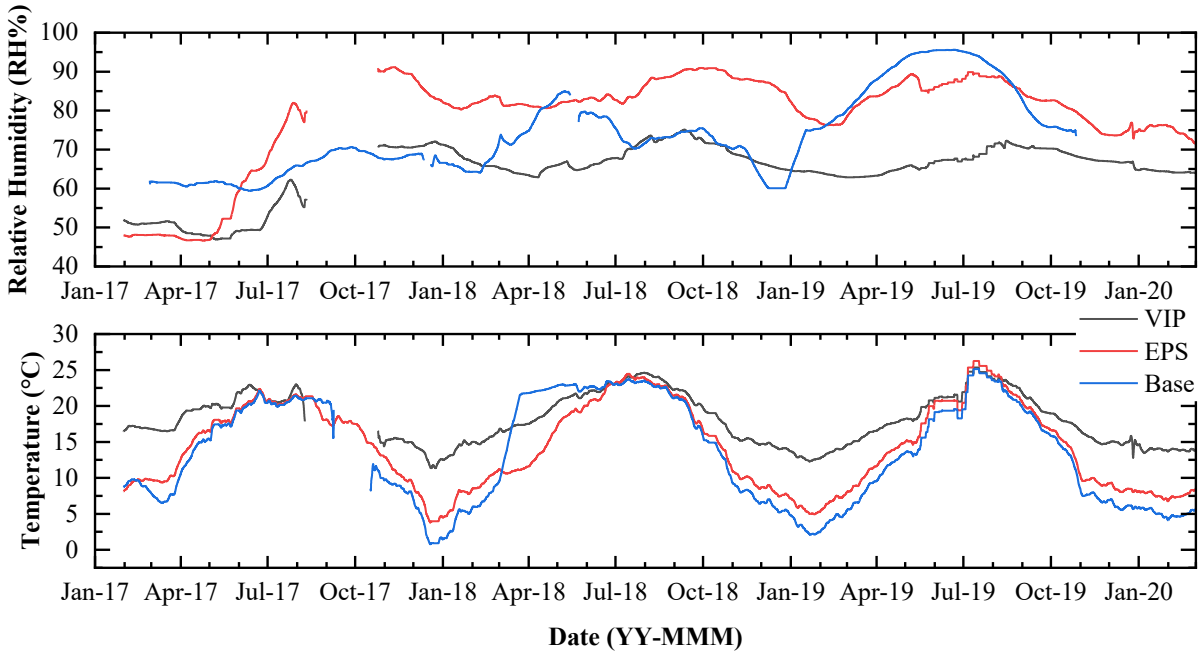

Figure 5-18: 30-Day Average RH (above) and Temperature (below) at the sheathing of 2x4 wood-framed wall retrofitted with CIP.

Instead of assigning a PASS/FAIL criterion for the enclosures, the number of hours that a surface was exposed to the outlined surface conditions was counted. The higher the number of hours that a surface is under a certain set of elevated surface conditions, the higher potential there is for mould growth at that surface in addition to the material and surface conditions.

The mould index was calculated using the surface temperature and relative humidity conditions and plotted in Figure 5-19. The mould index must stay below 3 to stay within the prescribed failure criteria, and as expected the Sheathing-EPS point is the main concern for the assembly. It steadily increases during the Fall of 2017 to the end of the plot and has sharp increases anytime the relative humidity at the surface reaches around 90%. The trend was alarming since it continued to increase per annum, however, it has just crossed into the Level-1 threshold after about 9 months of elevated humidity levels. Level-1 indicates that the conditions are favourable for microscopic bacterial growth on <25% of the surface. Since other studies ascertain that the mould

index does not provide conservative estimates, this assembly will be given another opportunity to dry during the upcoming winter months under normal interior conditions.

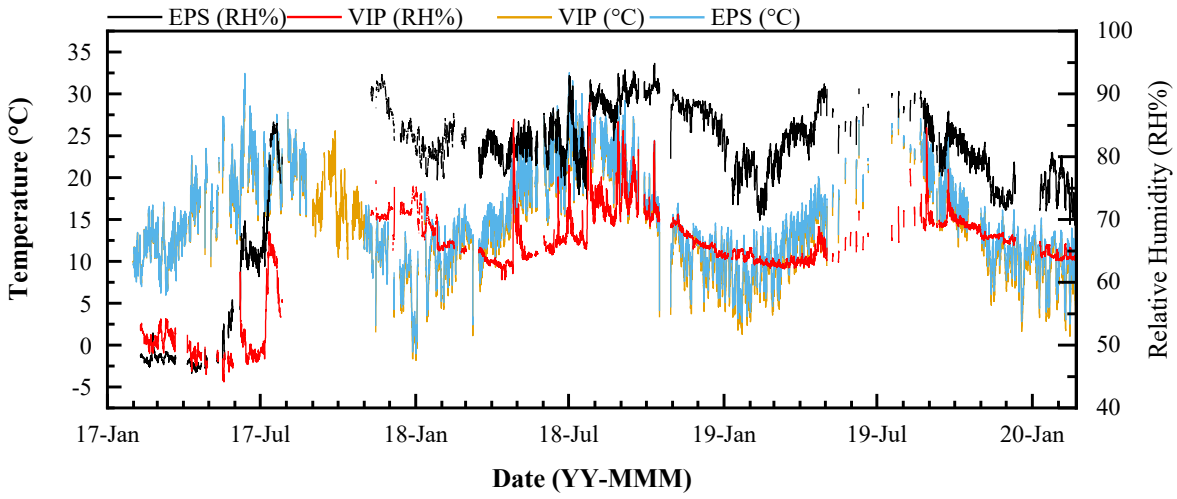

Figure 5-19: RH and Temperature at the sheathing surface used for mould index calculation

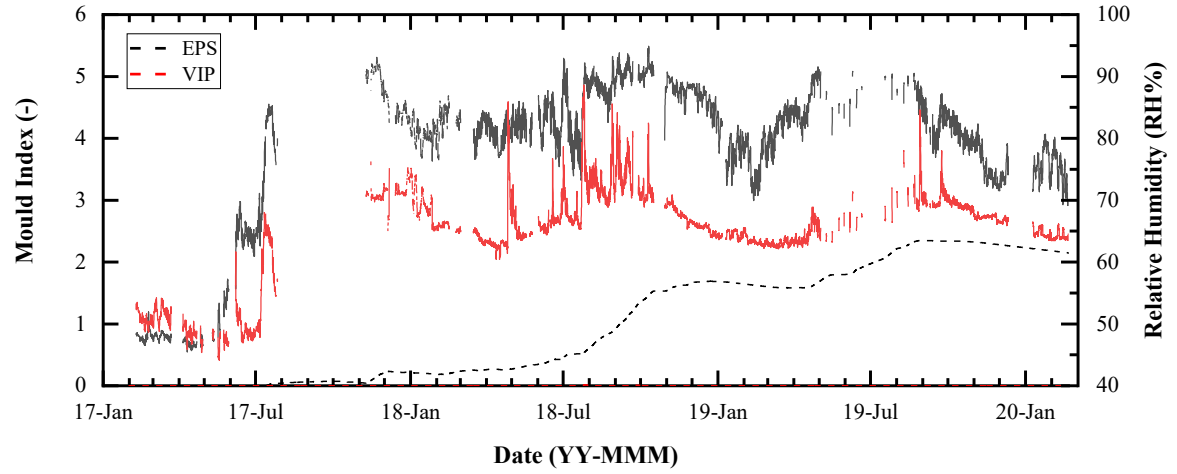

Figure 5-20: Calculated mould index (dashed line associated with the left axis) and RH (solid lines associated with the right axis) for a retrofit with VIPs over the test period.

The new construction assembly performed similarly, if not better, to the retrofitted assembly, which was expected since it contained an interior vapour barrier that limited the wetting from the interior during the winter months and was able to dry during these periods. They experienced the same wetting effects as the retrofit assemblies during the heating and should

season, which confirmed the effect that wind-driven rain and high exterior humidity have on the durability of these panels. In Figure 5-21, the relative humidity from the moisture content measurements in the OSB sheathing was plotted along with the average measured exterior OSB surface temperature. As the exterior surface temperature decreased in the winter months, the OSB surface relative humidity and moisture content rose above the 80%RH threshold. However, when the mould index, shown in Figure 5-22, and did not exceed the failure criteria since the critical relative humidity increases as the surface temperature decreases below 20°C.

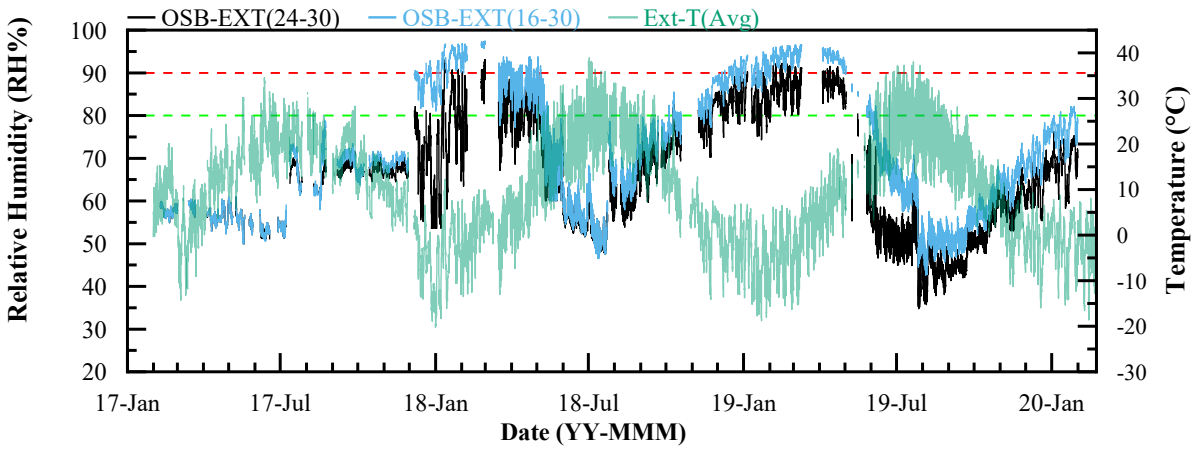

Figure 5-21: Measured RH and T for the new construction assembly over the test period

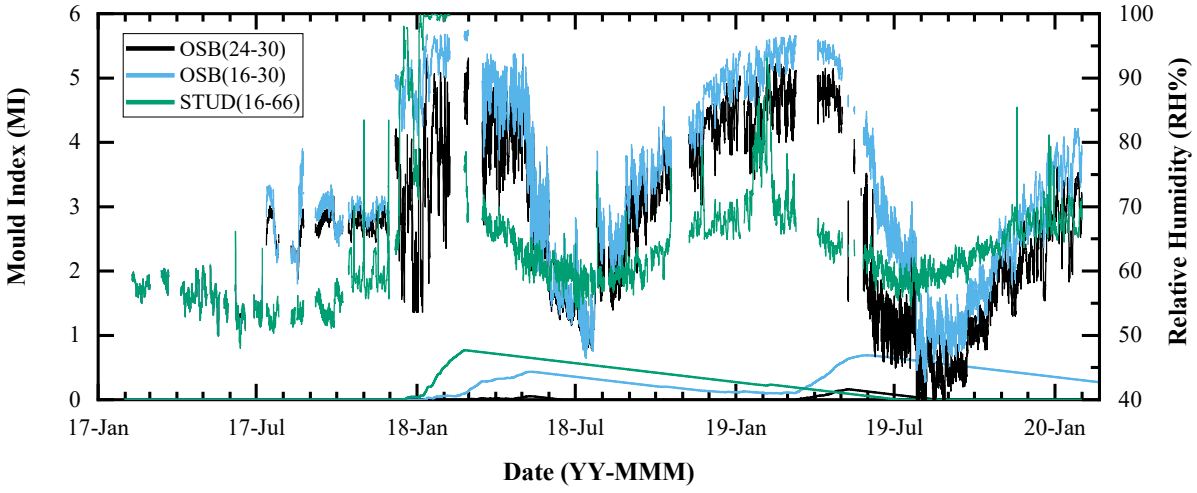

Figure 5-22: Calculated mould index and the measured RH for new construction with VIPs over the test period

For example, when the surface temperature was 5°C, the critical relative humidity changed to 95% RH. For this reason, it is possible that there will be a limited mould growth rate during the coldest months and a significant increase in the mould growth rate occurred during the Spring months (March to June) as observed in Figure 5-23. The measured relative humidity at area insulated by EPS had a limited increase during January 2019 with a monthly average of 90% surface RH because of an average -5°C surface temperature. Four months later, in April 2019, the surface conditions averaged 93%RH and 7.5°C which led to a mould index increase from 0.26 to 0.56. This highlights the importance of temperature on high relative humidity and the mould growth potential.

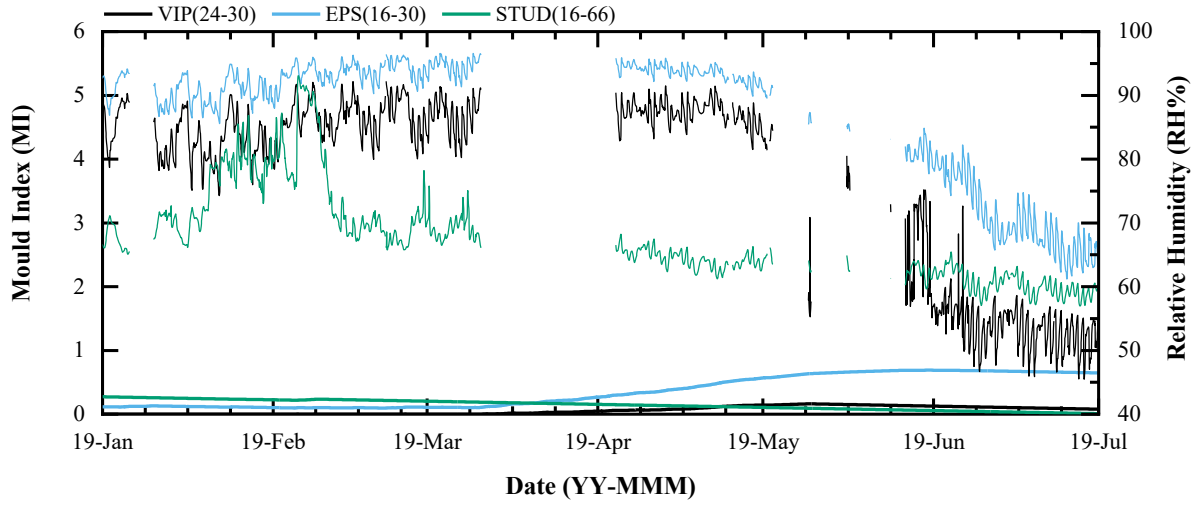

Figure 5-23: Mould index from January 2019 to July 2019 for new construction wall assembly

5.3 Discussion of Experimental Results

The objective of creating an insulation panel that could provide enough thermal and hygrothermal performance as well as be buildable with normal construction techniques was the view of managing the three variables to obtain an optimal orientation. The initial stages of the

project provided insights into whether a prototype product could be feasible from all aspects and yielded some insight into what future challenges could be presented.

5.3.1 Buildability of the Wall Assemblies

The buildability with VIPs is a barrier since the panels are simply too fragile to be handled on the construction site. However, this material is useful in significantly improving the enclosure without occupying a significant thickness. The solution was to encase the dimensionally smaller VIPs into open-cell insulation to provide a homogenous baseline value but improve the effective R-value. The VIPs selected for the initial design were considered the optimal for buildability, which is considered the largest barrier in this project. The VIP dimensions were 200 mm (8”) by 305 mm (12”), such that on 12”, 16” or 24” OC wood-framed spacing, there would be at least 50 mm (2”) strip around the perimeter of each VIP for fastening area. This was considered the highest performance in terms of buildability since the design provided the most fastening space.

The prototype panels also contained printing on the exterior surface where the VIPs would be located. This is useful during the installation process, and the printed area could be exaggerated compared to the actual VIP size to ensure there is not any puncture. One drawback observed during the installation of the panels at CE-BETH was the inability to add opaque layers to the exterior surface of the VIP-EPS panel at any point during construction. This issue arose when adding the WRB to the new construction's high-performance assembly. The exterior facing OSB had printing to differentiate the VIPs and EPS, however, after the WRB was added for vapour control, the printing was no longer visible with siding still needing to be fastened to the wall. This was not an issue for the retrofit assembly since the WRB was added interior to exterior insulation. In the future iterations of the OSB backer assembly, a combination WRB product with taped joints should be explored to avoid the issue of covering any markings.

5.3.2 Thermal Performance of the VIP-EPS Wall Assemblies

The VIP-EPS composite panel prototype was considered a multi-purpose product since it could be applied to many different wood-framed spacing, however, it led to the panel having a less than optimal VIP coverage area for augmented thermal performance. Since the buildability target was maintained constant for the first iteration of the project, it was anticipated that the thermal performance target could be reached. However, due to the thermal bridging and general underperformance of the first set of VIPs, the thermal performance targets were not met.

These issues were partially addressed with a better-quality VIP manufactured by Panasonic Inc., but improvements can be made by increasing the thickness or dimensions of the VIPs used for the prototype assembly. The drawback with improving the thermal performance is the reduction in buildability and change in hygrothermal performance. Evaluating the thermal performance of the in the guarded hot-box and by annual hygrothermal simulation programs of panels with different spacings could be further explored.

5.3.3 Hygrothermal Performance of the VIP-EPS Wall Assemblies

The experimental evaluation at CE-BETH began in January 2017 and the results are presented up to August 2018. The interior conditions were set to 35-40% interior relative humidity for the winter periods, which is conservative according to ASHRAE 160, and were allowed to float during the summertime, reaching a peak relative humidity of about 65%. During the monitoring periods, the relative humidity, temperature, and moisture content of sheathing and framing members were measured at 5-minute intervals. If gaps in the data exist, it could be due to a lack of power in the test facility, or low battery in the data loggers themselves.

The results were compared to the failure criteria outlined in the project objectives section of the introduction and the two prototype assemblies were found to pass most of the checks

required. The relative humidity in the retrofitted construction exceeded the maximum threshold for a prolonged period in 2018, however, the moisture content and mould index parameters remained well below the prescribed threshold. The ASHRAE 160 standard and mould index parameter have been criticized for being too stringent, based on case studies whereby failure predicted by these measures did not match the predicted mould growth at the end of the test period. These criticisms were outlined in the literature review section, through different case studies, however, it would be prudent to consider a strict metric to ensure enough long-term durability, since building envelopes are not meant to require significant maintenance over their lifetimes.

The in-situ study in Ottawa was completed in 2020 and showed promising results regarding the durability under the environmental loads between 2017 and 2020. Over the 3-year period, the wall assemblies were exposed to live weather condition under an East facing orientation with a flat room building. In Years 2 and 3 study, the moisture loads showed the hygrothermal load was repeated and did not have an annual increase of moisture within the assembly. Additionally, the seasonal moisture profile from Year 2 was repeated in Year 3. Therefore, it is expected that the wall will continue to perform in the same manner in the future for the given set of boundary conditions.

The experimental data can be compared to the numerical simulations with the measured boundary conditions and the wall assembly designs can be assessed in other climates across Canada to ensure they are sufficiently robust and durable.

The hygrothermal measurements continue to be logged in 2022, albeit with data acquisition challenges associated due to a lack of access to the in-situ facility between 2020 and 2022.

5.4 Summary

In summary, the experimental studies showed the thermal resistance of a rigid foam board of insulation could be increased however, the sizes of VIPs selected were insufficient to reach the targets. The guarded hot-box was used to evaluate the thermal resistance of a wood-frame wall with a composite and structural insulation panel comprised of VIPs to insulate the exterior. The steady-state testing found that including the VIPs in the exterior insulation as a 1:1 ratio improved the thermal resistance by 1-1.5 m^2K/W. It was found that the thermal bridging around the VIP edges was a significant factor based on the monitoring and infrared imaging. To meet the thermal resistance target of R-4.2 m^2K/W, the thickness of the VIPs or the VIP coverage area would need to increase.

The hygrothermal monitoring was undertaken over 4 years beginning in 2016. The moisture content, temperature and relative humidity readings during the monitored period showed that the enclosure had sufficient drying when exposed to high indoor humidity, and environmental conditions. Both wall systems did not exceed the mould index failure criteria and appear to have promise for long-term durability.

Chapter 6: Numerical Results

The following chapter presents the numerical results and analysis for a VIP insulated wall assembly using the methodology presented in Chapter 4. WUFI Pro 6.1 and WUFI 2D were used to evaluate the baseline performance of frequently used wall assemblies in Canadian low-rise housing from different vintages as old as 1960s-era construction. An analysis of the hygrothermal performance and feasibility on the above-grade walls retrofitted with the CIP and SIP systems. The numerical simulations were compared to the measured data acquired at CE-BETH, specifically the temperature and relative humidity at the sheathing surface. The model inputs were screened using an OAT method to qualitatively assess the model sensitivity to selected inputs. Finally, the VIP insulated wall system was evaluated in different climates across Canada to determine if there are climates that would not be suitable for this wall assembly design.

6.1 Baseline Stock Simulation across Canada

In WUFI Pro, a set of simulations was performed to access the baseline performance of Canada's current building stock. The building archetypes were created by dividing the existing building stock yearly vintage, the above-grade wall insulation levels, and the type of exterior cladding for wood-framed construction. The wall archetypes followed the data collected and work performed at CanmetENERGY under the EnerGuide for home evaluations program and Urban Archetypes Project as well as previous iterations of the National and Provincial building codes.

Based on those programs, the vintages were divided into 8 vintages with a variety of exterior cladding, vapour control and inboard insulation. These vintages were determined based on many houses within in date range and the building code iterations. While the proposed wall assemblies may not capture all homes within a certain vintage, they will provide a range of performance useful for assessing retrofits and VIP insulated assemblies.

The baseline above-grade wall assemblies were simulated using the WUFI Pro 6.1 hygrothermal modelling software. The wall assemblies were modelled using the best practices to estimate material properties, moisture and air sources, and boundary conditions. A simple drawing of the baseline assembly with air and moisture sources is presented in Figure 6-1, along with a description of the wall characteristics for the model assembly in Table 6-1. In summary, 10 baseline simulations were run to capture the expected array in performance of the current building stock in Ottawa, as well as determine the initial conditions if an enclosure retrofit were to take place.

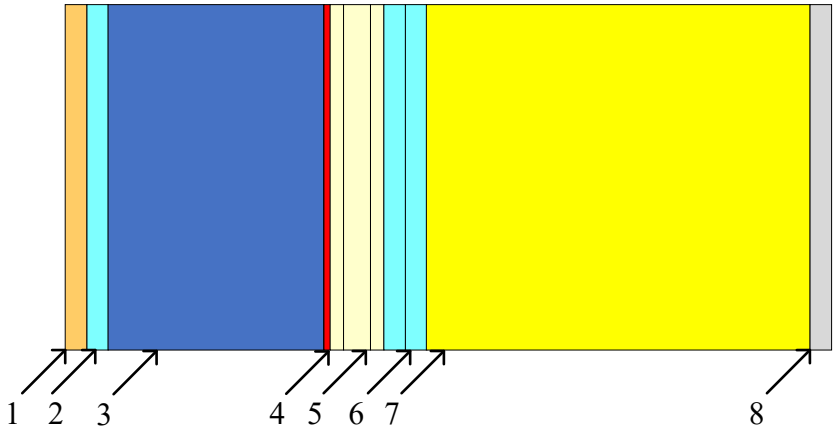

Figure 6-1: Simplified drawing of a baseline wall assembly including air and moisture sources.

1. Exterior Cladding with 1% WDR moisture source at the interior surface
2. Ventilated air space with 25-100 ACH air source tied to the exterior air
3. Exterior insulation with 10 ACH air source tied to the exterior air
4. Air control layer
5. Wood sheathing divided into 3 components with a 0.01% WDR moisture source at the exterior surface
6. Air layers with outer and inner lining leakage with two 10 ACH rates
7. Inboard insulation (fibreglass batts)
8. Gypsum board with vapour control layer

Table 6-1: Characteristics of the baseline above-grade walls

Vintage	Exterior Cladding	Sheathing	R-Value $\left[\frac{m^2K}{W}\right]$	Vapour Control
<1961	Brick, Wood	Fibreboard	1.9-2.2	n/a
1961-1977	Brick, Wood	Fibreboard OSB	1.9-2.2	Kraft paper
1977-1983	Brick, Wood	OSB	3.2-3.3	PE Membrane
1983-1995	Brick, Wood	OSB	3.2-3.3	PE Membrane
1995-2005	Wood	OSB	3.9-4.1	PE Membrane

The total water content in the assembly after the final timestep, presented in Table 6-2, and the water content profile through the assembly after the final timestep was exported and saved for simulations regarding an enclosure retrofit.

Table 6-2: End water content of the baseline above-grade walls

Vintage	Cladding	Sheathing	Vapour Control Interior (Exterior)	End Water Content [kg/m^2] Assembly (Sheathing)
1961	Brick Wood	Fibreboard	N.A.	1.45 (46 kg/m^3) 1.01 (30 kg/m^3)
1977-F	Brick Wood	Fibreboard	Kraft	1.98 (55 kg/m^3) 0.96 (24 kg/m^3)
1977-O	Brick Wood	OSB	Kraft	2.68 (103 kg/m^3) 1.37 (57 kg/m^3)
1983	Brick Wood	OSB	Vapour Barrier	2.25 (98 kg/m^3) 1.36 (56 kg/m^3)
1995	Brick Wood	OSB	Vapour Barrier (WRB)	2.63 (103 kg/m^3) 1.38 (58 kg/m^3)
2011	Wood	EPS+OSB	Vapour Barrier (WRB)	1.31 (52 kg/m^3)

The baseline simulations showed that there was no significant risk to mould growth on the sensitive layers. The end water content of the assemblies should that brick clad assemblies, and by extension, any absorptive type cladding will retain a significant amount of water after a rain event. This is an important distinction in the summary table and may pose an issue when looking into a retrofit involving insulating over the existing cladding after recent rainfall.

6.2 VIP Insulated Walls Simulation

The hygrothermal performance of the above-grade wall assemblies was simulated with VIPs included as the exterior insulation. The study focused on two types of high-performance assemblies: new construction and retrofit. The new construction assembly represents an above-grade wall that was built for a new dwelling while the retrofit construction utilized different materials and assemblies, along with initial conditions that were consistent with material conditions after 20+ years of use. The relative humidity, temperature, moisture content, mould index and RHT Index at the sheathing from the simulations are presented and compared to the simulations using baseline assemblies.

6.2.1 New Construction in Ottawa

The simulations were set up to represent wood-framed above-grade walls in new construction in Ottawa, CA with VIPs integrated into the exterior insulation. The simulations were performed in WUFI under the same modelling principles as the baseline simulations. Following the project's evaluation criteria, the temperature, relative humidity, mould index and RHT index are plotted below.

The simulated relative humidity and temperature of three components of the sheathing were plotted in Figure 6-2. The relative humidity at the inner, center and outer OSB nodes were plotted and may be compared in the plot. The temperature of the center OSB node was plotted to

represent the average OSB temperature during the simulation. The initial construction moisture, set at 80%RH and 20°C for all the materials, caused moisture levels to be elevated in the first year in comparison to the subsequent years. There are brief periods where the relative humidity spiked when the temperature dropped. This is expected since the parameters are inversely proportional. The results from the simulation show that the inner OSB surface is exposed to higher levels of relative humidity compared to the outer surface. These results are due to a combination of warm, moist interior air diffusion towards the exterior and air leakage from both boundaries on the interior OSB surface. While the inner OSB surface was exposed to the highest year-over-year relative humidity, the outer and center OSB nodes had higher relative humidity in the first year, presented in and those effects were obvious in the MI and RHT80 indices.

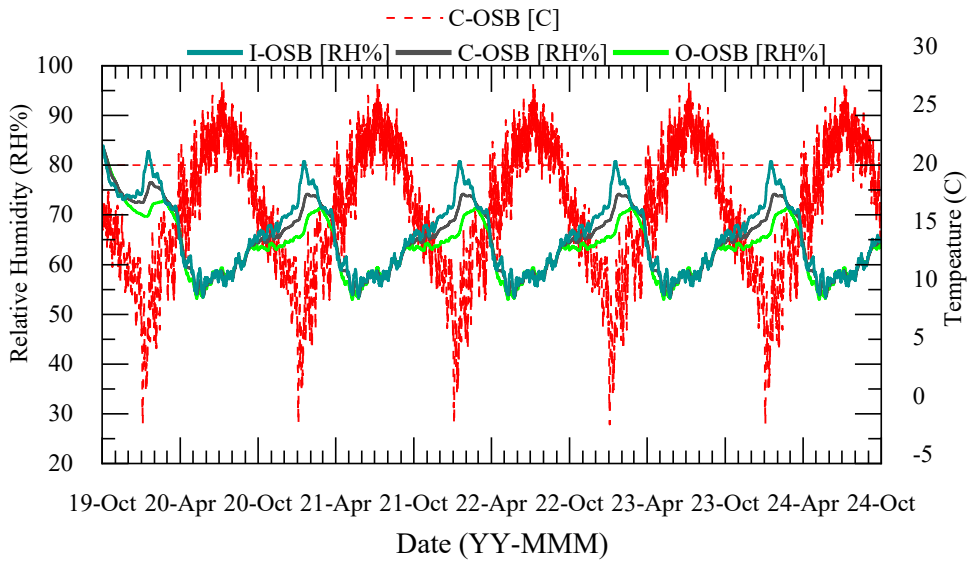

Figure 6-2: Simulated sheathing surface relative humidity (solid) and temperature (dashed) of an above-grade wall for new construction in Ottawa, CA

The M-Index and RHT80-Index were calculated and plotted for the VIP insulated new construction assembly in Ottawa, CA in Figure 6-3 (MI) and Figure 6-4 (RHT80). For the first two months, the results from the mould model suggested a higher value for mould growth potential, however, the values remained below the threshold for any kind of mould growth. Additionally, the

calculated RHT80 Index does not increase year-over-year for the most part. The inner OSB has very brief periods when the air conditions at the node meet the conditions necessary for the index. The first 8 months of the RHT80 index were plotted in Figure 6-5. It shows the RHT80 Index increasing at a similar rate during the first month for all nodes, before reaching a plateau. A small annual increase in RHT Index for the Inner OSB was observed, and was due to the temperature at the surface reaching 80%RH with a temperature above 5°C. At this temperature, the relative humidity is still below the critical relative humidity threshold for mould growth potential, however, it will trigger an increase in the RHT index

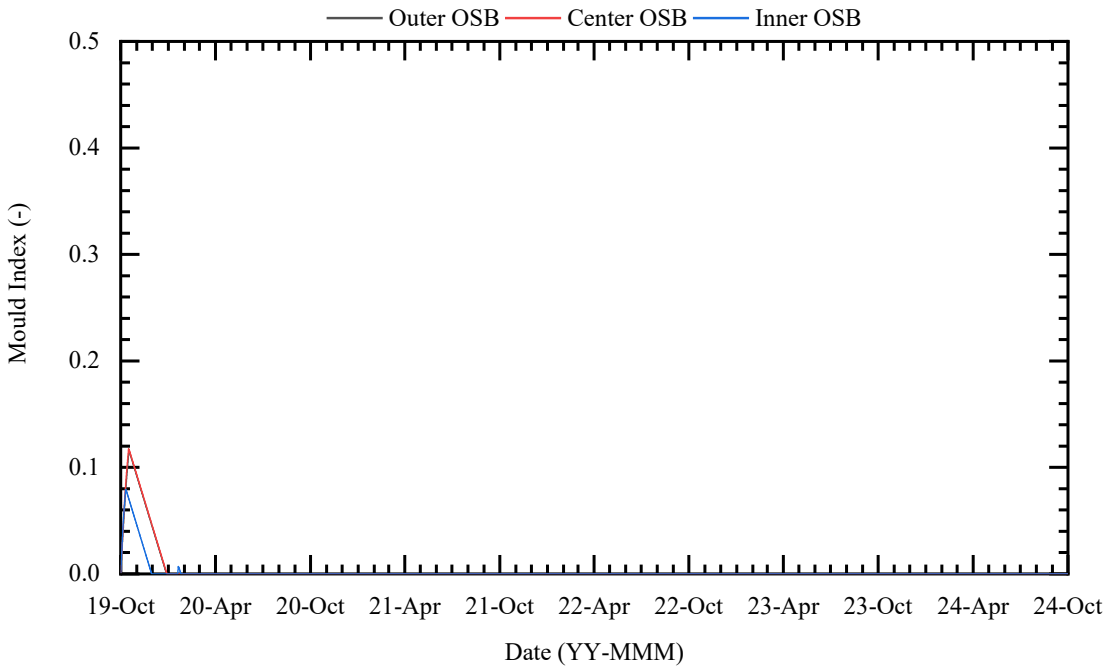

Figure 6-3: Calculated mould index for the simulated sheathing surface of an above-grade wall for new construction in Ottawa, CA

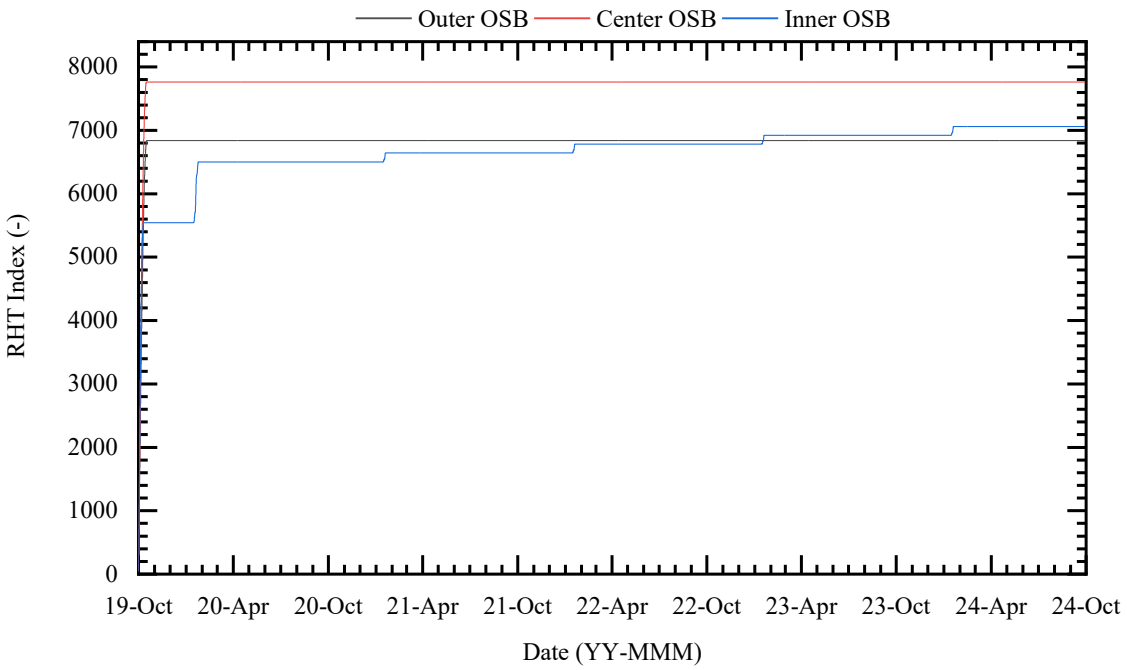

Figure 6-4: Calculated RHT80 for the simulated sheathing surface of an above-grade wall for new construction in Ottawa, CA

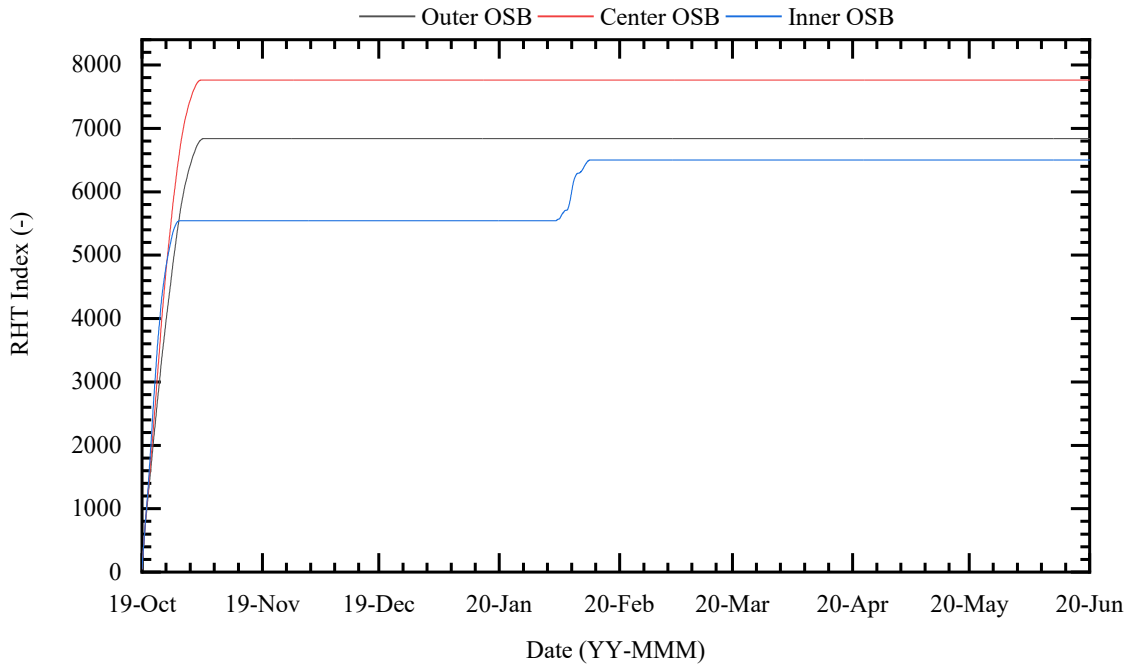

Figure 6-5: Calculated RHT80 for the simulated sheathing surface of an above-grade wall for new construction in Ottawa, CA during the first 8 months.

Overall, the simulations showed that VIP insulated new construction in Ottawa, CA would be safe from hygrothermal damage based on the 1D hygrothermal model.

6.2.2 Retrofit Construction in Ottawa

The building envelope retrofit simulated was performed to the exterior of the baseline vintages under two different approaches: removal of existing cladding or overcladding the existing assembly. From a hygrothermal standpoint, the amount of initial moisture in the existing building materials will change and the drying potential will differ based on the layered assembly.

In the cladding removal approach, all the material from the existing cladding up to the sheathing was removed before the retrofit. Under this approach, the sheathing could be checked for signs of long-term decay and the end of life materials can be removed. For this approach, a VIP insulated CIP was applied to the existing sheathing and cladding with a vented rainscreen and finished with composite wood siding.

In the overcladding approach, the existing cladding remains attached to the building, including the retained moisture by the absorptive materials, and new insulation and finish system are applied to the exterior. This approach could reduce the amount of waste and time required to complete the retrofit since there is less preparation required. For this style of retrofit, a VIP insulated SIP was applied to the exterior of the existing cladding.

The moisture profiles from the 20-year baseline stock simulations were used as initial conditions for these models. The water content in kg/m^3 from each material that would remain in place was applied to the same materials in the 5-year post-retrofit simulation. For the new materials used in the retrofit, the initial moisture and temperature were set to water content equivalent to 80% RH and 20°C. After the simulation was checked for convergence errors, the moisture in the sheathing was analyzed against the mould and RHT80 indexes. Simulations for both retrofit types

on five buildings vintages with brick and wood cladding were performed and the results were compared to the failure criteria.

For a cladding removal retrofit with a vacuum insulated CIP, the simulated relative humidity at the inner surface of existing sheathing (fibreboard or OSB) for all vintages evaluated had annual peaks between 50% and 70% RH after the initial dry out period, illustrated in Figure 6-6. During the first 6 months of the simulation, the existing sheathing dried from the elevated initial moisture content (between 24 kg/m^3 and 103 kg/m^3) from the baseline simulations. Furthermore, the calculated mould index for simulated retrofits, observed in Figure 6-7, showed that a low potential for mould growth exists and that the assembly could dry the initial moisture in the assembly before moisture-related issues could arise. Additionally, the masonry clad buildings showed tended to have a higher initial moisture content and were the only buildings to have conditions that could increase the potential for mould growth.

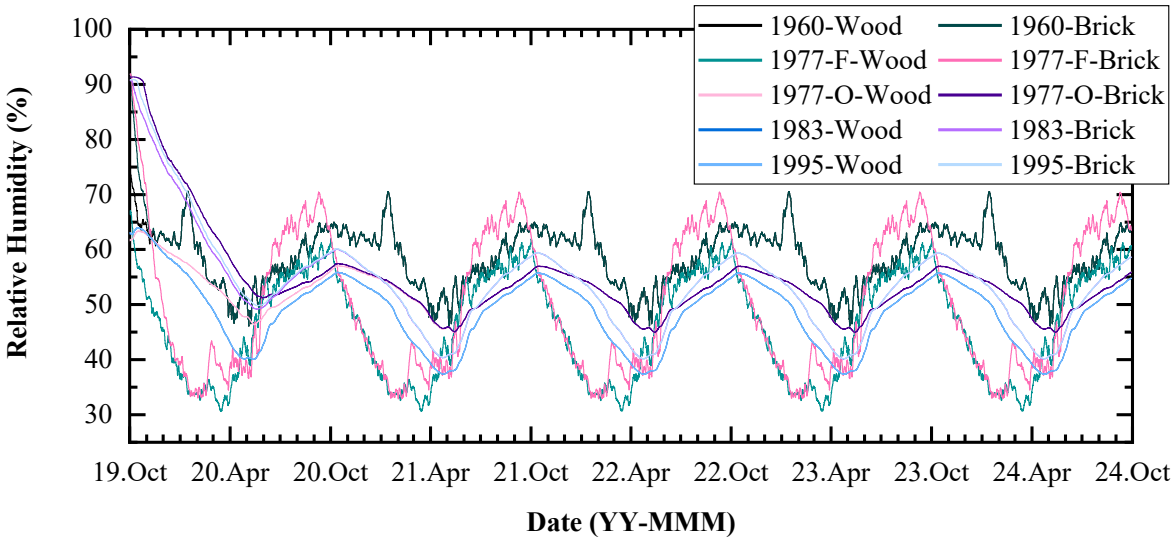

Figure 6-6: Simulated RH for the outer sheathing surface of an above-grade wall retrofitted with a CIP in Ottawa, CA. For 1977 Walls, F denotes fiberboard sheathing and O denotes OSB sheathing.

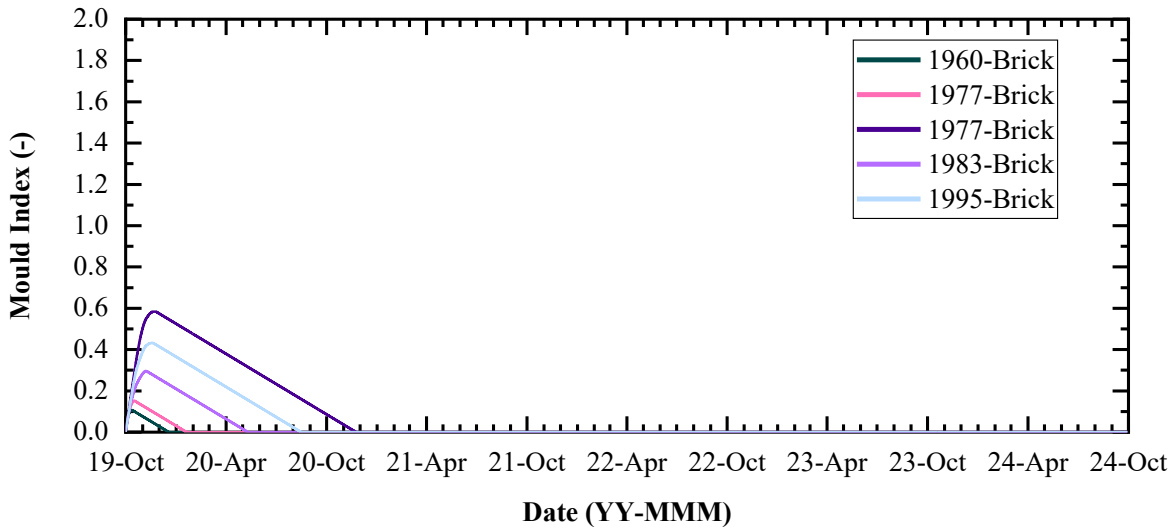

Figure 6-7: Calculated mould index for the outer sheathing surface of an above-grade wall retrofitted with a CIP in Ottawa, CA. For 1977 Walls, F denotes fiberboard sheathing and O denotes OSB sheathing.

In the overclad retrofit using a vacuum insulated SIP, two wood based materials would be susceptible to mould growth. For the OSB of the SIP, the simulated relative humidity varied between the vintages however did not eclipse the 80%RH threshold, except for intermittent periods between September and December. Since the simulated relative humidity was never greater than the critical relative humidity, there was no potential for mould growth at this surface.

At the outer surface of the existing sheathing, the initial moisture in the material varied with the vintage and was able to dry within the first 4-6 months post-retrofit. The initial moisture in the assembly was a concern after the retrofit since the surface temperatures inboard of the post-retrofit exterior insulation would increase. For the same amount of moisture content, an increase in temperature could cause the surface relative humidity to exceed the critical relative humidity for mould growth. Therefore, the mould index had to be calculated for this surface.

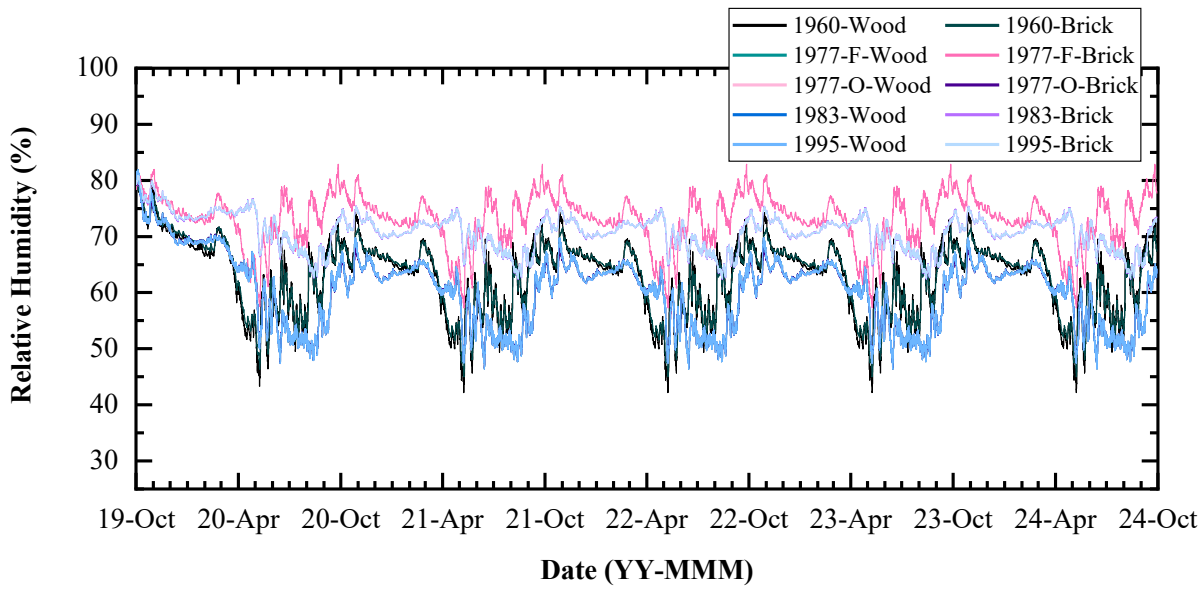

Figure 6-8: Simulated RHT for the new sheathing surface of an above-grade wall retrofitted with a SIP in Ottawa, CA. For 1977 Walls, F denotes fiberboard sheathing and O denotes OSB sheathing.

The mould index for retrofits overcladding brick buildings is presented in Figure 6-10 and shows that the peak mould index occurs during the dry out period. After the peak, there is a decline in the mould growth potential and there is no risk to mould growth on the exterior surface of the existing sheathing for any vintage of building after 1 year, and the mould index declines to 0 after 2.5 years post-retrofit. In total, two of the simulated vintages with a SIP retrofit exceed a mould index of 1, which means there is potential for small amounts of mould on the surface at a microscopic level.

The mould growth was greatest in the 1977 Brick clad wall assembly with OSB (1977-O) in both scenarios. Under the initial conditions from the baseline modelling, the 1977-O wall had the greatest amount of initial water content in the assembly. As such, the wall assembly took a longer time to dry the initial moisture, therefore had a larger peak mould growth index. Even though the wall assembly has a lower annual peak relative humidity in both the CIP and SIP panelized retrofits, the initial conditions dominated the mould growth potential in this study.

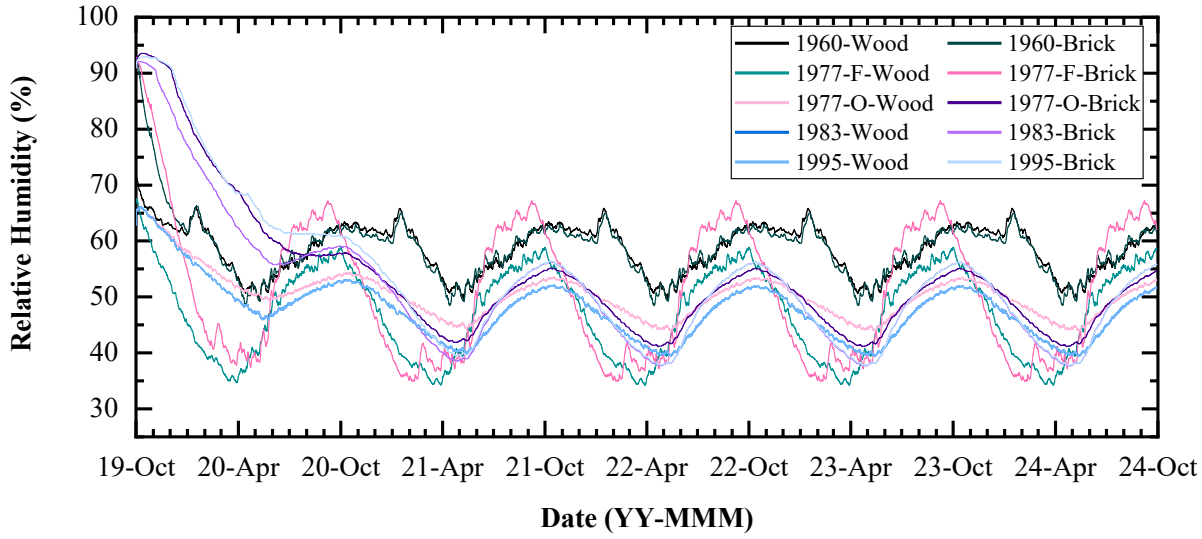

Figure 6-9: Simulated RHT for the existing sheathing surface of an above-grade wall retrofitted with a SIP in Ottawa, CA. For 1977 Walls, F denotes fiberboard sheathing and O denotes OSB sheathing.

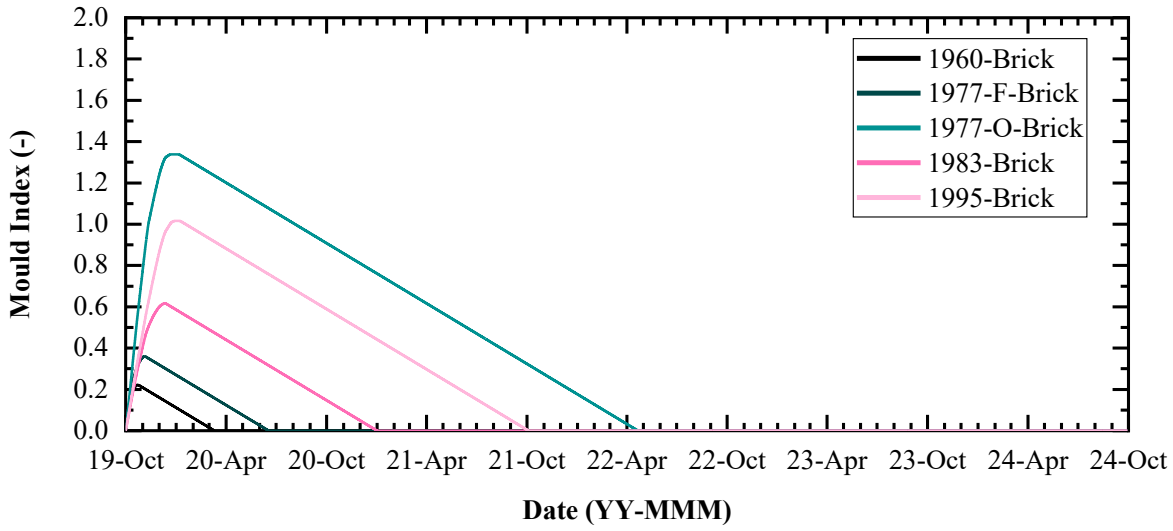

Figure 6-10: Calculated mould index for the existing sheathing surface of an above-grade wall retrofitted with a SIP in Ottawa, CA. For 1977 Walls, F denotes fiberboard sheathing and O denotes OSB sheathing.

6.3 Comparison to In-Situ Monitoring

The in-situ monitoring was compared to the simulations from the WUFI Pro 6.1 simulations. The hygrothermal modelling procedure used the measured initial conditions and boundary conditions (indoor and outdoor) from the in-situ testing. Material selection, air and

moisture sources and other model inputs used the best modelling practices described in Chapter 3. The model initial conditions were set to the first measured temperature and relative humidity or moisture content of the materials in the assembly, when available. A climate file was created using the measured interior conditions (T, RH) and used as the interior boundary condition in the simulation. Environment Canada's historical weather database was used to create an outdoor climate file including temperature, relative humidity, total rain, wind speed and wind direction using hourly and daily weather files from a nearby weather station. Since solar data was not recorded at the weather stations and not available on-site, the solar radiation data was taken from the ASHRAE Year 1 weather files for hygrothermal simulations.

No material properties were altered however, was expected that there could be some variation in properties between the materials selected for the simulation and the actual materials used for the experiment.

The in-situ monitoring used a SIP panel with VIPs on a 2x6 wood-frame wall with cavity insulation space on 400 mm (16") centers and a CIP panel with VIPs on a 2x4 wood-frame wall spaced on 400 mm (16") centers with cavity insulation and plywood sheathing.

6.3.1 Structural Insulation Panel (SIP)

The SIP system was installed in Bay A of CE-BETH in October 2015 and was monitored until February 2021. The system was installed on a 2x6 wood-frame wall with fibreglass batt insulation spaced on 400 mm (16") centers with a 6-mil poly vapour barrier finished with gypsum board and vapour-resistant paint. The sheathing was outboard of the insulation and was faced with Tyvek weather resistance barrier and vinyl siding. This assembly was meant to mimic an above-grade wall assembly that mimics what would be seen in a new build in Ottawa, CA.

The results from the in-situ testing at CE-BETH and the results from WUFI Pro 6.1 simulations were compared. In this assembly, the sheathing was uninsulated and placed outboard of the EPS and VIP insulation. Therefore, the measured surface temperature varied closely with the exterior temperature with a significant amount of variance caused by the environment. This was also reflected in the simulated results.

The simulated relative humidity was observed to be significantly different than the measured surface relative humidity. In Figure 6-11, the relative humidity at the exterior surface of the sheathing was plotted for a simulated wall assembly with VIP and failed VIPs, and the measured data. The model overpredicted the initial moisture in the assembly, as well as the relative humidity throughout the monitored period. The model had its best agreement with the model from April 2018 to April 2019 however, the results diverged afterwards.

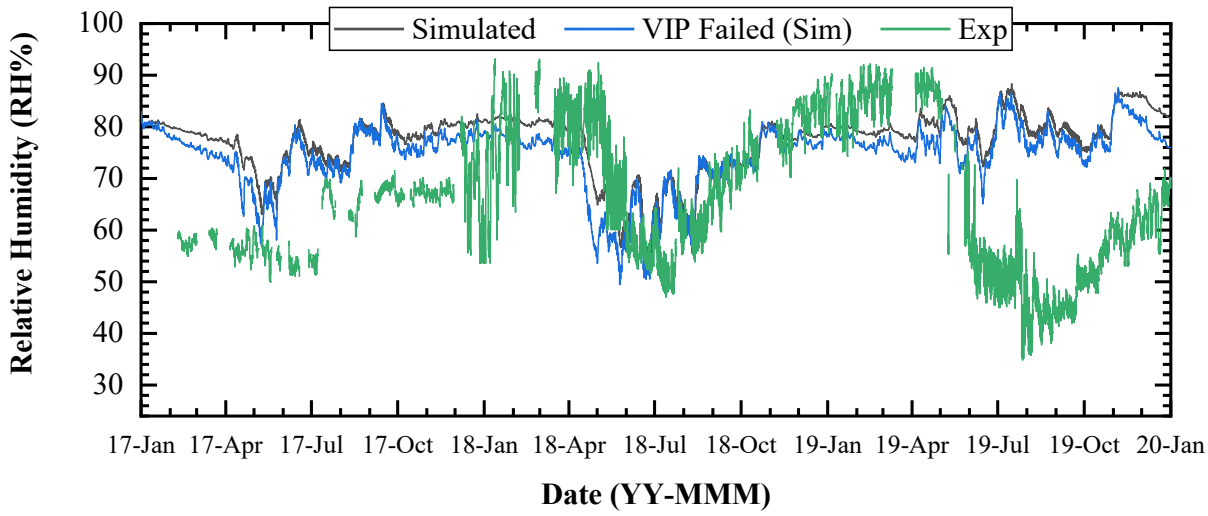

Figure 6-11: Measured and simulated inner sheathing surface temperature over the test period

During three warm months in 2018, the simulated and measured relative humidity was compared. The measured relative humidity was found to have a greater daily variance compared to the simulated data, presented in Figure 6-12. In this case, the exterior sheathing relative humidity

was likely influenced by the exterior conditions, rather than the interior due to its placement in the assembly and the interior vapour barrier. Reasons for the discrepancies in the results could include incorrect weather data, specifically solar radiation, differences in the measured and simulated material properties in the assembly, and differences in the wetting mechanisms.

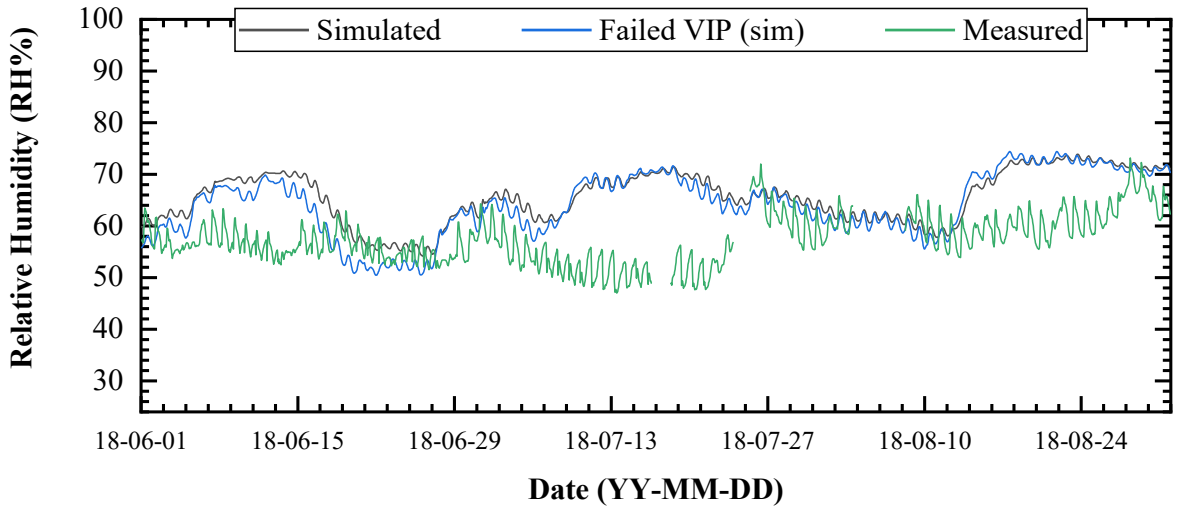

Figure 6-12: Measured and simulated sheathing surface relative humidity from June 2018 to September 2018

The measured and simulated results for the SIP panel showed agreement for one year out of the 3-years monitored. The sensors installed on the exterior surface of the sheathing had a high variance and as a result, made verifying the model challenging. Fortunately, the simulated results normally had a more conservative estimate for the surface relative humidity, which is useful during the building design stage and provide more confidence that this type of system would be durable long-term.

6.3.2 Composite Insulation Panel (CIP)

The CIP system was installed on a 2x4 wood-frame wall with fibreglass batt insulation spaced on 300 mm (12”) centers with vinyl siding at CE-BETH. This arrangement was used to replicate a retrofit of a 1980s vintage above-grade wall assembly. The WUFI simulation used the

best modelling practices described and specific material properties when possible. The measured moisture content, temperature and relative humidity from CE-BETH were compared to the simulated values to compare the expected values from the model to the measured values on-site.

The simulated and measured sheathing surface temperatures for 3 years are shown in Figure 6-13. The sheathing surface temperature insulated by VIP and EPS are included in the figure and plotted alongside the simulated sheathing surface temperature (black). When the same boundary conditions are applied to the simulated wall assembly, there appears to be an agreement between the measured and simulated trends. By looking at the results presented in Figure 6-14 during a cold week in 2018, when the temperature gradient through the wall assembly is greatest, the model underpredicted the temperature in the assembly. The simulated temperature was about 2°C colder than the measured temperatures at CE-BETH but followed the trend over the week well.

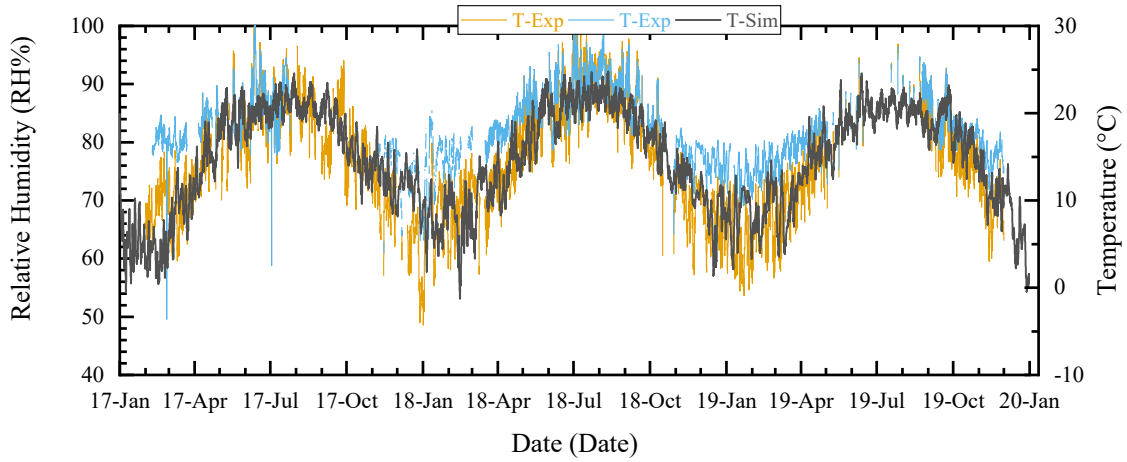

Figure 6-13: Measured and simulated inner sheathing surface temperature over the test period

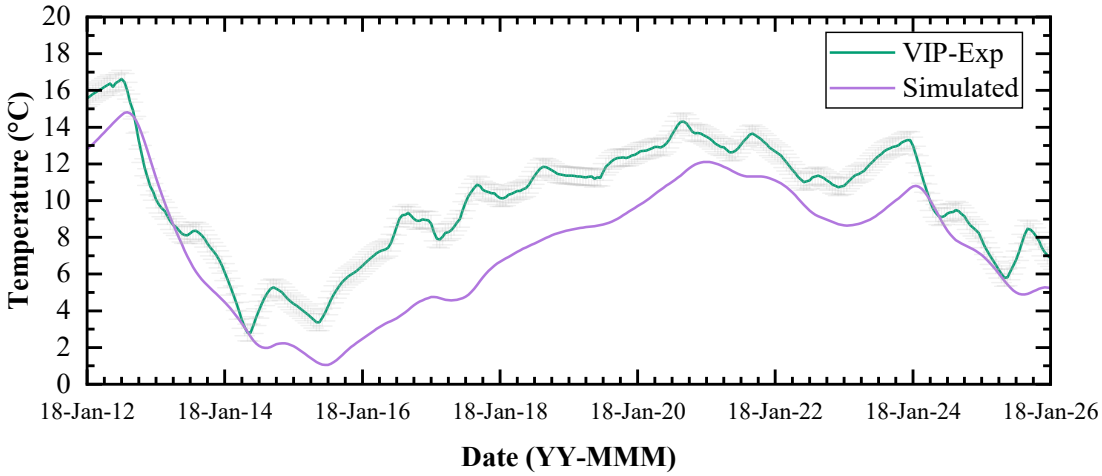

Figure 6-14: Measured and simulated inner sheathing surface temperature over a cold week. Sensor error denoted by the gray.

The measure and simulated RH at the inner sheathing surface did not correlate as well as the temperature values. The simulated relative humidity of the sheathing insulated with an intact and failed VIP is presented. The initial moisture conditions were overestimated in the model however, the simulated and measured conditions do converge within the first year.

There were instances when the simulated did not match with the measured data however the seasonal trends between the numerical and experimental results were consistent. Specifically, the periods between August 2017 and November 2017 (data collection gap) and February 2019 and April 2019 when the model predicts a wetting event of the sheathing. Reasons for the discrepancies could include variance in the redistribution of moisture in the experimental setup while the model only simulates a single dimension, variance in material properties between the experiment and model that were not considered, and the wetting assumptions used in the model could have been different than the actual wetting.

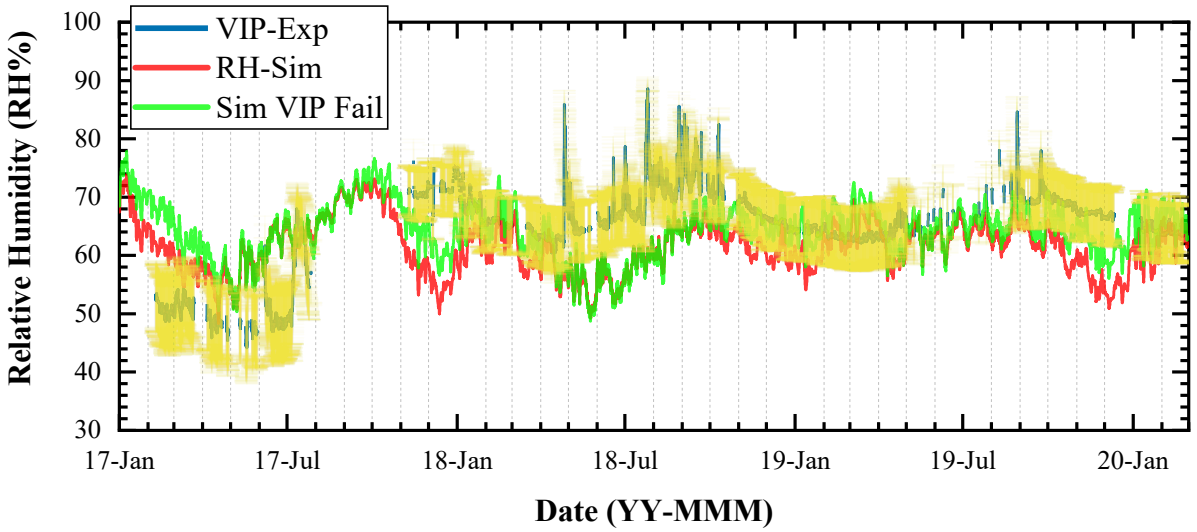

Figure 6-15: Measured and simulated RH over the measured period on the VIP insulated sheathing. Sensor error denoted by yellow.

Significant differences in measured and simulated RH were observed when looking at 1 month periods. During August 2018, a warm month, the measured relative humidity was greater than the simulated relative humidity and was influenced more by the interior relative humidity conditions than the simulation predicted presented in Figure 6-16. This is apparent in the daily cycles apparent in the measured data as well as the alignment of quick increases in RH for the interior and measured data.

During a cold month in 2018, the model would underpredict the relative humidity however, the trend over the month was noticeably closer than the summer. From Figure 6-17, the spread between the measured and simulated relative humidity varied between 4-12%RH during the period. The interior relative humidity was low during the winter (30% or less), and the daily cycling that was seen during the summer is no longer appear in the winter.

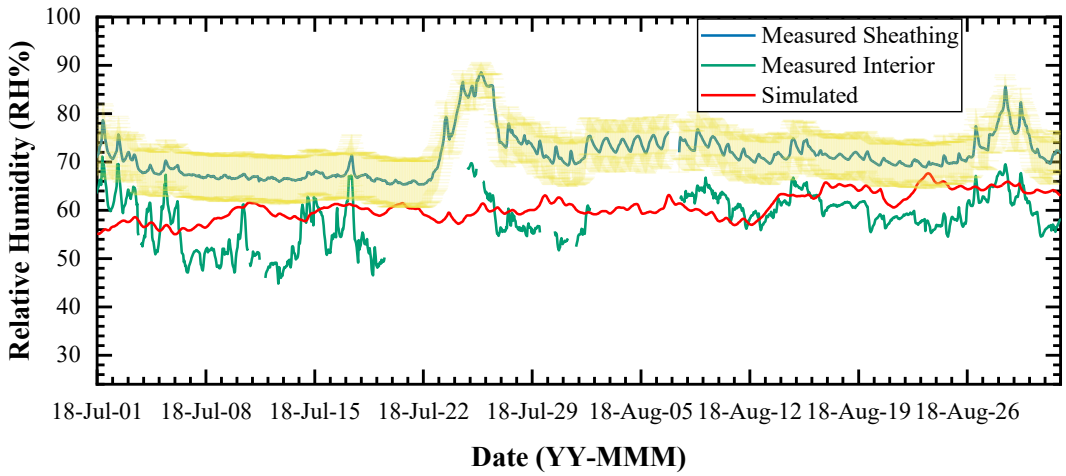

Figure 6-16: Measured and simulated RH on the VIP sheathing insulated over a warm period (July-Aug. 2018). Sensor error denoted by the yellow

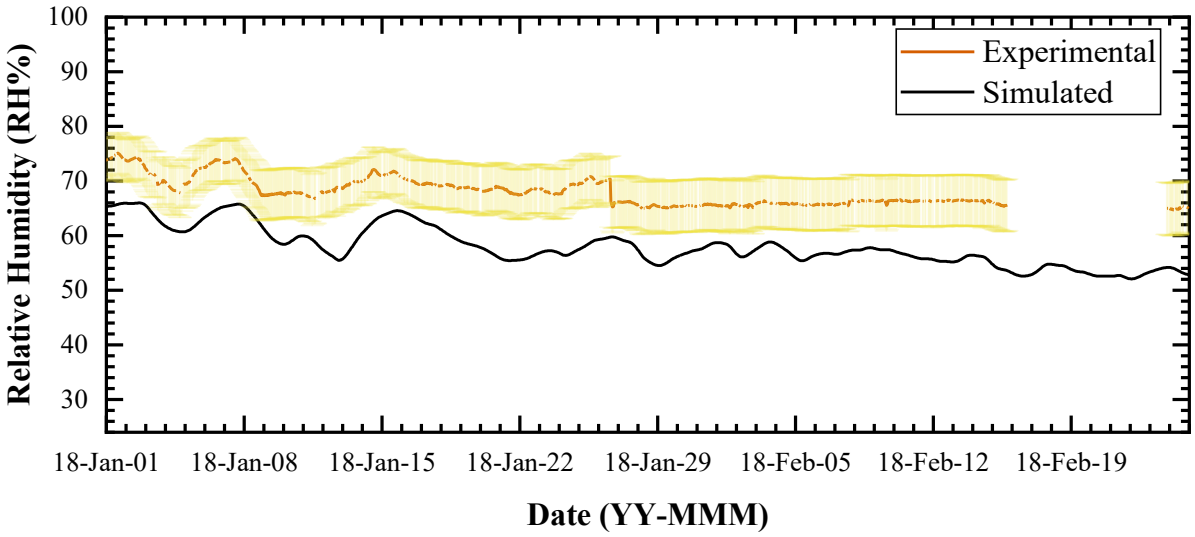

Figure 6-17: Measured and simulated RH at the VIP insulated sheathing during a cold month (Jan. 2018). Sensor error denoted by the yellow

The RSME was used to compare the experimental data to the modelled results using the measured boundary conditions and best practice assumptions. The RSME was calculated, and when a data gap existed, those points were excluded. The temperature and relative humidity at the inner sheathing surface insulated by a VIP was used for the comparison. From 2017 through 2019, the RSME between the experimental and modelled data was calculated to be 4.0°C and 7.3% RH.

The error between the data and modelling was not as accurate as expected and the unmonitored variables, such as air leakage and exact wetting from wind driven rain. Since these variables were not monitored in the in-situ study, they were estimated by using best practice assumptions for hygrothermal envelope modelling. To reduce the RMSE between the predicted and measured values, a more accurate and robust monitoring system for the boundary conditions, specifically the exterior boundary with temperature, humidity, wind velocity and direction, solar irradiation and wind driven rain on the surface. The parametric study of input modelling variables was performed to quantify the sensitivity of the input variables to the results, in lieu of the model calibration.

6.4 Parametric Study

The parametric study was performed using the WUFI Pro model and by simulating a wood-framed above-grade wall in Ottawa, CA. The process variables, described in a previous chapter, were varied with three different input levels and their relative impact was analyzed using the Morris Method. Each parameter evaluated below compared to the baseline conditions as well as the overall impact of each variable on the simulation.

6.4.1 Indoor Climate

The indoor climate is the interior boundary condition of the model and a source of heat and moisture for the model. The interior climate is a function of relative humidity and temperature that varies with each timestep through the simulation. The climate can be related to the (1) outdoor temperature and relative humidity, (2) number of occupants or activities within the building or (3) the setpoint if mechanical ventilation is available. In this study, the above-grade wall assembly was modelled using three interior climate files to measure the impact of varying the boundary condition.

A sine curve was utilized for the three indoor climate boundary conditions using the built-in WUFI conditions for low, medium, and high moisture load conditions. Effectively, the relative humidity setpoint increases by 7% for each step. From the simulation, the temperature and relative humidity from the nodes at the sheathing surfaces (interior and exterior) were extracted and plotted in Figure 6-18.

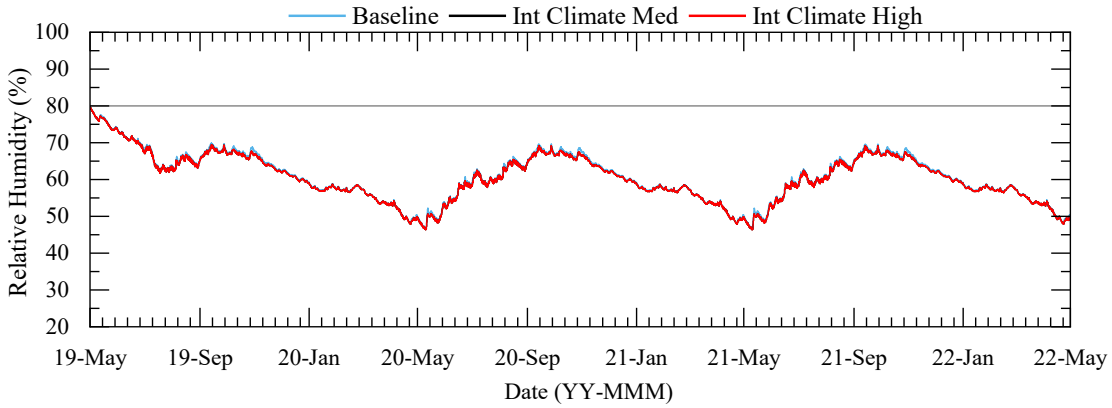

Figure 6-18: RH at the sheathing for various indoor climates

6.4.2 Wetting Plane

The wetting plane is the location that the wind-driven rain is deposited in the model. Based on modelling principles outlined by Lstiburek [124], the wind-driven rain (WDR) should be added to the enclosure as a moisture source within the assembly. They approximated that 1% of the WDR will make it to the outboard surface of the water control layer. Also, they predict that 1% of that 1% will penetrate inboard of the water control layer and represent a small water control leakage into the assembly. For this parametric study, the moisture source was added at the suggested surface, 1% inboard of the water control layer and 1% on the outboard surface of the sheathing. When the 1% WDR moisture source was applied inboard of the water control layer, the assumed water control leakage was included as a single moisture source. The simulations were used to examine the impact of the quality control layer on the hygrothermal performance of the enclosure,

and the parameters screening in the model. The temperature and relative humidity at the inboard and outboard sheathing surfaces are shown in Figure 6-19.

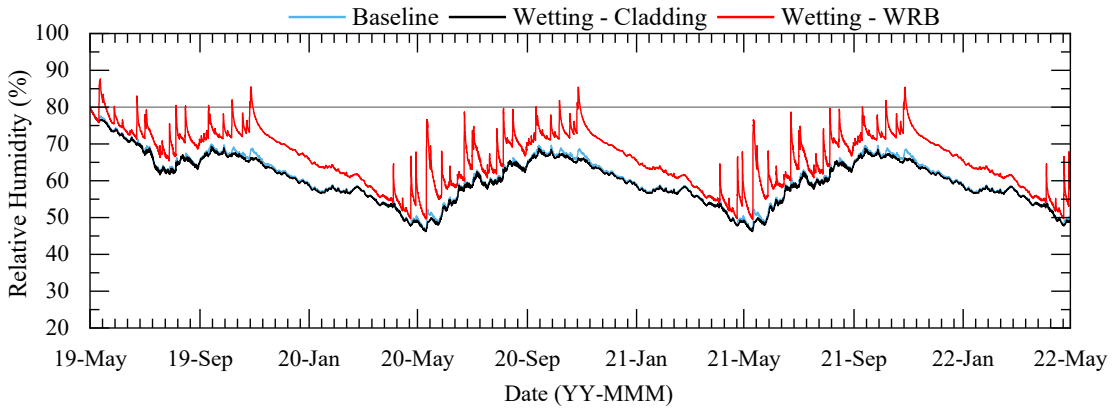

Figure 6-19: RH at the sheathing of an above-grade wall assembly with varied wetting planes.

6.4.3 WDR Moisture Source

Like the wetting, the moisture source was varied to evaluate the effect the amount of rain penetration has on the simulation results. The amount of WDR deposited outboard of the water control layer was varied from 1% up to 5% for the parametric study. The temperature and relative humidity for the inboard and outboard surfaces of the sheathing is presented in Figure 6-20.

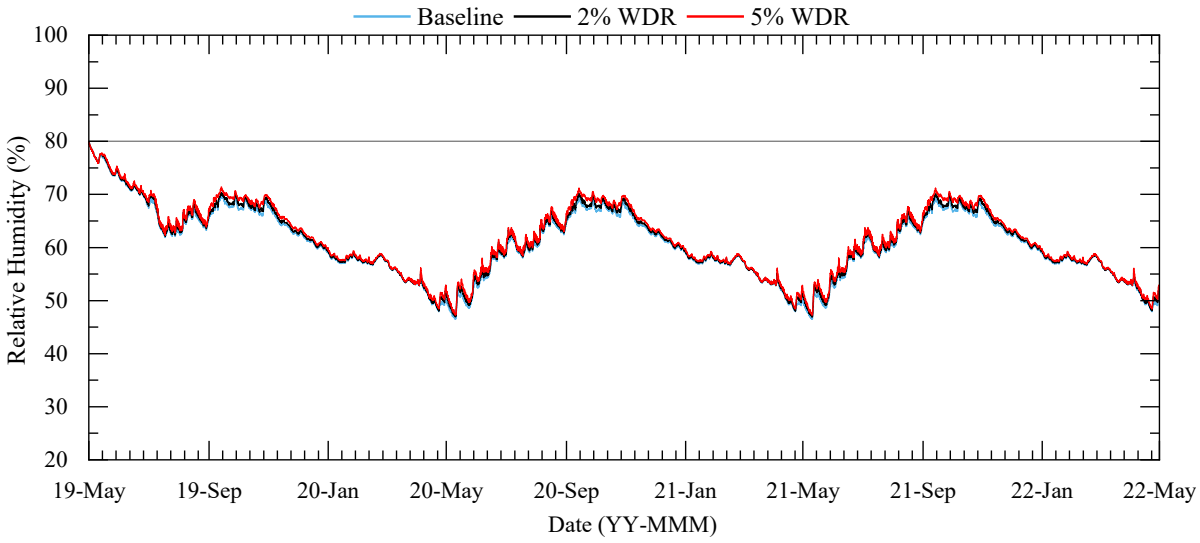

Figure 6-20: RH at the sheathing for varied % of wind-driven rain

The location of the WDR was kept constant for the initial study but was also varied with the different wetting planes outlined above, as it was anticipated the impact from these variables would be related.

6.4.4 Initial Construction Moisture

The initial construction moisture represents the amount of moisture in the system upon completion and occupation of the building. During the construction of a new or retrofit project, materials will spend an undefined amount of time exposed and unprotected from the elements. Materials, like brick and wood, have a level of moisture storage that could be a concern over a long time. The initial construction moisture was varied between 80% RH (common modelling practice) up to 90% RH to represent wet materials. The temperature was kept constant at 20°C for all materials to ensure that the maximum moisture capacity was consistent for the study. The temperature and relative humidity were plotted in Figure 6-21.

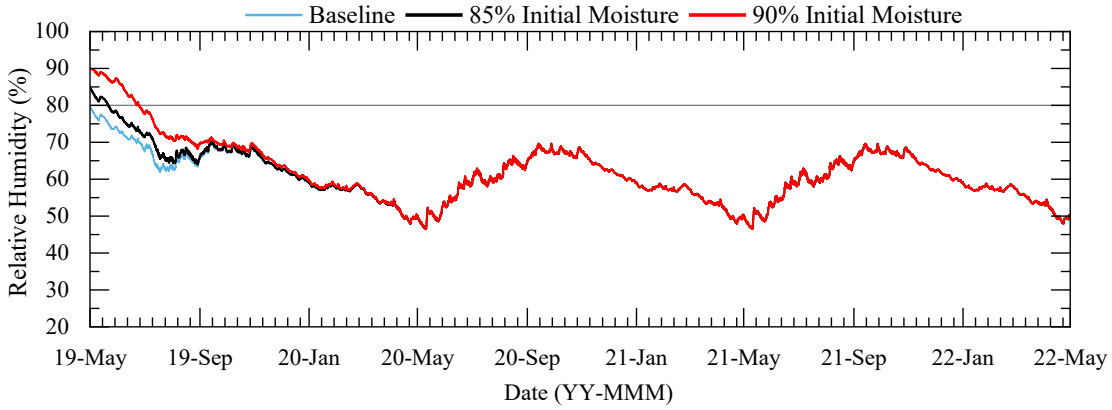

Figure 6-21: RH at the sheathing for various initial construction moistures

6.4.5 Season of Completion

The season of completion was varied because the heat and moisture fluxes and wetting were dependent on the exterior conditions. If the construction was completed during the Winter under a -20°C exterior temperature with a different radiation profile and limited wetting, it was

anticipated the above-grade was assembly would experience a different peak mould index compared to the same above-grade wall assembly with the same assumptions completed in the Summer with 20°C and more liquid rain wetting. The completion dates were varied as May 1, July 1st, and October 1st. Figure 6-22 plotted the changes in relative humidity and temperature during the first annum to highlight the difference the season impact makes on the

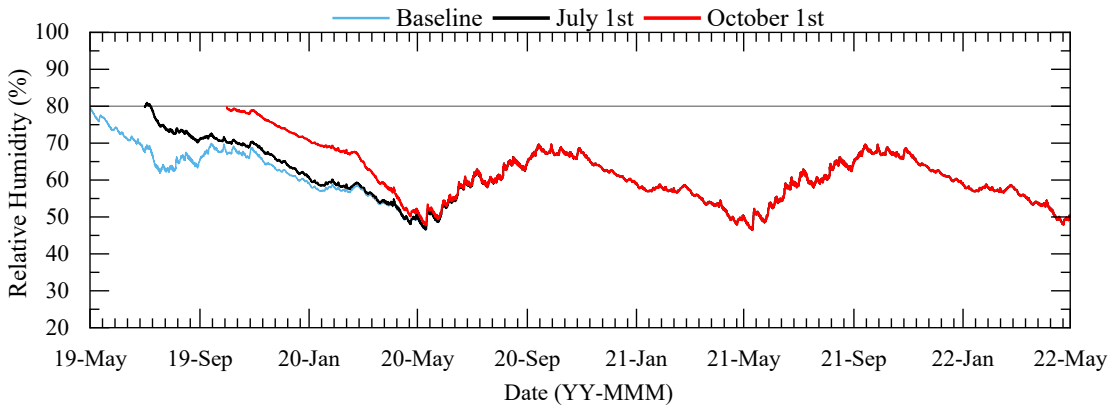

Figure 6-22: RH at the sheathing for various seasons of completion

6.4.6 Outboard Construction

The vapour permeability of the outboard construction affects the moisture drive through the assembly. With moisture permeable insulation used as continuous insulation, there is an increase in moisture drive and drying potential towards the exterior, generally the direction of moisture transport during the cold winters. In the simulations, the insulation and water control outboard of the sheathing was varied to assess the impact of a permeable and impermeable material on the sheathing moisture condition. Also, the rainscreen was removed from the above-grade wall construction and the moisture conditions at the sheathing were compared when a water control layer and effective drying plane is removed. Figure 6-23 shows the relative humidity and temperature of the sheathing for various outboard constructions.

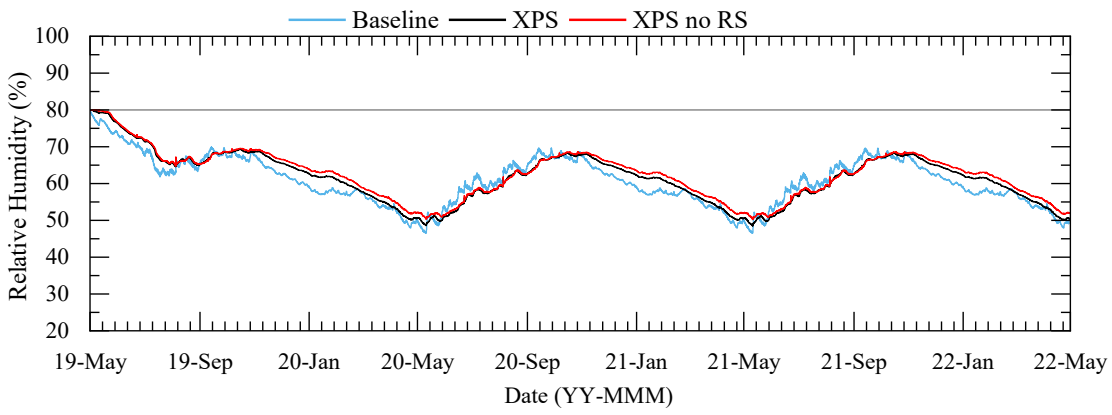

Figure 6-23: RH-T at the sheathing for varied vapour permeability outboard simulation

6.4.7 Vapour Control

The interior vapour control protects the sheathing from warm moist air diffusion towards a condensation plane within the above-grade wall assembly. Membranes for interior vapour control can be vapour impermeable or vapour retarding depending on the climate and the vintage of the home. The simulations were run using a vapour impermeable barrier, a vapour retarding barrier, and a barrierless above-grade wall assembly to assess the impact of each factor on the moisture conditions at the sheathing. The numerical results were plotted in Figure 6-24.

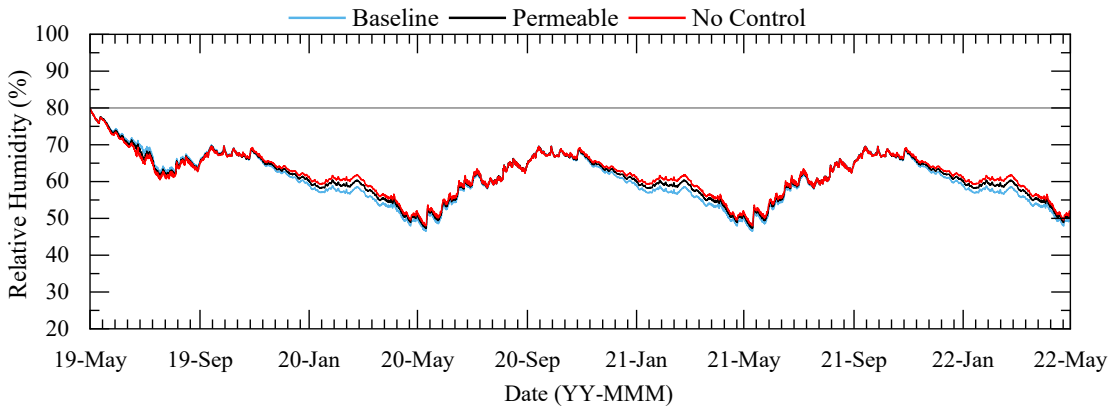

Figure 6-24: RH at the sheathing for various levels of interior vapour control

6.4.8 Above-Grade Wall Orientation

Different above-grade wall orientations will be exposed to different wind-driven rain wetting and solar exposure throughout the simulation. Those factors affect the moisture fluxes within the wall as the wind-driven rain acts as the moisture source within the assembly and a lack of solar exposure will reduce the amount of solar-driven moisture in the assembly. The orientation was varied between the North, South and East directions in the study to capture the extremes of solar exposure with a combination of wetting profiles. The moisture conditions at the surface of the sheathing are shown in Figure 6-25.

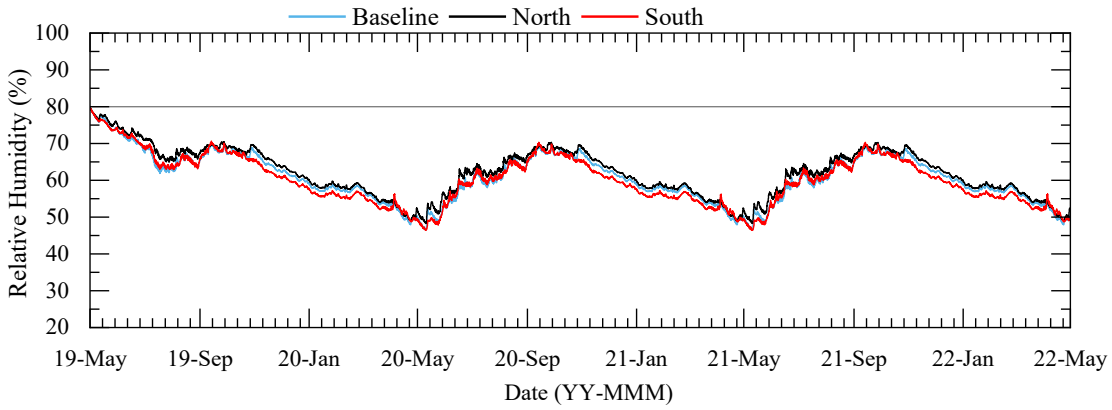

Figure 6-25: RH-T at the sheathing for various above-grade wall orientations

6.4.9 Random Sample and Elementary Effects

The objective of the parametric study was to screen the input parameters for a greater impact on the results of the WUFI hygrothermal models. The screening was used to reduce the computational time and narrow the broad range of input variables and vary the model inputs that have the greatest impact on the results. The elementary effect of each input parameter was calculated based on the final MI output from the simulation and the input parameters varied OAT. Screening the input variables and calculating the elementary effect meant the final sensitivity, μ, and the non-linear effects, σ, can be computed and compared for all values.

The random sample was generated using a randomly generated number between 1 and 3 in Excel. A number was generated for each variable for each simulation. The input level from Table 4-3 was assigned a value of 1 to 3 and was numerically evaluated in WUFI. From the result files, the mould index of the interior and exterior surfaces of the OSB sheathing was computed. In total, 10 variables and 33 simulations were defined based on the randomly generated value.

In total, a randomly generated matrix for 10 input values for 33 simulations was created as well as the elementary effects from each numerical simulation can be found in Appendix B.

6.4.10 μ^* and σ of Model Inputs

Following the calculation of the elementary effect of each input on the plot, the screening parameters could be computed according to Chapter 4. The μ_j^* and σ values represent the average difference in output caused by input, j, and the standard deviation of the change in output caused by input j, respectively. The greater the μ_j^*, the greater the sensitivity of the input on the model outputs. While large values of standard deviation would indicate that the effects of the model input have a non-linear effect on the output results. The results from the Morris Method are best represented as a plot of μ^* versus σ, shown below in Figure 6-26 and Figure 6-27. The two plots include the calculated values for all the input parameters of interest based on the calculated mould index on the interior and exterior sheathing surfaces.

Table 6-3: Mean and standard deviation of the input parameters studied in the Morris Method screening

Input Parameters	$MI_{interior}$		$MI_{exterior}$	
	μ^*	σ	μ^*	σ
Initial Construction Moisture	1.511	2.010	1.058	1.301
Construction Completion	1.429	1.668	0.929	1.097
Vapour Control	1.518	2.036	1.038	1.395
Orientation	1.542	2.165	0.951	1.420
WDR Past Water Control	1.312	1.797	0.942	1.346
WDR Past Vapour Control	1.040	1.470	0.645	1.042
Interior Conditions	1.124	1.791	0.950	1.636
Construction	1.549	2.059	1.421	2.230
Timestep	1.464	1.810	1.042	1.255

From the Morris Method screening, some clear trends were observed. The exterior and interior surfaces of the sheathings were both monitored to ensure that the observations were consistent. The values monitored on the exterior surface showed that the input with the largest impact on the mould index was the construction of the wall assembly, specifically the inclusion of a rainscreen and varying the permeability of the exterior insulation. These changes impacted the wetting and drying potential of the wall assemblies. In the case of an above-grade wall assembly without a rainscreen and vapour impermeable exterior insulation, the wetting would be higher, and the drying potential would be lower compared to the baseline assembly. Other inputs (e.g., orientation, vapour control, initial construction moisture, timestep, interior conditions, and

rain past the water control layer) were clustered with the same impact for the exterior sheathing. The plot shows the relative impact of one variable compared to another and that these input parameters have near equal significance in the modelling of an above-grade wall assembly.

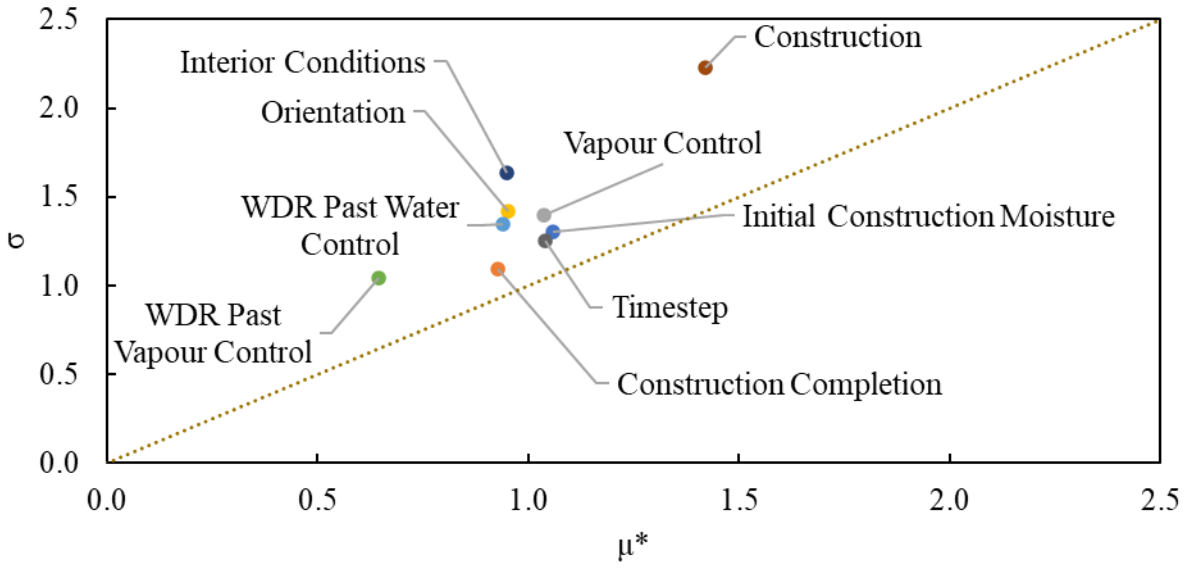

Figure 6-26: Morris Method results (μ^*, σ) on the exterior sheathing surface

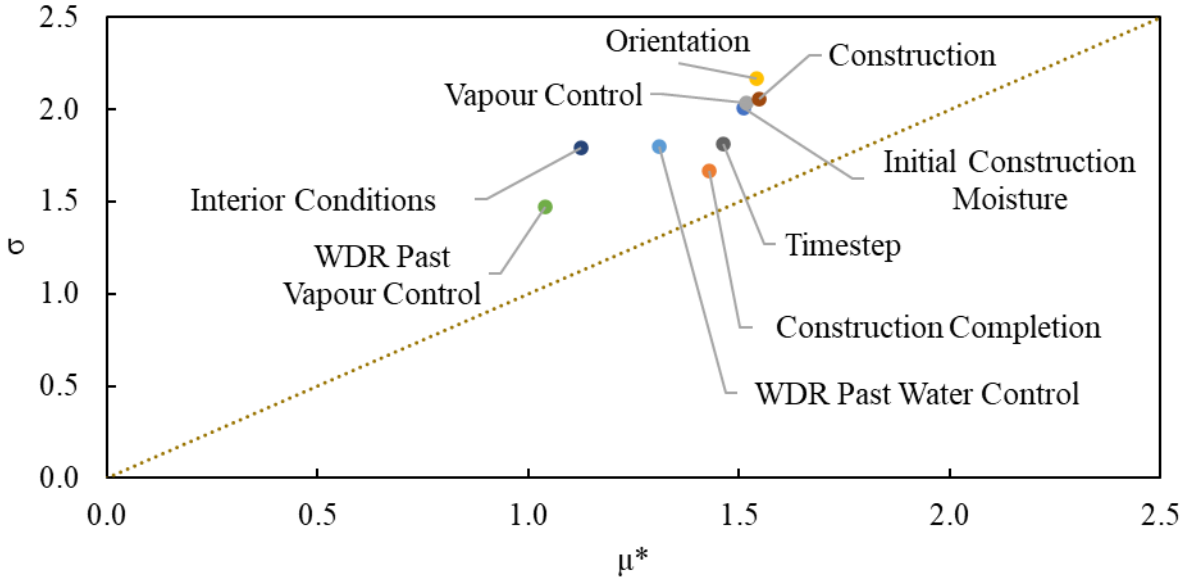

Figure 6-27: Morris Method results (μ^*, σ) on the interior sheathing surface

The interior sheathing surface showed a significant impact on the mould index output compared to the exterior sheathing surface. Four input parameters (construction, initial construction moisture, orientation, and vapour control) were clustered as the most sensitive parameters. The other parameters were mostly clustered together with a slightly lower impact on the mould index result.

In comparison to the exterior sheathing surface, the most sensitive input parameters for mould index exterior sheathing surface showed equal or greater significance on the mould index for the interior sheathing surface. The interior sheathing surface did show a greater impact on the mould index. During the other simulations, the trend of greater mould index on the interior surface was observed and agree with the results from the Morris Method screening.

6.5 VIP Insulated Assemblies Across Canada

The high-performance new construction and retrofit wall designs were evaluated in different Canadian climates through WUFI Pro because of the promising initial results from the experimental testing and numerical studies of the VIP insulated above-grade wall assembly in Ottawa, CA. The VIP exterior insulated above-grade wall assembly for new construction was simulated using a city-specific weather file as the outdoor conditions and simulating the orientation with the most wind-driven rain. The VIP exterior insulated above-grade wall assembly for retrofit construction was evaluated using a city-specific weather file with the worst-case orientation for wind-driven rain as well as adjusted initial conditions for moisture content. The initial moisture content of materials in the existing wall assembly was taken from a separate WUFI simulation of a wall assembly of 1960s vintage. The remaining numerical inputs were consistent with the proper hygrothermal modelling procedures outlined in Section 4.3.

6.5.1 VIP Insulated Above-Grade Wall Assembly for New Construction

The VIP insulated an above-grade wall assembly was evaluated using WUFI Pro 6.5 using different Canadian cities under a set of conservative conditions. A VIP insulated SIP and CIP systems were evaluated on a code-built wall assembly with a non-absorptive cladding material, such as vinyl siding or treated wood composite siding, with an air cavity behind the cladding. Additionally, a wood-framed wall with fibreglass batt insulation, interior vapour impermeable barrier and painted gypsum board. The wall assembly was selected as it best represented the expected wall construction across Canada for low-rise housing. The same modelling assumptions for Ottawa, ON were applied to other cities used in the cross-Canada study.

The relative humidity and temperature from nodes on both sides of any layer sensitive to potential mould growth were exported from the numerical simulation. In the new construction wall assemblies, the sensitive layers included both sides of the OSB skins for the SIP assembly and the OSB sheathing for the CIP assembly. The results were post-processed using MATLAB to calculate the mould index and the RHT index at each node. Additionally, the vapour pressure difference and vapour balance were calculated for each city for further comparison between climates.

The wall assembly insulated with a CIP panel was simulated in WUFI with monitors placed on the inner and outer OSB surfaces. The inner OSB surface was found to have a greater moisture content compared to the outer surface, therefore it was analyzed further. The relative humidity was exported from the monitors and the inner OSB surface was plotted in Figure 6-28 for the 5-year simulation period for each city. Based on the plot, the year-over-year relative humidity from the simulation was repeated, which shows a balance between the wetting and drying in the assembly. The numerical relative humidity at the inner OSB surface in each city except Whitehorse, YK tended to have comparable results. When the relative humidity does not exceed the 80% RH

threshold, the mould index and RHT index will be 0 or very low, which was the case for most cities investigated.

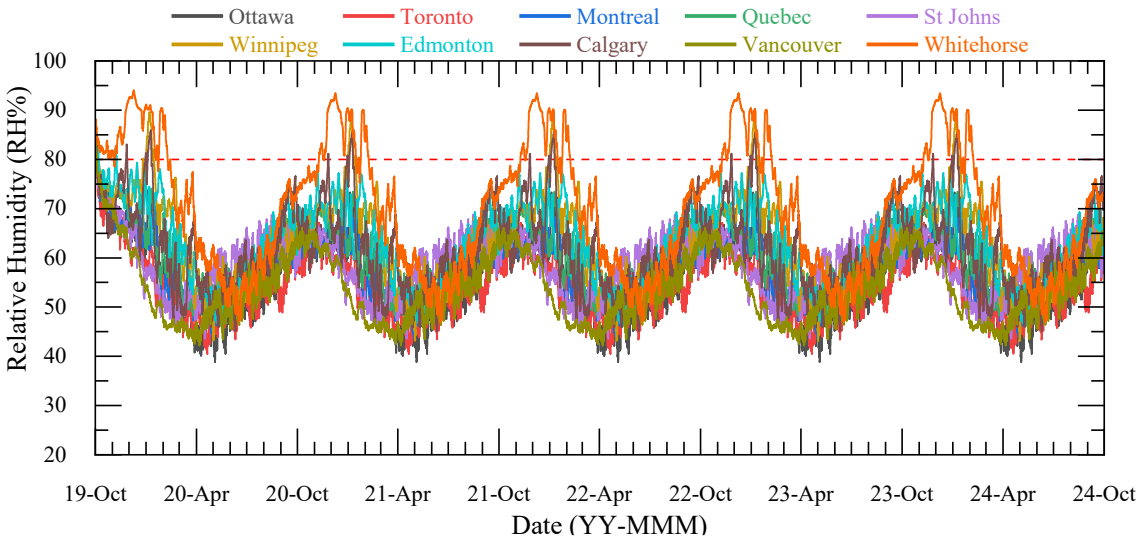

Figure 6-28: RH and T of VIP insulated wall assembly for CIP new construction over 5-year simulation.

The inner OSB surface RH during the first annum was used to evaluate the dry-out period for the assembly in each city. The dry out period is defined as the time required for the surface RH to drop below the 80% relative humidity threshold. In the case of new construction wall assemblies, it was assumed that all building materials would start at an EMC equivalent to 80%RH and 20°C. The dry out periods observed for this type of assembly, shown in Figure 6-33, were short since the initial moisture content levels were low, the exception was Whitehorse, YK. In Whitehorse, the inner OSB surface RH exceeds 80% for most of the heating season (Oct-19 to Feb-20) before dropping to less than 80% for the remainder of the first year. A long dry-out period is not an issue when compared to the failure criteria; however, it could lead to a higher mould index and RHT index that could lead to failure.

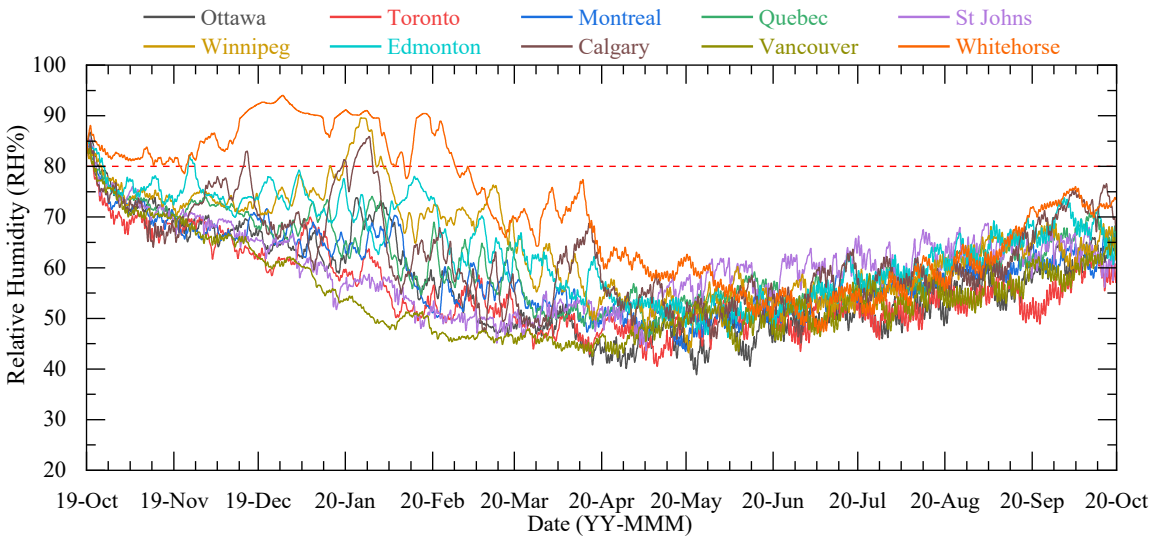

Figure 6-29: RH and T of VIP insulated wall assembly for CIP new construction during the first year of simulation.

As the inner OSB surface RH over the test period indicates, the mould index and RHT index for this assembly on that specific surface remains very low, as seen in Figures 6-30 and 6-31 respectively. For the mould index, there is an increase in the mould index during the first year that peaked well below 1 for all the cities. In the plot, the only cities with a visible mould index are Whitehorse, Calgary, and St. John's. Similarly, the RHT index at the inner OSB surface in the previous cities had a sharp increase during the first year, as well as a slight increase during the following years during the heating season. The inner OSB surface would be at no risk for potential mould growth in this type of assembly.

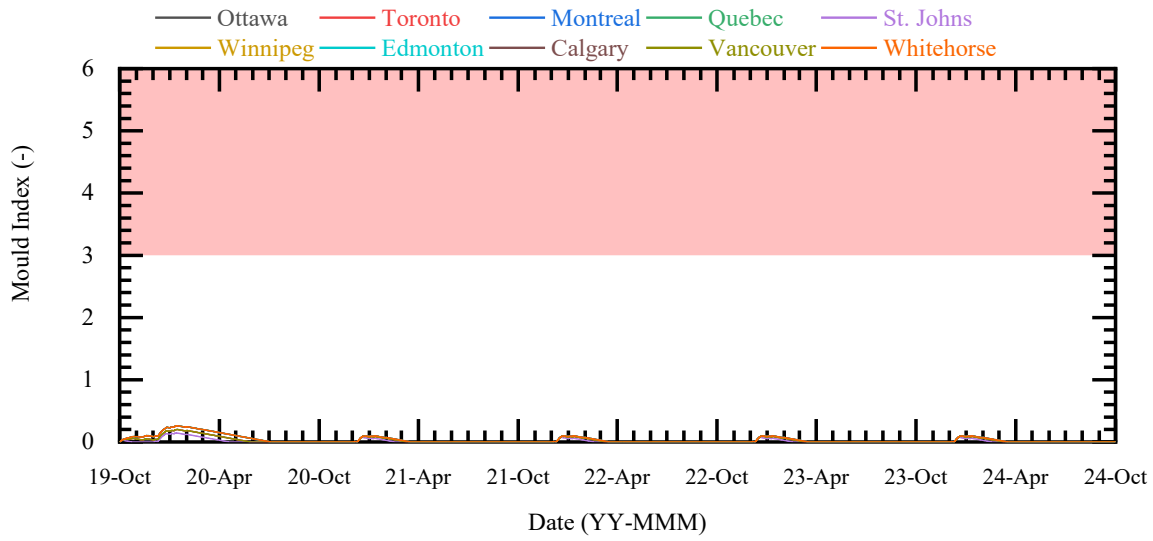

Figure 6-30: Calculated Mould Index for CIP wall assembly for new construction in Canadian cities.

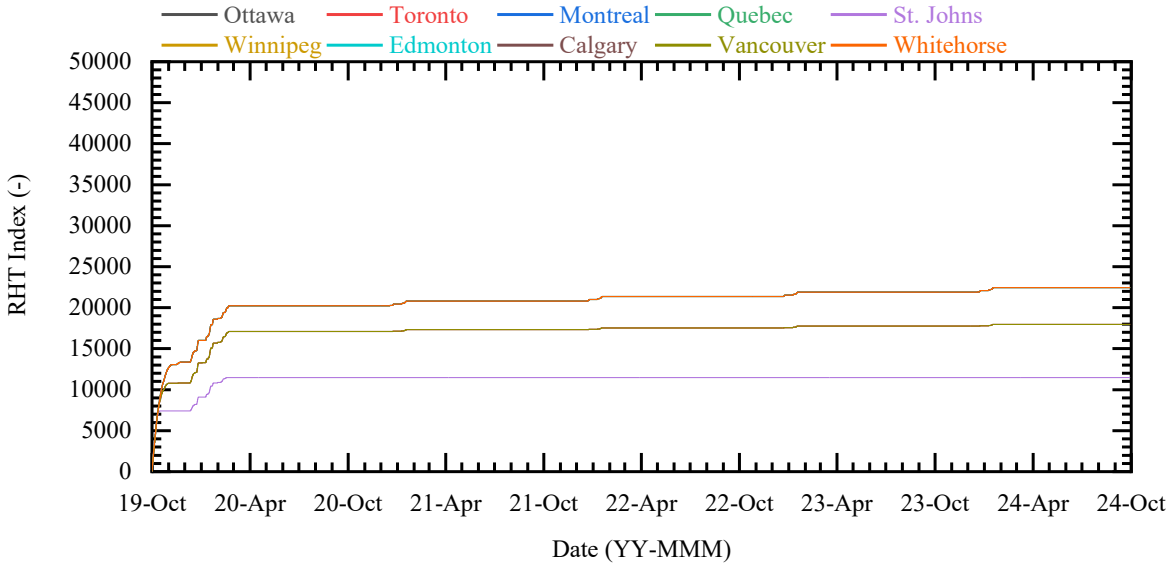

Figure 6-31: Calculated RHT Index for CIP wall assembly for new construction in Canadian cities.

In the CIP insulated wall assembly, the OSB sheathing was inboard of the insulation; therefore, kept warm and well protected from the outdoor elements, unlike the SIP panel. The sheathing used in the SIP assembly was outboard of the insulation and covered with 60-minute building paper to protect from liquid and bulk water. The inner and outer OSB sheathing surface was monitored because of the material sensitivity to mould growth and decay. The sheathing

surface was exposed to colder temperatures and greater vapour diffusion compared to the other panel type, which led to a higher surface relative humidity at the outer OSB surface, presented in Figure 6-32.

Over the 5-year simulation for a SIP-based above-grade wall assembly across Canada, the monitored relative humidity was higher than the CIP assembly for all the cities investigated. The outer OSB surface had more variance in the RH and T results due to the proximity to the exterior conditions, as expected with an uninsulated material. Over the 5-year simulation, a repeated cycle of RH was observed for each city and indicates a balance of wetting and drying within the enclosure. The initial surface relative humidity was 80%RH in all the cities and after 2 months the RH ranged between 100% and 60% across the cities investigated; including 3 cities where the outer OSB surface RH would exceed the 80% reference line. In those cities, the surface could be exposed to conditions where mould index would be greater than 0 if the surface temperature was high enough.

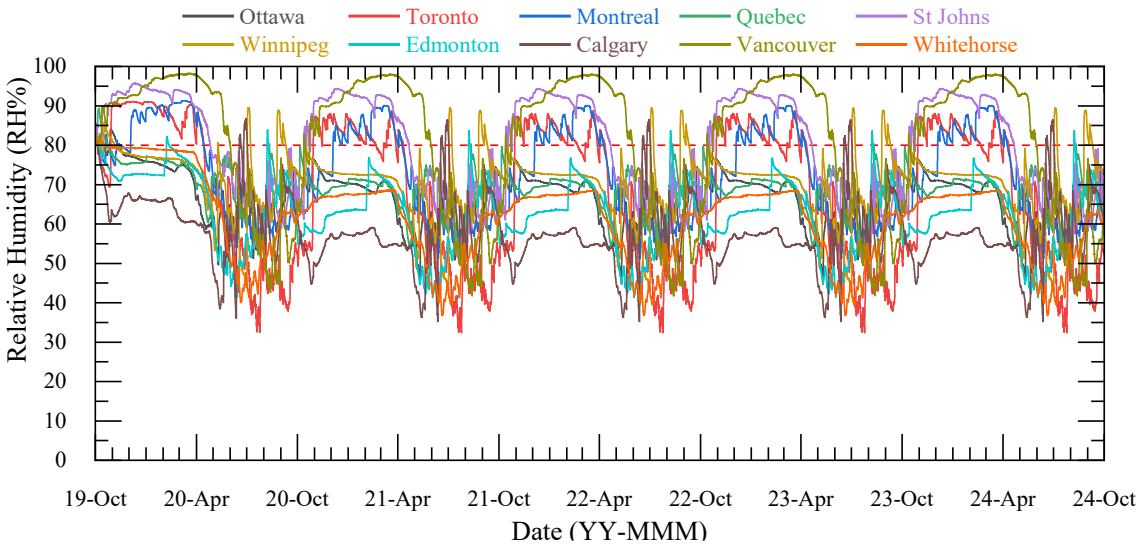

Figure 6-32: Outer OSB surface RH of SIP wall assembly for new construction over 5-year simulation.

The outer OSB surface relative humidity during the first year for three cities where the surface peaked over 80%RH annually and Ottawa were plotted in Figure 6-33. During the first year, the surface relative humidity in St. John's and Vancouver was above the 80% RH threshold between 7 and 8 months and could be a cause for concern for the potential for mould growth. In these two climates, the outdoor environment had a higher humidity level and vapour pressure, especially during the December through March months when in colder cities such as Ottawa, Whitehorse, and Edmonton where the colder temperatures allow for a greater vapour drive to the outdoors.

The average outdoor conditions in Vancouver and St. John's from the ASHRAE weather files, which are the most severe year concerning moisture-related damage within the building envelope, are approximately 5°C 85%RH and -2°C 85%RH, respectively. The higher humidity, the increased rainfall, and the longer periods of solar-driven moisture into the assembly have a greater impact on the relative humidity, moisture content and temperature of the OSB sheathing for a given wall assembly.

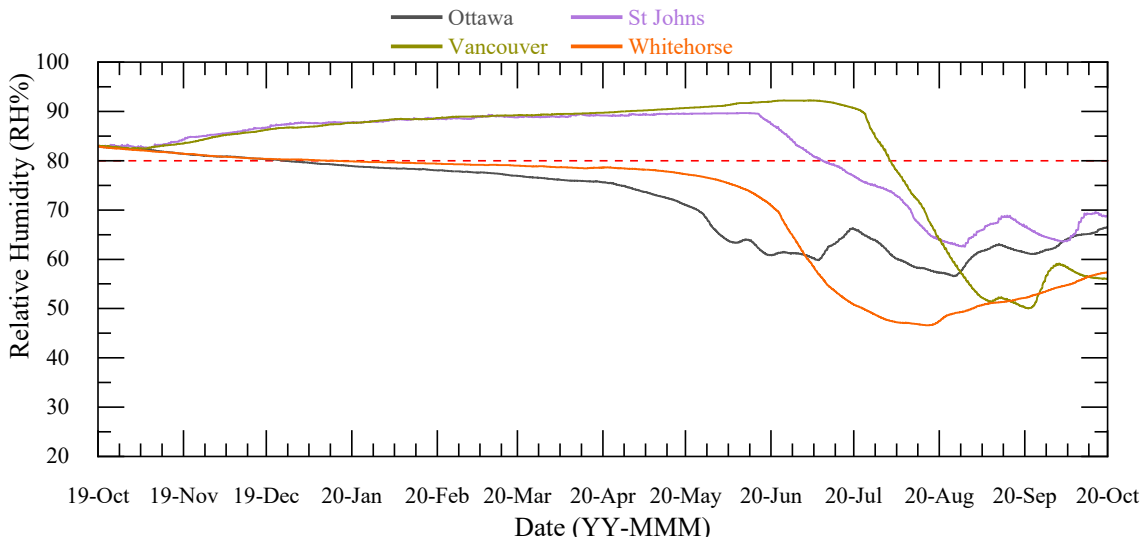

Figure 6-33: Outer OSB surface RH of SIP wall assembly for new construction during the first year of simulation.

The mould index on the outer OSB surface was less than 1 for all the cities, except for Vancouver, presented in Figure 6-34. The mould index was 0 for most of the cities and would have annual increases of less than one in Whitehorse. In Vancouver, the mould index increased above 1 in the first year, above 3 during year 3 of the simulation and failed the evaluation criteria overall. Since the mould index for the Vancouver case continued to increase year-over-year, it is unlikely that the initial moisture in the assembly is the cause of failure. Rather, the repeated outdoor environment and a lack of drying periods when the sheathing was wetted. The RHT index found similar trends; in Whitehorse and Vancouver, the index continues to increase every year, shown in Figure 6-35.

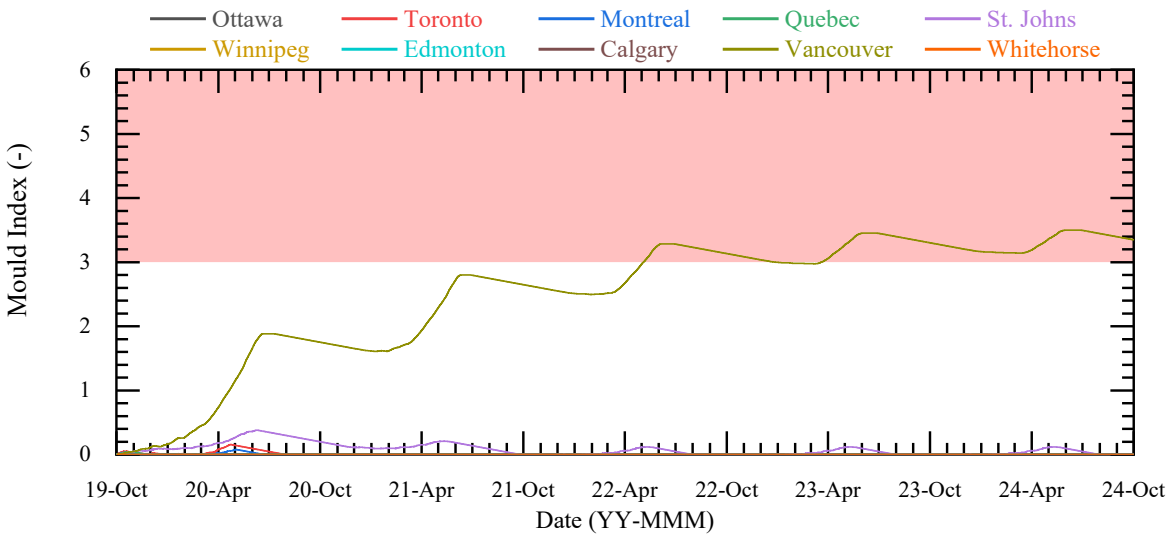

Figure 6-34: Calculated Mould Index for VIP insulated wall assembly for new construction in Canadian cities.

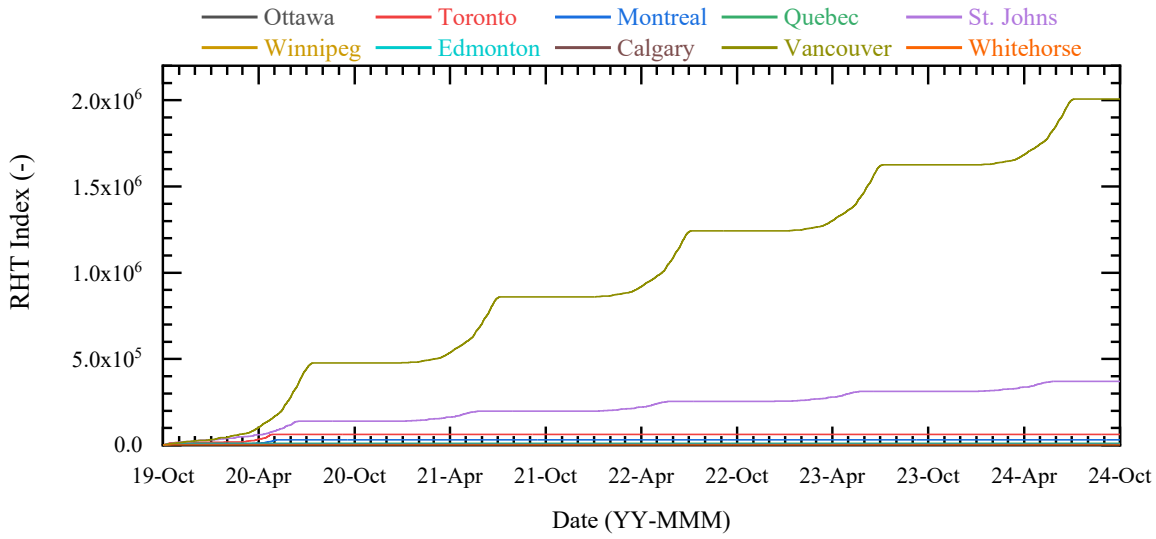

Figure 6-35: Calculated RHT Index for VIP insulated wall assembly for new construction in Canadian cities.

For new construction assemblies, both types of assemblies provided sufficient drying in most cities. The difference between the CIP and SIP insulated assemblies was the location of the sheathing. In the CIP assembly, the sheathing had thermal and moisture control layers on both surfaces. The difference in thermal control was the main component of what led to the low peak mould index in the assembly, tabulated in Table 6-4. The sheathing in this assembly was unaffected by the outdoor climate for the most part, in evidence from the RHT80 index values for the various cities, except for Whitehorse. However, when the sheathing was placed outboard of the insulation, the exterior climate had a larger impact on the hygrothermal performance. The mould index varied from 0 to 4 for the cities investigated, and the RHT80 index varied between 654 and $2x10^6$. The sheathing in the SIP assembly did not have outboard thermal control and was exposed to temperature and humidity variations. The building paper kept the sheathing dry from bulk wetting but was open to water vapour transmission. In areas where the humidity and rainfall were high (St. John's and Vancouver), the mould and RHT index were much higher than in the other cases.

In comparison to the results from the CIP assembly under the same conditions, it shows that an outboard sheathing or SIP assembly may not be as suitable for those climates.

Table 6-4: Peak Mould Index and RHT80 Index for VIP insulated wall assembly for new construction in Canadian cities

City	SIP – New Construction		CIP – New Construction	
	Mould Index	RHT80 Index	Mould Index	RHT80 Index
Ottawa, ON	0.02	7500	0.047	8000
Toronto, ON	0.33	134380	0.040	6890
Montreal, QC	0.08	31969	0.041	6690
Quebec, QC	0.7	11569	0.046	7120
St. John's, NL	1.1	443000	0.048	7212
Winnipeg, MB	0.06	186100	0.043	7077
Edmonton, AB	0.02	35351	0.031	5515
Calgary, AB	0.00	8640	0.041	7323
Vancouver, BC	4.7	2007600	0.049	7394
Whitehorse, YK	0.00	654	0.048	62146

6.5.2 VIP Insulated Above-Grade Wall Assembly for Retrofits

A wall assembly in need of retrofit is assumed to be nearing the end of its service life of approximately 50 years. The wall assembly, including all its materials, would be exposed to in-service conditions, including wetting from bulk water and air movement through leaks and degradation of seals, for its lifetime. When performing the retrofit, there would be an unknown level of moisture stored in the absorptive and hygroscopic materials before and after construction is completed. In contrast, the expectation for a newly constructed assembly would be that the materials were assembled dry and there would be limited moisture present in the assembly. For

design and modelling purposes, this differentiated the new construction from the retrofit cases the most.

The purpose of the modelling exercise was to evaluate a CIP panel appropriate for a retrofit under a realistic set of initial moisture conditions in the assembly. In Section 6.1, a set of baseline wall assemblies was simulated in WUFI Pro to calculate the moisture profiles for a wall assembly in Ottawa, ON. From the set of simulations, the 1960s above-grade wall built on 2x4 framing with kraft faced batt insulation and brick cladding had the highest peak moisture content and was selected to be the base wall for a CIP retrofit in different Canadian cities.

The wall assembly was simulated under the most severe year concerning moisture damage within building envelopes. The simulation was run until an annual moisture balance was found (approximately 3 years) and the wall surface was oriented in the direction of the highest wind-driven rain load. The inner and outer OSB surface relative humidity and temperature were plotted in Figure 6-36 and the annual repeated conditions are apparent. The moisture content profile for the assembly at the final timestep was plotted and was used in the next retrofit simulations and was presented in Figure 6-37. From the moisture profile, a steep gradient in moisture content was observed through the OSB at the end of the simulation and was used as the initial conditions for the retrofit simulations.

A similar simulation was created for each Canadian city using a climate file for the most severe weather concerning moisture-related damage within the building enclosure. The final moisture profile for the existing building materials (OSB to gypsum board) was exported and used for the retrofit simulations. The moisture content in the OSB layers was compiled into Table 6-5.

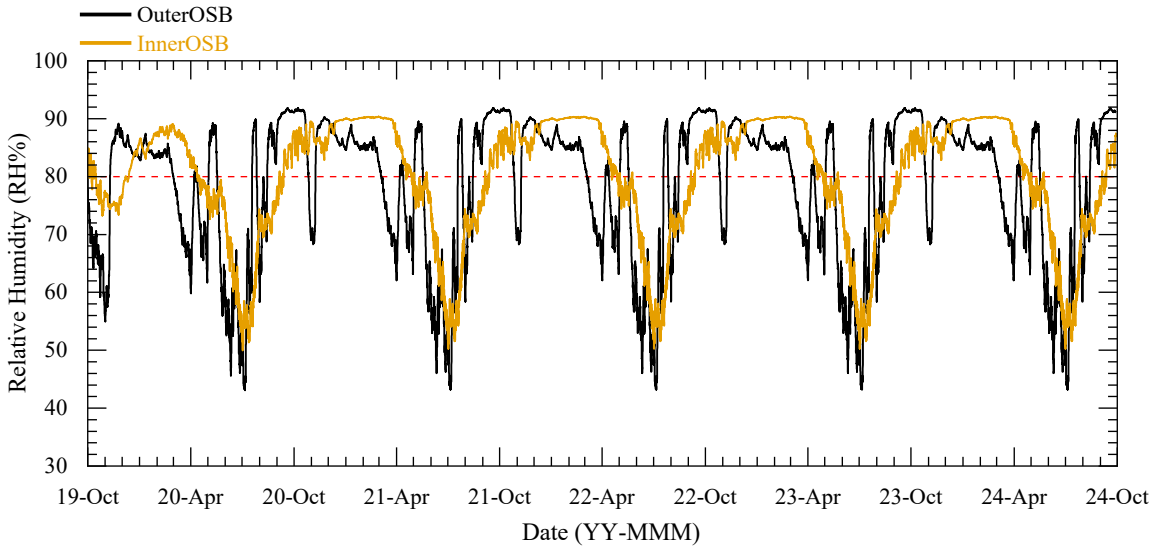

Figure 6-36: Inner and outer surface RH of 1960s wall assembly for retrofit construction at end of the 5-year simulation.

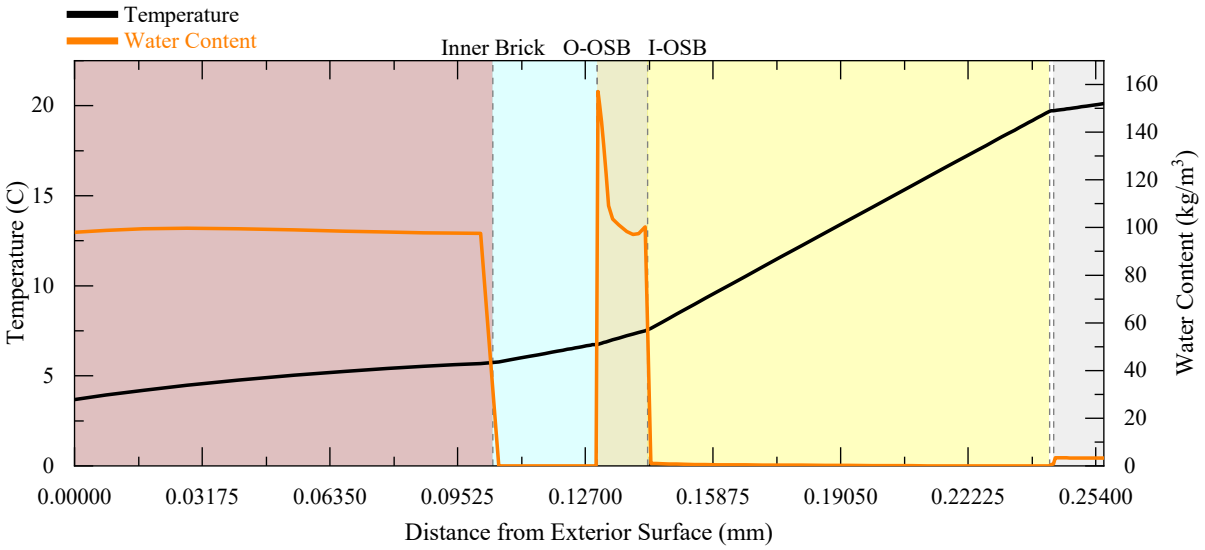

Figure 6-37: Water content profile of 1960s masonry clad wall at the end of a simulation for Ottawa, ON.

Table 6-5: End water content in OSB sheathing from existing materials in each Canadian city.

City	Average End Water Content (kg/m^3)	City	Average End Water Content (kg/m^3)
Ottawa, ON	123	Winnipeg, MB	46
Toronto, ON	109	Edmonton, AB	45
Montreal, QC	109	Calgary, AB	44
Quebec, QC	104	Vancouver, BC	53
St. John's, NL	70	Whitehorse, YK	39

For a 1960s retrofit, two cases were evaluated. In the first case, the CIP was installed on the existing with the existing cladding removed and in the second case, a SIP system was installed over the existing cladding.

With the brick cladding removed and the initial conditions from Table 6-5 added to the initial moisture content of the layers, the 1D hygrothermal model was designed for 10 Canadian cities. In this style of assembly, the existing sheathing was most sensitive to mould growth potential due to its position in the wall assembly and its organic material base. The outer OSB surface relative humidity was plotted in Figure 6-38 and an annual moisture balance was observed within the first two years. The annual peak in surface relative humidity stayed well below the 80%RH threshold and would be unlikely to develop significant mould growth potential. Additionally, limited variability in the surface relative humidity between the cities was observed. Based on the conservative estimates used in the simulation study, a wall assembly with a CIP would be suitable in an exterior envelope retrofit with the brick cladding removed.

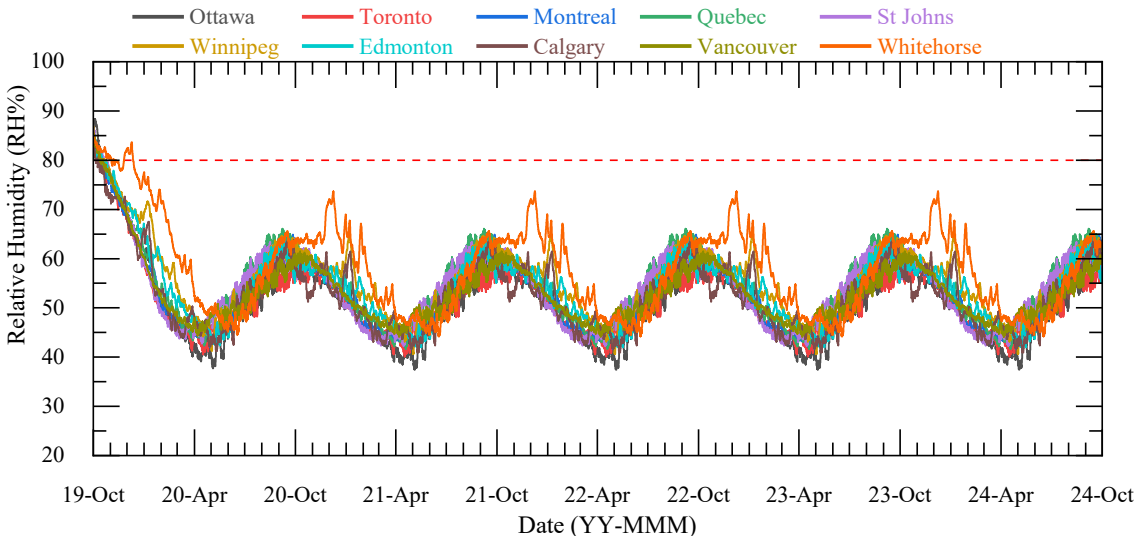

Figure 6-38: Outer OSB surface RH for CIP retrofit construction during 5-year simulation.

Despite the high initial moisture content in the OSB sheathing, the relative humidity decreased below the 80% threshold in the first quarter, plotted in Figure 6-39. Upon inspection of the animation film, the moisture flux from the OSB surfaces during the dry out period was towards the interior surface. The contributing factors would be the low vapour permeability to the exterior, the assumed air exchange rates at the inner OSB surface, and kraft faced batts instead of the polyethylene vapour barrier seen in new construction. The mould index plotted in Figure 6-40, rose due to the high initial moisture content but decayed to 0 before the end of the first year. The RHT index plotted in Figure 6-41, followed a similar trend as it plateaued early during simulation.

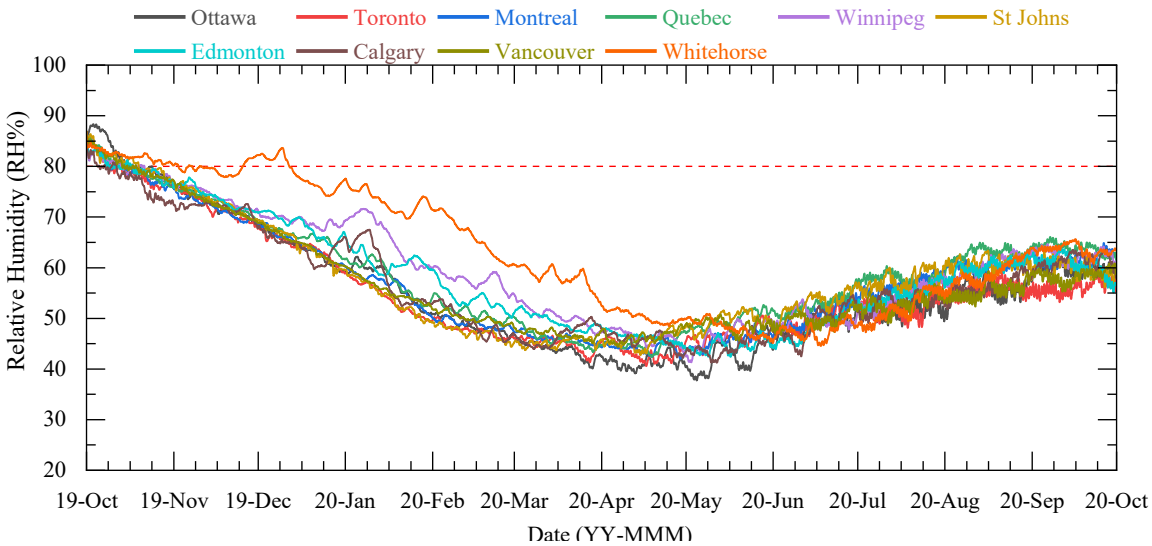

Figure 6-39: Outer OSB surface RH for CIP retrofit construction during the first year of simulation.

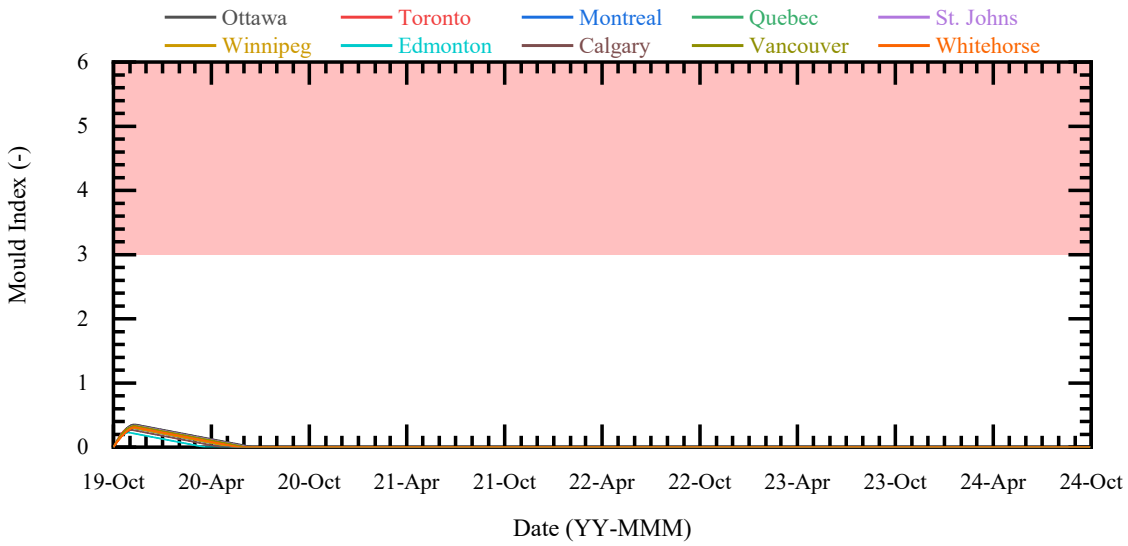

Figure 6-40: Calculated Mould Index for VIP insulated wall assembly for retrofit construction in Canadian cities.

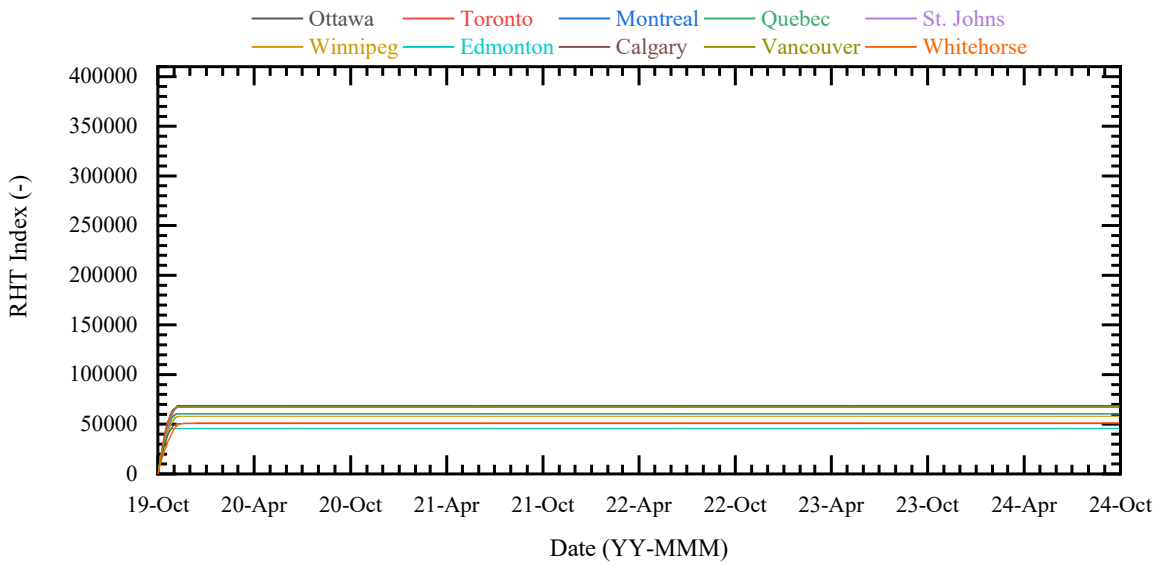

Figure 6-41: Calculated RHT Index for VIP insulated wall assembly for retrofit construction in Canadian cities.

Therefore, based on the mould and RHT indexes computed using the surface temperature and relative humidity, the CIP assembly would be a safe exterior envelope retrofit from a hygrothermal perspective. The mould index of 0 indicated that there would be no mould growth on the surface. The RHT index for the retrofit with the brick cladding removed was an approximate maximum of 83000, which was higher than the RHT Index calculated for a similar CIP wall assembly modelled for new construction. In the retrofit case, the enclosure has a higher initial moisture content with a higher permeability towards the interior. Since the low peak mould index for all the cities studied, this type of retrofit with vacuum insulation would be suitable for the climate, despite the exterior vapour barrier caused by the VIP.

For an overclad retrofit in different Canadian cities, a SIP system was applied over the existing masonry cladding. The results produced with WUFI Pro showed that the exterior sheathing of the retrofit panel was prone to a higher temperature and relative humidity conditions. The surface relative humidity over the 5 years is presented in Figure 6-42, and the trends were like SIP system used for new construction. In certain cities, namely Vancouver and St. John's, the

relative humidity at the exterior surface would annually exceed 90%RH, while most other cities would vary predominantly below 80% RH. During the first year of the simulation, presented in Figure 6-43, the only four cities that did not immediately dry below 80%RH were Vancouver, St. Johns, Toronto, and Montreal.

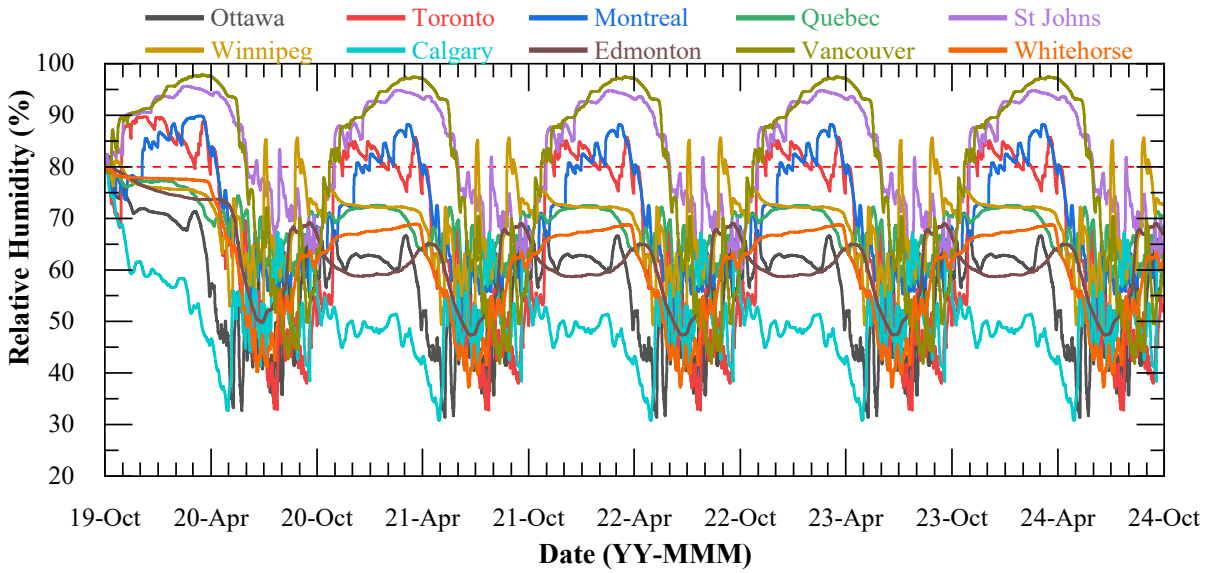

Figure 6-42: Simulated RH at the outer sheathing surface for a SIP retrofit in different Canadian cities.

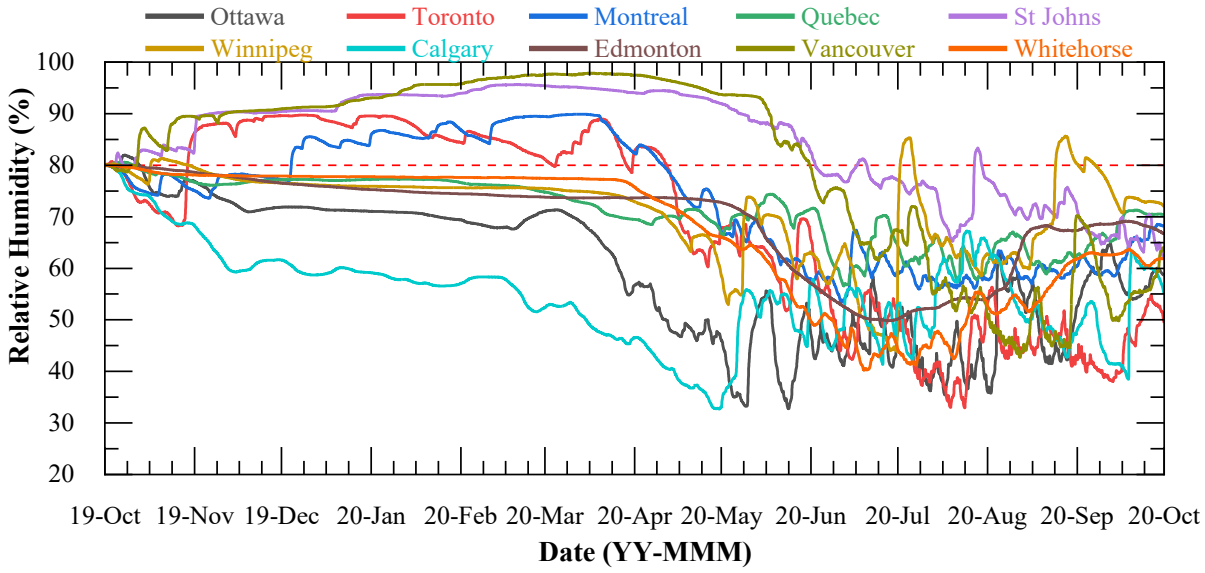

Figure 6-43: Simulated RH in the first year of a SIP retrofit in different Canadian cities.

Based on the simulated relative humidity, most cities were not likely to experience any potential mould growth on the surface because the air conditions were insufficient for mould growth. The mould index at the outer surface, shown in Figure 6-44, was only an issue for two Canadian cities that were exposed to high annual relative humidity. In Vancouver and St. Johns, the mould index peaked at 4.57 and 1.48, respectively. These results were consistent with the findings from the SIP system for new construction in coastal cities; and that this type of assembly may not be suitable in the coastal climate. The peak mould and RHT80 indexes were consolidated in Table 6-6.

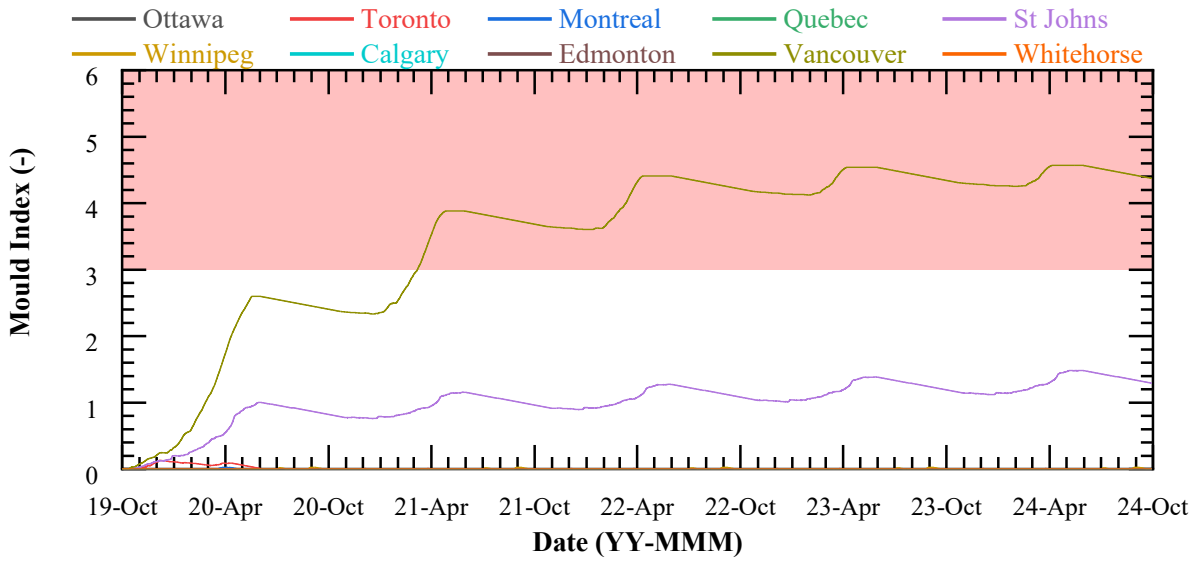

Figure 6-44: Calculated mould index for SIP retrofit in Canadian cities.

Table 6-6: Peak Mould Index and RHT80 Index for VIP insulated wall assembly for retrofit construction in Canadian cities

City	SIP – Retrofit		CIP - Retrofit	
	Mould Index	RHT80 Index	Mould Index	RHT80 Index
Ottawa, ON	0.00	1147	0.43	80038
Toronto, ON	0.13	66645	0.40	81752
Montreal, QC	0.03	14827	0.38	73078
Quebec, QC	0.00	215	0.38	72061
St. John's, NL	1.48	751760	0.43	81585
Winnipeg, MB	0.02	80690	0.38	70112
Edmonton, AB	0.00	5	0.30	56357
Calgary, AB	0.00	3	0.34	60203
Vancouver, BC	4.57	1854900	0.42	83097
Whitehorse, YK	0.00	0	0.38	58324

6.6 Modelling the Wall Assembly in 2D

The HAM transfers present in building envelopes are very rarely limited to 1D flow, especially in the case of the VIP insulated assemblies. There can be lateral heat and moisture flows when the plane does not have a constant temperature, humidity, or moisture content levels. In the building envelope, effects such as thermal bridges, lateral air leakage paths and degradation in seals and barriers may or may not exist in the assembly contributing to potentially 3D heat and moisture transport in the assembly. It is possible that these factors would vary from building to building, façade to façade, and were not within the scope of research to be evaluated. The research objective is to evaluate the hygrothermal performance of the insulation panels on the mould growth potential of the assembly. Since the inboard temperature caused by using non-homogenous exterior

insulation effects would not be captured in a 1D model; therefore, WUFI 2D 4.1 was selected to perform a 2D simulation.

The model inputs were selected using the assumptions and simplifications from Chapter 4 and the results from the parametric study and 1D modelling of VIP insulated assemblies. Since the outboard insulation was symmetric about every 300 mm or 400 mm section to match the framing spacing, the modelled cross sections were set to 300 mm and 400 mm. The 2D geometry was equal parts EPS and VIP in the outboard insulation and a smaller width would conserve computational time, as opposed to modelling a full wall section. For a 1-year hygrothermal simulation with hourly timesteps for a 400 mm width section, the computational time required is approximately 10+ hours of computational time. To simulate a full-scale 2400 mm (8') wall assembly needed multiple days to complete and would result in convergence errors. The materials selected were consistent with the materials selected in the 1D simulation and were taken from the WUFI material library. The initial moisture conditions used were consistent with the 1D simulations; new construction used the moisture content equivalent of 80%RH and 20°C, while retrofit used the moisture content profile exported from the 1960s simulation. The moisture content profile was constant across the width of the existing materials. Heat and moisture sources were consistent with the 1D model and conservatively assumed to be constant across the material width.

The outer OSB surface relative humidity in the CIP wall assembly was exported from the WUFI 2D post-processor. The OSB nodes were averaged based on whether the sheathing was insulated by EPS or VIP insulation outboard. The OSB nodes insulated by VIP and EPS were denoted as "VIP 2D" and "EPS-2D", respectively, in Figure 6-45. There was an agreement between the results from the WUFI Pro 1D and WUFI 2D in the plotted relative humidity that the EPS and VIP for the first year.

This gradient was largest during the first dry out period and was nearly non-existent during the cooling season. During the first 3 months (Oct-Jan), the calculated RH from the WUFI 2D showed followed the same trend calculated in the VIP 1D model. EPS 1D model had an outer OSB surface relative humidity, but after the initial dry out period (6 to 9 months) and warmer outdoor temperatures, the results from both simulations converged to similar results and followed the same trends within 5%. The 1D VIP results were lower in surface relative humidity for the duration, indicating that the WUFI 1D model might underestimate the hygrothermal performance of the assembly.

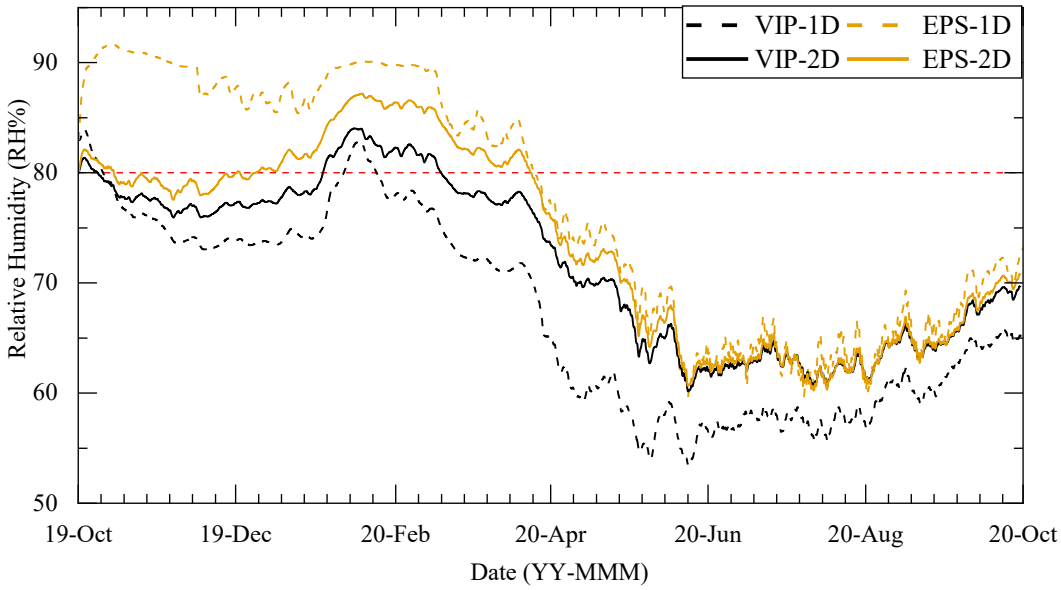

Figure 6-45: RH at the sheathing for a CIP above-grade wall assembly simulated in 2D.

An EPS to VIP ratio of 2:1 was used for the geometry in the simulations. However, it was shown that this type of ratio with a 20 cm thick VIP might not be sufficient to reach the desired R-value based on thermal modelling and GHB studies. Therefore, the 2D simulation was prepared using two different VIP ratios 3:4 and 1:4, as well as 2 additional thicknesses of 25 cm and 30 cm to assess the impact on the hygrothermal results. The geometry width was kept constant for the

simulations and was prepared using the CIP insulation panel with moisture sources, and initial conditions for a new construction above-grade wall assembly.

The OSB water content and equivalent relative humidity for the varied EPS:VIP ratio were simulated and post-processed in WUFI 2D. The water content and relative humidity were averaged for the first 6 mm of the OSB sheathing insulated by EPS or VIP; consistent with the previous sections. An increase in sheathing water content, plotted in Figure 6-46, was observed as the EPS:VIP ratio increased; thereby the water content in the sheathing increased as the amount of sheathing insulated by EPS increased. Additionally, the water content gradient between the VIP and EPS insulated areas was steeper when the ratio was greater. In terms of mould growth potential, the equivalent RH was plotted in Figure 6-47. Since the relative humidity was below 80% RH for the duration of the simulation, it could be assumed that the mould index would be less than 1 and probably close to 0.

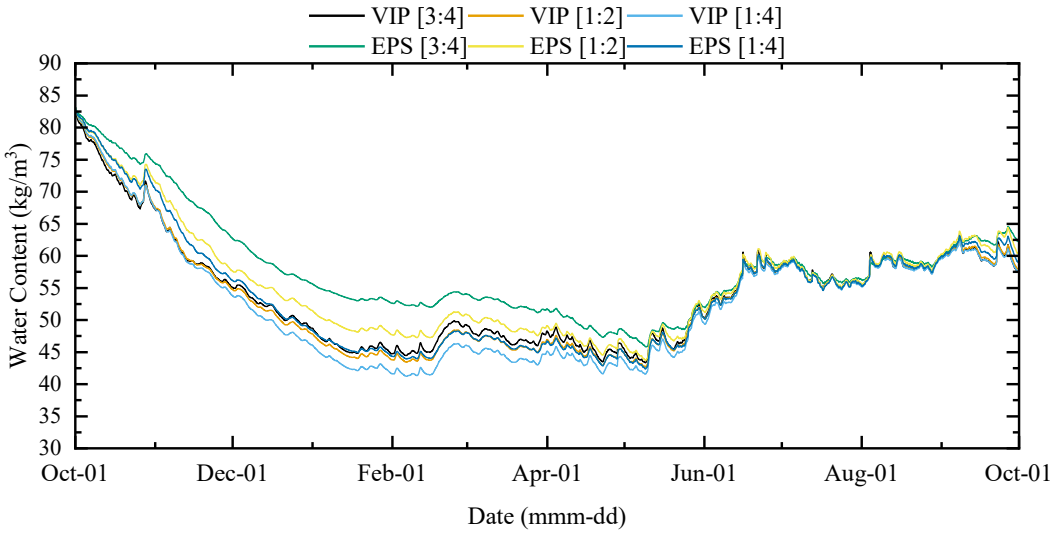

Figure 6-46: Sheathing WC for a CIP-based above-grade wall assembly for varied VIP-EPS ratio in 2D.

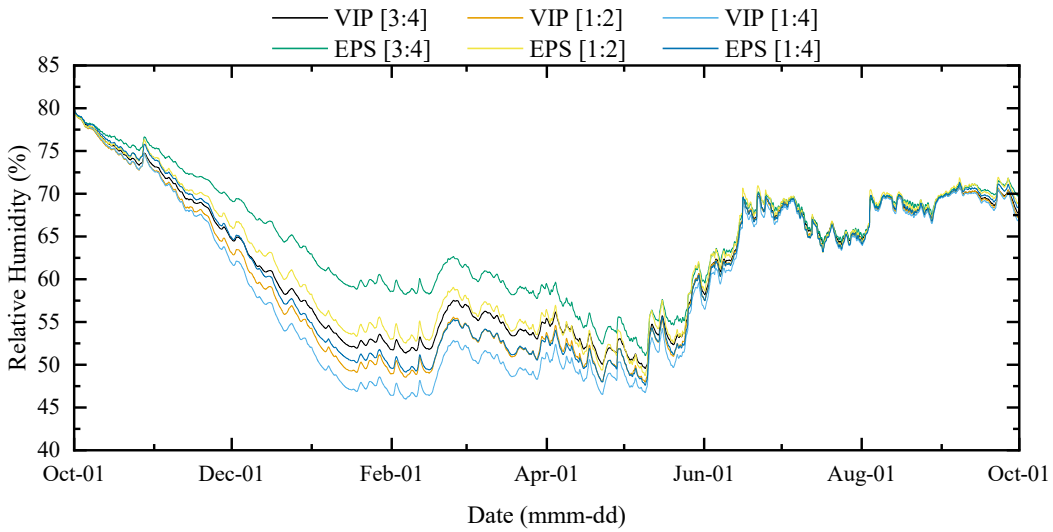

Figure 6-47: Sheathing RH for a CIP-based above-grade wall assembly for varied VIP-EPS ratio in 2D.

6.7 Discussion of Numerical Results

A discussion of the numerical results is provided in the section. The discussion includes a comparison of the experimental and numerical findings, the effect of vacuum insulation panels in different climates, the method to evaluate retrofit assemblies, the effect of simulation inputs on long-term durability of wood-framed walls and the comparison between the 1D and 2D models.

6.7.1 Comparison Between Experimental and Numerical

The experimental results from the in-situ monitoring and numerical results from WUFI Pro and WUFI 2D models were compared and were found to follow similar trends when the same boundary conditions were applied. Due to limitations on-site, the exact weather data for the in-situ study was not collected. An outdoor weather file was created using local weather stations and climate files for hygrothermal design purposes.

The comparison between the SIP insulated assembly on 2x6 wood framing to represent new construction was challenging since the sheathing was outboard of the insulation. The measured relative humidity followed the trend of the simulated data for about a third of the data

set based on the assumed initial conditions. The measured relative humidity at the surface would change rapidly from timestep to timestep, which was to be expected since it was heavily influenced by the outdoor conditions. The modelled values did not show the same rate of change between timesteps under the same conditions. It was expected that the amount of air exchange at the surface would have a significant effect on the values, but also the monitoring equipment and the longevity of the sensors placed at the surface. During the first year of monitoring, there were issues in data collection resulting in gaps in data. However, during the second year, the issues were resolved and the agreement between the measured data and simulated results increased. Overall, the comparison between the measured and simulated methods did not offer

The CIP insulated assembly was placed on a 2x4 wood-framed on 300 mm spacing used to represent an exterior retrofit with the existing cladding removed. The agreement between the measured and predicted values was generally greater than in the SIP panel. The relative humidity at the interior surface of the sheathing was found to follow the general trend well and came to the same conclusion that the interior sheathing would not be susceptible to moisture-related issues, such as potential mould growth. The measured wall assembly had a greater influence on the interior conditions, evident by the alignment of increases in interior and measured RH during the summer when there was not an interior RH setpoint. Overall, the measured and simulated results for the CIP good agreement over the long-term trend and provided confidence in the results that a VIP insulated CIP panel used in Ottawa would not contribute to moisture-related issues to the sheathing over the long-term without a vapour barrier on the interior, provided interior air conditions are kept at a comfortable level.

For both assemblies, the initial conditions assumptions for the sheathing were overpredicted in the model and should be corrected as an initial input to the model. Considering

the observations, the initial moisture assumption of equivalent moisture of 80%RH and 20°C was too high for this study and should be measured at the time of installation for the model input. In both scenarios, the initial moisture does not have a significant impact on the conclusions because the measure and simulated results converged during the first 6-12 months and does not have a significant impact on the annual moisture cycle of the wall assemblies, as shown in the study.

6.7.2 Vacuum Insulation in Different Climates and Cities

When the two insulation systems were evaluated across multiple cities in Canada, it was found that the CIP panel could be safely installed in all wall assemblies for new construction or exterior retrofits with the cladding removed. The differences between using new and retrofit assumptions did not alter the conclusions, albeit a slightly larger mould index was calculated for the retrofit cases compared to the new construction case.

For the SIP insulated wall assembly, the cities, and climates with a higher amount of annual driving rain and mean temperatures had a higher calculated mould index. The sheathing placed outboard of the insulation but behind a weather-resistant barrier, would be exposed to more wetting by bulk water and vapour diffusion compared to its counterparts in different cities. In the model, 0.01% of bulk water was assumed to bypass the weather-resistant barrier which is a small amount. Therefore, more of the wetting was found to occur through vapour diffusion that passed through the weather barrier. Due to the higher amount of rain in the cities, the outdoor humidity is expected to be higher and therefore be driven into the assembly. And since the mean temperature is greater, and the heating degree days are lower, the period when the sheathing can dry towards the exterior will be smaller, leading to a greater amount of moisture at the surface. The only city that failed the evaluation criteria for the SIP assembly was Vancouver, BC; and St. John’s received a cautionary pass, such that it requires more review and field investigation.

6.7.3 Screening Input Parameters

Input parameters for the hygrothermal model were dependent upon each other based on the Morris Method for screening variables. A total of 36 simulations were used to screen 9 different parameters under 3 different input levels. The parameters were assigned a range and subdivided into 3 categories to represent a low, expected, and high level. The screening was performed by randomizing the level for each input, running the simulations, calculating the mould index, and finding the μ^* and σ values for each input. The most sensitive parameters were found to be the layers in the construction, initial construction moisture, building orientation and vapour control. Other parameters, such as date of completion, interior conditions and timestep did not generate as large of an impact however, all the parameters were found to have non-linear related effects from other inputs.

The screening was a useful tool to inform the process of evaluating retrofits, specifically. As the number of completed building envelope retrofits increases, the questions regarding how to predict the long-term hygrothermal performance of these assemblies will become more important. Based on the screening for an insulated sheathing assembly, evaluating the initial construction moisture, good assumptions for the vapour control and vapour transport in the existing assembly and evaluating multiple orientations will be an important task during the retrofit design stage.

It will be more important to carefully select those parameters rather than the exact construction end date and post-retrofit interior conditions, which could be more challenging at that stage. It is also beneficial that the long-term durability of the wall assembly, while dependent on those parameters, may not be sacrificed if the construction schedule changes or the building is controlled differently post-retrofit by the occupants.

6.7.4 Comparison Between 1D and 2D Model

A deeper investigation of the impact of the initial conditions is needed but the annual wetting and drying from the exterior climate provided similar results from both models. Given that a WUFI 2D model required hours to complete the simulation compared to minutes for an assembly in WUFI Pro, a WUFI Pro model could be suitable for evaluating the wall assemblies. The gradient in relative humidity can be explained by the warmer temperature based on the lower conductivity of the exterior insulation. The comparison between the WUFI Pro and WUFI 2D hygrothermal models showed that after the dry out period, there was a 5% difference between the relative humidity at the sheathing.

Since the differences between the two types of models were small and the time required to complete the simulations was large (30 seconds to 8+ hours per year), it was found that WUFI Pro or an equivalent 1D model would be sufficient to assess the long-term hygrothermal performance of the assembly. In this study new and retrofit construction using a super insulating material, such as a VIP, were evaluated through the main wall assembly. The 2D model showed moisture redistribution behind the sheathing when the VIP is placed inside an insulative rigid foam board; the 2D analysis may be more useful when more substantial thermal bridging is present or when more than two boundaries are non-adiabatic. This would be the case at roof-to-wall or wall-to-foundation junctions; however, those points would not provide an accurate depiction of the long-term durability of the wall assembly as proposed. Other cases when a 2D analysis might provide better insight would be uninsulated steel structural components or thermal bridges that penetrate the thermal control layer, openings in the wall assembly such as doors and windows, evaluating bulk water leakage or an increased wetting event that causes more moisture redistribution within the assembly.

Chapter 7: Conclusions and Future Work

From the experimental and numerical research, the following conclusions were made about thin, high-performing building envelopes including vacuum insulation panels, hygrothermal monitoring and modelling of above-grade wall assemblies, and hygrothermal feasibility of exterior envelope retrofits in Canada.

7.1 Constructability of Composite Insulation Panel with VIPs

Vacuum insulation panels are a super insulation material that has 8-10 times lower thermal conductivity than fibreglass insulation currently used in low-rise housing, albeit with significant drawbacks. The vacuum contained with the membrane must remain intact to achieve the low thermal conductivity and a loss of vacuum within the panel is highly detrimental to the financial and scientific benefits of use. Therefore, VIP protection should be of utmost importance during use when used to insulate buildings.

Two concepts were explored during the research program to explore how VIPs could be introduced safely, economically, and easily to the building enclosure, specifically for low-rise housing. The concept was based on surrounding the VIPs in rigid foam-based insulation and providing accurate fastening points on the exterior face of the panel. The VIPs were embedded within EPS insulation with two different backer-based materials: OSB and EPS.

The prototypes were created using 1319 mm x 2438 mm (48” x 96”) Type 2 EPS base panel with 200 mm x 300 mm (8”x 12”) VIPs. The VIPs, smaller than what has been used in previous literature, were selected since it was expected that they would provide an improvement in constructability and shorten the required construction period while also meeting the RSI 3.4 m^2K/W (R-20) thermal performance target for the exterior insulation panel. These

prototypes were handled by the research team and were installed in the guarded hot-box and the in-situ test facility in Ottawa.

Both panel types were easy to handle and install on the 300 mm and 400 mm wood-framed wall spacing. The panels were considerably heavier than an EPS sheet of equal size from the embedded VIPs and OSB backer material. However, the panel could be moved and placed by one person. With the extra weight and EPS laminated, the CIP panel was flimsy compared to the SIP panel, with the OSB laminated on the backside. The SIP panel was easier to move around despite the excess weight, and despite initial concern, the OSB did not puncture any VIPs during lamination, verified by thermal imaging.

The EPS:VIP ratio used was beneficial to fastening the panel to the framing; however, suggested improvements to a second iteration would be changing the gap between VIPs. A 100 mm (4”) gap between VIP panels was more than necessary fastening area. In future iterations, it would be suggested to design the fastening area no more than 75 mm and no less than 50 mm. Since the wood studs used in Canadian construction are normally 38 mm in width, a 50 mm gap should be sufficient space to fasten to the assembly.

The prefabrication of the EPS-VIP panels made the installation quick on-site, however, only sections without penetrations were investigated. In a dwelling, penetrations (doors, windows, electrical etc.) will still exist and need to be accommodated. With the smaller VIPs, any penetrations through an area that included a VIP would be limited to a 200 mm by 300 mm area.

7.2 Insulation Panels Thermal Performance

The initial design was lower than the RSI-3.4 m^2K/W (R-20) thermal resistance criteria. The panel designs fell below expectations due to the VIP performance and the area insulated by VIPs. The edge effects from the VIPs caused a lower than expected thermal performance and was

verified in the guarded hot-box testing. The measured temperature difference showed that an increase in thermal conductivity exists along with VIP the perimeter, and when the perimeter to area ratio is increased, the effective thermal conductivity increases. In this study, the thermal bridge along the edges had a significant factor in the effective thermal resistance of the insulation panels, reducing the thermal resistance to below the expected values. The edge effects can be minimized by using different VIP dimensions; specifically using square VIPs.

Minimizing the perimeter means square VIP panels and multiple different sizes were presented. In the future iterations of the panel, a 375 mm by 375 mm (14.75" by 14.75") encapsulated VIP panel applied on 400 mm stud spacing would provide the passable hygrothermal performance, sufficient fastening area as well as meet the R 3.4 m^2K/W thermal resistance target.

7.3 In-Situ Monitoring of Building Enclosures

The in-situ monitoring of the two-panel types on two different assemblies was performed from 2016 until 2020. The temperature, relative humidity, and moisture content in the wood-based materials were monitored in addition to the boundary conditions. The mould index at the sensitive surfaces was calculated and found to be below the failure criteria threshold.

The monitoring was successful; however, the process was very slow when doing the long-term monitoring. To expedite the process, it is suggested to introduce controlled wetting and increase the initial moisture in the construction as opposed to high moisture interior boundary conditions. By introducing the moisture directly into the assembly, the drying potential of the assembly can be assessed in the first year. Bulk moisture wetting is much quicker than wetting from high interior humidity from air exchange and vapour diffusion. Therefore, conditioning the building materials to a specific equilibrium moisture content, for example, EMC 80%, would allow the drying potential in the assembly to be assessed quicker. Additionally, controlling the initial

moisture in the assembly would make comparing the results to a numerical model easier and more accurate.

Controlling the bulk wetting in the test assembly would be beneficially long-term because controlled moisture could be introduced during a forecasted dry week. During the week, the drying could be monitored for a given set of boundary conditions. These refined controls would give better and quicker insight into how heat and moisture are transferred in the assembly in a shorter period compared to only controlling the interior conditions.

In the future, it would be beneficial to use these assemblies on a building with an occupied interior space. In the in-situ monitoring, AHSARE 160 interior conditions were used to control the heat and moisture source however, the occupant interaction and occupant comfort would cause a different set of boundary conditions. Additionally, an occupied interior space would ensure that the minimum air conditions would be maintained, unlike the in-situ monitoring facility where periodic power outages and lack of connectivity caused the interior conditions to fall below comfort levels.

Additionally, decommissioning the existing test wall assemblies and measuring the thermal conductivity of the VIPs used for the study. The initial thermal conductivity of VIPs was measured at the beginning of the project. During the 5 years of in-situ monitoring, the air and humidity conditions around the VIP were measured. When the in-situ walls are decommissioned, the thermal conductivity of the aged VIP panel would be extremely useful in furthering the effective lifespan of VIPs under in-use conditions.

7.4 Monitoring and Modelling of Wall Assemblies and Exterior Envelope Retrofits

The moisture assessment of an exterior envelope retrofit was evaluated using experimental and numerical methods in Ottawa, CA and numerically in other Canadian cities. The moisture

assessment in Ottawa showed general agreement between the two types of analyses. The temperature and moisture profiles in the assemblies followed trends when the interior and exterior boundary conditions were used. The differences in results were attributed to the lack of material property testing for the materials used in the experimental study and unmeasured wetting in the enclosure. The material properties used in the simulations were taken from the WUFI library with adjusted thermal conductivity when appropriate; however, in the future, it is advisable to evaluate the moisture-related properties such as water vapour diffusion resistance factor, moisture storage function, and thermal conductivity for temperature and moisture dependence, for sensitive materials in the assembly. This could be done before or during the experimental phase and would be valuable when calibrating the WUFI simulation in a case study.

The monitored and numerical results from Ottawa and enclosures simulated in various cities showed that a VIP insulated above-grade wall would be not at risk of potential mould growth in most climates in the country. Among the cities and wall assemblies that were evaluated, a SIP panel in Vancouver was the only assembly to fail the criterion. The high outdoor humidity increased rainfall and longer periods of solar-driven moisture into the assembly were the contributors to the mould index on the outer OSB surface reaching 3.0 and failing. In the SIP panel simulations, the exterior OSB was outboard of the insulation and was covered with 60-minute building paper, a water-tight but vapour open barrier. This would be a case where a smart barrier might be beneficial in allowing vapour diffusion towards the exterior but not towards the interior.

In the retrofit evaluations, the enclosure dried when the sheathing with high moisture content was still able to dry during the first year. In all the locations evaluated with the CIP and sheathing inboard of insulations, the existing moisture was able to escape the assembly. The

calculated mould index indicated that the sensitive surfaces were not at risk of mould growth. The CIP panel proved to be a safe above-grade wall assembly for the cold humid climates in Canada.

For a monitored or modelling above-grade wall retrofit, there are some assumptions and factors that could be improved through a pilot project. The initial moisture in the building was estimated by running the WUFI model with best modelling practices and materials from the material library. In a pilot project, this could be refined by monitoring the temperature, relative humidity, and moisture content of materials for a period before retrofit construction and material property testing of samples taken from the retrofit building. By improving the inputs to the model, it would be easier to predict the long-term moisture assessment of assemblies and assumptions in the model.

7.5 Input Parameter Sensitivity for WUFI Pro

The WUFI Pro model was used for the input parameter sensitivity study. Eleven parameters that were deemed important and most sensitive were screened using the Morris Method with three different levels. In total, 36 simulations were conducted with a randomized set of input values. The construction was found to have the greatest effect on the results from the screening process. The variation in construction was the type of exterior insulation and the use of capillary breaks behind the rainscreen. These factors would alter the water vapour diffusion resistance factor within the assembly by changing the exterior insulation from EPS (WVDR = 46 at 80% RH) to XPS (WVDR = 170 at 80% RH). Secondary effects were orientation, initial construction moisture and interior vapour control affected the hygrothermal modelling results. The other parameters were found to be less impactful on the results and were clustered closely together in both the inner and outer OSB sheathing.

Non-linear effects were observed for all the parameters since the data points were not aligned with the centerline. This shows that changing one input parameter will influence another parameter as well as affect the result. For example, a change in construction alters the thermal and vapour components and a change in orientation alters the observed solar and rain loads on the surface. The construction, orientation, initial moisture, and interior vapour control were found to be the most sensitive parameters for an exterior insulated timber framed assembly. It would be best practice to perform this type of analysis for all future modelling studies of building enclosures.

WUFI was not the optimal tool to do a local or global sensitivity analysis due to the challenge in automating the process and requires a significant amount of user time to complete. If a similar task is required for a project, it is suggested that a different tool be used to obtain a better understanding of the uncertainty in the modelled results.

7.6 Future Work

The future work for this research would include address limitations from this study, as well as objectives that could build upon the work completed.

During this study, ASHRAE hygrothermal performance files were used. These files used past weather to build hygrothermal design files, however, the research did not account for future weather conditions and how that would impact the hygrothermal performance of the building enclosure. The presented numerical methodology could be used with the use of the climate change based weather files. These weather files should account for higher average temperature, higher average of precipitation and number of precipitation events.

The clear field assembly was evaluated in this research scope and excluded thermal bridging and moisture effects caused by the presence of windows, smart barriers, material decay and fasteners through the enclosure. The VIP insulated wood-framed wall assembly (CIP and SIP)

could be model using archetypes homes in Canada with specific window-to-wall ratios and psi-thermal bridge values for fasteners and connections. This work would be useful in determining whether a VIP insulated wood-frame building could comply with the NECB and be a construction in new and retrofitted homes in Canada in the future.

Finally, as retrofitting existing buildings become more prevalent, as will the embodied carbon and lifecycle emissions of building materials. In the future, the lifecycle emissions required for a VIP insulated wood-frame wall in Canada should be investigated to determine whether its greater than other types of building envelope retrofits and new buildings.

7.7 Contributions

This research contributes to the field of building science, hygrothermal monitoring and modelling and building envelope design. This includes:

- Measured the thermal resistance of two different manufacturers of VIPs in two different insulation systems for new and retrofit construction.
- Installed and monitored a wood-framed wall with composite and structural insulation panel systems with VIPs as exterior insulation in Ottawa, CA.
- Validated the results from a hygrothermal model with field data for a wood-frame wall insulated with VIPs.
- Used the Morris Method to screen the input variables for a hygrothermal model of a wood-framed wall.
- Introduced a modelling method to evaluate the risk potential for mould growth in a building envelope retrofit.
- Assessed the long-term hygrothermal performance of an exterior insulated VIP system across Canada.

Appendix A WUFI Material Properties

The following tables and graphs provide the material data for the WUFI Pro and WUFI 2D simulations. The material property data was taken from the WUFI material database.

Material: Composite Wood Siding

Property	Unit	Value
Bulk density	[kg/m³]	740
Porosity	[m³/m³]	0.666
Specific Heat Capacity, Dry	[J/(kg K)]	1880
Thermal Conductivity, Dry, 10°C	[W/(m K)]	0.094
Water Vapour Diffusion Resistance Factor	[-]	53.1
Reference Water Content	[kg/m³]	75.5
Free Water Saturation	[kg/m³]	347
Water Absorption Coefficient	[kg/(m² s^0.5)]	0.00072
Temp-dep. Thermal Cond. Supplement	[W/(m K²)]	0.0002

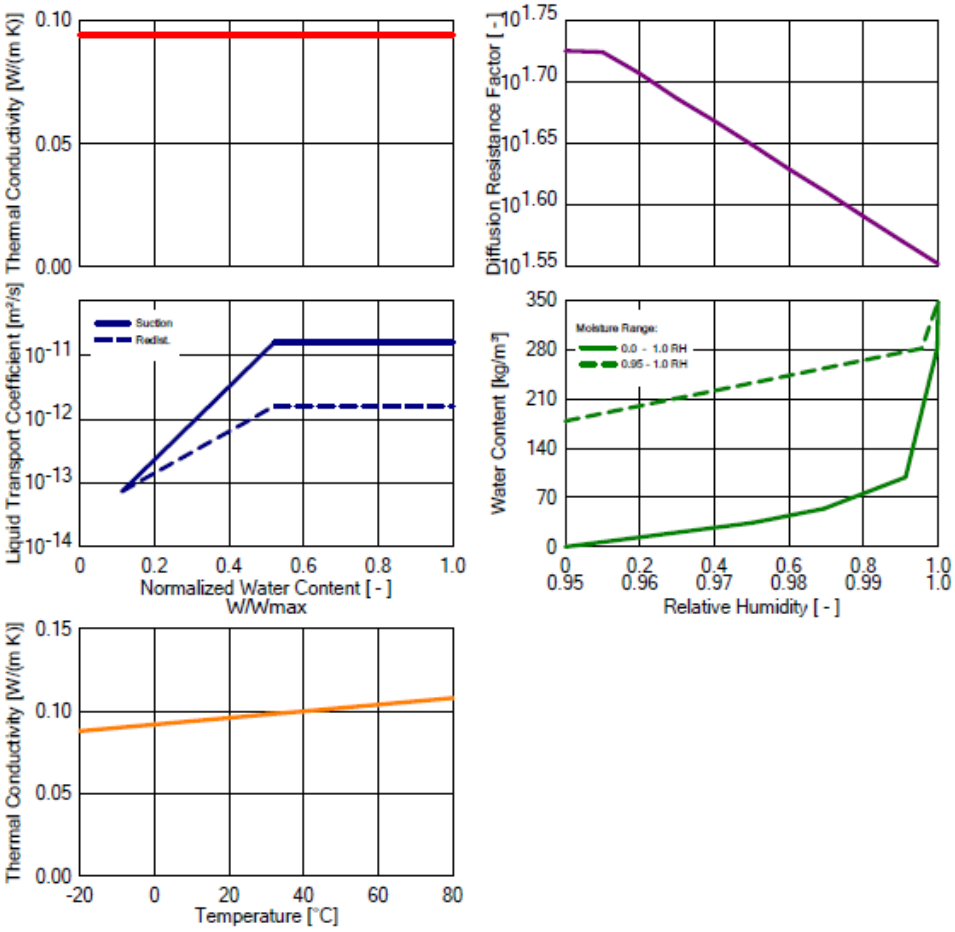

Material: 60 minute Building Paper

Property	Unit	Value
Bulk density	[kg/m³]	280
Porosity	[m³/m³]	0.001
Specific Heat Capacity, Dry	[J/(kg K)]	1500
Thermal Conductivity, Dry, 10°C	[W/(m K)]	2.3
Water Vapour Diffusion Resistance Factor	[-]	144
Temp-dep. Thermal Cond. Supplement	[W/(m K²)]	2.00000E-4

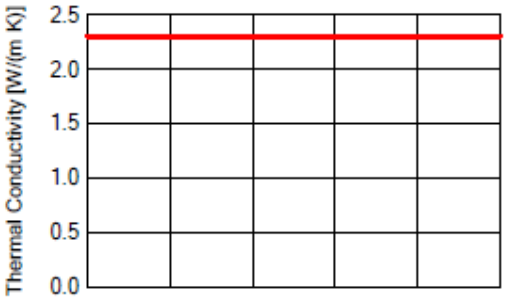

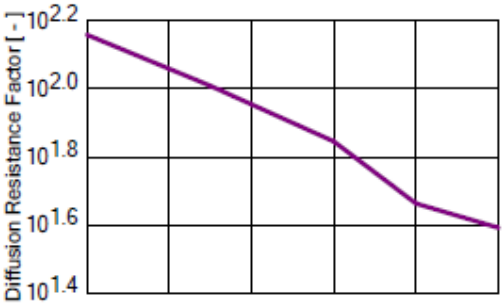

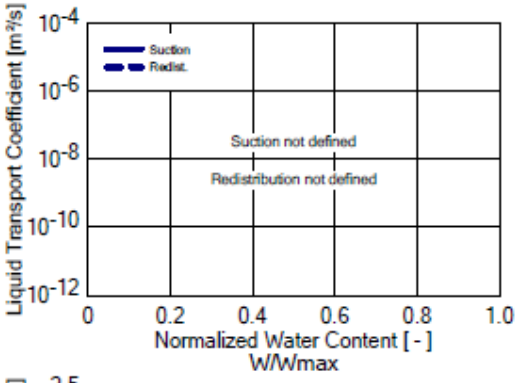

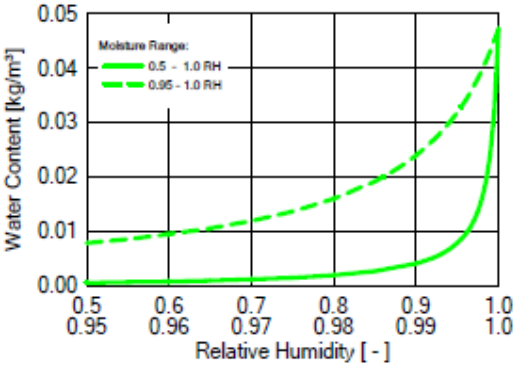

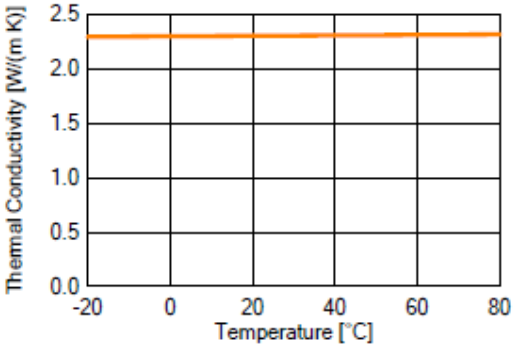

Material: Oriented Strand Board

Property	Unit	Value
Bulk density	[kg/m³]	650
Porosity	[m³/m³]	0.95
Specific Heat Capacity, Dry	[J/(kg K)]	1880
Thermal Conductivity, Dry, 10°C	[W/(m K)]	0.092
Water Vapour Diffusion Resistance Factor	[-]	812.8
Reference Water Content	[kg/m³]	83.3
Free Water Saturation	[kg/m³]	470
Water Absorption Coefficient	[kg/(m² s^0.5)]	0.0022
Temp-dep. Thermal Cond. Supplement	[W/(m K²)]	2.00000E-4

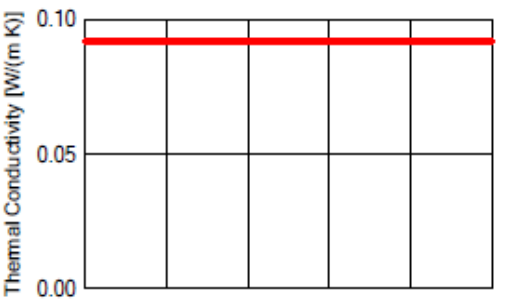

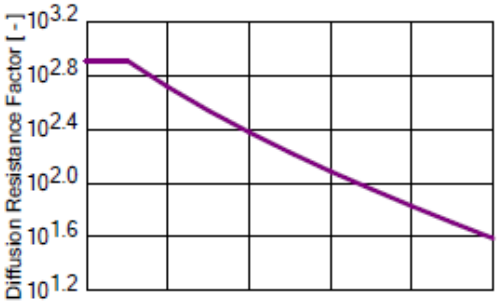

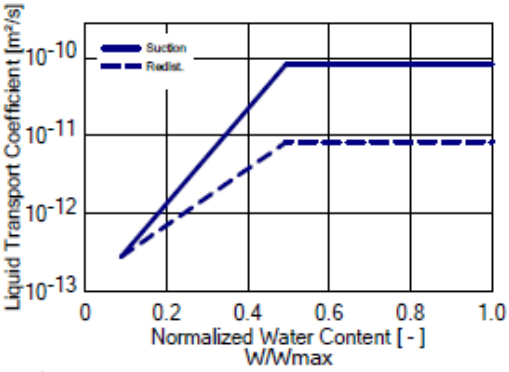

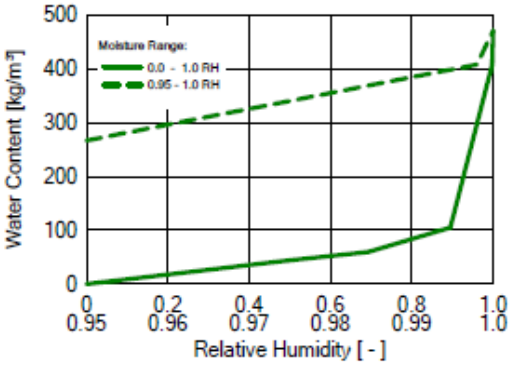

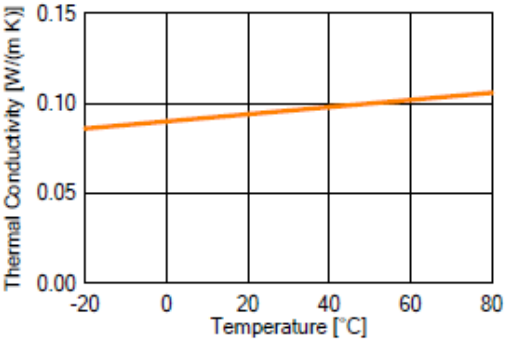

Material: VIP generic (0,007 W/m²K)

Property	Unit	Value
Bulk density	[kg/m³]	200
Porosity	[m³/m³]	0.001
Specific Heat Capacity, Dry	[J/(kg K)]	800
Thermal Conductivity, Dry, 10°C	[W/(m K)]	0.007
Water Vapour Diffusion Resistance Factor	[-]	1500000

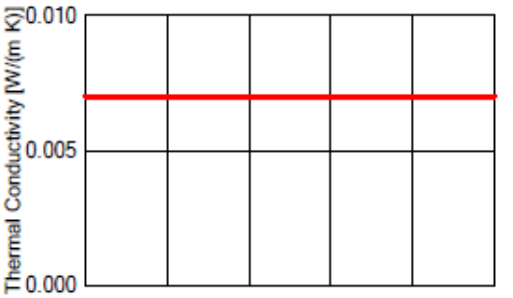

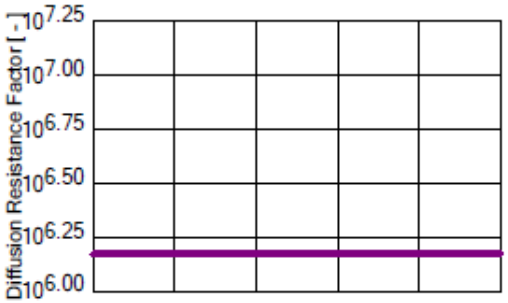

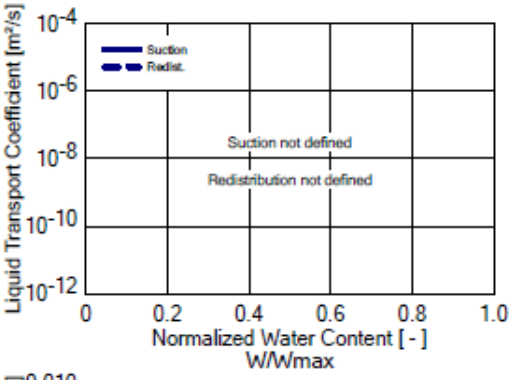

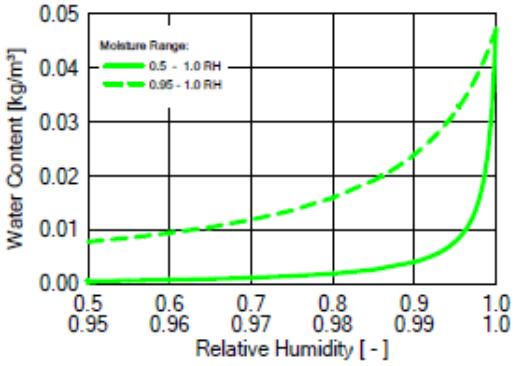

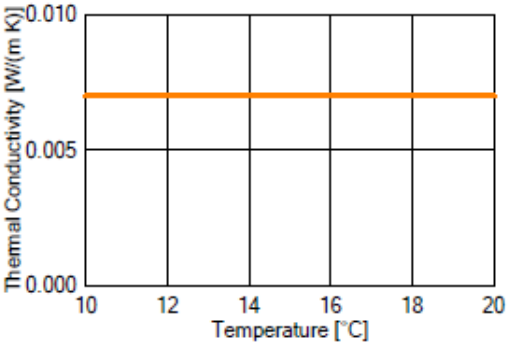

Material: Expanded Polystyrene Insulation

Property	Unit	Value
Bulk density	[kg/m³]	14.8
Porosity	[m³/m³]	0.99
Specific Heat Capacity, Dry	[J/(kg K)]	1470
Thermal Conductivity, Dry, 10°C	[W/(m K)]	0.036
Water Vapour Diffusion Resistance Factor	[-]	73.01
Temp-dep. Thermal Cond. Supplement	[W/(m K²)]	0.0002

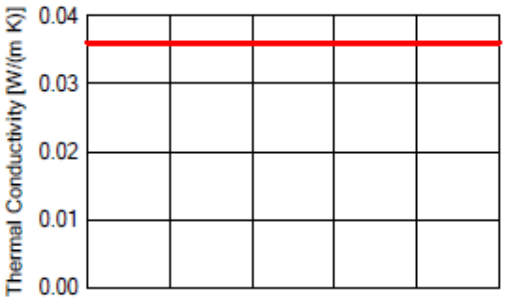

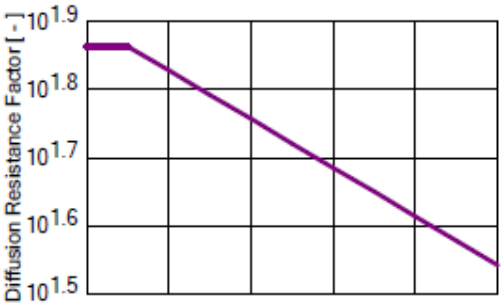

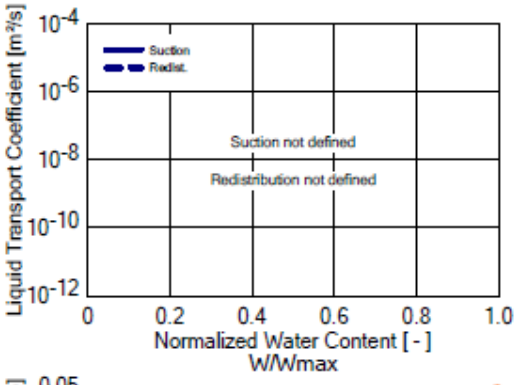

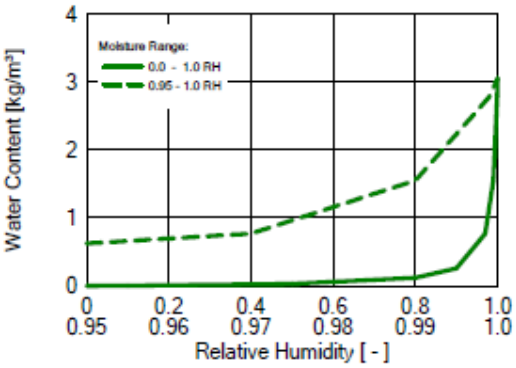

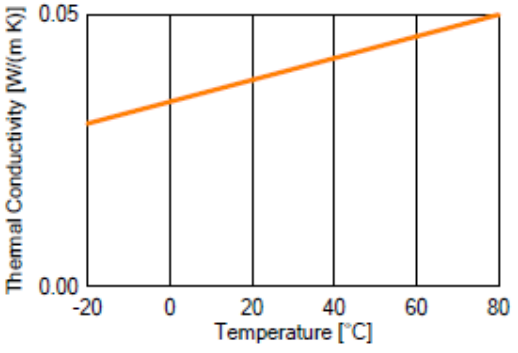

Material: Brick (old)

Property	Unit	Value
Bulk density	[kg/m³]	1670
Porosity	[m³/m³]	0.196
Specific Heat Capacity, Dry	[J/(kg K)]	840
Thermal Conductivity, Dry, 10°C	[W/(m K)]	0.4
Water Vapour Diffusion Resistance Factor	[-]	16
Moisture-dep. Thermal Cond. Supplement	[%/M.-%]	8
Temp-dep. Thermal Cond. Supplement	[W/(m K²)]	2.00000E-4

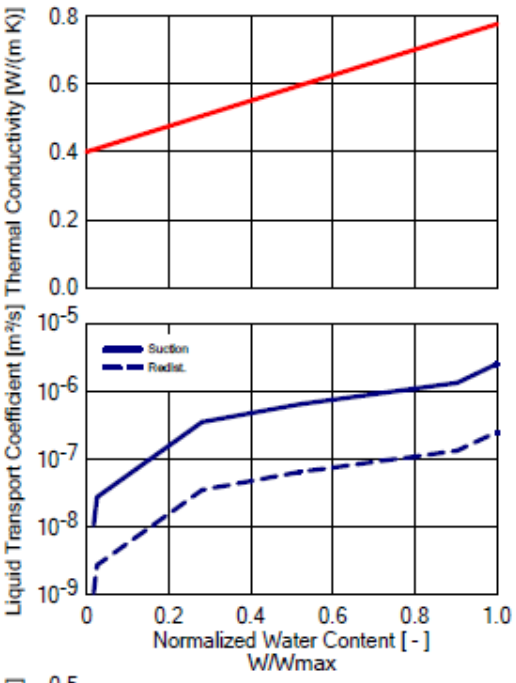

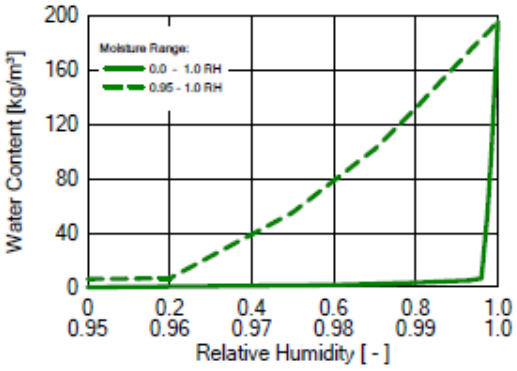

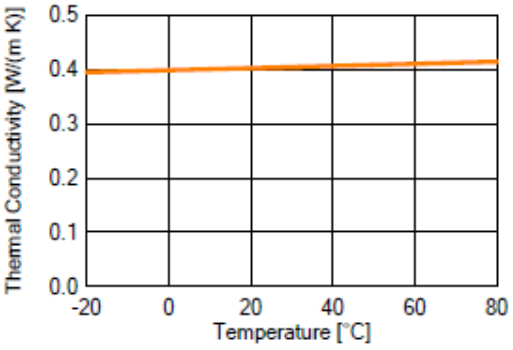

Material: Air Layer 5 mm; without additional moisture capacity

Property	Unit	Value
Bulk density	[kg/m³]	1.3
Porosity	[m³/m³]	0.999
Specific Heat Capacity, Dry	[J/(kg K)]	1000
Thermal Conductivity, Dry, 10°C	[W/(m K)]	0.047
Water Vapour Diffusion Resistance Factor	[-]	0.79

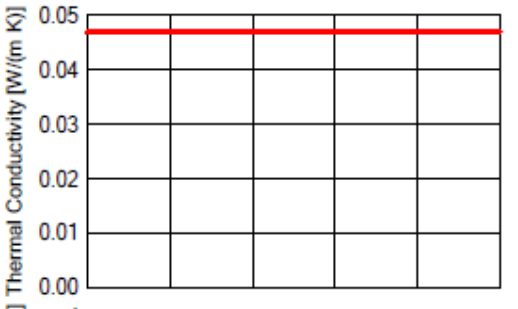

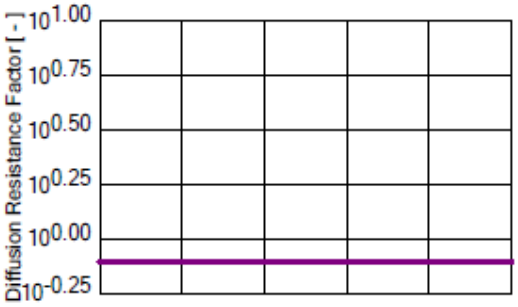

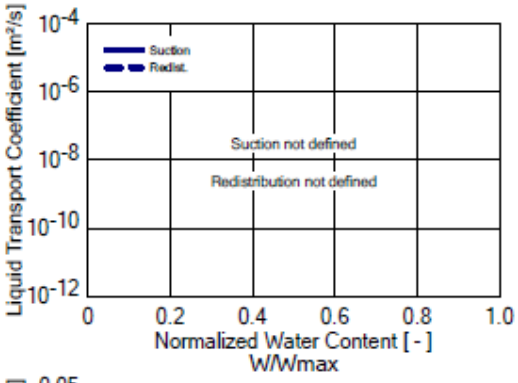

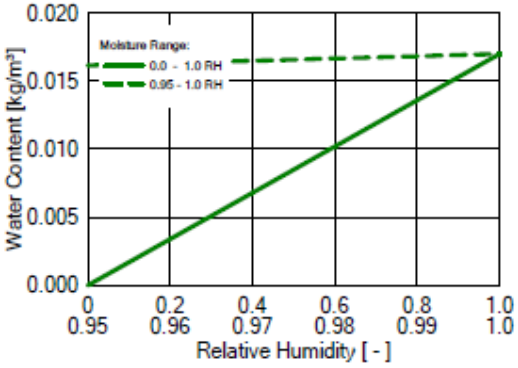

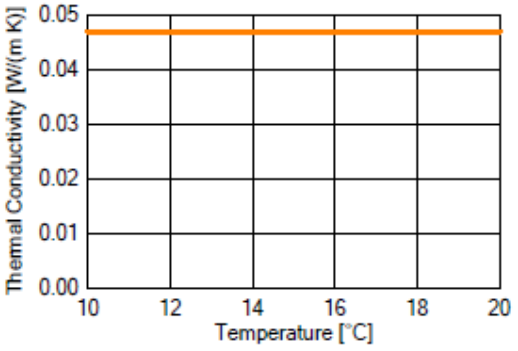

Material: Low Density Glass Fiber Batt Insulation

Property	Unit	Value
Bulk density	[kg/m³]	8.8
Porosity	[m³/m³]	0.999
Specific Heat Capacity, Dry	[J/(kg K)]	840
Thermal Conductivity, Dry, 10°C	[W/(m K)]	0.043
Water Vapour Diffusion Resistance Factor	[-]	1.21
Temp-dep. Thermal Cond. Supplement	[W/(m K²)]	2.00000E-4

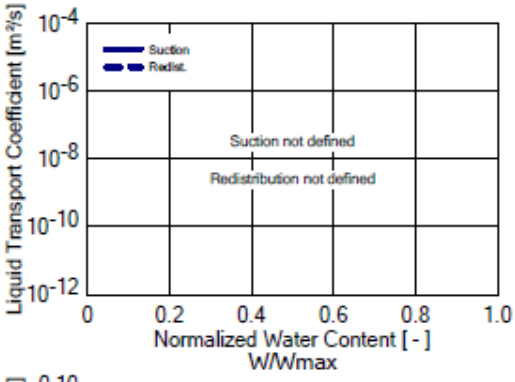

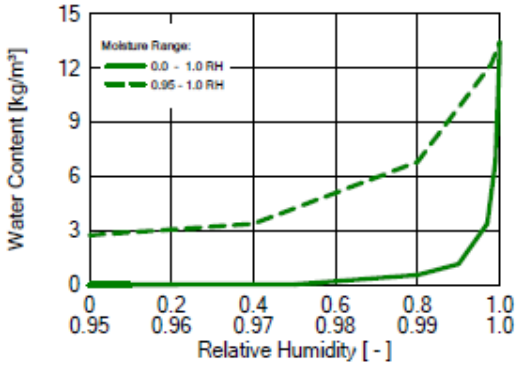

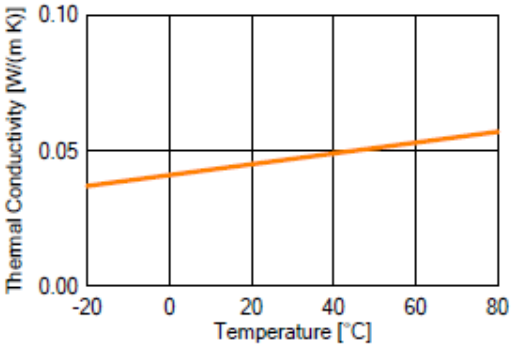

Material: Gypsum Board (USA)

Property	Unit	Value
Bulk density	[kg/m³]	850
Porosity	[m³/m³]	0.65
Specific Heat Capacity, Dry	[J/(kg K)]	870
Thermal Conductivity, Dry, 10°C	[W/(m K)]	0.163
Water Vapour Diffusion Resistance Factor	[-]	6
Moisture-dep. Thermal Cond. Supplement	[%/M.-%]	8
Temp-dep. Thermal Cond. Supplement	[W/(m K²)]	0.0002

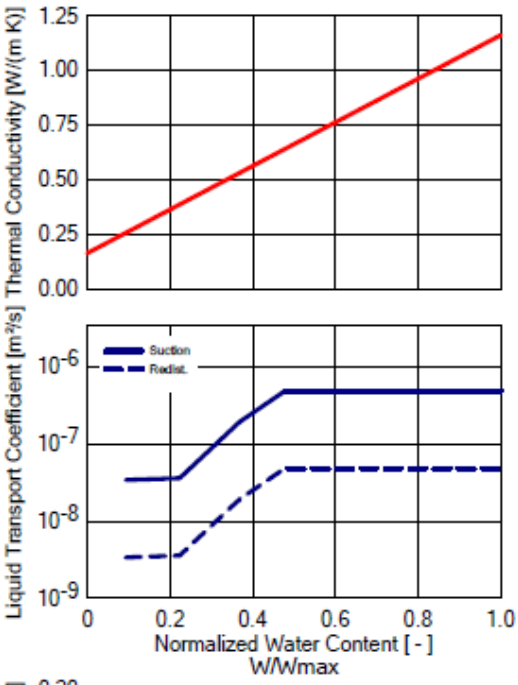

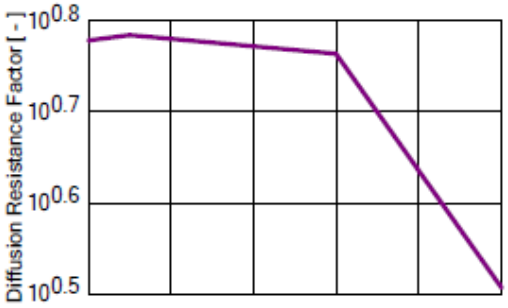

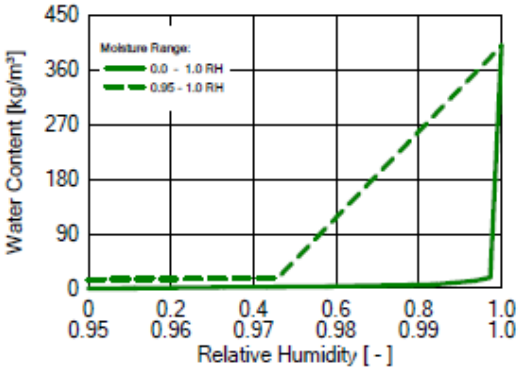

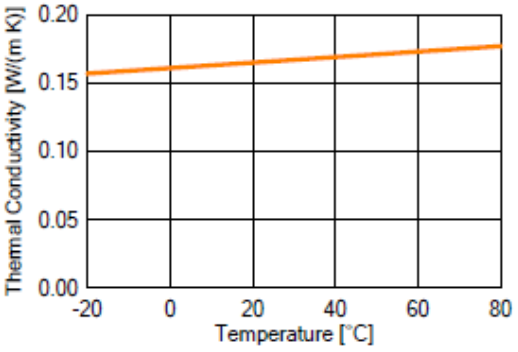

Appendix B Morris Method Randomly Generated Matrix

Using a random number generator in Excel and the variable situations, the following matrix of simulations was used to screen the input variables in WUFI.

Input/**Sim#**	**1**	**2**	**3**	**4**	**5**	**6**	**7**	**8**	**9**	**10**
Construction	XPS w/o RS	XPS w/ RS	EPS w/ RS	XPS w/ RS	XPS w/o RS	XPS w/ RS	XPS w/o RS	XPS w/ RS	XPS w/ RS	XPS w/ RS
WDR Past Water Control	0.02	0.05	0.02	0.01	0.02	0.01	0.02	0.05	0.01	0.05
WDR Past Vapour Control	0.0002	0.0005	0.0005	0.0002	0.0001	0.0005	0.0001	0.0001	0.0005	0.0001
Orientation	South	East	South	East	South	North	North	South	South	North
Vapour Control	None	None	Permeable	None	Impermeable	Impermeable	Impermeable	None	None	Impermeable
Initial Construction Moisture	0.85	0.8	0.8	0.8	0.85	0.8	0.9	0.85	0.9	0.8
Construction Completion	Spring	Fall	Fall	Spring	Summer	Spring	Summer	Fall	Summer	Spring
Timestep	0.33	0.5	1	1	0.5	0.5	0.5	0.5	0.33	0.5
Interior Conditions	Sinusoidal	Sin Med	Sinusoidal	Sinusoidal	Sin Med	Sinusoidal	Sin High	Sinusoidal	Sin Med	Sin High

Input/**Sim#**	**11**	**12**	**13**	**14**	**15**	**16**	**17**	**18**	**19**	**20**
Construction	XPS w/ RS	XPS w/o RS	EPS w/ RS	EPS w/ RS	XPS w/ RS	XPS w/ RS	EPS w/ RS	XPS w/ RS	EPS w/ RS	XPS w/o RS
WDR Past Water Control	0.02	0.05	0.01	0.05	0.02	0.05	0.02	0.05	0.02	0.05
WDR Past Vapour Control	0.0001	0.0001	0.0002	0.0002	0.0001	0.0005	0.0005	0.0005	0.0001	0.0001
Orientation	East	East	North	East	South	South	North	South	East	East
Vapour Control	None	Impermeable	Permeable	None	None	Impermeable	Permeable	Impermeable	None	Permeable
Initial Construction Moisture	0.8	0.85	0.8	0.8	0.8	0.85	0.85	0.85	0.9	0.9
Construction Completion	Spring	Summer	Spring	Fall	Fall	Summer	Summer	Spring	Summer	Fall
Timestep	1	0.5	0.33	1	1	0.33	0.33	0.5	0.5	0.5
Interior Conditions	Sinusoidal	Sin High	Sin Med	Sinusoidal	Sin High	Sin High	Sin High	Sin High	Sinusoidal	Sinusoidal

Input/**Sim#**	**21**	**22**	**23**	**24**	**25**	**26**	**27**	**28**	**29**	**30**
Construction	XPS w/o RS	XPS w/ RS	XPS w/ RS	XPS w/ RS	EPS w/ RS	XPS w/ RS	EPS w/ RS	XPS w/o RS	XPS w/o RS	XPS w/o RS
WDR Past Water Control	0.05	0.02	0.05	0.01	0.05	0.05	0.05	0.05	0.02	0.02
WDR Past Vapour Control	0.0001	0.0005	0.0002	0.0005	0.0002	0.0001	0.0001	0.0002	0.0005	0.0001
Orientation	East	South	East	North	North	North	North	East	East	North
Vapour Control	Permeable	None	Permeable	None	None	Impermeable	None	None	Permeable	Permeable
Initial Construction Moisture	0.85	0.85	0.8	0.85	0.85	0.8	0.9	0.9	0.9	0.85
Construction Completion	Summer	Summer	Fall	Fall	Summer	Spring	Fall	Fall	Spring	Summer
Timestep	0.33	0.5	0.33	0.33	1	0.33	1	0.5	0.5	1
Interior Conditions	Sin High	Sin Med	Sinusoidal	Sin Med	Sinusoidal	Sin High	Sinusoidal	Sin Med	Sin Med	Sin Med

Appendix C Mould Index Code

```
function M=MoldIndex(fileName, Class);
%MoldIndex returns a 2D vector of length (rows) equal to amount of time
%steps of input file, and columns equal to the amount of pairs of
%temperature RH data contained in the input file. Prints to outputfile.csv
%Each row data point is a Mold index value for that time step.
%If more than one pair of T and RH
%data are specified in the input file (nLayers>1) the multiple columns
%correspond to the different Mold index values for those pairs of T and RH
%data.
%fileName is a string of the input file name. e.g. 'test.csv'
%It should be formated with a header row,
%comma separated [can be changed, just change the line
%data=dlmread(fileName,',',1,0)]
%First column of input file should be date/time, second column should be layer
%temperature in degree C, third column should be RH in %, then alternate T and
%RH columns if required.
%nLayers is an integer of the amount of layers
%(i.e. pairs of T and RH data) being evaluated (e.g. 4).
%classVector is a 1D vector of integers corresponding the sensitivity class of materials being
%evaluated. Each component of the vector corresponds to one layer in the
%same order as they appear in the input file. (e.g. [1,2,1,3]). Integers
%are between 1 and 4 and correspond to the following sensitivity classes:
%1 - Very sensitive
%2 - Sensitive
%3 - Medium resistant
%4 - Resistant
%k3 is the decline coefficient and should be set to 0.1 unless a better
%value is known. (See Mold Growth Modeling of Building Structures Using
%Sensitivity Classes of Materials, Tuomo Ojanen Hannu Viitanen, Ruut
%Peuhkuri, Kimmo Lähdesmäki Juha Vinha, DSc Kati Salminen, 2010, Buildings
%XI)

%example of callout to MoldIndex: MoldIndex('test.csv', [2,2,2,2])

data=dlmread([fileName,'_MIInput.csv'],',',0,0);


M=0;
tdecl=0;
A = size(data);

nLayers = fix(A(2)/2);
classVector = Class*ones(nLayers);
k3 = 0.1;

for iLayer=1:(nLayers);
   deltaM=0;
   for itime=1:length(data);
```

```
        Ts=data(itime,iLayer*2-1);
        RHs=data(itime,iLayer*2);
%Checking the data for (1)NaN values, (2) outliers
        if RHs>100
           RHs=100;
        end
        if RHs<0
           RHs=40;
        end
        if isnan(RHs)==1
           if itime==1
              RHs=80;
           else
              RHs = RHs1;
           end
        end
        RHs1=RHs;
        if isnan(Ts)==1||Ts>60||Ts<-40
           if itime==1
              Ts = 20;
           else
              Ts = Ts1;
           end
        end
        Ts1 = Ts;

%Calculating Mould Growth with class vectors
      switch classVector(iLayer)
        case 1 %very sensitive
           if Ts<=20
              RHcrit=-0.00267*Ts^(3.0)+0.16*Ts^(2.0)-3.13*Ts+100;
           else
              RHcrit=80;
           end

           if M <1
              k1=1;
           else
              k1=2;
           end

           W=0;
           A=1;
           B=7;
           C=2;


        case 2 %sensitive
           if Ts<=20
              RHcrit=-0.00267*Ts^(3.0)+0.16*Ts^(2.0)-3.13*Ts+100;
           else
              RHcrit=80;
           end
```

```
        if M <1
           k1=0.578;
        else
           k1=0.386;
         end

        W=1;
        A=0.3;
        B=6;
        C=1;

    case 3 %Medium resistant
         if Ts<=7
           RHcrit=-0.00267*Ts^(3.0)+0.16*Ts^(2.0)-3.13*Ts+100;
        else
           RHcrit=80;
         end

        if M <1
           k1=0.072;
        else
           k1=0.097;
        end
        W=1;
        A=0;
        B=5;
        C=1.5;


    case 4 %resistant
         if Ts<=7
           RHcrit=-0.00267*Ts^(3.0)+0.16*Ts^(2.0)-3.13*Ts+100;
        else
           RHcrit=80;
         end

        if M <1
           k1=0.033;
        else
           k1=0.014;
        end
        W=1;
        A=0;
        B=3;
        C=1;
end

Mmax=A+B*(RHcrit-RHs)/(RHcrit-100)-C*((RHcrit-RHs)/(RHcrit-100))^2;
if itime==1
    k2=max(1-exp(2.3*(0-Mmax)),0);
else
   k2=max(1-exp(2.3*(M(itime-1,iLayer)-Mmax)),0);
```

```
    end



     if RHs>RHcrit && Ts>0
        deltaM=(k1*k2)/(168*exp(-0.68*log(Ts)-13.9*log(RHs)+0.14*W+66.02));
        tdecl=0;
     else
        tdecl=tdecl+1;

        if tdecl<=6
           deltaM=-0.00133*k3;
        elseif tdecl>6 && tdecl <= 24
           deltaM=0;
        else
           deltaM=-0.000667*k3;
        end
     end

    if itime==1
       M(itime,iLayer)=max(0+deltaM,0);
    else
       M(itime,iLayer)=max(M(itime-1,iLayer)+deltaM,0);
    end

  end
end
figure ('Name',fileName);
plot (M);
title('Mould Index Sheathing');
xlabel('Date');
ylabel('Mould Index (MI)');
ylim([0 6]);
% figure
% plot (RHp);
% figure
% plot (Tp);
dlmwrite([fileName,'_MI.csv'],M);
end
```

Appendix D RHT Index Code

```
function RHT80=RHTIndex(FileName,nCase)
%RHTIndex calculated the RHT Index for a given set of T and RH conditions
%The file needs to be an alternating set of temperature in °C, and RH in %.
%Data can be taken from experimental or numerical sources -- script is
%currently setup to run using a WUFI export file in the 'asc.' format,
%however a .csv format is provided below if desired.

%FileName is the filename of the T/RH source data from, and nCase would be
%the number of cases in your WUFI file (with 0 being the first case). The
%file will be start at 0 for the suffix of the data file.
%
%The script will output a cumulative RHT Index for RHT80 and RHT95 for each
%case; matching the order of the columns from the input file.
%
%ex. RHTIndex ('Ottawa_',9)


for jFile=0:nCase
   nFile = [FileName,num2str(jFile)];
% switch FileType
%     case 1 %From WUFI File RHT
      data=dlmread([nFile,'.asc'],'\t',1,1);
% %     case 2 %From Retrofit / MIInput File
%       data=dlmread([FileName,'_MIInput.csv'],',',0,0);


   A = size(data);
   nRHT = fix(A(2)/2);
   RHT80 = zeros(length(data),nRHT);
   RHT95 = zeros(length(data),nRHT);

   for iRHT=1:nRHT
      Ts = ones([length(data),1]);
      b = size(Ts);
      RHs = ones (length (data),1);

      for itime=1:length(data)

         Ts = data(itime,iRHT*2-1);
         RHs = data(itime,iRHT*2);

         if RHs>100
            RHs=100;
         end
         if isnan(Ts)==1||Ts>60||Ts<-40
            if itime==1
               Ts = 20;
            else
               Ts = Ts1;
            end
```

```
        end
        Ts1 = Ts;
        if isnan(RHs)==1
            if itime==1
                RHs=80;
            else
                RHs = RHs1;
            end
        end
        RHs1=RHs;

        %RH80Index
        if RHs>80 && Ts>5
            deltaRHT80 = (RHs-80)*(Ts-5);
        else
            deltaRHT80=0;
        end
        if itime==1
            RHT80(itime,iRHT) = deltaRHT80;
        else
            RHT80(itime,iRHT) = RHT80(itime-1,iRHT) + deltaRHT80;
        end

        %RHT95 Index
        if RHs>95 && Ts>5
            deltaRHT95 = (RHs-95)*(Ts-5);
        else
            deltaRHT95=0;
        end
        if itime==1
            RHT95(itime,iRHT) = deltaRHT95;
        else
            RHT95(itime,iRHT) = RHT95(itime-1,iRHT) + deltaRHT95;
        end

    end


  end


  dlmwrite([nFile,'_RHT80.csv'],RHT80);
  dlmwrite([nFile,'_RHT95.csv'],RHT95);
end
end
```

Appendix E Uncertainty for In-Situ Monitoring

The uncertainty for the critical relative is derived here. The critical relative humidity is calculated using Equation 2-1 and measured temperature was the only variable.

$$U_{\mathrm{RH_C}} = \frac{\delta RH_{\mathrm{c}}}{\delta T}\, U_{\mathrm{T}}$$

When the surface temperature is less than 20°C, the uncertainty of the critical relative follows the form:

$$U_{\mathrm{RH_C}} = \frac{\delta(-0.00267T^3 + 0.160T^2 - 3.13T + 100.0)}{\delta T}\, U_{\mathrm{T}}$$

$$U_{\mathrm{RH_C}} = (-0.00801T^2 + 0.320T - 3.13)U_{\mathrm{T}}$$

When the temperature is greater than 20°C, the critical relative humidity is equal to 80% RH for sensitive materials used in the study, and the uncertainty takes the following form:

$$U_{\mathrm{RH_C}} = \frac{\delta(80)}{\delta T} U_T$$

The measured temperature had an uncertainty of ±0.46°C or ±1.0°C for thermocouples and thermistors, respectively.

The uncertainty for the surface relative humidity derived from moisture content was calculated based on Equation 5-1 and was solely dependent on the moisture content, which has an error of 1% MC between 8% and 30% and a resolution of 0.01% MC [134].

$$RH_{\mathrm{MC}} = \left(1 - e^{\left(-26.655 * \mathrm{MC}^{1.55}\right)}\right) * 100$$

$$U_{\mathrm{RH_{MC}}} = \frac{\delta RH_{\mathrm{MC}}}{\delta MC}\, U_{\mathrm{MC}}$$

$$U_{\mathrm{RH_{MC}}} = \left[\left(41.31 \cdot e^{26.655(M)^{1.55}} (M)^{0.55}\right)(0.01)\right] * 100\%$$

References

[1] Canadian Mortgage and Housing Corporation, "Number of Households: Canada, Provinces and Territories 1976–2036," Canada Mortgage and Housing Corporation, Ottawa, 2018.

[2] Natural Resources Canada, "Energy Use Data Handbook 2000 - 2018," Natural Resources Canada - Office of Energy Efficiency, Ottawa, Ontario, 2015.

[3] United States Department of Energy, "International Energy Outlook 2016," U.S. Department of Energy, Washington, DC, 2016.

[4] EuroStat, "Final Energy Consumption , EU-28, 2014," European Commission, 2016.

[5] Environment and Climate Change Canada, "Pan-Canadian Framework on Clean Growth and Climate Change : Canada's plan to address climate change and grow the economy.," Environment and Climate Change Canada, Gatineau, QC, 2016.

[6] Statistics Canada, "2011 National Household Survey," Statistics Canada, 23 11 2016. [Online]. Available: http://www12.statcan.gc.ca/nhs-enm/2011. [Accessed 27 06 2017].

[7] "National Building Code of Canada 2015," Institute for Research in Construction, National Research Council of Canada, Ottawa, Canada, 2015.

[8] Ministry of Municipal Affairs, "Ontario Building Code," Minisitry of Municipal Affairs - Building and Developement Brach, Toronto, Ont, 2014.

[9] "National Energy Code of Canada for Buildings," 2022. [Online]. Available: https://www.nationalcodes.ca. [Accessed 28 03 2022].

[10] Natural Resources Canada, "Residential End-Use Model," February 2016. [Online]. Available: http://oee.nrcan.gc.ca/corporate/statistics/neud/dpa/menus/trends/comprehensive_tables/list.cfm. [Accessed January 2018].

[11] B. Conley, C. Baldwin, C. A. Cruickshank and M. Carver, "Challenges associated with High RSI-value Building Envelope Retrofits," in *Proceedings of the 15th Canadian Conference on Building Science and Technology*, Vancouver, Canada, 2017.

[12] J. W. Lstiburek, "The Perfect Wall," *ASHRAE Journal,* vol. 49, no. 5, pp. 74-78, May 2007.

[13] A. Parek, *Next Generation Standards for Housing Efficiency,* FP Innovations, 2012.

[14] B. Conley, C. A. Cruickshank and C. Baldwin, "2.24 Insulation Materials," in *Comprehensive Energy Systems*, Elsevier, 2018, pp. 760-795.

[15] L. L. S. Zalewski and D. B. K. Rousse, "Experimental and numerical characterization of thermal bridges in prefabricated building walls," *Energy Conversion and Management,* no. 51, pp. 2869-2877, 2010.

[16] J. Fricke, H. Schwab and U. Heinemann, "Vacuum insulation panels -- Exciting thermal properties and most challenging applications," *International Journal of Thermophysics,* vol. 27, no. 4, pp. 1123-1139, 2006.

[17] P. Mukhopadhyaya, D. MacLean, J. Korn, D. van Reenen and S. Melleti, "Building applications and thermal performance of vacuum inuslation panels (VIPs) in Canadian subarctic climate," *Energy and Buildings,* vol. 85, pp. 672-680, 2014.

[18] B. Jelle, "Traditional, state-of-the-art and future thermal building insulation materials and solutions - Properties, requirements and possibilities," *Energy and Buildings,* vol. 43, no. 10, pp. 2549-2563, 2011.

[19] M. A. Lacasse, G. Hua, M. Hegel, R. Jutras, A. Laouadi, G. Sturgeon and J. Wells, "Guideline on Design for Durability of Building Envelopes," National Research Council, Ottawa, 2018.

[20] ISO, "13823:2008 - General principles on the design of structures for durability," Geneva, Switzerland, 2007.

[21] J. Jermer, "WoodExter - Service life and performance of exterior wood above ground," SP Technical Research Institute Sweden,, Boras, 2011:53.

[22] "BS 7543:2015 Guide to durability of building and building elements, products and components," British Standards Institution, London, 2015.

[23] CSA, "S487-95 - Guideline on Durability in Buildings," CSA Group, Toronto, 2007.

[24] H. R. Trechsel, "Moisture analysis and condensation control in building envelopes," American Society for Testing and Materails, West Conshohocken, PA, 2001.

[25] J. Lstiburek, "Moisture Control for Buildings," *ASHRAE Journal,* February 2002.

[26] J. Lstiburek, "Understanding Vapour Barriers," Building Science Corporation, 2005.

[27] U.S. Environmental Protection Agency, "Moisture Control Guidance for Building Design," U.S. Environmental Protection Agency, Washington, 2013.

[28] J. Straube and E. F. P. Burnett, Building Science for Building Enclosure Design, Westford, MA: Building Science Press, 2005.

[29] J. Straube, "Moisture in Buildings," *ASHRAE Journal,* vol. 44, no. 1, pp. 15-19, 2002.

[30] ANSI/ASHRAE, "Criteria for Moisture Control Design Analysis in Buildings," ASHRAE, 2016.

[31] A. Hukka and H. Viitanen, "A mathematical model of mould growth on wooden material," *Wood Science and Technology,* vol. 33, no. 6, pp. 475-485, 1999.

[32] H. Viitanen, T. Toratti, L. Makkonen, S. Thelandersson, T. Isaksson, E. Fruhwald, J. Jermer, F. Englund and E. Suttie, "Modelling of service life and durability of wooden structures," in *9th Nordic Symposium on Building Physics*, Tampere, Finland, 2011.

[33] T. Ojanen, H. Viitanen, R. Peuhkuri, K. Lahdesmaki, J. Vinha and K. Salminen, "Mold Growth Modeling of Building Structures Using Sensitivity Classes of Materials," in *Thermal Performance Exterior Envelope Buildings XI*, 2010.

[34] A. TenWolde, "A Review of ASHRAE Standard 160-Criteria for Moisture Control Design Analysis in Building," *Journal of Testing and Evaluation,* vol. 39, no. 1, 2011.

[35] J. Straube and J. Smegal, "High-R Walls Case Study Analysis," Building Science Corporation, Somerville, MA, 2009.

[36] J. F. Straube, "High R-Value Enclosures for High Performance Residential Buildings in All Climates," U.S. Department of Energy, Washington, DC, 2011.

[37] International Energy Agency, "Energy in Buildings and Communities Programme," 09 April 2019. [Online]. Available: http://www.iea-ebc.org/projects/project?AnnexID=24.

[38] International Energy Agency, "Energy in Buildings and Communities Programme," 09 April 2019. [Online]. Available: http://www.iea-ebc.org/projects/project?AnnexID=32.

[39] International Energy Agency, "Energy in Buildings and Communities Programme," 09 April 2019. [Online]. Available: http://www.iea-ebc.org/projects/project?AnnexID=39.

[40] International Energy Agency, "Energy in Buildings and Communities Programme," 09 April 2019. [Online]. Available: http://www.iea-ebc.org/projects/project?AnnexID=41.

[41] International Energy Agency, "Energy in Buildings and Communities Programme," 09 April 2019. [Online]. Available: http://www.iea-ebc.org/projects/project?AnnexID=65.

[42] M. A. Lacasse and M. Morelli, "Approach to assessing the long-term performance of wall assemblies: durability of low-rise wood-frame walls," in *14th International Conference on Durability of Building Materials and Components*, Ghent University, Belgium, 2017.

[43] G. Hall and S. Flock, "In-Situ Moisture Testing of Building Products as a Predictor of Actual Conditions," in *Proceedings of the 3rd Building Enclsoure Science and Technology Conference*, Atlants, 2012.

[44] J. Smegal and J. Straube, "High-R Walls for the Pacific Northwest - A Hygrothermal Anslysis of Various Exterior Wall Systems," Building Science Press, Sommerville, MA, 2010.

[45] R. Lepage, C. Schumaker and A. Lukachko, "Moisture Management for High R-Value Walls," U.S. Department of Energy, Springfiled, VA, 2013.

[46] A. Abdul Hamid and P. Wallenten, "Hygrothermal Assessment of Internally Added Thermal Insulation on External Brick Walls in Swedish Multifamily Buildings," *Building and Environment,* vol. 123, pp. 351-362, 207.

[47] T. Trainor, "The Hygrothermal Performance of Exterior Insulated Wall Systems," University of Waterloo, Waterloo, ON, 2014.

[48] M. A. Lacasse, H. H. Saber, W. Maref, G. Ganapathy and M. Nicholls, "Evaluation of Thermal and Moisutre Response of Highly INsulated Wood-Frame Wall Assemblies - Part I: Experimental trials in the Field Exposure of Walls test Facility - Phase 1 and 2," National Research Council Canada, Ottawa, Canada, 2016.

[49] H. H. Saber and G. Ganapathy, "Evaluation of Thermal and Moisutre Response of Highly Insulated Wood-Frame Wall Assemblies Phase 1 Part II Numerical Modelling," National Research Coucil, Ottawa, 2016.

[50] T. Moore, M. Bartko and M. Lacasse, "Evaluation of thermal and moisture response of highly insulated wood-frame wall assemlbies: Part II: parametric numerical simulation evaluation for risk of condensation," National Research Council, Ottawa, 2016.

[51] H. H. Saber and G. Ganapathy, "Evaluation of thermal and moisture response of highly insulated woodframe wall assemblies, phase 2, Part II numerical modelling," National Research Council, Ottawa, 2016.

[52] M. Bartko, R. Jonkman, M. A. Lacasse, T. Moore, A. Parekh and S. Plescia, "An Overview of Studies to Assess the Thermal and Hygrothermal Performance of Highly Insulated and Zero Energy Ready Wall Assemblies," in *15th Canadian Conference on Building Science and Technology*, Vancouver, 2017.

[53] R. Wang, H. Ge and M. Gul, "Hygrothermal Modelling of Multi-Functional Wood Composite Panel (MFP): Comparison of Simulation Results with Field Measurements,"

in *Thermal Performance of the Exterior Envelopes of Whole Buildings XIV International Conference*, Atlanta, 2019.

[54] H. Awad, L. Secchi, M. Gul, H. Ge, R. Knudson and M. Al-Hussein, "Thermal Resistance of Multi-Functional panels in cold climate regions," *Journal of Building Engineering,* vol. 33, 2021.

[55] T. Kawasaki and S. Kawai, "Thermal insulation properties of wood-based sandwich panels for use as structural insulated walls and floors," *Journal of Wood Science,* no. 52, pp. 75-83, 2006.

[56] C. St-Ongea, P. Mukhopadhyayab, G. Torokc and T. Moore, "Canadian Construction materials centre guidelines for the evaluation of vacuum insulated panels," in *1st International Conference on New Horizons in Green Civil Engineeringn*, Victoria, BC, 2018.

[57] M. Schiedel, C. A. Cruickshank and C. Baldwin, "In-Situ Experimental Validation of THERM Finite Element Analysis for a High R-Value Using Vacuum Insulation Panels," in *Proceedings of the ASME 2013 7th International Conference on Energy Sustainability*, Minneapolis, 2013.

[58] C. Baldwin, C. A. Cruickshank, M. Schiedel and B. Conley, "Comparison of steady-state and in-situ testing of high thermal resistance walls incorporating vacuum insulation panels," in *6th Internation Building Physics Conference*, Turino, 2015.

[59] P. Mukhopadhyaya, M. Kumaran, G. Sherrer and D. van Reenen, "An Investigation on Long-Term Thermal Performance of Vacuum Insulation Panels (VIPs)," in *Proceedings of the 10th International Vacuum Insulation Symposium*, Ottawa, 2011.

[60] A. Parekh and C. Mattock, "Incorporation of Vacuum Insulation Panels in a Wood Frame Net Zero Energy Home," *International Vacuum Insulation Symposium,* no. 10, pp. 46-50, 2011.

[61] M. Carver, A. Parehk, C. Baldwin and B. Conley, "Field Evaluation of Hygrothermal Performance and Constructability of Vacuum-Insulated, Thin Wood-Framed Assembly," in *15th Canadian Conference on Building Science and Technology*, Vancouver, BC, 2017.

[62] B. Conley, C. Baldwin, C. A. Cruickshank and M. Carver, "Comparison and Validation of Modelling Methods for Non-Homogenous Walls Incorporating Vacuum Insulation Panels," in *International High Performance Buildings Conference*, West Lafayette, USA, 2016.

[63] M. Zerger and H. Klein, "Integration of VIPs into external wall insulation systems," in *Proceedings of the 7th INternational Vacuum Insulation Symposium*, Duebendorf/Zurich, Switzerland, 2005.

[64] T. Voellinger, A. Bassi and M. Heitel, "Facilitating the incorporation of VIP into precast concrete sandwich panels," *Energy and Buildings,* no. 85, pp. 666-671, 2014.

[65] L. Kubina, "LockPlate System ETICS with integrated VIP - Experience from Building Practice," in *Proceedings of the 10th International Vacuum Insulation Symposium*, Ottawa, Canada, 2011.

[66] K. Gudmundsson, "A Parametric Study of a Metal Sandwich VIP," in *Proceedings of the 9th International Vacuum Insulation Symposium*, London, UK, 2009.

[67] P. Mukhopadhyaya, K. Kumaran, F. Ping and N. Normandin, "Use of vacuum insulation panel in building envelope construction: advantages and challenges," in *13 th Canadian Conference on Building Science and Technology*, Winnipeg, 2011.

[68] B. Conley, "Thermal Evaluation of Vacuum Insulation Panels within Residential Building Envelopes," Carleton University, Ottawa, Canada, 2017.

[69] B. Conley and C. A. Cruickshank, "Evaluation of Thermal Bridges in Vacuum Insulation Panels Assemblies through Steady-State Testing in a Guarded Hot Box," in *eSim 2016*, Hamilton, 2016.

[70] S. Grynning, B. P. Jelle, S. Uvslokk, A. Gustavsen, R. Baetens, R. Caps and V. Meloysund, "Hot box investigations and theoretical assessments of miscellaneous vacuum insulation panel configurations in building envelopes," *Journal of Building Physics,* vol. 34, no. 4, pp. 297-324, 2010.

[71] A. A. Binz, G. Steinke, U. Schonhardt, F. Fregnan, H. Simmler, S. Brunner, K. Ghazi, R. Bundi, U. Heinemann, H. Schwab, H. Cauberg, M. Tenpierik, G. Johannesson and T. Thorsell, "Vacuum Insulation in the Building Sector - Systems and Applications (Subtask B)," in *IEA/ECBCS Annex 39*, 2005, pp. 1-134.

[72] P. Karami, "Robust and Durable Vacuum Insulation Technology for Buildings," KTH Royal Institute of Technology, Stockholm, Sweden, 2015.

[73] A. Batard, T. Duforestel, L. Flandin and B. Yrieix, "Prediction method of the long-term thermal performance of Vacuum Insulation Panels installed in building thermal insulation applications," *Energy and Buildings,* vol. 178, no. 1, pp. 1-10, 2018.

[74] T. K. Ulmer, "Predicting the Lifespan of Vacuum Insulation Panels in Buildings Using Hygrothermal Simulation," Carleton University, Ottawa, Canada, 2019.

[75] M. Nikafkar, "Experimental Verification of Theoretical Ageing and Service Life Prediction Model fo Vacuum Insulation Panels," Ryerson University, Toronto, Canada, 2019.

[76] H. Simmler, S. H. U. S. H. Brunner, K. M. P. Kumaran, D. S. H. Quenard, K. Noller, E. Kuecuekpinar-Niarchos, C. Stramm, M. Tenpierik, H. Cauberg and M. Erb, "Vacuum Insulation Panels - Study on VIP-components and panels for service life prediction of VIP in building applications (Subtask A)," Switzerland, 2005.

[77] P. Johansson, B. Adl-Zarrabi and A. Berge, "Evaluation of long-term performance of VIPs," *6th International Building Physics Conference,* vol. 78, pp. 388-393, 2015.

[78] C. Campbell, "Durability Characterization of a High Performance Building Envelope with Vacuum Insulation Panels and Energy Recovery Ventilation," Carleton University, Ottawa, ON, 2021.

[79] T. V. Moore, "Evaluating the thermal resistance of a vacuum insulation panel wall assembly containing thermal bridges using industry standard calculation methods and numerical simulation techniques," Carleton University, Ottawa, ON, 2017.

[80] U. Berardi, "Aerogel-enhanced insulation for building applications," in *Nanotechnology in Eco-efficient Construction*, Woodhead Publishing Series in Civil and Structural Engineering, 2019, pp. 395-416.

[81] M. Ibrahim, E. Wurtz, P. Biwole, P. Achard and H. Sallee, "Hygrothermal Performance of Exterior Walls Covered with Aerogel-Based Insulating Rendering," *Energy in Buildings,* Vols. 241-251, p. 84, 2017.

[82] P. Beaulieu, M. T. Bomberg, S. M. Cornick, W. A. Dalgliesh, G. Desmarais, R. Djebbar, M. K. Kumaran, M. A. Lacasse, J. C. Lackey, W. Maref, P. Mukhopadhyaya, M. Nofal, N. Normandin, M. Nicholls, T. O'Connor, J. D. Quirt, M. Z. Rousseau, M. Said, M. Swinton, F. Tariku and van Reenen, D. , "Final Report from Task 8 of MEWS Project (T8-03) - Hygrothermal Response of Exterior Wall Systems to Climate Loading: Methodology and Interpretation of Results for Stucco, EIFS, Masonry and Siding-Clad Wood-Frame Walls," National Research Council Canada, Ottawa, 2002.

[83] M. Benkhaled, S.-E. Ouldboukhitine, A. Bakkour and S. Amziane, "Sensitivity analysis of the parameters for assessing a hygrothermal transfer model HAM in bio-based hemp concrete material," *International Communications in Heat and Mass Transfer,* vol. 132, 2022.

[84] M. Steeman, M. Van Belleghem, M. De Paepe and A. Janssens, "Experimental validation and sensitivity analysis of a coupled BES-HAM model," *Building and Environment,* vol. 45, no. 10, pp. 2202-2217, 2010.

[85] M. Van Belleghem, H.-J. Steeman, M. Steeman, A. Janssens and M. De Paepe, "Sensitivity analysis of CFD coupled non-isothermal heat and moisture modelling," *Building and Environment,* vol. 45, no. 11, pp. 2485-2496, 2010.

[86] J. Goffart, M. Rabouille and N. Mendes, "Uncertainty and sensitivity analysis applied to hygrothermal simulation of a brick building in a hot and humid climate," *Journal of Building Performance Simulation,* vol. 10, no. 1, pp. 37-57, 2017.

[87] P. Johansson, S. Geving, C.-E. Hagentoft, B. Jelle, E. Rognvik and A. S. T. B. Kalagasidis, "Interior insulation retrofit of a historical brick wall using vacuum insulation panels: Hygrothermal numerical simulations and laboratory investigations," *Built and Environment,* vol. 79, no. 1, pp. 31-45, 2014.

[88] D. I. Kolaitis, E. Malliotakis, D. A. Kontogeorgos, I. Mandilaras, D. I. Katsourinis and M. A. Founti, "Comparative Assessment of Internal and External Thermal Insulation Systems for Energy Efficient Retrofitting of Residential Buildings," *Energy and Buildings,* vol. 64, pp. 123-131, 2013.

[89] T. Stovall, T. Petrie, J. Kosny, P. Childs, J. Atchley and K. Sissom, "An Exploration of Wall Retrofit Best Practices," Oak Ridge National Laboratories, Oak Ridge, TN, 2007.

[90] B. Arregi and J. Little, "Hygrothermal Risk Evaluation for the Retrofit of a Typical Solid-Walled Dwelling," *Journal of Sustainable Design & Applied Research Journal of Sustainable Design & Applied Research,* vol. 4, no. 1, pp. 16-26, 2016.

[91] K. Ueno, "Residential Exterior Wall Superinsulation Retrofit Details and Analysis," in *ASHRAE Buildings XI*, 2010.

[92] S. Brideau, M. Carver, A. Parekh and B. Conley, "Monitoring and modelling of a prefabricated exterior envelope retrofit," in *In Healthy, Intelligent, and Resilient Buildings and Urban Environments*, Syracuse, NY, 2018.

[93] M. Carver, J. Armstrong and B. Conley, "Prefabricated Wall Panels for Rapid Exterior Enclosure Retrofits of Low-Rise Residential Buildings: Concept and Pilot Design," *Journal of Facade Design and Engineering,* 2020.

[94] "PEER – Prefabricated Exterior Energy Retrofit," Natural Resources Canada, 04 10 2021. [Online]. Available: https://www.nrcan.gc.ca/energy-efficiency/data-research-insights-energy-efficiency/housing-innovation/peer-prefabricated-exterior-energy-retrofit/19406. [Accessed 30 03 2022].

[95] B. Conley, M. Carver and S. Brideau, "Hygrothermal Monitoring of Two Pilot Prefabricated Exterior Energy Retrofit Panel Designs," *Journal of Physics: Conference Series,* vol. 2069, no. 1, pp. 12-28, 2021.

[96] C. Capener, K. Sandin, M. Molnar and J. Jonsson, "Energy efficient retrofitting of a 1950s multi-dwelling block house considering hygrothermal properties - field measurements and simulation," in *Proceedings of 5th International Building Physics Conference*, Kyoto, Japan, 2012.

[97] C.-M. Capener and K. Sandin, "Performance of a Retrofitted 1950's Multi-Unit Residential Building: Measurements and Calculated Transient Hygrothermal Behaviour," in *Thermal Performance of the Exterior Envelopes of Whole Buildings XII International Conference*, Clearwater, USA, 2013.

[98] C. Craven and R. Gaber-Slaught, "Exterior insulation envelope retrofits in cold climates: Implications for moisture control," *HVAC&R Research,* vol. 20, no. 4, pp. 384-394, 2014.

[99] P. Johansson, S. Geving, E. Hagentoft, B. P. Jelle, E. Rognvik, A. Kalagasdis and B. Time, "Interior Insulation Retrofit of a Historical Brick Wall using Vacuum Insulation Panels:

Hygrothermal Numerical Simulations and Laboratory investigations," *Buildings and Environment,* vol. 79, pp. 31-45, September 2014.

[100] D. Maclean, P. Mukhopadhyaya, J. Korn and S. Mooney, "Design details and long-term performance of VIPs in Canada's North," in *8th International Conference on Sustainability in Energy and Buildings*, Turin, Italy, 2016.

[101] V. T. Chan, M. D. Ooms, J. Korn, D. MacLean, S. Mooney, S. Andre and P. Mukhopadhyaya, "Critical Analysis of in situ Performance of Glass Fiber Core VIPs in Extreme Cold Climate," *Frontier Energy Research,* 2019.

[102] D. MacLean, J. Korn and P. Mukhopadhyaya, "Vacuum Insulation Panels (VIPs) arrive in northern Canada: Institutional building pilot retrofit in Yukon," in *Proceedings of International Vacuum Insulation Symposium*, Ottawa, 2011.

[103] S. Fantucci, S. Garbaccio, A. Lorenzati and M. Perino, "Thermo-economic analysis of building energy retrofits using VIP - Vacuum Insulation Panels," *Energy and Buildings,* vol. 196, no. 1, pp. 269-279, 2019.

[104] F. E. Boafo, J.-G. Ahn, J.-T. Kim and J.-H. Kim, "Computing thermal bridge of VIP in building retrofits using DesignBuilder," *Energy Procedia,* vol. 78, pp. 400-405, 2015.

[105] ASTM International, "Standard Test Method for Thermal Performance of Building Materials and Envelope Assesmblies by Means of a Hot Box Apparatus," ASTM International, West Conshohocken, PA, 2011.

[106] C. Baldwin, "Design and Construction of an Experimental Apparatus to Assess the Performance of a Solar Absorption Chiller with Integrated Thermal Storage," Carleton University, Ottawa, 2013.

[107] "Standard Test Method for Calibration of Thermocouples By Comparison Techniques," ASTM International, West Conshohocken, USA, 2021.

[108] National Instruments, "LabVIEW," National Instruments, Austin, TX, 2014.

[109] S. V. Glass and S. L. Zelinka, "Moisture Relations and Physical Properties of Wood," in *Wood handbook : wood as an engineering material; FPL, Centennial ed. General technical report; GTR-190*, Madison, WI., U.S. Dept. of Agriculture, Forest Service, Forest Products Laboratory, 2010, pp. 4.1-4.19.

[110] Vaisala, "Humidity and Temperature Probe HMP60," 2020. [Online]. Available: https://www.vaisala.com/en/products/instruments-sensors-and-other-measurement-devices/instruments-industrial-measurements/hmp60. [Accessed 26 09 2021].

[111] Honeywell, "HIH-5030/5031 Series," 03 2010. [Online]. Available: https://sps.honeywell.com/ca/en/products/advanced-sensing-technologies/healthcare-sensing/humidity-with-temperature-sensors/hih-5030-5031-series. [Accessed 06 04 2022].

[112] Environment Canada, "Historical Climate Data," Government of Canada, 21 March 2019. [Online]. Available: climate.weather.gc.ca. [Accessed 1 January 2019].

[113] LBNL, *THERM Version 7.7.07,* Lawrence Berkeley National Laboratory, 2019.

[114] "THERM 7 / WINDOW 7 NFRC Simulation Manual," National Fenestration Rating Council, Inc. , 2017.

[115] H. Künzle, "Untersuchungen über Feuchtigkeitsverhältnisse in verchiedenen Flachdachkonstruktionen," *Berihte aus der Bauforschung,* vol. 48, 1966.

[116] O. S. Hagerstedt and J. Arfvidsson, "Comparison of Field Measurements and Calculations of Relative humidity and Temperature in Wood Framed Walls," in *Thermophysics 2010*, Valtice, Czech Republic, 2010.

[117] S. Olof Mundt-Peterson and L.-E. Harderup, "Validation of a One-Dimensional Transient Heat and Moisture Calculation Tool under Real Conditions," in *Thermal Performance of Exterior Envelopes of Whole Buildings XII - International Conference*, Florida, USA, 2013.

[118] U. Alev, A. Uus, M. Teder, M.-J. Miljan and T. Kalamees, "Air leakage and hygrothermal performance of an internally insulated log house," in *10th Nordic Symposium on Building Phsyics*, Lund, Sweden, 2014.

[119] E. 15026, "Hygrothermal performance of building components and building elements. Assessment of moisture transfer by numerical simulation," 2007.

[120] E. I. 13788, "Hygrothermal performance of building components and building elements – Internal surface temperature to avoid critical surface humidity and interstitial condensation – Calculation methods.," Brussels, Belgium, 2012.

[121] J. F. Straube and E. F. P. Burnette, "Simplified Prediction of Driving Rain on Buildings," in *International Building Physics Conference*, Eindhoven, Netherlands, 2000.

[122] J. Straube and E. Burnette, "Driving Rain and Masonry Veneer," in *Water Leakage Through Building Facades, ASTM STP 1314*, Philadelphia, USA, 1997.

[123] J. F. Straube and C. Schumacher, "Driving rain loads for Canadian Building Design," in *Proceedings of 10th Canadian Building Science and Technology Conference*, Ottawa, 2006.

[124] J. Lstiburek, K. Ueno and S. Musunuru, "Strategy Guideline: Modeling Enclosure Design in Above-Grade Walls," U.S. Department of Energy, Oak Ridge, TN, 2016.

[125] T. V. Moore and M. A. Lacasse, "Approach to Incorporating Water Entry and Water Loads to Wall Assemblies When Completing Hygrothermal Modelling," in *Building Science and the Physics of Building Enclosure Performance*, D. Lemieux and J. Keegan, Eds., West Conshohocken, PA, ASTM International, 2020, pp. 157-176.

[126] ISO, "Hygrothermal performance of building components and building elements — Internal surface temperature to avoid critical surface humidity and interstitial condensation — Calculation methods," 17 02 2020. [Online]. Available: https://www.iso.org/standard/51615.html.

[127] ASHRAE, "RP-1325: Environmental Weather Loads for Hygrothermal Analysis and Design of Buildings," American Society for Heating, Refrigeration and Air-Conditioning Engineers, Atlanta, 2011.

[128] M. D. Morris, "Factorial Sampling Plan for Preliminary Computational Experiments," *Technometrics,* vol. 2, no. 33, 1991.

[129] T. Homma and A. Saltelli, "Importance measures in global sensitivity analysis of nonlinear models," *Reliability Engineering and System Safety,* vol. 52, no. 1, pp. 1-17, 1996.

[130] I. Sobol, "Global sensitivity indices for nonlinear mathematical," *Mathematics and Computers in Simulation,* no. 55, pp. 271-280, 2001.

[131] Natural Resources Canada, "National Energy Use Database," 2016. [Online]. Available: http://oee.nrcan.gc.ca/corporate/statistics/neud/dpa/data_e/databases.cfm?attr=0. [Accessed 01 01 2018].

[132] Natural Resources Canada Office of Energy Efficiency, "EnerGuide for Houses -- Grants for Homeowners," Office of energy Efficiency, Ottawa, ON, 2004.

[133] Office of Energy Efficiency; National Research Council, "Survery of Household Energy Use: Detailed Statistical Report," Natural Resources Canada Office of Energy Efficiency, Ottawa, ON, 2007.

[134] E. Schmidt and M. Riggo, "Monitoring Moisture Performance of Cross-Laminated Timber Building Elements during Construction," *Buildings,* vol. 6, no. 9, p. 144, 2019.

[135] A. TenWolde and I. Walker, "Interior moisure design load for residences," in *Proceedings of Exterior Envelopes of Whole Buildings VIII International Conference*, Atlanta, 2001.

[136] T. Ojanen and K. Kumaran, "Effect of exfiltration on the hygrothermal behaviour of a residential wall assembly," *Journal of Thermal Insulation and Building Envelopes,* no. 19, pp. 215-227, 1996.

[137] H. Schwab, C. Strak, W. Johannes, H.-P. Ebert and J. Fricke, "Thermal Bridges in Vacuum-insulated Building Facades," *Journal of Building Physics,* vol. 28, no. 4, pp. 345-355, 2005.

[138] C. R. Mero, "Design Construction of a Guarded Hot Box Facility for Evaluating the Thermal Performance of Building Wall Materials," Texas A&M University, 2012.

[139] K. Martin, C. E. A. Escuder, I. Flores and J. Sala, "Equivalent wall method for dynamic characterisation of thermal bridges," *Energy and Buildings,* no. 55, pp. 704-714, 2012.

[140] F. Bianchi, A. L. Pisello, G. Baldinelli and F. Asdrubali, "Infrared Thermography Assessment of Thermal Bridges in Building Envelope: Experimental Validation in a Test Room Setup," *Sustainability,* vol. 6, pp. 7107-7120, 2014.

[141] F. Asdrubali and G. Baldinelli, "Thermal transmittance measurements with the hot box method: Calibration, experimental procedures and uncertainty analyses of three different approaches," *Energy and Buildings,* vol. 43, no. 7, pp. 1618-1626, 2011.

[142] International Organization for Standardization, "Thermal insulation -- Determination of steady-state thermal transmission properties -- Calibrated and guarded hot box," Geneva, 2013.

[143] C. Aggarwal, M. Defo, T. Moore, M. A. Lacasse, S. Sahyoun and H. Ge, "Validation of Three Methods of Selecting Moisture Reference Years for Hygrothermal Simulations," in *XV International Conference on Durability of Building Materials and Components*, Barcelona, 2020.

[144] P. Johansson, C.-E. Hagentoft and A. S. Kalagasidis, "Retrofitting of a listed brick and wood building using vacuum insulation panels on the exterior of the facads: Measurements and simulations," *Energy and Buildings,* vol. 73, pp. 92-104, April 2014.

[145] M. Rossi and V. Rocco, "Application of VIP: Evaluation of Winter and Summer Energy Performance of External Walls with VIP in Buildings located in Middle Latitudes," in *International Vacuum Insulation Symposium*, Ottawa, 2011.

[146] M. Mullens and M. Arif, "Structural Insulated Panels: Impact on the Residential Construction Process," *Construction Engineering and Management,* vol. 132, no. 7, pp. 786-794, 2006.